University of Southampton

Faculty of Medicine

Clinical and Experimental Sciences

The functional effect of CD1c responsive T cells in human Tuberculosis (TB)

https://doi.org/10.5258/SOTON/D2892

by

Sahar Hazem Farag

ORCID ID 0000-0003-2360-7094

Thesis for the degree of Doctor of Philosophy

April 2024

University of Southampton

Abstract

Faculty of Medicine

Clinical and Experimental Sciences

Doctor of Philosophy

The functional effect of CD1c responsive T cells in human Tuberculosis (TB)

by

Sahar Hazem Farag

Tuberculosis (TB) is an infectious disease with one of the highest rates of mortality, and remains a global health pandemic. Despite major research programmes over the last two decades, outcomes of novel interventions for TB have been disappointing; and the consistent emergence of multi-drug resistant strains continue to pose a challenge. Thus, a deeper understanding of the host-pathogen interaction is urgently required for the development of more efficacious treatments. *Mycobacterium Tuberculosis (Mtb)*, the causative agent of TB, owes its high virulence to its lipid-rich cell wall, many of which can trigger a host-mediated immune response during infection. Mycobacterial derived lipids are presented by the CD1 family of proteins, which include CD1c. During the natural course of *Mtb* infection, CD1 proteins bind lipid antigens and present them to T cells. An increase in CD1c-restricted *Mtb*-lipid specific T cells in the peripheral blood of TB patients has been documented. Importantly, the majority of CD1c-restricted T cells are also autoreactive as they recognise CD1c in the absence of exogenous lipid antigens. Hence, CD1c-autoreactive T cells recognise CD1c proteins when they are bound to endogenous self-lipid antigens. Nevertheless, the exact role that CD1c-autoreactive T cells play in the host response to TB is yet to be elucidated. In this study, we aimed to identify whether CD1c-autoreactive T cells have an as of yet undetermined anti-TB function. Henceforth, we optimised cellular *in vitro* assays to facilitate the detection, isolation, and expansion of CD1c-autoreative T cells before investigating their anti-TB functions. We explored various methods of expanding CD1c-autoreactive T cell populations from pan T cells derived from human blood, and determined that THP1-CD1c mediated expansion was the most effective method of enriching these populations. Following expansion with THP1-CD1c, we employed CD1c-tetramers to isolate CD1c-autoreactive T cells. T cell reactivity to CD1c was validated through a combination of tetramer studies and functional assays. Importantly, CD1c-autoreactive T cells were significantly cytotoxic towards *Mtb* infected THP1-CD1c target cells, but not towards uninfected target cells, nor towards target cells that did not express CD1c, irrespective of their infection status. In addition, while CD1c-autoreactive T cells released cytokines in response to uninfected $CD1c^+$ target cells in an autoreactive manner, they produced significantly enhanced amounts of a variety of anti-microbial cytokines including TNF-α, IFN-γ, GM-CSF, IL-4, IL-5, and IL-13 in response to *Mtb* infected $CD1c^+$ targets. Moreover, phenotypical studies confirmed that our CD1c-autoreactive T cells were $CD4^+$ and are polyclonal as they expressed αβ- or hybrid δ/αβ-TCRs. Lastly, to better understand the TCR repertoire of CD1c-autoreactive T cells we completed sequencing studies which identified eight unique TCRs, four of which were αβ-TCRs, and four were γδ-TCRs. Altogether, the data highlights that while these T cells are overtly self-reactive towards CD1c, they also respond even more strongly to a specific human infection such as *Mtb*. Hence, these findings suggest a specific functional role for CD1c-autoreactive T cells in the immune response to TB, and sheds light on a potential protective mechanism that could be manipulated to design future therapeutic interventions.

Table of Contents

Table of Tables

Table of Figures

List of Accompanying Materials

DOI: https://doi.org/10.5258/SOTON/D2892

Research Thesis: Declaration of Authorship

Print name: Sahar Hazem Farag

Title of thesis: The functional effect of CD1c responsive T cells in human Tuberculosis (TB)

I declare that this thesis and the work presented in it are my own and has been generated by me as the result of my own original research.

I confirm that:

1. This work was done wholly or mainly while in candidature for a research degree at this University;
2. Where any part of this thesis has previously been submitted for a degree or any other qualification at this University or any other institution, this has been clearly stated;
3. Where I have consulted the published work of others, this is always clearly attributed;
4. Where I have quoted from the work of others, the source is always given. With the exception of such quotations, this thesis is entirely my own work;
5. I have acknowledged all main sources of help;
6. Where the thesis is based on work done by myself jointly with others, I have made clear exactly what was done by others and what I have contributed myself;
7. None of this work has been published before submission

Signature: Date: 10th April 2024

Acknowledgments

Firstly, I would like to thank my supervisors, Dr Salah Mansour and Professor Paul Elkington. I am grateful for this opportunity, and for their ongoing guidance, support, and patience. I am also thankful to be part of the CD1-TB family, which has some of the kindest hearts, and brilliant minds; thank you for your friendship and encouragement. Additionally, thank you to the wider community of Level E for making the department a pleasant and welcoming environment to work in.

I'd also like to thank my industrial supervisors, Dr Dave Cole, Dr Marco Lepore and Dr Chris Holland; and the Discovery Research group at Immunocore for their advice, help, and kindness. They made carrying out an industrial placement during a global pandemic as pleasant of an experience as possible. I thoroughly enjoyed my time at Immunocore and learnt a great deal about the industry as well as myself. Also, thank you to the MRC and Immunocore for funding my PhD and allowing me to pursue my passion.

Lastly, thank you to my family, friends, Cein and Kiki for being a constant source of support, love, and happiness. To my parents, Hazem and Kauser Farag, who I dedicate this PhD to. You walked so I could run. Thank you for believing in me and supporting me unconditionally. Daddy, thank you for encouraging me to always dream bigger, and not be afraid to fall. My love for all things science began because of you, so this PhD is as much yours as it is mine. Mama, thank you for being the best role model anyone could ask for, I grew up in awe of your strength, kindness, and determination. You filled our lives with so much love and warmth and will always be my greatest source of inspiration.

To my siblings, Ibrahim, Soha, and Yousef, thank you for anchoring me and looking after me, each in your own way; you are the most wonderful people I will ever know, and a blessing. To my husband, Ayman, thank you for all that you are, all that you do, and the light and happiness that you bring.

Alhamdulillah.

Definitions and Abbreviations

α-GalCer	alpha-Galactosylceramide
Ac2SGL	Diacylated Sulphoglycolipid
AEC	Airway Epithelial Cell
AIM	Activation Induced Marker
AK	Adenylate Kinase
ALF	Alveolar Lining Fluid
AM	Alveolar Macrophage
AMP	Antimicrobial Peptide
APC	Antigen Presenting Cell
ATI	Alveolar Type 1
ATII	Alveolar Type 2
β2m	Beta-2-microglobulin
BCG	Bacillus Calmette Guérin
BSA	Bovine Serum Albumin
CCR6	C-C Chemokine Receptor Type 6
CD1	Cluster of Differentiation 1
CFP	Culture Filtrate Protein 10
CFU	Colony Forming Unit
CIITA	Class II Transactivator
CL3	Containment Level 3
CLR	C-type Lectin Receptor
CMV	Cytomegalovirus
CTV	Cell Trace Violet
DC	Dendritic Cell
DDM	Dideoxymycobactin
DMSO	Dimethyl Sulfoxide
DN	Double Negative
EBV	Epstein-Barr Virus
ECM	Extracellular Matrix
ELISA	Enzyme-linked Immunosorbent Assay
ELISPOT	Enzyme-linked Immune Absorbent Spot
ESAT-6	6-kDa Early Secretory Antigenic Target
FBS	Foetal Bovine Serum

FPLC	Fast Pulse Liquid Chromatography
GMM	Glucose Monomycolate
GM-CSF	Granulocyte Monocyte-Colony Stimulating Factor
HBD-2	Human β-defensin-2
HEK	Human Embryonic Kidney
HIV	Human Immunodeficiency Virus
HLA	Human Leukocyte Antigen
HSP70	Heat Shock Protein 70
IB	Inclusion Body
IFN	Interferon
iNKT	Invariant Natural Killer T Cell
IL	Interleukin
ILT4	Ig-Like Transcript 4
IPTG	Isopropyl-β-D-thiogalactoside
KO	Knockout
LAM	Lipoarabinomannan
LB	Luria-Bertani Broth
mLPA	methyl-Lysophosphatidic Acid
LPS	Lipopolysaccharide
LTBI	Latent TB Infection
M1	Classically Activated Macrophages
M2	Alternatively Activated Macrophages
MA	Mycolic Acid
MACS	Magnetic Activated Cell Sorting
MAG	Monoacylglycerol
MAIT	Mucosal-associated Invariant T cells
MAMP	Microbe Associated Molecular Pattern
MFI	Mean Fluorescence Intensity
MHC	Major Histocompatibility Complex
MIG	Monokine Induced by Interferon gamma
MMP	Matrix Metalloproteinase
MoDC	Monocyte-derived Dendritic Cell
MOI	Multiplicity of Infection
MPD	Mannosyl Phosphodolichols
MPM	Mannosyl-β1-phosphomycoketide

MR1	Major Histocompatibility Complex Class I Related Protein
Mtb	*Mycobacterium Tuberculosis*
NHP	Non-human Primate
NK	Natural Killer Cell
NKT	Natural Killer T Cell
NOD2	Nucleotide-binding Oligomerisation Domain containing protein 2
NOS	Nitric Oxide Synthase
PAMP	Pathogen Associated Molecular Pattern
PBMC	Peripheral Blood Mononuclear Cell
PBS	Phosphate Buffered Saline
PC	Phosphatidylcholine
PCR	Polymerase Chain Reaction
PD-L1	Programmed Death Ligand 1
PG	Phosphatidylglycerol
PHA	Phytohemagglutinin
PI	Phosphatidylinositol
PI3K	Phosphatidylinositol 3 kinase
PM	Phosphomycoketide
PRR	Pathogen Recognition Receptor
RANTES	Regulated on Activation, Normal T cell Expressed and Secreted
ROS	Reactive Oxygen Species
RLU	Relative Luminescence Units
SDS-PAGE	Sodium Dodecyl Sulphate-Polyacrylamide Gel Electrophoresis
SEC	Size Exclusion Chromatography
DC-SIGN	DC Specific Intercellular adhesion molecule-3 Grabbing Non-integrin receptor
SL	Spacer Lipid
SM	Sphingomyelin
SP	Surfactant Protein
TAP	Transporter Associated Antigen processing protein
TB	Tuberculosis
TCR	T Cell Receptor
TGF	Transforming Growth Factor
TIMP	Tissue Inhibitors of Metalloproteinases
TLR	Toll-Like Receptor
TNF	Tumour Necrosis Factor

UV	Ultraviolet
WHO	World Health Organisation
WT	Wild Type

Chapter 1 Introduction

Tuberculosis (TB)

Mycobacterium tuberculosis (*Mtb*) is the aetiological agent of human Tuberculosis (TB) infection. The spread of *Mtb* across the world is thought to have occurred due to human migration from Africa where it originally emerged approximately 70,000 years ago [2, 3]. To date, approximately a third of the world's population is infected with latent TB, and an estimated 10% of these cases are likely to reactivate and become infectious in their lifetime, thus continuing the dissemination of TB in humans [4]. TB poses an even greater risk to immunocompromised individuals, such as infants, the elderly, and those with other health conditions such as human immunodeficiency virus (HIV); with 30% of deaths amongst HIV patients being due to TB [4]. Biochemical analyses as well as techniques such as electron microscopy, and cryoelectron tomography, were able to demonstrate that the cell wall of *Mtb* is functionally similar to gram-negative bacteria, and is rich in mycolic acids and glycolipids [5, 6]. These molecules give TB its thick waxy structure that results in its high virulence and provides an almost impenetrable barrier to compounds and drugs, thus ensuring its survival and persistence, making *Mtb* the successful pathogen it is today.

Due to the complexity of the immune response to *Mtb*, the development of effective vaccines, diagnostic tests and treatments poses a great challenge. Murine models and human studies have both demonstrated that Interferon gamma (IFN-γ), IL-12 [7-9], CD4 T cells [8, 9], and Tumour Necrosis Factor alpha (TNF-α) [10, 11] are essential in the host's ability to control the infection. However, the underlying causes for why some hosts are able to clear the infection whilst others do not, remain unknown [12]; although, well established risk factors include HIV coinfection, diabetes, and malnutrition [13].

Mtb infection

The host immune response to *Mtb* infection remains poorly understood as the pathogen has developed ways to evade the innate and adaptive immune responses it encounters. Mycobacteria have a conserved complex cellular envelope that comprises a variety of unique lipids [14]. This cell wall plays an integral role in the survival and propagation of the bacilli [15]. Cell wall derived lipid antigens are presented to immune cells to initiate a response. However, mycobacteria have

developed strategies to evade or interfere with lipid antigen presentation, suggesting that this is an important mechanism of defence against *Mtb* infection [16].

Mtb infection is usually transmitted via the inhalation of airborne droplets containing tubercle bacilli from a patient with active TB. There are several outcomes possible following the inhalation of these droplets by a host (Figure 1), (a) the bacilli are killed in the alveoli upon initially encountering macrophages, (b) the bacteria is able to overcome the initial response by the macrophages, this results in a primary infection following high bacterial burden, (c) the bacteria is contained by the immune system, the host is rendered asymptomatic and non-contagious, this is known as Latent TB Infection (LTBI), (d) the bacteria are able to reactivate at a later time point and active infection occurs [17].

The first line of defence upon inhalation of bacilli are the airway epithelial cells (AECs) and phagocytes which include macrophages, dendritic cells (DCs) and neutrophils [18]. Depending on bacterial load, these cells are usually able to clear the infection; however, several other factors may influence their ability to overcome the infection. *Mtb* is able to infect alveolar macrophages and DCs as well as the non-phagocytic pneumocytes [19]. *Mtb* replicating within the infected macrophages then spreads to extra pulmonary sites via the lymph nodes where the adaptive immune system response develops [20]. The relationship between host and bacterial factors are multifaceted and varied. Here, we discuss the role of some of the immune cells and the processes that take place during TB infection and how *Mtb* is able to evade these responses.

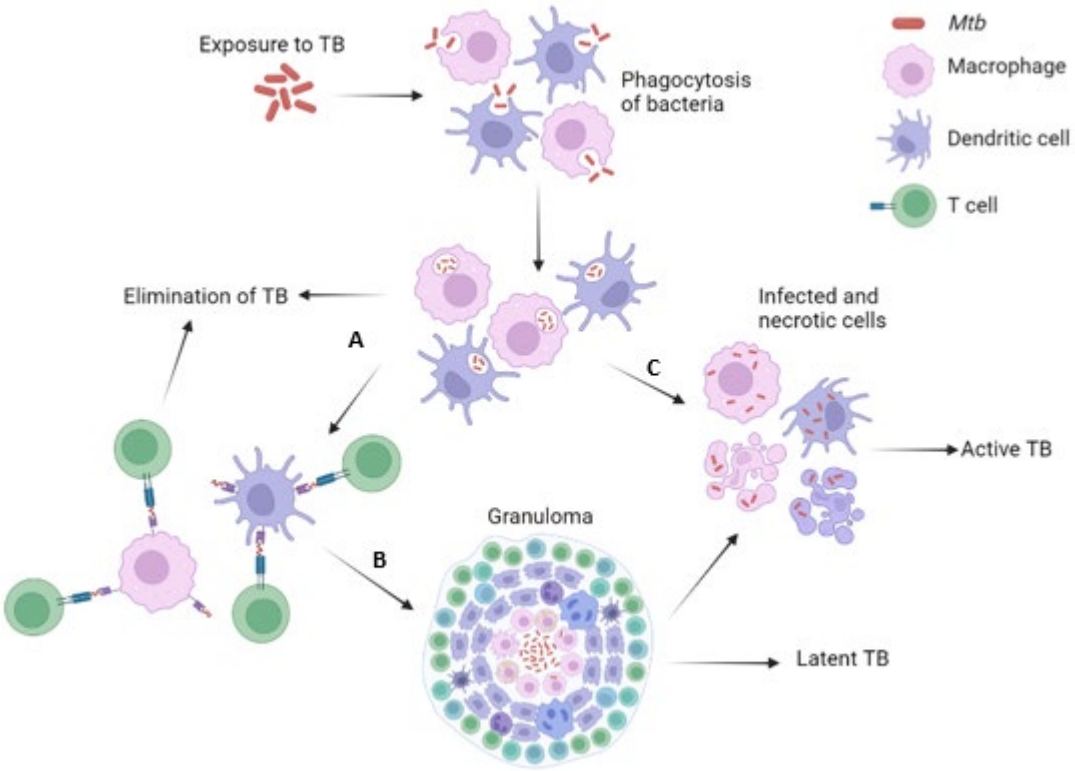

Figure 1: TB infection cycle. Upon entry into the lungs, *Mtb* is phagocytosed by cells such as macrophages and dendritic cells, the infection is then either eliminated by the innate or adaptive immune responses (**A**), contained in a granuloma which could possibly cause reinfection (**B**), or overcomes the immune response and causes active TB (**C**)**.**

Immune response to TB

Host airways

The human trachea, bronchi and bronchioles are composed of different types of tightly adhered airway epithelial cells (AECs) that serve to protect the airways both physically and immunologically from intruders. These cell types include ciliated cells that physically trap foreign material, club cells that produce glycosaminoglycans that coat and protect the airway, and goblet cells that produce mucus that covers the airways and facilitates the clearance of foreign pathogens and particles via the mucocilliary escalator [21]. The AECs produce a mucus that lines the airways and contains an array of proteins including immunoglobulins, mucins, and defensins [22]. These components serve to protect the airways from foreign pathogens in different ways. Secretory immunoglobulins A (IgA) present on mucosal surfaces neutralise toxins and interfere with the adherence of pathogens to the airways, thus preventing internalisation [23]. Mucins are large heavily glycosylated proteins that are

responsible for the viscosity of the mucus layer, and for physically trapping microbes [24]. Defensins are also an important bactericidal constituent of the airway mucus and have been shown to disrupt the mycobacterial cell wall [25]. Additionally, the presence of functional pathogen recognition receptors (PRRs) on AECs allows them to sense invading pathogens, resulting in the secretion of cytokines such as TNF-α, chemokines, and growth factors such as granulocyte macrophage colony-stimulating factor (GM-CSF) that recruit phagocytes to the site of infection where pathogens are eliminated by phagocytosis [26].

The alveoli are composed of specialised cells known as alveolar type 1 (ATI) and alveolar type 2 (ATII) which also have dedicated functions in the maintenance and protection of the lungs [27]. In the alveoli, alveolar lining fluid (ALF) produced by ATI and ATII cells also contains components of the complement pathway such as C2, C3, C4, and C5 which is an important pathway of the innate immune system [28]. Lung hydrolases present in the ALF have been shown to decrease *Mtb* adhesion and intracellular survival within macrophages by modifying its cellular envelope [29], as well as augmenting TNF-α and IL-8 expression in neutrophils infected with hydrolase exposed *Mtb* [30]. Overall, mucosal barriers of the airways are well equipped to initially defend against inhaled *Mtb* as well as other pathogens, providing that the host is not immunocompromised, and the bacterial load is manageable. However, as well as being protective, a role for AECs in the degradation of lung tissue has been highlighted by Elkington et al. [31] as mentioned below.

Whilst ATII cells are non-phagocytic, they play an important role in the response to *Mtb* infection [32]. These cells express Dectin-1 which was initially characterised as a fungal PRR that binds to β-glucan. In the context of *Mtb*, an ATII cell line (A549 cells) infected with *Mtb* resulted in the induction of Dectin-1 in a Toll-like receptor 2 (TLR2) dependent manner and demonstrated a synergy between both proteins, which enhanced cytokine production [32, 33]. The production of ROS was also dependent on the increased expression of Dectin-1 [32]. Other studies have demonstrated a role for Dectin-1 in antimycobacterial immunity, such as its role in promoting IL-12p40 production in response to *Mtb* infection from macrophages and DCs, which subsequently activate T cells [33].

Additionally, surfactant proteins (SPs) secreted from ATII and club cells also play a role in the recognition of pathogens and contribute to developing an adaptive immune response during infection [34]. There are four known SPs, SP-A, B, C, and D. These are all composed of phospholipids and proteins; their main role is to reduce surface tension in the alveoli during breathing by allowing lungs to expand during inhalation [35]. SP-A has been shown to play a role in the capture and phagocytosis of *Mtb* by alveolar macrophages [36]. Additionally, several *in vivo* and *in vitro* studies have demonstrated a role for SP-A and SP-D in the host defence against *Mtb* [37, 38].

TLRs are amongst the most important PRRs and are expressed on AECs. They mediate host-pathogen interaction via the recognition of pathogen associated molecular patterns (PAMPs) expressed on pathogens. Upon activation, they initiate a signalling event that results in the recruitment of immune cells to the site of infection [39].

There are 10 TLRs expressed in humans (TLR1 to 10). TLR1, TLR2, TLR4, TLR5, TLR6, and TLR10 have been found to be expressed on AECs where they recognise bacterial proteins, lipoproteins, and polysaccharides. Upon activation with their ligand, each of these TLRs triggers the appropriate downstream signalling cascade to launch an immune response [40, 41]. As well as TLRs, AECs also present an assortment of cell surface proteins such as the C-type lectin receptors (CLRs), Dectin-1, DC specific adhesion molecule-3 grabbing non-integrin receptor (DC-SIGN also known as CD209), and mannose receptors; as well as nucleotide-binding oligomerisation domain containing protein 2 (NOD2) [39].

In alveolar cells, TLR2 form heterodimers with TLR1 or TLR6, the major ligand for these TLRs are lipoproteins that are ubiquitously expressed on the outer membranes of gram-negative bacteria [42]. This heterodimerisation is thought to have evolved as a means of expanding the ligand repertoire of lipoproteins and peptides that TLRs can recognise [43, 44]. During *Mtb* infection, the TLRs become activated in response to lipoarabinomannan (LAM) present in the cell wall of *Mtb*, this results in the downstream activation of the MyD88 signalling pathway, which in turn activates NF-kB; this results in the production of pro-inflammatory cytokines and the subsequent activation of T cells [45]. In particular, the activation of TLR2 also results in the production of IL-8 and an antimicrobial peptide known as human β-defensin-2 (HBD-2). IL-8 is a neutrophil chemoattractant and so recruits them to the site of infection; whilst HBD-2 has been shown to act via a chemokine receptor, C-C chemokine receptor type 6 (CCR6) to recruit dendritic cells (DCs) and T cells to the site of infection [46].

Additionally, studies have demonstrated a role for TLR1 through to TLR6, as well as TLR9 [39] in the immune response of bronchial epithelial cells to *Mtb* infection. These cells have also been shown to regulate the sensitivity of the bronchi in the recognition of microbes by managing TLR expression in mucosal surfaces [47]. AECs also present antigens to mucosal-associated invariant T cells (MAITs) [48] and stimulate them to release IFN-γ, TNF-α and granzyme; these are factors that aid in the clearance of the bacilli. The fast response of MAIT cells provides an IFN-γ boost that activates macrophages [49]. Once in the alveoli, *Mtb* encounters alveolar macrophages (AMs), DCs and neutrophils, which are all phagocytic.

Macrophages

One of the most important cells of the immune system are macrophages, these cells are often the first to engage with invading pathogens, they phagocytose and degrade them, and subsequently trigger an immune response that instructs cells of the adaptive immune system in order to resolve the infection [50]. Upon recognition of *Mtb* MAMPs by PRRs on alveolar macrophages (AMs), the bacteria is phagocytosed and contained in a phagosome where it is then degraded, however, certain *Mtb* proteins have been shown to inhibit this process [51]. Pro-inflammatory cytokines and chemokines such as GM-CSF, TNF-α, IL-1β, and IL-6 can also be upregulated by AMs in order to recruit and activate other immune cells such as T cells to help combat the infection [52, 53]. $CD4^+$ T cells recruited to the site of infection produce IFN-γ which activates macrophages and results in the recruitment of more lymphocytes. The IFN-γ mediated stimulation of macrophages along with other mediators such as vitamin D, play a very important role in containing *Mtb* within the macrophage [54]. Vitamin D supports the production of an antimicrobial peptide (AMP) known as cathelicidin, this protein activates the transcription of autophagy related genes [55]. As a result, vitamin D deficiency supports the growth and survival of *Mtb* within cells.

However, *Mtb* has been shown to survive within macrophages, and circumvent or delay the onset of several processes involved in the innate immune response, as well as causing a delay in initiation of the adaptive immune response. Once inside the macrophage, *Mtb* is able to manipulate its environment, making it more favourable for its survival and replication. Some of the functions *Mtb* is able to disrupt include phagosome maturation, apoptosis, and the production of ROS and cytokines [50].

Furthermore, another way in which *Mtb* evades the host immune response is by inhibiting phagosome maturation. During the course of infection, *Mtb* infects macrophages and survives. The macrophage forms a phagosome around the bacteria, this phagosome would typically fuse with a lysosome, thus forming a phagolysosome that degrades the pathogen upon acidification. However, *Mtb* can disrupt the maturation of the phagosome, preventing its fusion with a lysosome and subsequently inhibiting its acidification, and therefore survives [56, 57]. The inability of macrophages to form phagolysosomes causes cellular necrosis, this in turn results in the release of *Mtb* and consequently allows it to infect other cells [56]. Bacterial proteins such as early secretory protein 6 (ESAT 6) disrupt the maturation of phagosomes by preventing the accumulation of vacuolar ATP and GTP enzymes, thus maintaining pH at 6 – 6.5. Normally, the accumulation of these enzymes decreases the pH by facilitating luminal acidification and allow the maturation of the phagosome [58]. Additionally, ESAT 6 has been shown to create membrane spanning pores in the membranes of phagosomes, which allows the escape of *Mtb* and its virulence factors into the cytosol where *Mtb* replicates and ultimately results in cell death and dissemination of the bacteria [59, 60]. ESAT 6 along with its chaperone protein, culture filtrate protein 10 (CFP 10), form complexes and are able to

enter the endoplasmic reticulum where it sequesters β2-microglobulin (β2m), resulting in the inhibition of cell surface expression of MHC class I, and consequently downregulating antigen presentation [61]. The importance of ESAT 6 as a virulence factor is documented in the literature. Studies have demonstrated that the integration of the gene encoding for ESAT 6 (RD1) in mycobacterium species that do not otherwise express it such as *M. bovis*, and *M. microti*, increase virulence of these strains [59, 62], whilst the deletion of this gene in *Mtb* attenuates the strain [63].

Moreover, *Mtb* is able to manipulate the expression of various important markers such TACO/coronin 1. This is an actin binding host protein which is typically released before the fusion of lysosomes with phagosomes [64]. The recruitment and retention of TACO/coronin 1 to phagosomal compartments containing *Mtb* arrests the maturation of the phagosome, stops the fusions of the lysosome, and allows *Mtb* to persist [65]. Furthermore, the amount of TACO/coronin 1 positively correlates with the amount and activity of *Mtb* in phagosomes [66].

Additionally, AMs are essential for the maintenance of airway immune homeostasis. They can differentiate either into classically activated macrophages, known as M1, these are proinflammatory; or into alternatively activated macrophages, known as M2; these have anti-inflammatory properties. The subset they differentiate into is dependent on the biomolecular signals they are stimulated with during infection [67, 68]. Whilst macrophages can trigger an immune response against *Mtb* infection, AMs collected from TB patients were found to be anti-inflammatory of the M2 phenotype and have a diminished ability to control the infection [69, 70].

Studies have shown that *Mtb* is capable of polarising AMs towards an M2 phenotype by upregulating anti-inflammatory cytokines such as IL-10 and TGFβ [71, 72], as well as making AMs less effective at presenting antigens [73]. The ability of *Mtb* to manipulate AMs makes them an ideal vessel for mycobacterial survival in the host.

The *Mtb* cell wall is composed of many lipids and lipoproteins, some of which interact with components of the hosts' cells, allowing it to alter the immune response and ensuring its survival [74]. The bacterial lipoprotein LprG binds to lipoglycans such as LAM and enables the transfer of LAM from the plasma membrane to the cell envelope, this increases the surface exposed LAM which inhibits phagolysosomal fusion [75]. LAM derived from the *Mtb* cell wall has been found to block calcium signalling and inhibits type III phosphatidylinositol 3 kinase (PI3K) which is vital for the fusion of vesicles involved in phagosomal maturation [76, 77].

Neutrophils

In the airways of patients with active TB, neutrophils have been found in abundance [78]. Nevertheless, their role in the progression of TB seems to depend on various factors, such as *Mtb* virulence and host genetics [79]. Neutrophils can be phagocytosed by *Mtb* infected macrophages, the antimicrobial granules of neutrophils are able to fuse with *Mtb* containing phagosomes in macrophages to improve killing of the bacteria [80]. Neutrophils also result in the recruitment and activation of other immune cells following stimulation by *Mtb* [81]. However, despite their beneficial properties, neutrophils have also been shown to have a negative impact during the immune response and can result in tissue damage due to the excessive production of antimicrobial proteins [82]. Additionally, they are able to negatively regulate lymphocytes. The proportion of neutrophils expressing Programmed death ligand 1 (PD-L1) is high in TB patients; this ligand interacts with its receptor, Programmed death receptor 1 (PD-1), which is expressed on lymphocytes and triggers their loss of function and eventually apoptosis, thereby decreasing the number of lymphocytes fighting the infection [83].

Nevertheless, similarly to macrophages, neutrophils are also able to produce AMPs such as cathelicidin as well as lipocalin 2 which helps with containing the bacteria [84]. Additionally, both cell types work together to recruit and activate more immune cells via the production of granules and cytokines [80, 85]. Neutrophils have also been found to produce extracellular vesicles that promote the production of ROS in macrophages, thus increasing their autophagic activity [86].

Dendritic cells (DCs)

Another cell type that *Mtb* can hijack are DCs, these cells are professional antigen presenting cells (APCs) and are able to activate $CD4^+$ T cells by presenting antigens to them, as well as via the production of cytokines [87]. However, upon infection with *Mtb*, these cells can also become vessels for its survival and their functional abilities to activate T cells weakens [88]. Following the phagocytosis of *Mtb***,** DCs mature and present antigens via Major Histocompatibility Complex (MHC) class I and II to T cells in the local lymph node [89], forming the link between innate and adaptive immune responses. However, as well as studies finding that DCs are valuable in boosting the cellular immune response to *Mtb*, it has also previously been reported that *Mtb* is capable of impairing DC function and their ability to prime an immune response to ameliorate the infection [90].

Under normal conditions, DCs presenting pathogen-derived antigens migrate to the lymph nodes where they prime T cells; this migration is facilitated by the binding of CD209 which is expressed on DCs to CD54 which is present on endothelial cells. However, during an infection, CD209 facilitates

the entry of *Mtb* in to DCs [88]. The interaction of mannosylated lipoarabinomannan (ManLAM) present on the cell membrane of *Mtb* with CD209 results in the disruption of the cellular function of DCs and results in the downregulation of IL-12 production and the upregulation of IL-10, leading to the suppression of T cell activity [91, 92]. This hindrance in the maturation of DCs and subsequent lack of activation of T cells is one of the ways whereby *Mtb* bests the immune response and gains time to establish a foothold in the host [93].

Additionally, alpha glucan derived from *Mtb* cell wall has been shown to differentiate monocytes into DCs (Glu MoDCs). These cells were found to be CD1 negative and were not able to present sulphatides to CD1-restricted T cell clones [94]. The downregulation of CD1c by *Mtb* in DCs which otherwise express high levels of it, was determined to be due to the ability of live *Mtb* infection to decrease CD1 mRNA levels [95, 96], thus evading $CD4^+$ T cell responses that have been previously reported in the literature to be mediated by $CD1c^+$ MoDCs [97].

Natural Killer cells (NK)

NK cells play an integral role in fighting off infections, and are often activated by infected macrophages. A role for NK cells in *Mtb* infection is highlighted by studies in patients with active TB where the number of NK cells in peripheral blood is increased [98], as well as elevated levels of NK cells in pleural fluid from TB patients, which are not found in the pleural fluid of patients with other lung pathologies [99]. However, NK cells from patients with active TB produced significantly lower amounts of IFN-γ and degranulation in response to *Mtb* antigens; and treatment of TB correlates with reduced numbers of $CD57^+$ NK cells, these cells have reduced cytokine responsiveness. This suggests that altering the NK repertoire to cells that are more responsive to cytokines and activation leads to more success in fighting off the infection [100]. Furthermore, NK cells found at the site of infection were mostly of the $CD56^{hi}$ subset; these cells have a higher cytokine secreting activity and a lower cytotoxic activity as opposed to their counterparts, the $CD56^{lo}$ subset which have better cytotoxic function but a lower ability to secrete cytokines [101]. As well as being activated by macrophages, NK cells can also be activated via their Nkp44 receptors upon recognition of *Mtb* cell wall components [102]. Further evidence of a direct interaction between *Mtb* and NK cells is established by the production of IFN-γ by $CD56^{hi}$ cells in response to *Mtb* in the absence of cells expressing CD3, CD14 or CD19 [99]. During the early stages of an infection, it is likely that NK cells provide and early source of IFN-γ before the adaptive response begins to take place [101]. They are also able to lyse DCs or macrophages that are not capable of controlling the intracellular growth of the bacteria, this results in the bacteria being released in the extracellular space but allows better

access for NK cells to interact with ligands and further activate NK, and other phagocytic cells present locally [103, 104]. The production of IL-12 and TNF-α by DCs and macrophages initially results in copious amounts of IFN-γ being produced by NK cells; this initial response may influence the $CD4^+$ T cell repertoire by inducing activated $CD4^+$ T cells to differentiate into Th1 cells [101].

Myeloid-derived suppressor cells (MDSC)

Regulatory immune cells are an essential compartment of the immune system and ensure that the immune response remains in check to prevent immunopathology. Over the past 15 years, MDSCs, which are a population of myeloid regulatory cells, have been shown to play a role as an innate immune checkpoint, but with an inhibitory, and deleterious effect on the host immune response [105, 106]. MDSCs are a heterogeneous group of cells that are mostly monocytic and polymorphonuclear cells, and are phagocytic [107]. They are overproduced during chronic infections and suppress host T cell-mediated response [108]. They have been extensively studied in both human and murine models in the context of cancer [107, 109-111], and have been found to expand in cancer as well as during chronic infection, whilst being below detection levels in healthy controls [110-113]. More recently, MDSCs with potent inhibitory effects have been shown to be present during TB infection [112, 114, 115].

Following infection with *Mtb*, typically, $CD4^+$ Th1 cells trigger an adaptive immune response in order to clear the infection. However, should this response fail, and the infection persist, a chronic inflammatory state takes hold which could result in tissue damage [106]. Consequently, regulatory mechanisms are activated to return to homeostasis. Under normal conditions, immature myeloid cell (IMC) precursors differentiate into mature monocytes, DCs, NK cells, neutrophils, basophils, eosinophils, and mast cells [116]. However, during chronic infection, the presence of cytokines and growth factors such as GM-CSF, IL-6, VEGF, PGE_2, IL-1β, and IFN-γ, results in the generation of MDSCs from IMCs that have not fully matured, and develop a suppressive phenotype [112, 116-118].

MDSCs have been shown to suppress immune responses mediated by other immune cells such as NK cells, CD4 and CD8 T cells, in both antigen-specific and non-antigen specific manners [112, 119-121]. Despite there being a few studies on the role of MDSCs in TB, most studies have been carried out in cancer models, nevertheless, certain mechanisms found in cancer studies can be applied to infectious diseases such as TB. For example, arginase 1 becomes upregulated which results in the depletion of arginine and the consequent inhibition of T cell activation and proliferation; this has been demonstrated in human TB and mouse models [112, 122, 123]. Additionally, the upregulation of inducible nitric oxide synthase (iNOS) results in the production of nitric oxide, which has been

shown in both humans and mouse models of TB [109, 124-126]. This can result in the nitrosylation of the TCR and a loss of the TCR zeta chain, as has also been demonstrated in human TB [112, 116]. Lastly, MDSCs upregulate CTLA-4 and PD-1, which results in the induction of T cells apoptosis. This has also been observed in human *in vitro* TB models [122].

Whilst regulatory and immune suppressive mechanisms are in place to play a protective role in reducing tissue damage and averting immunopathology [110], MDSCs are almost too effective at reducing innate cytokines and suppressing Th1 responses [127].

Within the tumour microenvironment in cancer, lipid transport receptors have been found to be upregulated in MDSCs due to signal transducer and activator of transcription (STAT) 3 and STAT5 signalling, which is mediated via tumour associated growth factors such as GM-CSF, and encourages lipid accumulation [128]. Similarly, the environment of granulomas found in TB are lipid rich, and abundant with foamy macrophages, which add to this richness. These macrophages are originally derived from normal macrophages that have experienced a metabolic shift and an imbalance in low density lipoprotein (LDL) influx and efflux [129]. The imbalance is caused by an increase in the internalisation of LDL components such as triacylglycerides, phospholipids, and cholesterol, by macrophages [129, 130], which upon accumulation, induce the differentiation of normal macrophages into foamy macrophages [129]. Studies have demonstrated that *Mtb* is able to dysregulate host lipid metabolism and synthesis in order to survive [130-132]; the presence of large amounts of foamy macrophages in TB granulomas, is suggestive of *Mtb* using these cells as nutritional stores that allow the bacteria to survive within the granuloma and for the disease to persist [133]. Metabolic and imaging analyses have shown that upon being phagocytosed by foamy macrophages, *Mtb* undergoes phenotypic and metabolic changes that result in the increase of both the uptake and use of fatty acids such as cholesterol that has been derived exogenously [133-135].

Furthermore, mouse models of TB have demonstrated the ability of macrophages to result in the expansion of MDSCs. Lipid bodies associated with macrophages result in an increase in COX-2 and PGE_2, these molecules induce the expansion of MDSCs [136-138], and contribute towards the suppression of factors that are important for the control of *Mtb* infection such as the Th1 response, and generation of TNF [139]. The accumulation of MSDCs has also been shown in a mouse model infected with BCG [124], and in TB patients where MSDCs were found in abundance in pleural effusion fluid, as well as in peripheral blood [112]. Additionally, Du Plessis et al. demonstrated that in these patients, mycobacteria killing capacity was decreased and T cell proliferation was inhibited; this provided the first evidence for a functional role of MDSCs in TB disease [112]. Moreover, MDSCs were found to simultaneously suppress Th1 responses [110], and internalise *Mtb*, where the bacteria

is able to survive within the cells and use its lipid rich stores as a source of carbon for energy [128, 133, 140]. Furthermore, following internalisation of *Mtb*, MDSCs were found to promote haematopoiesis, and resulted in the production and recruitment of MDSCs to the lung [141].

Whilst compelling evidence has emerged regarding the role of MDSCs during TB in studies carried out in humans, and mouse models. The extent to which these cells inhibit the immune response, and the complete mechanisms by which they achieve their effects are yet to be elucidated.

Granulomas

Perhaps the most destructive way by which *Mtb* is thought to evade the immune response is by being able to survive within granulomas. These structures are a hallmark of *Mtb* infection and are a host protective mechanism by which the *Mtb* is physically contained, they are achieved by the collective effort of cells from the innate and adaptive immune systems, forming an organised multicellular structure. At the centre are infected macrophages, foamy macrophages, giant cells and epithelioid cells which are essential for its formation [18, 142]. The granulomas may calcify and encapsulate the *Mtb* [143]; whilst this contains the infection, it does not eradicate it, the *Mtb* is simply dormant and able to survive [144, 145]. As well as granulomas being a protective structure for the host, it also provides *Mtb* with a microenvironment in which it can survive until the opportunity arises for it to become reactivated [58]. The environment within the granuloma is sub optimal, with cholesterol being the only source of carbon, nutrients being inaccessible and the depletion of oxygen levels resulting in hypoxia [146]. Belton et al. were the first to carry out a detailed study of the hypoxic status of TB granulomas in humans, as well as their deleterious effect on tissue destruction. They demonstrated that lung granulomas are severely hypoxic, and this condition resulted in the upregulation of matrix metalloproteinase-1 (MMP-1) [147]. MMP-1 is a collagenase that degrades tissues and drives the immunopathology observed in pulmonary TB [148, 149]. Airway epithelial cells adjacent to granulomas were found to express high levels of MMP-1 [31] which results in the destruction of the tissue surrounding granulomas. MMP-1 activity is regulated by tissue inhibitors of metalloproteinases activity (TIMPs), which negatively regulate MMP-1 [147]. During *Mtb* infection, the secretion of TIMP by pulmonary epithelial cells was found to be suppressed [31], further promoting the destruction of tissues.

Adaptive immune response

Following the innate immune response, if a pathogen is able to persist, the adaptive immune response sets in. Whilst the adaptive immune response takes a lengthier time to become active, it is longer lasting and more specific than the innate response. Its importance in TB is highlighted by studies carried out in HIV patients. The reduction of $CD4^+$ cells in HIV patients co-infected with TB has been correlated with increased dissemination of *Mtb*, as well as a higher bacterial load [150].

APCs such as DCs or macrophages phagocytose pathogens at the site of infection, they then migrate to the lymph nodes via chemotaxis; once there, they present antigens bound to their MHC class I and II proteins to immature T cells. Binding of MHC class I via $CD8^+$ T cells results in the maturation and proliferation of cytotoxic T cells, whilst the binding of MHC class II via $CD4^+$ T cells results in the activation and proliferation of helper T cells. Activated $CD4^+$ T cells release inflammatory cytokines such as IFN-γ and TNF-α, this results in the activation of macrophages [151], and enhances their killing capacity by stimulating the release of ROS [152]. Activated $CD8^+$ cytotoxic T cells destroy infected cells and can destroy pathogens directly by recognising the same antigen they were initially activated by [153].

T cells that are activated by antigens bound to MHC class I and II are known as 'conventional' T cells. MHC class I and II are highly polymorphic and bind an array of pathogen-derived peptide antigens which they present to T cells expressing a diverse repertoire of αβ T cell receptors (TCRs). The diversity of these TCRs is essential in enabling the recognition of a range of peptide antigens [30].

In comparison, 'unconventional' T cells are non-MHC restricted, some but not all express TCRs of limited diversity, and recognise non-peptide antigens. CD1-restricted, MR1 and γδ T cells recognise antigens such as lipids, vitamin B metabolites, and phosphoantigens, respectively. As such, these unconventional T cells have all been demonstrated to play a role in the response to *Mtb* infection to varying degrees by responding to bacterial derived antigens [154]. The overall adaptive immune response and roles of the conventional and unconventional T cells to *Mtb* are discussed here.

Conventional T cells

CD4⁺ T cells

$CD4^+$ T cells undergo developmental processes that ensure they recognise a wide range of antigens. Activation of naïve $CD4^+$ T cells by antigens presented on APCs results in their differentiation into different effector T cells in order to clear infections [155]. Cytokines produced by effector $CD4^+$ T cells result in the activation of various immune cells such as, macrophages that recruit other immune cells, cytotoxic CD8 T cells that target infected cells, and B cells that produce antibodies [156-158].

There are five main subsets of $CD4^+$ T helper (Th) cells which are classed based on their signature cytokine profiles and their expression of specific transcription factors, these are Th1, Th2, Th17, T regulatory (Treg), and follicular T helper (Tfh) cells. Th1 cells produce IFN-γ and express T-bet; Th2 cells produce IL-4, IL-5, and IL-13, and express GATA3; Th17 cells produce IL-17 and IL-22, and express RORγt; Treg cells produce IL-10, and TGF-β, and express Foxp3; and Tfh cells produce IL-21, and express Bcl6 [159]. The different $CD4^+$ T cell subsets respond to different pathogens and generate an array of responses. Type 1 immune responses that activate M1 macrophages and protect against intracellular pathogens such as viruses and bacteria are mediated by Th1 cells [157]; type 2 responses are mediated by Th2 cells in response to large parasites such as helminths, and recruit other lymphocytes such as mast cells and eosinophils, and activate M2 macrophages [160]. Meanwhile, type 3 responses are mediated by Th17 cells at mucosal surfaces such as in lungs and intestines, in response to extracellular pathogens such as fungi and bacteria. They induce the production of AMPs by epithelial cells, and recruit neutrophils [161]. Tregs have been shown to play a role in immune homeostasis and prevent the development of autoimmune diseases [162, 163]. Lastly, Tfh cells have been found to play an important role in the generation of antibodies by B cells, they promote germinal centre formation, and affinity maturation [164].

Th1 cells

Cytokines signals are the main determinants for T cell lineage differentiation. Cytokines released upon antigen recognition bind and activate their receptors on T cells, which activate STAT factors. Upon translocation into the nucleus, STAT molecules bind master regulator genes, these encode for lineage specific transcription factors, and other effector cytokines, thus determining the lineage of the differentiated T helper cell [165].

$CD4^+$ T cells activated by peptides presented on MHC class II molecules, as well as IL-12 produced by macrophages, results in the production of copious amounts of IFN-γ, which is the signature cytokine produced by Th1 cells. The production of IFN-γ is essential for promoting the differentiation and proliferation of Th1 cells; it induces STAT1, which synergises with STAT4 to activate T-bet, and can directly activate Th1 related genes [166, 167]. IFN-γ produced by Th1 cells activates macrophages, B cells, and CD8 T cells during infections [158]. During TB infection, the maturation of phagosomes is facilitated by this IFN-γ and is an essential step in the destruction of the *Mtb* confined within the phagosome [9].

Additionally, the IL-12 produced by macrophages binds to the IL-12 receptor on the surface of T cells. This induces STAT4, which also induces T-bet. Th1 specific genes are bound by T-bet, which promotes their expression [168]. Additionally, the presence of both molecules simultaneously is essential in producing optimal levels of IFN-γ, as T-bet on its own is unable to do so. Furthermore, deficiencies in T-bet and STAT4 completely diminishes IFN-γ production [157, 168, 169]. As well as promoting the expression of Th1 genes, T-bet also inhibits the expression of Th2 and Th17 specific genes, thus inhibits the differentiation of $CD4^+$ T cells into Th2 and Th17 subsets [170]. Additionally, as well as being generated from naive $CD4^+$ T cells, the plasticity of $CD4^+$ T cells allows for Th1 cells to also be generated from other CD4 subsets such as Treg, Th17, and Tfh cells [157, 171-173].

Evidence for the importance of the $CD4^+$ T cell response, particularly for Th1 cells in TB, is highlighted by *in vivo* studies using various animal models. TB infection of murine models that are either knockouts for MHC class II or have depleted levels of $CD4^+$ T cells, leads to high levels of fatality due to the inability of the immune system to fight off the infection [174, 175]. Additionally, mice deficient in $CD4^+$ T cells [173, 176-178], T-bet [179], or IFN-γ [180, 181], were found to be more susceptible to TB infection.

Additionally, antibody mediated depletion of $CD4^+$ T cells in cynomolgus macaques resulted in a reduced ability to control the disease, as well as reactivation with latent infection [182]. Whilst *Mtb* may not directly impact $CD4^+$ T cells, infection results in the impairment of antigen presentation by MHC class II in macrophages, thus affecting CD4 mediated responses [183]. An efficient immune response to infection is heavily based on the ability of macrophages to activate and recruit antigen specific $CD4^+$ T cells to the site of infection, where they secrete IFN-γ to further activate macrophages which are able to recruit more lymphocytes to the site of infection [183]. Furthermore, studies of animal models as well as humans have demonstrated the importance of $CD4^+$ T cell derived IFN-γ in resisting *Mtb* infection. Mouse models with aberrant CD4 T cells are extremely vulnerable to TB [176]. Furthermore, a study using an adoptive transfer mouse model where all cells except $CD4^+$ T cells were able to produce IFN-γ highlighted that unless the IFN-γ was particularly derived from $CD4^+$

T cells, the mice were unable to control bacterial growth, and succumb to infection [184]. Moreover, individuals who develop autoantibodies that neutralise IFN-γ [185], as well as those with congenital defects in the IL-12/IFN-γ axis have extreme susceptibility to TB [186].

Th2 cells

Naïve $CD4^+$ T cells differentiate into Th2 cells after being activated by DCs [160]. In activated $CD4^+$ T cells, IL-4 activates the Th2 master transcription factor GATA3 via STAT6, this ensures their differentiation and function [157, 187]. Differentiation into a Th2 lineage is achieved by GATA3 by also suppressing the expression of other lineage transcription factors such as RORγt, and T-bet [188-190]. During infection, Th2 cells take part in type 2 responses and produce IL-4, IL-5, and IL-13. IL-4 promotes antibody class switching to IgE in B cells; IL-5 recruits other immune cells such as eosinophils to the site of infections, and IL-13 promotes mucus production by goblet cells [160].

Th17 cells

In response to extracellular pathogens such as bacteria and fungi, APCs produce pro-inflammatory cytokines such as IL-6, IL-1β, and IL-23 which result in the differentiation of naïve CD4 T cells into Th17 cells [158]. The expression of the Th17 master transcription factor RORγt is induced by STAT3, which is activated by IL-6 and IL-23 [191, 192]. Th17 cells play an important role in response to fungi and extracellular bacteria, however, they've also been shown to play a pathogenic role in autoimmune diseases such as multiple sclerosis [193]. Upon differentiation, Th17 cells produce several cytokines such as IL-17A, IL-17F, and IL-22. These cytokines result in the activation of immune cells and lead to the production of MMPs, AMPs, and nitric oxide; thus facilitating in the clearance of pathogens [158, 194-196].

Treg cells

The discovery of a subset of immune cells that maintain immune homeostasis was made in 1995, Sakaguchi et al. identified a subset of $CD4^+$ T cells that highly expressed CD25 (a high affinity IL-2 receptor), and displayed an immune regulatory function [197]. The discovery of the well-established Treg master transcription factor, Foxp3, came in 2003, by three separate groups [198-200]. Tregs develop in the thymus [199] and make up 2-3% of peripheral blood [201]. They can also differentiate

from mature $CD4^+$ T cells outside the thymus due to chronic antigen stimulation, or due to stimulation by cytokines such as TGF-β [202] or IL-10 [203]. The expression of Foxp3 is induced upon activation of STAT5 and SMAD2/3, which are promoted by IL-2 and TGF-β, respectively [204-206].

Several ways have been identified by which Tregs exert their regulatory functions. They secrete cytokines such as TGF-β, IL-10 and IL-35, that are able to counteract the effects of Th1 and Th2 cells [207], and consume IL-2 which further hinders the proliferation of $CD4^+$ T cells [208, 209]; they can also directly kill APCs as they express granzyme B and perforins [210]. Furthermore, they can induce trogocytosis, which is a process by which cells "nibble" each other, thereby are able to remove specific antigen-MHC complexes from APCs [211].

Lastly, Tregs express immune checkpoint extracellular receptors that are inhibitory such as CTLA-4 [162, 212]. Treg cells have also been identified in mouse models during TB infection and were first observed in a C57BL/6 line [213]. Whilst mouse models do not recapitulate many aspects of the human disease, they do have some similarities, and have been extensively used in TB research to further shed light on important immunological processes. Models using aerosolised low-dose exposure of *Mtb* in mice are similar to how infection occurs in humans, this model demonstrated that Th1 $CD4^+$ T cells that arrive in the lung following infection produce IFN-γ [9], however, unless the resident immune cells are able to clear the bacilli, by the time Th1 cells arrive at the site of infection, the bacteria is able to form a stronghold and infect the lungs [214]. Additionally, similar to in humans, following *Mtb* exposure in mice, the number of Tregs increases at the site of infection, this can disturb the balance required between Th1/Th2/Treg cells to control the infection [215-217].

Tfh cells

The differentiation of Tfh cells from naïve CD4 T cells is mediated by IL-6 and IL-21, which activate STAT3, this results in the expression of the transcription factor Bcl6 [218-220]. Tfh cells are mostly found in germinal centres (GCs), where their main role is to support antibody production, and affinity maturation in B cell follicles in the spleen and lymph nodes [221]. Additionally, Tfh cells express CD40L, which mediates the formation of high affinity plasma cells [222], and produce IL-21 which controls the maintenance and affinity maturation of GC responses [221, 223, 224].

Summary

The main $CD4^+$ T cell subsets that have been found to respond to *Mtb* infection are Th1 and Th17. Whilst Tregs and Th2 have also been identified at sites of infection [225], they have been found to suppress the effector functions of Th1 and Th17 cells, as well as the cytotoxic effect of CD8 T cells [226].

During TB infection, Th1 and Th17 cells promote protective inflammatory and antimicrobial functions to kill *Mtb,* and encourage granuloma formation to physically contain the bacteria [227, 228]. Meanwhile, Th2 and Treg cells have been shown to counteract the protective effects of the immune response found during TB infection, and can lead to its exacerbation [229, 230]. This was also demonstrated in several studies carried out in patients with active pulmonary TB, where Treg levels were increased at the site of infection, and it was suggested that *Mtb* induces immunosuppressive effects via Tregs in order to persist [231, 232]. Additionally, Treg cells isolated from blood samples of patients with active TB were shown to dampen the proliferative response of $CD4^+$ T cells and their IFN-γ production [233]. Additionally, they were also shown to negatively impact the ability of monocyte derived macrophages, and alveolar macrophages to inhibit the intracellular growth of TB in the presence of $CD4^+$ effector cells [234]. Furthermore, PBMCs depleted of Treg cells from patients with active TB recovered their antigen-specific IFN-γ responses [235]. Collectively, these studies reinforce the notion that Tregs play a role in hindering antimycobacterial immunity in TB, and this has not only been documented with $CD4^+$ T cells, they were also able to suppress the functional effects of non-$CD4^+$ T cells such as Vδ2 T cells, by suppressing their production of IFN-γ and granulysin [236, 237].

Th2 cells have been shown to impair the degradation of intracellular bacteria by inhibiting Th1-induced autophagy [238]. Additionally, they impact the control of *Mtb* infection. Cytokines produced by Th2 cells such as IL-4 and IL-13 have been shown to suppress the production of IFN-γ by Th1 cells, and therefore suppresses the activation of M1 macrophages, which is mediated by IFN-γ [229, 239]. Furthermore, IL-4 has been shown to induce and expand mature Treg cells [240]. Although IL-10 and IL-4 promote Th2 differentiation and inhibit Th1 T cells, resulting in predominantly only one of these subsets being present at a time; Th1 and Th2 cells demonstrate some plasticity, whereby they are able to co-express Th1 and Th2 transcription factors and cytokines [241].

The significance of the Th1 response during TB infection has been highlighted in humans. Mutations in cytokine receptor subunits such as the IFN-γ receptor ligand binding chain, and the β1 chain in the IL-12 receptor, results in increased susceptibility to different types of mycobacteria, BCG, and *Mtb*

[242-244]. This has also been demonstrated in mouse models whereby mice with deficiencies in $CD4^+$ T cells and Th1 cytokines are unable to manage *Mtb* infection and succumb to it [174, 181, 245].

In a mouse model of latent TB, although the IFN-γ response remained unchanged despite depleting $CD4^+$ T cells, it was insufficient to control the infection [246]. Other studies have also reported a correlation between antigen specific $CD4^+$ T cell-derived IFN-γ and a decrease in *Mtb* bacterial load [247]. It has been suggested that this protection is due to IFN-γ limiting the function of Th17 cells, which drive the infection by mediating tissue damage, and inducing pathogenic neutrophilic inflammation, as opposed to inhibiting *Mtb* replication by increasing antibacterial activity [248].

When comparing the different subsets of $CD4^+$ helper T cells in the context of TB infection, Gallegos et al. derived ESAT-6 specific Th1, Th2, and Th17 cells from mice that were either wild type or had impairments in factors associated with Th1 responses such as TNF-α or IFN-γ, in order to investigate their role during TB infection in an adoptive transfer model. They found that Th2 cells did not result in any protection against *Mtb* replication, and whilst Th17 cells provided some protection, Th1 cells did so to a greater extent, however their activity was not dependent on IFN-γ [249].

Various studies have demonstrated that PD-1 deficiency in mice leads to mortality during TB infection. Although these mice have a wild type like CD4 and IFN-γ response during infection, they succumb to the disease due to increased lung pathology, higher bacterial load, and increased proinflammatory cytokines expression. Interestingly, depletion of $CD4^+$ T cells in PD-1 -/- mice resulted in the consequent depletion of IFN-γ and other cytokines, and greater survival. [250, 251].

Overall, despite the importance of Th1 responses, in particular IFN-γ, and its role in mediating protective mechanisms during TB infection, on its own, it is not sufficient to control *Mtb* infection. Mice deficient in IL-6, TNF-α, or GM-CSF were unable to combat TB with only IFN-γ [252]. Some studies have even demonstrated that Th1 mediated IFN-γ responses were anti-inflammatory and resulted in TB immunopathology [170, 248, 253]. Additionally, Th1 cells have also been found to secrete IL-10. Bronchoalveolar lavage from patients with active TB have detectable levels of $CD4^+$ T cells that secrete both IFN-γ and IL-10 [254], and IL-10 is increased in the serum and lungs of patients with active TB [255-257]. The secretion of IL-10 by effector T cells has been shown to be due to high antigen load [258], and is thought to be a way by which pro-inflammatory T cells can regulate their own activity in situations where there is chronic infection. IL-10 derived from $CD4^+$ T cells has been found to impair the control of infection [259]. Furthermore, mice with an IL-10 deficiency have a decreased susceptibility to *Mtb* infection and have a better proinflammatory response [260].

There is no doubt that $CD4^+$ T cells play an important role in combating TB infection, and their production of vital cytokines such as IFN-γ and TNF-α lead to downstream events that allow the host to control the infection [261, 262]. However, vaccines which aim to solely drive the Th1 response, and upregulate the release of IFN-γ have not proven to be effective [263].

The existence of polyfunctional $CD4^+$ T cells that are able to produce multiple cytokines, and displayed a protective phenotype, were first identified in patients with Leishmania [264], and HIV [265, 266]. Studies carried out in mouse models have demonstrated that T cells that produce IFN-γ/TNF-α/IL-2, or IFN-γ/IL-2, were able to fight off/better protected against TB infection [267-270]. Additionally, an NHP model demonstrated that following BCG being administered intravenously, polyfunctional $CD4^+$ T cells that produce both IFN-γ and TNF-α were stimulated, and were associated with less severe pathology [271]. It is clear that a fine balance of immune responses is required to effectively tackle the infection, with multiple cytokines and T cell responses being involved.

$CD8^+$ T cells

$CD8^+$ T cells are activated upon the binding of T cells expressing CD8 to a peptide-MHC class I complex. *Mtb* derived peptides such as 19-kDa protein (a membrane bond lipoprotein), as well as from ESAT 6 have been identified as ligands for $CD8^+$ T cells when presented on MHC class I molecules [272, 273]. Upon activation, these cells can directly lyse infected cells as well as intracellular bacteria. $CD8^+$ T cells release granulysin which is an antimicrobial peptide that directly kills intracellular *Mtb* [274], and perforins that lyse infected macrophages [275, 276].

In a mouse model lacking transporter associated antigen processing 1 (TAP-1) proteins, *Mtb* infection results in rapid onset and inability to manage the infection in comparison to wild type controls. This is due to TAP-1 being involved in the loading of peptides on MHC class I molecules; disruptions in this process result in lack of CD8 mediated responses and the consequent inability to manage infection [277].

Whilst the ability of conventional $CD8^+$ T cells to become activated via the peptide-MHC class I complex is extremely important in recognising and fighting off invading pathogens, the HLA-A, -B, and -C genes which encode MHC class I result in highly polymorphic proteins [263]. This polymorphism makes identifying specific TCRs or antigen presenting molecules that are involved in successfully overcoming infections, and applicable to a large enough population impossible. Hence, developing immunotherapies by taking advantage of these interactions is not feasible.

However, there are other subsets of T cells shown to recognise *Mtb* antigens known as unconventional T cells. These cells have been shown to bind molecules that are non-polymorphic and thereby not restricted to a specific donor. The molecules include MR1, CD1, and a specific MHC class I molecule encoded by the HLA-E gene [49, 278-281].

Unconventional T cells involved in the immune response to TB

There are several types of unconventional T cells that are involved in the immune response to TB. They are present in the peripheral circulation and possess invariant or semi-invariant TCRs that recognise conserved antigens such as bacterial lipids or metabolites. They are also identified as innate-like due to their immediate and rapid response to infection upon recognition of antigens and secrete pro-inflammatory cytokines to escalate the immune response [27]. These cells form a bridge between the innate and adaptive immune responses. The various populations of unconventional T cells are discussed here.

Mucosal-associated invariant T (MAIT) cells

MAIT cells are highly abundant in mucosal tissues such as the lungs and the intestinal tract, and are thought to be involved in local immune surveillance of these tissues. They are restricted by the MHC related protein 1 (MR1) [282]. MR1 is an antigen presenting molecule that presents riboflavin and folate related metabolite antigens derived from pathogenic bacteria to MAIT cells [283]. They are either $CD8^+$ or $CD4^-CD8^-$(DN), and have also been shown to exert cytotoxic functions in response to bacterial antigens. They can also secrete high levels of IL-17 [284] to recruit neutrophils to the site of infection and further drive an immune response. Combined with their non-polymorphic nature, this potentially makes them an appealing target for vaccines [285].

In the context of *Mtb* infection, studies have demonstrated that MAIT cells respond to *Mtb* infected lung epithelial cells and produce IFN-γ, granzymes, and TNF-α [49, 286]. In TB patients, the numbers of MAIT cells circulating in peripheral blood was found to be lower than that of healthy controls, and were not found to accumulate in the lungs of patients with active TB [286, 287]. They were also found to be functionally deficient and did not produce IFN-γ irrespective of their mode of stimulation [287]. Moreover, in a rhesus macaque model of TB, recruitment of MAIT cells to granulomas was

modest [288]. Overall, it remains unclear whether deficient MAIT cell responses correlate with susceptibility to *Mtb* infection and whether they make good therapeutic targets in the case of TB.

Natural Killer T (NKT) cells

NKT cells respond to a range of lipids presented by CD1d molecules. However, there are two subtypes of NKT cells, type I, these are known as invariant NKTs (iNKTs) due to their invariant TCRs, and type II NKTs which have a more diverse TCR repertoire [281]. iNKTs have been shown to recognise *Mtb* infected cells [289] and produce proinflammatory cytokines upon activation [281]. However, several studies have demonstrated that during active TB, the frequency of iNKTs in the circulation is reduced [290-292]. While there is indirect evidence that these cells may help control the infection, an exact role for them is yet to be defined. Furthermore, the role of diverse NKTs is yet to be established but is thought to be involved in immune regulation of infectious diseases and tumours [281].

Gamma delta (γδ) T cells

γδ T cells are $CD4^-$ $CD8^-$ and have the ability to recognise ligands in a TCR-dependent as well as independent manner. They express PRRs on their cell surface so can be stimulated by bacterial derived PAMPs [27]. Upon activation, they produce protective inflammatory cytokines such as TNF-α, IFN-γ, and IL-17. The production of IL-17 by γδ T cells has been shown to support the formation of granulomas as a means of suppressing the infection [293]. Moreover, a study using a cohort from the same household with an active TB case demonstrated that γδ and MAIT cells played a role in the host resistance to initial infection [294]. However, similarly to MAITs and iNKTs, the levels of γδ T cells are lower in patients with active TB [27].

CD1-restricted T cells

CD1 protein

CD1 proteins bind and present hydrophobic molecules such as lipids, to T cells. The five members of the CD1 family are encoded by 5 non-polymorphic genes and divided into 3 groups. These are Group 1 (CD1a, CD1b, and CD1c), Group 2 (CD1d) and Group 3 (CD1e). The proteins are composed of a heavy CD1 chain associated with β2m and are structurally similar to MHC class I molecules. The heavy chain consists of 3 domains (α1, α2, and α3). The α1 and α2 helices make up the antigen binding portion of the molecule while the α3 helix associates with the β_2m and has a transmembrane domain which continues into an intracytoplasmic tail [16, 295].

The classification of CD1 family members into three groups is contingent on their structural differences, cellular function, sequence homology and tissue distribution [296]. All group 1 family members are expressed on professional APCs such as DCs. However, they are also expressed independently on different cells. For example, CD1a is expressed on Langerhans cells in the skin and is a unique marker for a specific cell population; whereas CD1b is expressed on DCs, and CD1c is expressed on a population of B cells and DCs. CD1d is expressed on myeloid, lymphoid and non-haematopoietic cells such as vascular smooth muscle cells. CD1e is the only member of the CD1 family that is not expressed on the cell surface; it is expressed intracellularly in the Golgi complex and late endosomes/lysosomes where it facilitates lipid antigen loading of other CD1 molecules, such as the loading of mycobacterial lipids on CD1b and CD1c [295].

CD1 proteins as a whole bind diverse lipid structures, this is due to the binding domains of each member of the family being of different size and shape (Figure 2) [16]. Each protein has structural differences specific to it that makes it suited to present certain lipids that other members cannot present. Each member of the CD1 family has an A' and an F' pocket which interact with and bind the ligand. CD1a has the smallest groove of all the CD1 proteins; despite being restrictive, the short A' pocket binds alkyl chains; whereas the F' pocket is more permissive and allows larger lipid moieties to bind [16, 297, 298], as well as peptide fragments such as a lipopeptide analogue of the *Mtb* derived didehydroxymycobactin [299]. CD1b has the largest antigen binding domain in comparison to other CD1 molecules due to its additional C' pocket and T' tunnel. Collectively, the A', T' and F' pockets form a super channel, thus allowing it to bind and present long mycobacteria derived

mycolic acids [300]. The T' tunnel also allows lipid alkyl chains to stick out through the bottom of the pocket [300, 301].

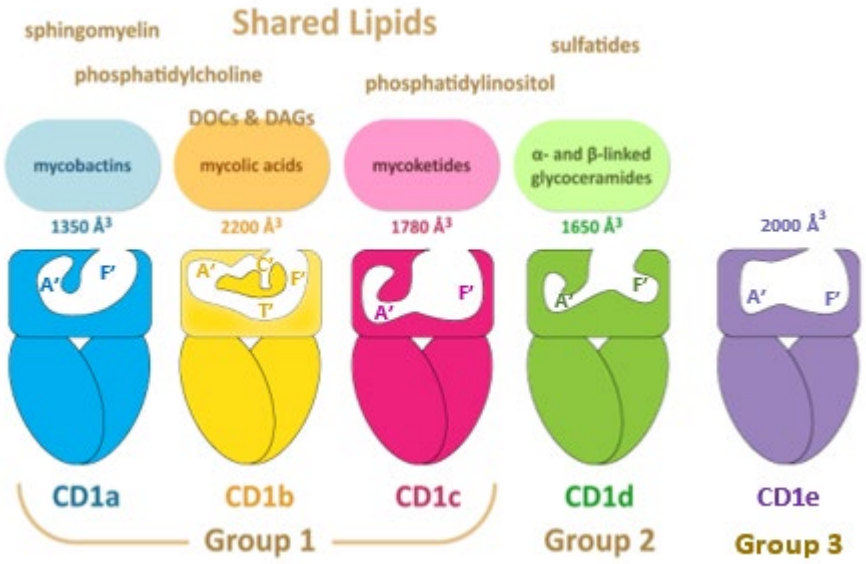

Figure 2: Structures of binding domains of CD1 proteins. Illustration of members of the CD1 family of proteins. The proteins vary in the shapes and sizes of their binding domains, hence are able to bind a diverse repertoire of self and non-self lipid antigens (Adapted from Kaczmarek et al., 2017 [1]).

The A' and F' pockets of CD1c are surrounded by hydrophobic amino acids which makes them an ideal place for apolar alkyl chains of lipids to bind. Uniquely, the central pocket of the CD1c molecule allows the protrusion of the hydrophilic moiety of bound antigens whilst the A' pocket houses the alkyl chain of the antigen [302]. The A' and F' pockets of CD1c can present various lipid antigens, typically these were flexible and linear alkyl chains. Mansour et al. demonstrated that CD1c can also bind more rigid structures such as cholesteryl-esters [303], this finding was significant as it brought to light more information regarding the TCR binding surface of CD1c; it was found that the F' pocket is more "open" than that of other members and depending on the ligand bound, has been shown to adopt 'open' and 'closed' conformations [303]. The A' and F' pockets of CD1d can bind a variety of lipids such as diacylglycerol and phospholipids; but its most well-known ligand is α-galactosylceramide (α-GalCer), which is a potent agonist of iNKT cells [304]. Its fatty-acyl chain occupies the A' pocket while its sphingosine chain occupies its F' pocket [305, 306].

The interaction of the CD1-restricted TCRs and the antigens/antigen presenting molecule was thought to be similar to that of MHC class I and its bound peptide, whereby the TCR interacts with the antigen as well as the antigen presenting molecule in order to become activated. However, CD1-

restricted TCRs have been found to interact with CD1 proteins in different ways (Figure 3). The structure of CD1a-lipid bound to an autoreactive TCR determined that the TCR binds the CD1a protein itself without interacting with the bound ligand, and that protruding ligands with larger head groups may actually interfere with this interaction [307]. This method of CD1-TCR interaction became known as "absence of interference" where the TCR makes contact with the closed portion of the A' roof with minimal or no contact with the bound ligand [308]. Furthermore, a recent study identified the same method of CD1-TCR interaction in the case of CD1c [309]. The 3C8 TCR is one of the first CD1c-autoreactive TCRs to be identified; in this study it was found to specifically bind CD1c proteins loaded with sequestered lipids that were fully seated within the protein, this meant that the TCR interacted specifically with the CD1c protein itself rather than the lipid bound. Additionally, lipids with larger head groups that protruded from the protein abrogated this binding [309]. It is also worth noting that the closed roof conformation adopted by the CD1c proteins bound to sequestered lipids is akin to the CD1c-SL proteins made by our group [303]; which corroborates that CD1c-SL is a good surrogate protein complex for binding and identifying autoreactive T cells. Mansour et al. did indeed isolate a CD1c autoreactive TCR which was shown to recognise the CD1c protein itself as opposed to its cargo, since the lipids were enclosed within the protein [303]. They first generated CD1c proteins using a bacterial expression system (*E. coli*), in the absence of additional lipids and demonstrated that CD1c refolded with spacer lipids (CD1c-SL). These lipids were identified via electron density experiments as three hydrocarbon chain spacer lipids which filled the A' and F' channels of the protein and are integrated either from the expression system or during refolding [303].

The other method of interaction between CD1 proteins and TCRs is via the co-recognition of the CD1 molecule and the protruding head group of the bound ligand such as phosphate or hydrophilic head groups that stick out of the F' pocket [301, 310]. Co-recognition applies to CD1a bound to didehydroxymycobactin [298], however, a TCR has been found to interact sideways with CD1a and a part of its β2m molecule, independent of the bound sulfatide ligand [311]. CD1d bound to sulfatides, phospholipids, and sphingomyelin have also been shown to be co-recognised by TCRs [312, 313].

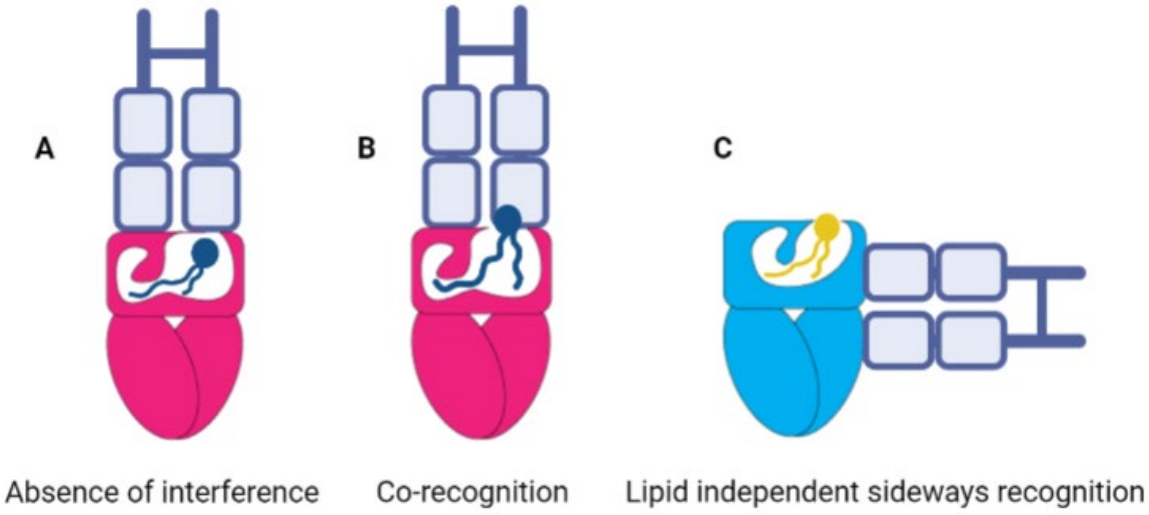

Figure 3: CD1-restricted TCRs interact with lipid loaded CD1 proteins in various ways. Depending on the CD1 protein and the lipid antigen bound, recognition of the CD1-antigen complex may occur differently. The TCR recognises the CD1 protein when an antigen is bound, and interacts with the CD1 protein only whilst the lipid antigen is fully seated within the protein (**A**), or the TCR recognises and interacts with the lipid antigen as well as the CD1 protein (**B**), or the TCR binds and interacts with the CD1 protein sideways, independent of the antigen (**C**).

CD1 mediated responses in TB

Mycobacterial glycolipids, lipopeptides, and lipids form stable complexes with different members of the CD1 family; these complexes interact with and activate T cells bearing specific TCRs that are CD1 restricted. A number of *Mtb* derived lipid antigens presented by group 1 members of the CD1 family have been identified [314]. CD1 molecules were found to be upregulated in response to *Mtb* infection in *in vivo* as well as *in vitro* studies [315, 316]; and in the bronchoalveolar lavage fluid of TB patients [317].

CD1a has been shown to present the lipopeptide dideoxymycobactin (DDM) to T cells and results in their activation [318]. Mycobactin promotes *Mtb* cell growth; during its synthesis, DDM is produced in trace amounts [319]. Therefore, the identification of cells presenting DDM by CD1a-restricted T cells could be useful for detecting *Mtb* infected cells. Moreover, the discovery that CD1a presented lipopeptides was suggestive of it being similar to MHC-peptide complexes. However, the crystal structure of CD1a-DDM revealed that the highly hydrophobic peptide segment was bent into the antigen binding groove, as opposed to the linear conformation adopted by MHC class I peptides [298].

To date, CD1b has been found to present the most mycobacterial cell wall derived lipid antigens including mycolic acids (MA) [320], glucose monomycolate (GMM) [321], and sulphoglycolipids [322], which activate CD1b-restricted T cells. CD1b-MA reactive T cells were identified in the lungs and blood of TB patients, were found to display markers of memory and effector T cells, and continued to be detected for months following successful treatment [323]. On the other hand, CD1b-lipoglycan reactive T cells isolated from bronchoalveolar lavage of TB patients were found to have cytotoxic properties and were able to inhibit intracellular *Mtb* growth [324].

However, whilst CD1b binds the most diverse lipid antigen repertoire, its function is impaired by the inhibition of phagolysosomal acidification caused by *Mtb* [56], as some lipids such as long chain mycolyl lipids require low pH to bind CD1b [325, 326]. Nevertheless, CD1b plays an important role in presenting mycobacterial lipid antigens; for example, it is the only CD1 protein capable of presenting certain mycolic acid related lipids that have particularly long fatty acid chains [16].

The initial evidence for the role of CD1c in the presentation of *Mtb* derived antigens came almost 25 years ago. The study demonstrated that $CD1^+$ monocytes presenting an *Mtb* sonicate were able to stimulate the proliferation of T cells, whilst $CD1^+$ monocytes presenting sonicates of *E. Coli*, and *E. Toxoid* antigens were not able to stimulate T cells to the same extent. Moreover, the proliferative response was lost when CD1c was blocked, but maintained when other members of the CD1 family were blocked, as well as MHC class I and class II proteins [327]. Furthermore, the proliferative T cells were negative for both CD4, and CD8, further emphasising the CD1-mediated nature of their activation [327]. However, in another study, CD1-restricted T cells responding in a similar manner to *Mtb* sonicate were found to be $CD8^+$, however, blocking MHC class I and II proteins did not attenuate their proliferative responses [328].

In signifying a role for CD1c-restricted T cells during TB infection *in vivo* for the first time; Moody et al. demonstrated that blood lymphocytes from TB patients had a significantly higher proliferative response to *Mtb* derived isoprenoid glycolipids presented by CD1c, whilst those from healthy controls did not [329]. They also showed that blocking CD1c in particular resulted in substantial inhibition of the proliferative response. Additionally, they identified $CD8^+$ T cells that were CD1c-restricted, and responded to CD1c presenting synthetic mannosyl phosphodolichols (MPD) which are structurally related to mycobacterial mannosyl-β1-phosphomycoketide (MPM) [329].

The most widely studied CD1 restricted T cells by far are iNKT cells which are CD1d responsive. These cells were originally identified due to their high affinity to CD1d bound to the glycosphingolipid α-

GalCer, which was originally extracted from the marine sponge *Agelas mauritianus* [330]. However, CD1d also binds *Mtb* derived phosphatidylinositol (PI) [331] and results in the activation of iNKT cells. It has been well established that patients with active TB have depleted numbers of iNKT cells in their blood [332, 333]. iNKT cells demonstrated the ability to inhibit the intracellular growth of *Mtb* via the production of GM-CSF [334]; and their abundance had a direct correlation with a resistance phenotype to *Mtb* challenge in a macaque model and was found to be protective [335]. *In vivo*, iNKTs also result in the maturation of DCs and facilitates their presentation of soluble antigens which increases the priming of $CD8^+$ T cell responses [336]. In the context of TB, this leads to the expansion of antigen specific $CD8^+$ T cells that play a role in protective immunity [276].

Similarly to MAIT cells, numbers and function of circulating iNKT cells in patients with active TB is decreased [290]. However, a study demonstrated that patients with latent TB infection have increased levels of iNKT cells [27]. *In vitro* studies have demonstrated that upon recognition of *Mtb* infected cells, iNKT cells produced IFN-γ and granulysin, thus restricting bacterial replication [289, 337]. The manipulation of NKT responses using synthetic glycolipids is a viable approach for immunotherapy-based therapeutics in diseases such as cancer as well as TB [338].

CD1 autoreactive T cells

Over the past decade, a handful of studies have been published exploring the role of autoreactive T cells in various diseases. CD1-restricted autoreactive T cells are activated by self-lipid bound CD1, with each member binding distinct self-lipids [339]; upon activation by self-antigen, these T cell lines were found to produce IFN-γ, IL-17 and TNF-α [340]. They comprise a substantial part of the circulating T cell repertoire with between 1 in 10 and 1 in 300 being CD1-autoreactive [341]. Moreover, CD1-autoreactive T cells have been found to infiltrate organs during autoimmune diseases [342], and have also been implicated in allergic skin diseases such as psoriasis [343]. Additionally, they are also involved in anti-tumour immunity; this is indicative of the role that autoreactive T cells play in balancing tolerance and responding to potentially harmful cell types or pathogens.

Most recently, Cotton et al. established that CD1a-autoreactive T cells from skin can recognise CD1a irrespective of the bound ligand and are present in high frequencies. Using a mammalian expression system, the CD1a monomers produced were left “untreated”, as they were already loaded with approximately 100 endogenous lipids from the mammalian expression system they were generated in, and tetramerised. The study demonstrated that regardless of the endogenous lipid bound, CD1a

autoreactive T cells recognised these tetramers. The TCR recognition was mapped to a portion of the CD1a protein where bound ligands would not be able to interact with the TCR. The authors suggested that the antigenic target of CD1a autoreactive T cells is CD1a itself, and due to the prevalence and high frequency of these lipid-independent cells, they are a normal component of the T cell repertoire in human skin [344]. However, it is important to remember that the presence of lipid antigens is essential for the CD1a molecule to traffic to the cell surface where it can be "seen" by T cells. Therefore, whilst the T cell does not interact with the antigen, the presence of the antigen remains vital for the recognition of CD1a by its cognate TCR.

A study by Shahine et al. aimed at identifying new targets of CD1b-mediated responses found that despite using CD1b tetramers pulsed with various foreign lipid antigens or extracts to isolate CD1b-reactive T cells, the cells derived were found to be autoreactive in response to monocyte-derived dendritic cells. To further confirm autoreactivity of these cells, the TCRs were found to bind CD1b-endo tetramers [345]. Moreover, a study using phosphatidylglycerol (PG) which is a lipid antigen present in both humans and bacteria, demonstrated that CD1b-PG complexes, loaded with either bacterial or host derived PG, resulted in the activation of CD1b-autoreactive T cells [346]. Furthermore, PG is present in mammalian mitochondria as well as in bacteria and is released during bacterial infection and mitochondrial stress. Whilst CD1-restricted T cells are activated by this antigen, it has been suggested that this occurs in a concentration dependent manner; PG is much more abundant in bacteria as opposed to mammalian cells, and so while T cells "see" the self-PG, it remains below the threshold of detection, and they become activated by the bacterial PG instead due to its abundance [347]. Furthermore, another important role of autoreactive T cells is the recognition of self-glycosphingolipids which bind CD1b in conditions unfavourable for antigen processing [348]. This mechanism is useful as it circumvents the issue of *Mtb* interfering with phagolysosome fusion, which is essential for lipid antigen processing [56].

A high frequency of CD1c-reactive cells are readily detected in healthy human blood [341] as well as in the blood of human TB patients [329]. In addition, CD1c has been found to be strongly upregulated on foamy macrophages; these cells are foamy in appearance due to the intracellular build-up of cholesterol and other derivatives such as cholesteryl esters [349]. Whilst they are most commonly found in atherosclerotic plaques, they are also present in lung TB granulomas [350]. Mansour et al. have demonstrated that autoreactive T cells recognise CD1c bound to self-cholesteryl esters and could therefore be driving inflammation in the context of TB granulomas [164]. This potentially highlights a role for CD1c-restricted T cells in the pathogenesis of TB. Indeed, a previous study indicated that $CD1^+$ foamy macrophages, similar to those present in atherosclerotic plaques, can activate CD1-autoreactive T cells [351].

The notion of the CD1 molecule itself resulting in autoreactivity by directly interacting with the TCR as with CD1a, is echoed with CD1c and its cognate TCR. CD1c-restricted cells were found to recognise CD1c proteins loaded with various chemically diverse self-lipids [303, 309]. This was found to be due to either ligands being small enough to be fully seated within the CD1c protein [309], or the ligand causing the protein to adopt different conformations [303], thus allowing for the F' roof to develop a "closed" conformation. The TCR then interacts directly with the CD1c protein without interacting with the lipid ligand within. These studies indicate that despite not interacting with the TCR, the lipid can determine autoreactive responses [303, 309].

Additionally, Lepore et al. demonstrated that CD1c autoreactive T cells recognise methyl-lysophosphatidic acid, a self-lipid that is found to accumulate in leukaemia cells. CD1c autoreactive T cells targeted and lysed $CD1c^+$ acute leukaemia cells and poorly recognised non-tumour CD1c expressing B cells. This highlights a role for CD1 restricted T cells in anti-tumour immunity [352].

Almost 2% of all αβ T cells are reactive to CD1c presenting self-lipids [341, 353]; however, CD1c has also been reported to stimulate a population of γδ T cells that are autoreactive [354, 355]. Vδ1 cells in particular were found to be CD1c-reactive. Whilst the γδ enriched T cells were expanded in the presence of *Mtb* antigens, they were found to proliferate in response to $CD1^+$ DCs in the absence of *Mtb* antigens, indicating their autoreactivity. Furthermore, functional assays revealed that these cells produced inflammatory cytokines, contained bactericidal granulysin, and were able to kill $CD1c^+$ targets [355].

Co-receptor expression

$CD4^+$ T cells are typically associated with MHC class II and produce cytokines that activate other subsets of T cells to drive an immune response; and $CD8^+$ T cells are associated with MHC class I where they lyse target cells upon activation. The binding and activation of these T cells via MHC molecules requires the recognition of peptide antigens. However, $CD4^+$ and $CD8^+$ T cells have been shown to recognise non-peptide antigens such as lipids. Although the reactivity of CD1-restricted T cells is independent of MHC class I and class II, a few studies have determined the expression of CD4 and CD8 on these cells. However, a systematic analysis of the co-receptor status of unconventional T cells has not yet been carried out, and their functional role (if any) in the modulation of the activity of these T cells has not yet been determined.

Studies on group 1 members of the CD1 family have identified different populations of T cells that are either double negative for CD4 and CD8 (DN), single positive for CD4, or single positive for CD8 [328, 356, 357], with each population exhibiting different functional responses in some cases where this has been investigated. Without directly studying how the expression of CD4 and CD8 impacts the functionality of these T cells, it is challenging to ascertain whether the function of the T cells is modulated by them.

Initially, CD1a- and CD1c-restricted T cells were found to be DN; and exhibited cytolytic activity when encountering APCs expressing either CD1a, or CD1c. This was confirmed using blocking assays that identified CD1a or CD1c mediated responses [307]. A later study identified the expression of CD8 [358], as well as CD4 on CD1a-restricted T cells. Cells that were either $CD4^+$ or $CD8^+$ and were CD1a-reactive produced IFN-γ as well as TNF-α in response to APCs expressing CD1a [359]. Furthermore, CD1a- and CD1c-restricted T cells isolated from peripheral blood were identified to be $CD8^+$, and displayed potent cytotoxicity against monocytes infected with *Mtb* [275], this releases the bacteria within these cells and exposes them to other host effector cells to facilitate their eradication. Additionally, $CD8^+$ cells have been shown to produce Th1 cytokines similar to those produced by $CD4^+$ T cells such as IFN-γ, which can activate neighbouring cells [328].

An expansion of $CD4^+$ CD1b-restricted T cells have been identified in subjects infected with *Mtb* but not in healthy controls [360]. $CD4^+$ CD1b- and CD1c-restricted T cells have been demonstrated to produce the Th1 cytokines IFN-γ as well as GM-CSF, indicative of the protective role these T cells play during infection [356]. The protective role IFN-γ plays is well established as evidenced by the increased susceptibility of IFN-γ-KO mice to *Mtb* infection [180, 181], whilst GM-CSF induces the expression of CD1 on monocytes, resulting in a greater frequency of lipid antigens presented to T cells [356]. Furthermore, the functional effect of CD4 was investigated in this study and was found to not contribute to the ability of the CD1-restricted T cells in recognising antigens. Blocking CD4 did not impact the proliferative response of these T cells to APCs or decrease the production of IFN-γ [356]. This indicates that whilst CD4 was expressed on the CD1b- and CD1c-restricted T cells isolated, it did not play a role in modulating their function, however, the production of Th1 type cytokines is suggestive of the contribution of these T cells in cell-mediated immunity during infection.

CD1b-restricted T cells were identified in patients with latent TB, as well as those who have recovered from TB infection [324]. CD1b-restricted T cells isolated from these subjects that displayed cytotoxic properties were $CD8^+$, and released IFN-γ, granulysin, perforin and granzyme B to limit *Mtb* growth when cultured with *Mtb* infected APCs. Moreover, this cytotoxic response was confirmed to be mediated via the recognition of CD1b, as blocking CD1b resulted in the growth and viability of *Mtb.* The study concludes that frequency of these T cells in latent TB infected individuals

was greater than those who recovered from TB, suggesting that this subset of T cells plays a role in preventing the disease from developing to active TB [324].

Human iNKTs have been found to be either $CD4^+$, $CD8^+$, or DN [361]. These subsets are defined either as $CD4^+$ and produce both Th1 and Th2 cytokines and can play an immunoregulatory role, or $CD4^-$ (which includes $CD8^+$ and DN cells) and produce Th1 cytokines and have cytotoxic properties [362, 363]. Amongst the $CD4^-$ subset, $CD8^+$ cells produce greater amounts of IFN-γ than DN cells and have a higher potency for cytotoxicity [364].

Whilst the direct interaction between CD8 and CD1d has not yet been determined, one study demonstrated that CD4 is able to bind CD1d and potentiate the activation of $CD4^+$ iNKTs. CD4 blocking assays inhibited antigen-dependent activation of $CD4^+$ iNKTs when cultured with APCs expressing CD1d and significantly reduced their production of IFN-γ. Furthermore, in order to eliminate the interaction of CD4 and MHC class II as a way by which the activity of iNKT is enhanced, iNKTs were activated using an APC-free system whereby plates coated with CD1d were used to activate them; again, blocking CD4 significantly decreased the production of IFN-γ in the absence of MHC class II [365].

Overall, studies have highlighted the expression or absence of the co-receptors on CD1-restricted T cells, but not all studies have investigated whether the co-receptors play a role in modulating the function of these T cells. Determining whether or not they play a role would be beneficial in helping inform better decisions when developing therapeutics.

CD1 tetramers

The first tetramers developed were based on MHC class I and II molecules. These were assembled by binding biotinylated proteins with fluorescently labelled streptavidin molecules in a 4:1 molecular ratio. Altman et al. tetramerised antigen-presenting molecules loaded with known antigens to stain individual antigen specific T cells [366]. Whilst this greatly improved our understanding of T cells and their peptide antigens, MHC class I and class II proteins are highly polymorphic, therefore they are limited in their application [366]. Due to the non-polymorphic nature of CD1 proteins, tetramers can in theory be applied to a genetically varied human population to analyse antigen-specific T cell responses [319, 367]. Consequently, this increases the prospects of using lipid antigens as an approach for immunodiagnosis and immunomodulation [319]. Lipid-loaded CD1 tetramers developed almost 20 years ago have allowed the field to make great strides in investigating T cell functions and phenotypes *ex vivo* [368-370].

CD1-lipid loaded tetramers

Although initially developed for CD1d, tetramers have been applied to CD1a, CD1b, and CD1c. Whilst some of these tetramers were loaded with *Mtb* derived lipid antigens and used to identify CD1-reactive T cells in patients with active and latent TB [371-373], they had not yet been validated for use in assays that could be applied clinically. The development of standardised assays that enumerate and characterise lipid antigen specific T cells in clinical samples has been lacking. Layton et al. have combined the use of CD1b tetramers loaded with mycobacterial lipid GMM into a multi-parameter flow cytometry assay [367]. Their assay has robustly detected GMM-specific T cells in South African subjects with LTBI not present in U.S. healthy controls. They have suggested that their assay can be used in studies of disease progression, vaccine development and mycobacterial infection by including additional tetramers and/or phenotypic markers to characterise GMM-specific T cells.

As opposed to monomers, the multimerisation of MHC and CD1 tetramers results in a higher avidity binding due to multiple low-affinity interactions with several TCRs on one cell. Dextramers have yet an even better staining ability and intensity in comparison to tetramers, this is due to their lengthier interaction half-lives with T cells [374]; Van Rhijn et al. demonstrated this using CD1b dextramers [346]. Despite their better performance, dextramers are less commonly used predominantly in academic research labs due to the high costs associated with producing and purchasing them, particularly for long term experiments.

The most significant contribution of the use of tetramers in the field have so far been that firstly, they have shown that T cell clones that recognise mycobacterial lipid antigens were not as rare as previously thought, and are present in many TB patients [375, 376]. Secondly, the concept of highly conserved TCRs was established based on the discovery of CD1d restricted NKT cells [377]. The existence of conserved CD1a, CD1b and CD1c TCRs was proven among individuals which was consistent with the non-polymorphic nature of CD1 proteins [375, 376].

Interestingly, until recently, CD1c-phosphomycoketide (CD1c-PM) tetramers were the only CD1c-tetramer tool available. However, since then, two groups, including ours, have published results using new CD1c tetramer tools such as CD1c-SL and CD1c-PC tetramers [303, 378]. Using CD1c-PM tetramers, PM was identified as a new *Mtb* derived antigen, whereby T cell populations from TB patient blood readily stained with CD1c-PM tetramers [373]. Additionally, the use of CD1c-SL tetramers allowed for the identification of an additional conformation that CD1c adopts when bound

to cholesteryl esters, this conformation means that the lipid does not interact with the TCR, thus the TCR directly interacts with the CD1c molecule and becomes activated [303].

Perhaps most importantly, CD1c tetramers have been used to isolate and expand cell types that are otherwise difficult to expand and study *in vitro* due to having an anergic phenotype, such as γδ T cells [379, 380]. CD1c-MPM and CD1c-PM tetramers allow the successful isolation and expansion of γδ T cells *in vitro* [381]. Moreover, these T cells also demonstrated binding to CD1c proteins with endogenous lipids derived from an insect cell expression system, demonstrating their cross reactivity [381].

CD1-endogenous (CD1-endo) lipids tetramers

Whilst the use of lipid loaded CD1 tetramers has allowed for a better understanding of the CD1-restricted T cell repertoire, the use of tetramers loaded with endogenous lipids from within the mammalian expression system from which the proteins are generated has also allowed for important discoveries to be made regarding the autoreactivity of CD1-restricted T cells.

Using CD1a-endo tetramers that bind ~100 endogenous lipids, a study determined that CD1a-reactive TCRs bind directly to the CD1a protein itself irrespective to the ligand bound. The binding of the TCR was mapped to a portion of the protein that covers the antigen within as opposed to an exposed site where the TCR can interact with the ligand. Additionally, the study suggests that by bypassing the need to load specific lipids to detect CD1a-restricted T cells, as well as the non-polymorphic nature of the CD1 protein, the CD1a tetramers can be used to track CD1a-restricted T cells in clinical diseases [344].

The use of CD1b-endo tetramers demonstrated that despite CD1b-restricted T cells being isolated and expanded using CD1b-lipid loaded tetramers, the cells were autoreactive and bound to CD1b-endo tetramers. To further validate their autoreactivity, these cells displayed functional autoreactivity to CD1b transfected human cells in the absence of exogenous lipid antigens and released IFN-γ [345].

CD1c-endo tetramers were found to consistently stain a large proportion of T cells and have been used to further understand the mechanism by which the TCRs of CD1c-restricted T cells interact with CD1c. CD1c-restricted T cells isolated using CD1c-endo tetramers demonstrated functional autoreactivity in response to human cell lines transduced to express CD1c, by releasing IFN-γ. Additionally, the interaction of the TCR with the CD1c was determined to be via direct recognition of the CD1c protein rather than with bound lipids [309].

The use of fluorescently tagged tetramers in general, allows for the labelling of single antigen specific T cells among millions of freshly isolated T cells. The cells can then be sorted by flow cytometry and enriched via different methods. The enriched populations subsequently used in functional assays and/or multi-parameter flow cytometric analyses for phenotyping [319]. Using CD1-endo tetramers allows the identification and isolation of CD1 autoreactive T cells. Upon isolation and expansion, these cells can then be stained with CD1 tetramers loaded with *Mtb* derived lipids and/or cultured with *Mtb* infected APCs to study their cross reactivity and response to bacterial ligands.

Current models of Mtb infection

The use of different experimental models have greatly advanced our knowledge of the immune response to *Mtb* infection. However, the need for more relevant models that better recapitulate the events that occur during infection, and are more translatable to humans, remains. *In vivo* models range from zebrafish to non-human primates (NHPs); and *in vitro* models have developed sophisticated 3D systems.

Despite being the smallest animal model that TB infection is studied in, experiments in zebrafish have provided useful information in terms of disease pathogenesis. Although zebrafish can only be infected with *Mycobacterium marinum (M. marinum),* which is genetically related to *Mtb* and infects cold blooded aquatic animals [382]; they can develop granulomatous structures upon infection with *M. marinum* that are histologically similar to those formed in human *Mtb* infection [383, 384]. One of the most significant aspects of this model is that larval zebrafish are transparent which allows the application of high-resolution microscopy [385]. It can also be easily genetically manipulated, with genes being inactivated by antisense oligonucleotides [386]. Using a zebrafish model, an important question regarding how the mycobacteria are able to survive within phagocytes was addressed by Cambier et al.; they demonstrated that mycobacteria are able to selectively enhance the phagocytic activity of specific subsets of macrophages that are deficient for inducible nitric oxide synthase (iNOS), thereby reducing microbial activity and promoting their survival [387]. However, zebrafish larvae do not have T cells, and so can only be used to study mycobacterial-macrophage interactions.

Mouse models of infection are the most commonly used due to the range of tools and strains available. However, their main drawback is that most models do not reproduce the human pathologies, in particular granulomas similar to those seen in humans. Granulomas formed in mice tend to be less compact and do not caseate, which is a hallmark of human *Mtb* granulomas [388].

Nevertheless, several groups have succeeded in generating humanised mouse models that recapitulate this hallmark [389-393].

Heuts et al. generated a humanised mouse model by transplanting human CD34 hematopoietic stem cells (chord blood progenitor cells) which differentiate into human immune cells [394-396] in order to study the human immune response to *M.bovis* and *Mtb* infection, and to shed light on the differences between key events that occur during BCG or TB infection. They observed that humanised mice had a greater bacterial load in their organs relative to non-humanised mice, and that this was mediated by $CD4^+$ T cells, as it was associated with an increase in PD1 expression [390].

Similar to human TB disease, $CD4^+$ T cells have been shown to be essential in the formation of granulomas in mouse models, as well as in mediating the Th1 immune response [397]. Additionally, TNF is well established to play a role in the response to *Mtb* infection as it is involved in cytokine production, macrophage activation, and granuloma formation in mice [10, 388, 398]. Heuts et al. demonstrated that in humanised mice, infection with *Mtb* or BCG resulted in the formation of structured granulomas that contain macrophages and T cells, and resembled those seen in human TB [390]. However, the mice were unable to control bacterial growth and had impaired T cell function.

Additionally, the group demonstrated that TNF helps control the bacterial load within the granuloma, and the extent of inflammation. The treatment of infected humanised mice with a TNF neutralising TNF receptor fusion protein resulted in more necrosis in granulomas formed during *Mtb* infection. In BCG infected mice, although their granulomas remained structurally sound, they had higher levels of intracellular bacilli, further highlighting the importance of TNF in the immune response. Additionally, the group showed that $CD4^+$ T cells in particular, play a role in granuloma formation in humanised mice. The high bacterial load seen in humanised mice was decreased by depleting $CD4^+$ T cells, which also resulted in smaller and sparser lesions. Huets et al. suggested that humanised mice such as these can be used to better understand the formation of granulomas and the factors that allow the persistence in human TB [390].

Another humanised mouse model used to study TB is a mouse model engrafted with human foetal bone marrow, liver and thymus (BLT) tissue. This model has been used to study diseases and pathogens such as Dengue fever [399], *Salmonella* Typhi [400], and *Plasmodium falciparum* [401], as well as HIV [402, 403]. Caledron et al. generated this humanised mouse model by engrafting BLT tissue to study TB infection [392]. At 12 weeks post engraftment they confirmed the expression of human T cells, macrophages, monocytes, and NK cells. Flow cytometric analysis confirmed that the T cells were functional in response to stimuli such as anti-CD3/28 and produced effector molecules such as perforins and IFN-γ [392]. The mice were infected with *Mtb* intranasally, within 2-8 weeks

the infection had taken hold in the lungs and disseminated to the liver and spleen, and human T cells were found at these locations. Additionally, human T cells were also found in granulomas that had formed in the lungs. Caseous necrosis was also observed, as well as crystallised cholesterol deposits [392]. Calderon et al. have suggested that the similarities between the pathology this mouse model develops and those seen in human TB, as well as the distribution and function of immune cells, and disease dissemination, makes this mouse model a good candidate for not only TB studies, but also for potentially studying co-infection of HIV and *Mtb* [392]. This was achieved in 2016 by the same group [389].

A novel co-infection mouse model of *Mtb* and HIV was generated by first producing BLT mice, which were then infected with HIV via a tail vein injection, and infected with *Mtb* intranasally [389]. They created this co-infection model to better understand the detrimental effect that HIV infection has on the ability of the host to control *Mtb* infection. Similar to what is found in humans, the study found that co-infection resulted in greater progression of TB disease, loss of granuloma structure, and an increase in bacterial load [404]. Additionally, the study found that co-infection amplifies a non-protective proinflammatory response in a HIV-dependent manner, and has deleterious effects such as worsening lung pathology, and resulting in an increase in recruitment of neutrophils. *Ex vivo* studies carried out using human cells demonstrated that HIV impaired both the function of $CD4^+$ T cells and cytotoxic T cells [405-407], as well as antigen presentation by macrophages, and disrupted the antibacterial capacity of immune cells [408-410]. In patients, a significant loss of CD4+ T cells is a clinical hallmark of HIV infection and results in immune suppression [407, 411]. In this co-infection model, the group identified deleterious *in vivo* effects prior to a large decrease in $CD4^+$ T cells, allowing for a better understanding of the immune dynamic during TB/HIV co-infection [389].

Although NHPs are the most ideal animal model, high costs associated with maintaining NHPs makes them better suited for end stage development of vaccines as opposed to early-stage screening. Humanised mice are easier to maintain and can be a powerful tool in helping uncover important aspects of the human immune response to disease; humanised mice produce responses that are highly similar to those found in humans and can help with vaccine development.

Grover et al. used a humanised mouse model that was generated by engrafting mice with CD34 hematopoietic progenitor cells which resulted in >50% human leukocytes in the mice, which expressed $CD3^+$, $CD4^+$ and $CD8^+$ T cells [391]. This model was used to study the effect of a vaccine on the immune response to TB infection. Previously, several studies using humanised mice demonstrated the presence of T cells within granulomas in BCG and *Mtb* infected mice that were infected with two different strains of *Mtb* [390, 392]. Additionally, T cells from a BCG infected mouse

model displayed anergy to *Mtb* derived antigens but were responsive to stimulation by a mitogen [412]. Having seen human $CD4^+$ and $CD8^+$ T cells respond to infection in humanised mice, the effect of a liposome-based vaccine on *Mtb* infection was studied [391]. The aim was to determine whether the vaccine could elicit a cytokine response reminiscent to what is observed in humans. Mice were vaccinated with either BCG or an ESAT-6 containing liposome-based formulation, and their response was compared to two other commonly used animal models for testing TB vaccines, the C57BL/6 mouse model, and Hartley guinea pig model of TB. In humanised mice vaccinated with either BCG or the liposome-based formulation, human $CD4^+$ and $CD8^+$ T cells were able to undergo differentiation and produced effector cytokines such as TNF-α, IFN-γ and IL-2. The response observed in humanised mice differed from that of the C57BL/6 mice and Hartley guinea pigs, and more closely reflected that of the human response [391]. Having demonstrated that a vaccine results in a human immune response, Grover et al. have suggested that the humanised mouse model can be used to study novel vaccines and the human immune response *in vivo* [391].

A humanised mouse model was also generated by Arrey et al. to further investigate granulomas. The group generated a humanised mouse model by engrafting mice with human foetal liver derived stem cells [393]. Following *Mtb* infection, the mice were used to further examine the cellular composition and structure of granulomas. They found that mice developed various pulmonary lesions and caseous necrotic granulomas, which had a similar immunophenotype, cellular and organisational structure to those seen in humans with TB [393], particularly those found in immunocompromised or paediatric patients [413]. Current TB treatment regimens are lengthy and consequently lead to reduced compliance and the emergence of drug resistant strains [414]. Moxifloxacin, an antibiotic that has been proposed as an addition to current TB drugs such as Rifampicin and Isoniazid, it was proposed that its addition could shorten treatment time by approximately 30% [415]. The group used this humanised mouse model to study whether Moxifloxacin in conjunction with other TB drugs had a beneficial impact on clearing the disease, they found that over a prolonged period of time, adding Moxifloxacin to the treatment regimen did not confer any advantages [393], as has been previously observed in a clinical setting [415]. Having observed findings that align with those made in clinic, and most importantly, with this model developing similar pathology as that seen in human TB, Arrey et al. suggested that the model has enough parallels with human TB, that it could be used as a *in vivo* pre-clinical tool for the development of drugs [393].

Additionally, mouse models have provided significant data in terms of highlighting the essential role of IFN-γ using IFN-γ-KO mice [180, 181], and the roles of TNF-α in murine *Mtb* infection such as its anti-necrotic effect on granulomas and the stimulation of nitrogen production by macrophages in early infection [10].

Also, it is worth noting that in the context of studying CD1-mediated responses in TB infection, mice do not express Group 1 CD1 proteins [18]. To overcome this, Felio et al. generated a transgenic CD1 mouse model (hCD1Tg), which expressed group 1 CD1-restricted T cells (CD1a-, CD1b-, and CD1c) [416]. After immunising with *Mtb*, the majority of CD1-restricted T cell lines isolated from hCD1Tg mice were found to be autoreactive and were able to lyse both human cell lines expressing CD1, as well as DCs derived from hCD1Tg mice. This implies that the self-antigens presented by both these cell types are conserved between humans and mice, and that *Mtb* drives CD1 autoreactive T cells *in vivo* [416].

The most clinically relevant model yet is the NHP model, in particular macaques [417]. However, due to the extremely high costs associated with husbandry, ethical considerations and time course of studies, this is not very widely used [418]. Disease pathogenesis in NHPs parallels that of humans [419]; they are also able to develop LTBI [417]. Perhaps most significantly, NHP models are able to display susceptibility to TB in the presence of well-established risk factors such as HIV and anti-TNF-α treatment [420, 421].

Naturally, no animal model is perfect and has its own limitations in terms of extrapolating findings across species. The application of more human relevant/based models is essential in reducing the use of animals as well as complementing findings already made *in vivo.* Important pathophysiological aspects of TB such as granulomas can be studied in 3D cell culture models that lend themselves to better understanding cellular events specific to TB granulomas.

Complex cell culture systems allow mechanistic studies to be carried out that would not be possible in humans, and would be challenging in animals [422]. Cell biology is modulated by extracellular matrix (ECM), and 3D systems allow the incorporation of ECM in culture [423]. Tezera et al. have developed a system that incorporates live *Mtb*, and primary human blood mononuclear cells in a collagen-alginate matrix to form microspheres (Figure 4), this allows the investigation of host-pathogen interaction in a more relevant setting than traditional cell culture. They have demonstrated that the ECM regulates cell survival in TB, while its destruction leads to disease dissemination [424]. They have also optimised the system to give multi-parameter read outs such as cytokine secretion and immunoaugmentation. One of the most important features of this model is being able to use live *Mtb*, including clinically relevant *Mtb* strains. There is evidence in the literature demonstrating that macrophages process heat-killed *Mtb* more rapidly than live *Mtb* when presenting antigens to T cells [425]. This indicates that viability is an important factor in antigen

processing, and consequently in triggering an immune response; further supporting the importance of using a live *Mtb* model of infection to study the host-pathogen interaction more accurately during infection.

This 3D system has the potential to be used to study the effect of CD1-restricted T cells during *Mtb* infection. The frequency of CD1c-restricted T cells growing in the microspheres can be measured using CD1c tetramers. Additionally, peripheral blood mononuclear cells (PBMCs) can be supplemented with autologous CD1c-restricted T cells that have been enriched *in vitro* and multi parameter read outs can be measured, such as cytokine secretion, cell toxicity and *Mtb* growth. Furthermore, the effect of lipid antigen specific T cells on *Mtb* growth can also be studied. This will give insight into the functional role of these cells in infection.

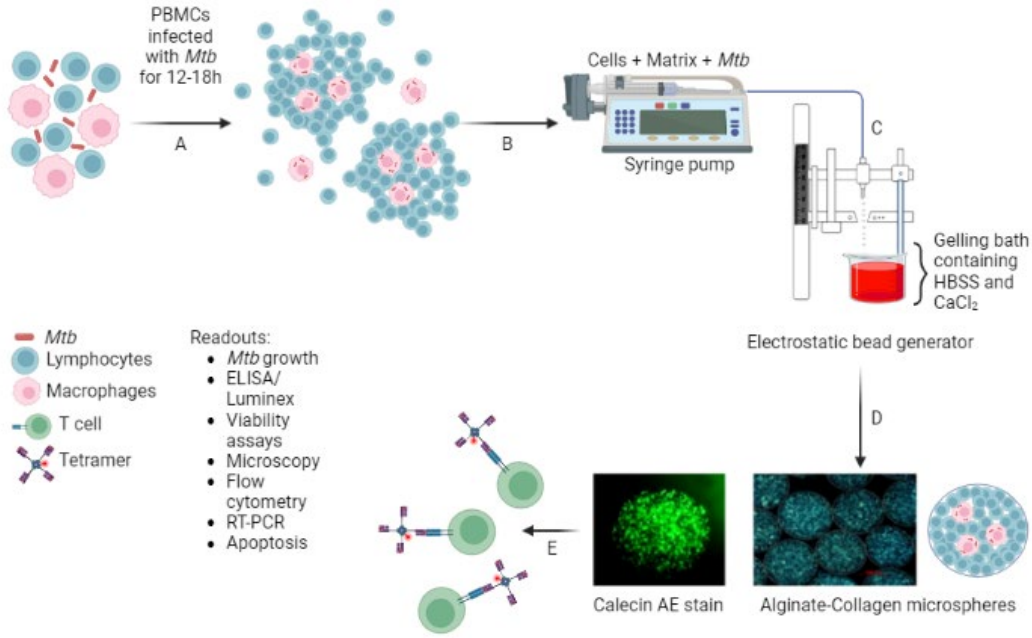

Figure 4: Schematic of Bioelectrospray microsphere generation workflow. PBMCs are infected with *Mtb* and mixed with alginate collagen, which is representative of cellular matrix. Upon being passed through the bioelectrospray, alginate collagen encapsulated 3D microspheres form. The process involves the following steps, (**A**) PBMCs are infected with *Mtb* overnight, (**B**) Cells are mixed with alginate-collagen matrix and loaded in a syringe, (**C**) Matrix in syringe is injected into the bioelectrospray machine to generate beads that fall into a HBSS solution. (**D**) Cells that are infected with fluorescently labelled *Mtb* and can be visualised**.** (**E**) Following being cultured in microspheres, the cells can be stained with CD1c tetramers after 7-14 days following decapsulation (Adapted from Tezera et al., 2017 [253]).

TB vaccines

The Bacillus Calmette Guérin (BCG) vaccine was developed more than 100 years ago and is used routinely worldwide with the exception of a few regions [426]. However, despite having some protective effects in children, it does not protect against primary infection or reactivation of pulmonary TB in adults [427]; thus the need for a more effective vaccine remains. Antigens used in vaccines to drive a T cell response are typically peptides and are presented by the MHC I and II proteins, which are polymorphic. Following infection with *Mtb,* the adaptive immune response has been found to take approximately 2 weeks before it is observed [9, 428]. New vaccines developed against TB aim to hasten this response time. Although most vaccines are developed to drive T cell mediated responses, antibody mediated responses have also been shown to play a role in the immune response to TB. Studies carried out in macaques demonstrated that the BCG vaccine administered via intravenous or mucosal routes almost completely eliminated *Mtb* infection, and that this clearance correlated with *Mtb* specific antibodies such as IgA, IgM and IgG in the blood and bronchoalveolar lavage (BAL) fluid [429-432]. Furthermore, *in* vitro, IgM and IgG antibodies isolated from the vaccinated macaques were found to increase bacterial uptake of *Mtb* by macrophages [431]. Additionally, although a direct relationship has not yet clearly been defined, antigen specific IgM titres were found to correlate with reduced bacterial burden [429]. Additionally, in a study in Japanese healthcare workers, similar to *Mtb* infection, BCG vaccination resulted in the generation of high avidity IgG antibodies to bulk surface antigens, including tuberculosis glycolipid [433, 434].

In a macaque model comparing MTBVAC which is a live attenuated genetically modified *Mtb* vaccine, and BCG; MTBVAC was shown to induce a swift and robust adaptive immune response, as well as opsonising antibodies [431]. BCG has a smaller antigen repertoire than *Mtb,* however, the antibodies generated following BCG vaccination have some overlap with *Mtb* targets, such as antibodies against LAM [435, 436].

In a study carried out in humans in the UK, arabinomannan (AM)-specific IgG antibodies increased in the serum, following intradermal administration of a BCG vaccine, and correlated with macrophages killing BCG and opsonisation [437]. Additionally, mice immunised with antibodies against AM were shown to survive for longer and had a reduction in bacterial load in a dose dependent manner [438]. Serum collected following the immunisation of healthy volunteers with BCG demonstrated that it stimulated both cell mediated and humoral immunity [437]. Additionally, the serum was found to result in the opsonisation of *Mtb*, resulting in increased phagocytosis, inhibition of intracellular bacterial growth, and enhancing phagolysosomal fusion. The antibodies produced were found to be against cell surface glycolipids such as LAM and AM [437]. Whilst there is clear correlation between

these antibodies and protection against TB [437, 439], another study has suggested that antibody mediated protection occurs independent of these antigens [440].

A TB vaccine that showed a lot of promise recently was the Modified Vaccinia virus Ankara expressing Ag85A from *Mtb* (MVA85A). Ag85A induces $CD4^+$ T cell responses which produce IFN-γ [441], in animal studies, this has been shown to be essential in protecting against *Mtb* infection [180, 442]. In infants, this vaccine resulted in increased levels of Ag85A-specific IgG in serum and was linked to a decrease in the risk of TB infection [443], however, during phase 2b of the trial, infants that were vaccinated with BCG and boosted with MVA85A were followed for 3 years, and no improvement against TB was detected [444]. Additionally, mice primed with BCG vaccine prior to receiving MVA85A expressed high levels of antigen specific $CD4^+$ and $CD8^+$ T cells [445]. However, NHPs that were inoculated with both BCG and MV85A vaccines had higher mortality rates than control animals that received BCG alone [444, 446].

Furthermore, in a study carried out in adults with HIV, whilst MVA85A elicited T cell responses that produced IFN-γ, it did not produce detectable levels of antibodies [447], although not yet confirmed, this has been pinpointed as one of the potential reasons that the MVA85A vaccine is not able to protect against *Mtb* infection [448]. Moreover, this aligns with findings made in infants whereby despite an increase in cytokine expression and T cell frequency, MVA85A was not protective following being used as a booster to BCG [449].

Some vaccines against TB that have been shown to be protective failed to have the same effects when given as a booster following BCG being the initial vaccine [450, 451]. One such vaccine is a cytomegalovirus (CMV) based vaccine, where the CMV vector expressed 6 or 9 Mtb antigens which included Ag85A, and ESAT-6 [450]. In a macaque model, this vaccine was highly protective against TB and induced robust $CD4^+$ and $CD8^+$ T cell responses, as well as cytokines such as IFN-γ and TNF; and produced evidence of complete elimination of the disease in some of the animals [450]. Furthermore, despite inducing a marked cellular response, the vaccine did not produce significant antibody responses, demonstrating that the protective responses were T cell mediated, and gene expression profiling also suggested a protective role for neutrophils [450]. However, the protective effects of this vaccine were not reproduced when given as a booster to the BCG vaccine [450].

Despite the CMV based vaccine showing promising results as a TB vaccine, the deleterious effect of pre-vaccination with BCG makes on the protective function of this vaccine makes it an unviable option. The BCG vaccine is administered to children in most countries as part of routine vaccinations, its impact on new vaccines that show promising results in its absence adds another layer to the development of a new TB vaccine. The process of developing a new vaccine that would protect

adults from primary infection or reactivation of pulmonary TB must take into account that a BCG vaccine has already been administered and whether or not it impacts the new vaccines' function and efficacy.

When considering protective responses against TB, cell mediated immune responses are often the main focus. *In vivo* studies carried out in mice demonstrated that when important components of cell mediated immunity such as T cells, or cytokines such as IFN-γ and TNF are impaired, the susceptibility to TB increases [452], as has also been seen in patients with HIV who become immunocompromised as a result of the diseases [453].

With regards to B cells, studies in TB infected cynomolgus macaques demonstrated that the granulomas that formed were surrounded by B cell clusters that secreted *Mtb* specific antibodies [454], although the depletion of B cells using Rituximab, which is a monoclonal antibody, did result in a change in granulomas by altering local cytokine and T cell responses, overall, it did not impact disease pathology or outcome [455]. Whilst B cell mediated responses are an essential compartment of the immune response, animal studies are yet to highlight their involvement and whether this can be manipulated for the sake of developing therapies.

Altogether, the immunological criteria required for an effective TB vaccine is yet to be outlined and requires a better understanding of the host pathogen interaction in TB, including responses driven by unconventional T cells [456]. Many non-peptide derived *Mtb* antigens that are recognised by both αβ- and γδ-TCRs have been identified over the past few decades, and are presented by proteins other than the polymorphic MHC proteins, such as CD1, MR1, and HLA-E. The non-polymorphic nature of these antigen presenting molecules not only widens the scope for targets of the vaccines, but it also means that the vaccines can be applied globally despite the genetic diversity of the population [457].

Several studies investigating lipid-based vaccines in guinea pig animal models have been published [458-460]. Guinea pigs were normally used as they express homologs of the CD1 proteins [319], and the way in which granulomatous inflammation occurs in them is similar to that in humans [460]. Dascher et al. demonstrated that guinea pigs immunised with total lipids derived from *Mtb* before being challenged with aerosolised *Mtb* had a reduced bacterial load and less severe pathology [459]. Furthermore, guinea pigs immunised with a mixture of mycobacterial lipids were shown to have a lipid specific CD1 restricted response [458]. More specifically, guinea pigs inoculated with purified *Mtb* lipid antigens such as diacylated sulphoglycolipids (Ac2SGL), and phosphatidyl-myo-inositol, had a lesser bacterial load in the spleen, which was consistently reduced in comparison to the

unvaccinated group [461]. Additionally, guinea pigs receiving the lipid-based vaccine had a lower number of lung and splenic lesions than the unvaccinated control group with lower severity of immunopathology [461]. The protective effects attained by the lipid antigens was comparable to that of protein antigens in the same guinea pig model, however, targeting non-polymorphic proteins allows for greater applicability [461].

In terms of mouse models, several a few groups generated transgenic mouse models (hCD1Tg) that express these proteins and utilised them to study lipid based vaccines [416, 462]. Felio et al.found that immunising hCD1Tg mice with *Mtb* lipids elicited Th1 responses by CD1-restricted *Mtb* lipid antigen specific T cells, and were able to lyse mouse as well as human cell lines in the absence of exogenous lipid antigens, demonstrating autoreactivity across species [416]. They further validated the CD1 mediated responses by demonstrating that during *Mtb* infection, CD1-restricted T cell responses were inhibited in the presence of monoclonal anti-CD1 antibodies. This provided direct evidence that group 1 CD1-restricted T cell responses are induced by TB infection *in vivo* and may be involved in the immune response against TB [416].

Overall, animal models have presented compelling evidence that the induction of the CD1-restricted T cells by *Mtb* infection could be exploited to develop lipid-based vaccines. This initial promising data, along with the continued efforts to determine the role of CD1-restricted T cells in TB could pave the way for the generation of lipid-based TB vaccines.

Hypothesis and aims

Despite major research programmes over the last two decades, recent outcomes of novel interventions for TB have been disappointing. Thus, a better understanding of the host-pathogen interaction is urgently required to inform better future therapeutic interventions. A growing body of evidence suggests a functional role for CD1c and its restricted T cells in human TB. This project will study immune responses to TB mediated by CD1c molecules, and the functional impact of CD1c immunity in human TB, in particular CD1c-autoreactive T cells. *We hypothesise that CD1c and its restricted T cells regulate the host-pathogen interaction in human TB*.

The overarching aim of this project is to investigate the functional effect of CD1c-autoreactive T cells in human TB infection. We will address this aim with the following key objectives:

A) Optimise the methodology pipeline to facilitate the expansion, specific isolation, and enrichment of CD1c-autoreactive T cells *in vitro* for downstream functional studies
B) Determine the phenotype of CD1c-autoreactive T cells by flow cytometry
C) Investigate the anti-TB function of CD1c-autoreactive T cells using a 2D *Mtb* infection model
D) Define the clonal diversity of CD1c-autoreactive T cells through TCR-sequencing

Chapter 2 Materials and methods

Ethical approval statement

University of Southampton

The work with human blood cells is approved by the NRES Committee South Central - Southampton A (REC reference 13/SC/0043; IRAS project ID 109038) and the University of Southampton research ethics office (ERGO 14291). The analysis of human tissues has been approved by the Southampton Research Biorepository (REC reference 12/NW/0794; RHM SRB0005; HTA licence number 12009; ERGO 12332). Approval for infection of human cells with *Mycobacterium tuberculosis* has been approved by the UK Health and Safety Executive and the University of Southampton Biological Safety Committee (GMBSC-41).

Immunocore

The work with human blood cells is approved by the NRES Committee South Central – Oxford A (REC reference 13/SC/0226), Immunocore study protocol number IMCres02.

Generating CD1c tetramers

Bacterial expression system

Expression and purification of inclusion bodies

Escherichia coli (E. Coli) Rosetta strain (Novagen) expressing recombinant proteins of the CD1c heavy chain and human β2m were separately propagated overnight at 37°C. The following day, 10ml of the bacterial culture was added to 2L of low salt Luria-Bertani (LB) broth (20g Tryptone, 10g yeast extract, and 10g NaCl in 2L dH_2O) and incubated at 37°C whilst monitoring absorbance at 600nm (OD_{600}). Cultures were then stimulated with Isopropyl-β-D-thiogalactoside (IPTG) (Melford) when the OD_{600} was between 0.4-0.6 and incubated for a further 4 hours to allow for protein synthesis. The bacteria were pelleted at 6000rpm for 6 minutes using a high-speed centrifuge (Beckman Coulter). The supernatant was discarded, and the pellets were resuspended in Phosphate Buffered Saline

(PBS) (Lonza) and sonicated on ice to isolate inclusion bodies (IBs). IBs were pelleted at 10000rpm for 30 minutes before resuspending in Wash buffer (50mM Tris pH 7.5, 100mM NaCl, 1mM DTT, 1mM EDTA, 0.5% Triton X, 0.1% NaN_3). They were then homogenised using a Dounce homogeniser before being pelleted again at 10000rpm for 10 minutes; this was repeated three times. Next, they were resuspended in Resuspension buffer (50mM Tris pH 7.5, 100mM NaCl, 1mM DTT, 0.5mM EDTA), homogenised and pelleted at 10000rpm for 10 minutes; this was repeated three times. Finally, the IBs were fully denatured in 6M guanidine-HCL and reduced with 20mM DTT and then stored at -20°C.

Refolding of CD1c lipid complexes

Completely denatured and reduced inclusion body proteins for both CD1c heavy chain and β_2m were refolded via oxidative refolding and purified as previously described [463]. Briefly, 39.22mg CD1c and 49.21mg β_2m were added to the refolding buffer (1M Tris, 500mM EDTA, 300mM 1M L-Arginine, 6% Urea) containing oxidised and reduced glutathione (1.835g and 917.6mg, respectively), and 6ml vehicle (150mM NaCl, 0.5% Tween-20) at 4°C overnight with constant stirring. Refolded proteins were concentrated using a Vivaflow crossflow filtration system (Sartorius) down to approximately 10ml before being purified by Fast Pulse Liquid Chromatography (FPLC) by size-exclusion and anion-exchange chromatography using preparatory grade SD75 26/600, SD75 10/300, and MonoQ 4.6/100 columns (GE Healthcare).

CD1c-SL tetramers assembly

Refolded and purified CD1c-SL monomers were biotinylated via an engineered BirA motif at the C-terminus of CD1c using a BirA Enzyme biotinylation kit (GeneCopoeia) and subsequently re-purified by size exclusion chromatography (SEC). A biotin ELISA was carried out to confirm biotinylation of the monomers prior to tetramerisation. Briefly, 1µg of protein was mixed with 100µl PBS (Lonza) in triplicate wells, non-biotinylated CD1c-SL monomers were used as a control. The plate was incubated at 37°C for 1 hour. The wells were then washed with PBS before adding Blocking buffer (PBS, 0.5% FBS, 0.1% sodium azide), and incubated at 37°C for 30 minutes. The wells were washed again and streptavidin-HRP (1:2000) (Sigma) was added and placed at room temperature for 30 minutes. Following another wash, TMB ELISA substrate (Invitrogen) was added, and the plate was incubated at room temperature for 30 minutes in the dark. Fluorescence was measured at 450nm following the addition of 1M H_2SO_4. Upon confirmation of biotinylation, the CD1c-SL monomers were

conjugated to phycoerythrin (PE) or Brilliant Violet 421 (BV421) -streptavidin (BioLegend) to generate fluorescently labelled CD1c-SL tetramers.

Mammalian expression system

Expression and purification of proteins

Biotinylated CD1c monomers loaded with endogenous lipids (CD1c-endo) were produced in transfected Expi293F HEK cells using the ExpiFectamine 293 Transfection Kit, following the manufacturer's instructions (Gibco). HEK cells were grown in suspension in Expi293 Expression Medium at 37°C, 8% CO_2 whilst shaking at 120rpm. The day before transfection, they were split to a final density of 2.5 –3 × 10^6 viable cells/ml and left to grow overnight. The next day they were counted again to ensure they have reached a density of approximately 4.5-5.5 × 10^6 viable cells/ml, with cell viability between 95–99%. This ensures the cultures are healthy enough to proceed with the transfection. The cells were then diluted to a density of 3 × 10^6 viable cells/ml in 100ml using fresh pre-warmed Expi293 Expression Medium and incubated at 37°C, 8% CO_2, shaking at 120rpm, whilst the DNA plasmid was prepared. The DNA plasmid was added at 1µg/ml of cells, this was prepared by diluting 100µg of plasmid in Opti-MEM (reduced serum media), as well as diluting the required volume of ExpiFectamine 293 reagent in Opti-MEM in separate tubes and incubating them at room temperature for 5 minutes. The diluted ExpiFectamine 293 reagent and DNA plasmid were mixed and incubated at room temperature for 20 minutes and then slowly added to the flask of cells whilst swirling the flask. The cells were incubated again at 37°C, 8% CO_2 whilst shaking at 120rpm overnight. The next day (18-22 hours post transfection), 600µl ExpiFectamine 293 Transfection Enhancer 1 and Enhancer 2, and 2ml Biotin (100nM final concentration) (Sigma) were added to the flask and the cells were incubated at 37°C, 8% CO_2 whilst shaking at 120rpm for 5 days.

After 5 days, the proteins were harvested by spinning the cultures at 4000rpm for 30 minutes at 4°C. The supernatant was then triple filtered through a 0.8µm pore size vacuum filter unit, followed by filtration through a 0.45µm filter, and finally a 0.22µm filter (all filter units were from Corning). The protein was then purified by FPLC, initially using a HisTrap excel nickel column (Cytiva), the sample was eluted off the column in 500µl fractions; these were then analysed on an SDS-PAGE gel as described below. The protein was further purified using a SEC column Superdex 200 Increase (Cytiva) and was eluted off the column in 500µl fractions; these fractions were also analysed on an SDS-PAGE gel as described below. The fractions were then concentrated using a centrifugal concentrator by

centrifuging at 3000rpm at 4 °C, aliquots were then made and snap frozen on dry ice before storing at -80 °C.

CD1c-endo tetramers and dextramers

Assembly

Biotinylated CD1c-endo monomers were conjugated to PE-conjugated streptavidin (eBioscience) to generate fluorescently labelled CD1c-endo tetramers. A 25% excess of streptavidin-PE was added to the monomers to ensure maximum efficiency of tetramerisation. The total volume of streptavidin-PE was added in 5 increments over a 1-hour time period, with 10 minutes incubation at room temperature in the dark between each addition. To generate dextramers, the same process was repeated as above, with PE-labelled dextran backbones (Dex-PE) (Immudex), as opposed to PE-conjugated streptavidin.

SDS-PAGE gel analysis

CD1c-SL

A 12% SDS-PAGE gel was prepared in gel cassettes (Bio-Rad). Firstly, 12% resolving gel was made (dH_2O, 30% acrylamide, 1M Tris pH 6.8, TEMED, 10% SDS, 10% Ammonium persulfate) and poured into the cassette; 3ml of isopropanol (Fisher Scientific) was added to level the surface of the top of the gel. The isopropanol was poured out after the gel had set, and a 12% stacking gel (dH_2O, 30% acrylamide, 1.5M Tris pH 8.8, TEMED, 10% SDS, 10% Ammonium persulfate) was added to the cassette, followed by a 10-well comb. After the gel had fully set, the comb was removed, and the cassette was placed securely in a tank (Bio-Rad) and filled with 1X Tris-glycine-SDS (TGS) (Sigma,) running buffer. Ten µg of protein was mixed with loading dye and boiled for 10 minutes at 95°C before loading onto the gel. The samples were run at 20V through the stacking gel, followed by 130V through the resolving gel until they reached the bottom. The gel was then removed and rinsed with water, followed by gently shaking in InstantBlue Coomassie Protein Stain (Expedeon) for at least 1 hour. Gel images were then taken on the ChemiDoc MP Imaging System (Bio-Rad).

CD1c-endo

Reduced and non-reduced fractions of the protein were analysed post HisTrap filtration as well as post SEC. A 4-12% SDS-PAGE gel (Invitrogen) was placed securely in a tank (Invitrogen) and filled with 1X Tris-glycine-SDS (TGS) (Sigma) running buffer. The gel was then loaded with 10µl of ladder and samples. For the non-reduced samples, 5µl of protein was mixed with 10µl of laemelli sample buffer (Bio-Rad); for the reduced samples, 5µl of protein was mixed with 10µl of laemelli sample buffer (Bio-Rad), DTT, and boiled for 5 minutes at 95^{o}C before loading onto the gel. The samples ran for 25 minutes at 200V. The gel was then removed and rinsed with water, followed by gently shaking in InstantBlue Coomassie Protein Stain (Abcam) for at least 1 hour. Gel images were then taken on the Gel Doc EZ Imager (Bio-Rad).

Isolation of CD14^{+} monocytes and CD3^{+} T cells from human blood

Blood was collected from various donors, these include healthy subjects, as well as those who have been previously exposed to *Mtb* and do not currently have an active infection. Approximately 50ml was collected in heparinised tubes and diluted 1:1 in PBS prior to layering 25ml over 15ml of Ficoll-Paque (GE Healthcare) in 4 x 50ml tubes and centrifuged at 2000rpm for 20 minutes. The buffy coat was harvested and washed in PBS followed by centrifugation at 1500rpm for 5 minutes to pellet cells. CD14^{+} monocytes were isolated using CD14 Microbeads (Miltenyi). Briefly, cell pellets were resuspended in MACS buffer (PBS, 0.5% BSA, 2mM EDTA) and incubated with CD14 microbeads at 4^{o}C to allow binding of beads to CD14^{+} cells before passing through a magnet-mounted MS column where microbeads bound to CD14^{+} cells remain for harvesting. The effluent was also collected to isolate autologous CD3^{+} T cells using the pan T cell isolation kit (Miltenyi). Briefly, the cells were pelleted and resuspended in an appropriate amount of MACS buffer before adding the antibody cocktail and incubating at 4^{o}C, microbeads were then added and the cell suspension was passed through the magnet mounted LS column where unlabelled CD3^{+} cells passed through. The CD3^{+} cells were cryopreserved in freezing medium (FBS, 10% DMSO) for later use.

Generation of CD1c$^+$ APCs

Trained monocyte-derived dendritic cells (MoDCs)

CD14$^+$ monocytes were seeded at 2x10^5 cells per well of a 24-well plate and cultured in Complete media (RPMI 1640, 1% Penicillin/Streptomycin Glutamine, 10% FBS) supplemented with either Lipopolysaccharide (LPS) (50ng/ml), β-glucan (5µg/ml), Mevalonate (500µM) (all Sigma) or UV-killed TB at multiplicity of infection = 1 (MOI=1) (Pasteur Institute, Paris) for 24 hours. The next day they were washed and cultured in Complete media supplemented with 20ng/ml IL-4 and 20ng/ml GM-CSF (MoDC media) for 5 days. CD1c is a marker for MoDCs, and its expression was analysed at day 5 by flow cytometry; trained MoDCs were stained with anti-CD1c-PE or its isotype control (BioLegend), PI, and acquired on FACSAria IIU (BD Biosciences) to confirm CD1c expression prior to co-culturing with T cells.

Traditional MoDCs

CD14$^+$ monocytes were seeded at 2x10^5 cells per well in a 24-well plate and cultured in MoDC media for 5 days to differentiate monocytes to MoDCs. CD1c expression was analysed at day 5 by flow cytometry; MoDCs were stained with anti-CD1c-PE or its isotype control (BioLegend), PI, and acquired on FACSAria IIU (BD Biosciences) to confirm CD1c expression prior to culturing with T cells.

Ex vivo expansion of T cells

CD1c coated MACSi beads

MACSi beads were coated with CD1c and used as artificial APCs (aAPCs) to stimulate T cell proliferation. Five million MACSi anti-biotin beads (Miltenyi) were placed in a sterile tube; 10µg of biotinylated CD2, 10µg of biotinylated CD28 (both Milentyi), and 10µg of biotinylated CD1c-SL monomers were added. The total volume was made up to 1ml using MACS buffer, this mixture was rotated at 4^{o}C overnight to allow the binding of proteins to the beads. Control beads were generated in the same way without the addition of the CD1c-SL monomers. The following day, one million beads were washed in media and pelleted at 400rpm for 5 minutes, before resuspending in 1ml of T

cell media 2 (RPMI, 10% human serum, 1% Penicillin/Streptomycin Glutamine, 1% Non-essential amino acids, 1% amino acid, 1% HEPES buffer). Beads were cultured with T cells (1:1 ratio) for 5 days. The media was supplemented at day 2 with 5 IU/ml IL-2 (Proleukin, Novartis) and was changed every other day. At day 5, some cells were stained with CD1c-SL tetramers, whilst the rest of the cells were re-stimulated by adding matching beads to each well for 24 hours. Those cells were stained at day 6 with T cell activation markers CD25 and CD137 before analysing by flow cytometry.

Trained and traditional MoDC-T cell cultures

Five days post differentiation of MoDCs, autologous T cells were added at $2x10^6$ per well and cultured in T cell media 2 (RPMI, 10% human serum, 1% Penicillin/Streptomycin Glutamine, 1% Non-essential amino acids, 1% amino acid, 1% HEPES buffer) supplemented with 100 IU/ml IL-2 (Proleukin, Novartis). The media was changed every 2 days and cells were stained and analysed by flow cytometry after 2 weeks.

THP1-mediated expansion

8 days method

Pan T cells purified by negative selection were labelled with CellTrace Violet (CTV) (Thermo Fisher) as per the manufacturer's instructions. Next, they were stimulated with irradiated (80 Grays) THP1 cells expressing CD1c (THP1-CD1c) at a 6:1 ratio, or with THP1 cells that were knockout for CD1c (THP1-KO) as a control. 4 days post stimulation, 10 IU/ml IL-2 (Proleukin, Novartis) was added per well. At 8 days post stimulation, cells were either stained with CD1c tetramers, or re-stimulated with THP1-KO or THP1-CD1c for 24 hours, and stained with the activation markers, CD25 and CD137. Cells were cultured in T cell media 2.

12 days method

Pan T cells from 3 healthy donors purified by negative selection were labelled with Tag-it Violet Proliferation Tracking Dye (BioLegend) as per the manufacturer's instructions and stimulated with irradiated (50 Grays) THP1-CD1c at a 10:1 ratio, or without THP1 cells, as a control. At On days 4, 6,

8, 10 and 12 post stimulation, 10 IU/ml IL-2 (Peprotech) was added. At 12 days post stimulation, cells were stained and sorted on live $CD3^+$ CTV^{lo} cells as described below. Cells were cultured in T cell media (RPMI, 5% Human Serum, 1% Penicillin/Streptomycin, 2mM Glutamine, 1% Non-essential Amino Acids, 1% Sodium Pyruvate).

Flow cytometry

The antibodies listed in *Table 1* recognising the indicated cell surface antigens were used (all BioLegend). For cell viability, either PI or LIVE/DEAD Dead Cell stains were used (Invitrogen). Prior to staining with antibodies of choice for 30 minutes at 4°C, T cells were blocked with 50% Human Serum (Sigma) for 20 minutes at 4°C, and washed with Sorting Buffer (HBSS, 1% Human Serum, 10mM HEPES, 2mM EDTA). Where T cells were also stained with tetramers, they were incubated with the kinase inhibitor Dasatinib (Cell Signaling) for 30 minutes at 37°C after being blocked with human serum, followed by a 30-minute incubation period with the tetramer, and then stained with the antibodies of choice for 30 minutes at 4°C. All data acquired was analysed using FlowJo v10 (FlowJo LLC).

Table 1: Antibodies and clones used during flow cytometry experiments.

Antibody target	**Clone**
CD3	UCHT1
CD4	RPA-T4
CD8	HIT8a
CD14	M5E2
CD25	M-A251
CD69	FN50
CD137	4-1BB
CD1c	L161
HLA-A, -B, -C	W6/32
HLA-DR, -DP, -DQ	Tü39
αβ-TCR	IP26
γδ-TCR	B1
β2m	A17082A
Isotype control	MOPC-21

CD1c expression

MoDCs: $CD14^+$ monocytes were differentiated to MoDCs as described above. On days 0, 4, and 6, CD1c expression was measured by flow cytometry. Cells were stained with anti-CD1c-PE or its isotype control (BioLegend), Propidium Iodide (PI), and acquired on FACSAria IIU (BD Biosciences) in order to determine the optimal time point for peak CD1c expression on MoDCs prior to culturing with T cells.

THP1 lines: THP1-CD1c and THP1-KO lines were stained with anti-CD1c-PE and its isotype control (BioLegend) and Live/Dead Aqua (Invitrogen). Cells were acquired on FACSAria IIU (BD Biosciences) to confirm the expression CD1c on THP1 cells.

Tetramer staining

CD1c-endo tetramers titration

Pan T cells from 3 donors, a positive control line (CD1c-restricted T cells) and a negative control T cell line were stained with tetramers and dextramers (made as described above) at 6 different concentrations per $1x10^6$ cells; 0.011, 0.033, 0.055, 0.11, 0.33, and 0.55µM. The cells were blocked with 50% Human Serum for 20 minutes at 4°C, washed with Sorting Buffer (HBSS, 1% Human Serum, 10mM HEPES, 2mM EDTA), and then incubated with the kinase inhibitor Dasatinib (Cell Signaling) for 30 minutes at 37°C, this prevents the down regulation of TCRs. They were then stained with the various amounts of CD1c-endo-PE tetramers or dextramers for 30 minutes at 4°C in the dark, followed by staining with anti-CD3-PerCP-Cy.5 (BioLegend), and LIVE/DEAD Violet Dead Cells stain (Invitrogen) for 30 minutes at 4°C in the dark. The stained cells were acquired on the IntelliCyt iQue Screener (Sartorius).

Expanded T cell cultures

MoDC and MACSi beads expanded cultures: cells were stained with 0.3µg of CD1c-SL-PE and CD1c-SL-BV421 tetramers, anti-CD3-APC (BioLegend), and PI. Live $CD3^+$ CD1c-SL^+CD1c-$endo^+$ T cells were sorted and cultured further to expand CD1c-restricted T cell populations where possible.

THP1 mediated T cell expansion: to determine the efficiency of the expansion prior to sorting, T cells were stained with 0.3µg of CD1c-SL-PE and CD1c-SL-BV421 tetramers, anti-CD3-FITC (BioLegend), Live/Dead Aqua (Thermo Fisher); the cells were acquired and sorted using the FACSAria IIU (BD Biosciences). Additionally, the cells were stained with 0.33 µM CD1c-endo-PE tetramer, anti-CD3-APC (BioLegend), and LIVE/DEAD Violet Dead Cells stain (Invitrogen); the cells were acquired using the IntelliCyt iQue Screener (Sartorius).

Functional assays

Activation induced marker (AIM) assay

MACSi beads: T cells stimulated with CD1c coated MACSi beads for an extra 24 hours were stained with anti-CD25-PE, anti-CD137-APC, anti-CD3-FITC (All BioLegend), and Live/Dead Aqua (Thermo Fisher).

THP1 cell lines: Pan T cells that were expanded with THP1-KO and THP1-CD1c were re-stimulated with THP1-KO or THP1-CD1c for 24 hours. The cells were then stained with LIVE/DEAD Violet Dead Cells stain (Invitrogen), anti-CD3-PerCP-Cy5.5, and the activation markers, anti-CD69-PE, and anti-CD137-PE/Cy7 (all from BioLegend). All cells were acquired using the MA900 Cell Sorter (Sony) and analysed using FlowJo v10 (FlowJo LLC).

IFN-γ assay

THP1-WT, THP1-KO, and THP1-CD1c cells were cultured overnight in Complete media (RPMI 1640, 10% FBS, 1% Penicillin/Streptomycin, 1% L-Glutamine), in the presence or absence of IFN-γ (1ng/ml). The next day they were stained with LIVE/DEAD Violet Dead Cells stain (Invitrogen), anti-HLA-A, -B, -C-PE, anti-HLA-DR, -DP,-DQ-FITC, anti-CD1c-APC, and anti-β2m-PerCP-Cy5.5 (BioLegend). All cells were acquired using the SH800 flow cytometer (Sony) and analysed using FlowJo v10 (FlowJo LLC).

T cells sorting and expansion

MoDC stimulated cultures

The FACSAria IIU (BD Biosciences) machine was set up to sort Live $CD3^+$ CD1c-SL-PE^+ CD1c-SL-$BV421^+$ T cells into a single tube. Depending on the number of cells sorted, 100-500 cells were placed in U-bottom wells of a 96-well plate with 150,000 irradiated feeder cells (PBMCs) in T cell media 2 supplemented with 1.6µg/ml phytohemagglutinin (PHA) (Sigma) and incubated at 37°C, 5% CO_2. Two days later, 100 IU/ml IL-2 was added per well and cell pellets from every set of 8 wells were transferred into 1 well of a 24-well plate when they become large, round and uniform. After 14 days, cells were stained with 0.3µg of CD1c-SL-PE and CD1c-SL-BV421 tetramers, anti-CD3-APC and PI. Live $CD3^+$ double $tetramer^+$ T cells were then sorted and cultured again as above; this was repeated 4 times until an enrichment in CD1c-reactive T cells was clearly visible.

THP1-CD1c expanded cultures

Two rounds of sorting were carried out for THP1-CD1c expanded T cells. In the first round, the FACSAria IIU (BD Biosciences) machine was set up to bulk sort either live $CD3^+$ CTV^{lo} CD1c-SL^+ cells, or live $CD3^+CD25^+CD137^+$ cells into single tubes. 20 cells were then transferred per well into round bottom wells of a 96-well plate with 200,000 irradiated feeder cells (PBMCs) in T cell media 2 supplemented with 1.6µg/ml PHA (Sigma) and incubated at 37°C, 5% CO_2. Two days later, 100 IU/ml IL-2 was added per well and cell pellets from every set of 8 wells were transferred into 1 well of a 24-well plate when they become large, round and uniform. After 21 days, cells were stained with 0.3µg of CD1c-SL-PE tetramer, anti-CD3-APC, and Live/Dead Aqua. Live $CD3^+$ CD1c-SL^+ T cells were then bulk sorted. Between 1 and 3 cells were transferred per well into round bottom wells of a 96-well plate with 200,000 irradiated feeder cells (PBMCs) in T cell media 2 supplemented with 1.6µg/ml PHA (Sigma) and incubated at 37°C, 5% CO_2. Two days later, 100 IU/ml IL-2 was added per well and cell pellets were pooled into 1 well of a 24-well plate when they become large, round and uniform. Additionally, following a separate round of expansion, the cells were stained and sorted twice. In the first round of sorting, live $CD3^+$ CTV^{lo} cells were sorted and placed in wells of a flat bottom 96-well plate with 200,000 irradiated feeder cells in T cell media supplemented with 1µg/ml PHA (Thermo Scientific), 100 IU/ml IL-2 (Peprotech), and incubated at 37°C, 5% CO_2. The cells were fed and/or split as and when required depending on growth rate. When a sufficient number of cells proliferated, they

were stained and sorted again. In the second round of sorting, previously sorted $CD3^+$ CTV^{lo} cells were stained with CD1c-endo-PE tetramer, anti-CD3-PerCP-Cy.5 (BioLegend), and LIVE/DEAD Violet Dead Cells stain (Invitrogen). Live $CD3^+$ CD1c-endo-PE $tetramer^+$ cells were sorted and seeded in flat bottom wells of a 96-well plate with 200,000 irradiated feeder cells in T cell media supplemented with 1µg/ml PHA (Thermo Scientific), 100 IU/ml IL-2 (Peprotech), and incubated at 37°C, 5% CO_2. All cells were acquired, and bulk sorted using the MA900 Cell Sorter (Sony). Although the cells were bulk sorted, they were seeded in six wells and treated as separate lines. Following expansion, the cells were cryopreserved.

Single cell sort for sequencing

Pan T cells from 3 donors were previously expanded with THP1-CD1c and live $CD3^+$ CTV^{lo} cells were sorted; following bulking up by stimulating with PHA, IL-2, and feeder cells as described above, live $CD3^+$ CD1c-endo $tetramer^+$ cells were single cell sorted directly into 96-well PCR plates. All cells were acquired and sorted using the MA900 Cell Sorter (Sony).

UV killed TB infection model

CD1c expression on TB infected THP1 cells

THP1-CD1c cells were infected with a range of MOIs of UV killed TB which was prepared in the CL3 lab by Dr L Tezera (Elkington group, University of Southampton). Briefly, *Mtb* was grown to an optical density of 0.60 when measured on the WPA cell density meter (this corresponds to 1 x 10^8 CFU/ml). The *Mtb* was then transferred to a UV illuminator and killed by exposure to high intensity UV light for 90 minutes. A stock suspension with an MOI of 10 was first prepared, 10-fold serial dilutions were carried out until an MOI of 0.0001 was reached. 50,000 cells were infected per MOI (0.0001, 0.001, 0.01, 0.1, 1, 10) and incubated in T cell media for 3 days. The cells were stained with anti-CD1c (BioLegend) at three time points (day 1, 2, and 3); cells infected with an MOI of 10 were also stained with an isotype control (BioLegend) at each time point. All cells were acquired using the FACSAria IIU (BD Biosciences).

THP1-T cell co-culture

THP1 cell lines were infected with UV killed TB at a chosen MOI. 50,000 infected cells were seeded per well in a 96-well plate, along with the control conditions; all cells were seeded in a volume of 100µl. 24 hours later, T cells of each line (CD1c-restricted and a control T cell line) were added to the THP1 cells at the desired ratio in a volume of 100µl, making the total media volume 200µl per well. The cultures were then incubated at 37^{o}C, and 5% CO_2 for 48 hours post the addition of the T cells. During the initial optimisation experiments, a 24-hour readout time point was included. In experiments where the effect of increasing the T cell ratio was investigated, T cell lines were added at ratios of 0.3, 1, and 10. In experiments where the effect of increasing the MOI of TB was investigated, the cells were infected with UV killed TB at three MOIs (0.1, 1, and 10). A stock suspension of an MOI of 10 was first prepared, 10-fold serial dilutions were then carried out until the desired MOIs were reached. The T cells were added at a 1:1 ratio. Each condition was set up in triplicate repeats, and the cultures were incubated for 48 hours before cytotoxicity was measured using the ToxiLight assay as described below.

ToxiLight cytotoxicity assay

T cell cytotoxicity against *Mtb* infected target cells was measured using a ToxiLight assay (Lonza), which was carried out as per the manufacturer's instructions. Briefly, 20µl of media from each well was transferred to a luminometer compatible 96-well plate, 100µl of ToxiLight reagent was then added. Following a 5-minute incubation period, the plate was read using a Glomax 20/20 Luminometer.

Luminex cytokine release assay

Cytokine release in cell culture supernatants was measured using a Cytokine Human Magnetic Panel for Luminex Platform assay (Invitrogen), which was carried out as per the manufacturer's instructions. Briefly, 25 µl of 1X antibody beads were incubated on a magnetic 96-well plate for 60 seconds before the liquid was discarded and the beads were washed twice with 200 µl of 1X Wash Solution. 25 µl of the Incubation buffer, Assay Diluent, and samples were then added to each well, and were incubated for 2 hours at room temperature in the dark whilst shaking. Following two washes with 200 µl of 1X Wash Solution, 50 µl of 1X SAV-RPE was added per well and incubated for

30 minutes at room temperature in the dark whilst shaking. Following three washes with 200 µl of 1X Wash Solution, 150 µl of 1X Wash Solution was added per well and incubated for 3 minutes whist shaking, before the plate was read on a Bio-Plex 200 machine (Bio-Rad).

TCR sequencing

Following single cells sorting, the Sequencing Team at Immunocore processed the samples to generate sequences. Briefly, after sorting the single cells into each well, they were lysed and an Oligo-dT primer was annealed to the Poly A tails of the mRNA, and reverse transcription is carried out to generate cDNA. During reverse transcription, unique adaptor PCR arms are added to the cDNA, primers that anneal to the unique PCR adaptor arms are then added to allow for the universal PCR amplification of all cDNA. Targeted PCRs were then preformed for each single cell to amplify the variable regions of TCRs, the products are barcoded with an 8-bp DNA sequence unique to each well. This results in each well containing paired alpha and beta, or gamma and delta chains from a single cell barcoded with the same well specific sequence. The PCR products were then purified and DNA fragments of 500-600bp were targeted. NGS libraries of the size-selected fragments were then prepared and barcoded using NEB kits, and sequenced using the MiSeq platform. Sequences of the CDR3, variable, and constant regions were obtained. The TCRseq was then further analysed using Seven Bridges software to generate the final sequences.

Amplification of gBlock DNA fragments

TCR sequences were synthesised as gBlock DNA fragments between 1586–1745 bases by Integrated DNA Technologies (IDT). Attempts to amplify the gBlock gene fragments were made using primer pairs and Q5 High-Fidelity DNA polymerase PCR reaction (NEB). The reactions were made in 50µl with 10ng of gBlock DNA fragments, and 0.5µM total concentration of each forward and reverse primers (*Table 2*), and the PCR programme used has been outlined below (*Table 3*). Temperature gradient PCR for a few samples were also carried out under the same conditions, with one modification, whereby a temperature range was tested from 56 ^{o}C - 66^{o}C. In all cases, the resulting PCR products were separated by electrophoresis on a 1.5% agarose gel at 90V for 30 minutes and visualised on a GelDoc machine (BioRad).

Table 2: Primer pairs for gBlock fragments amplification

TCR	V	Primer (5'-3')	Sequence
1	TRDV2	Forward	AAG CTG GCT AGC CAC CGC CAT TGA GTT G
	TRGV9	Reverse	TTG ATT GTC GAC TTT ATG ATT TCT CTC C
2	TRDV2	Forward	AAG CTG GCT AGC CAC CGC CAT TGA GTT G
	TRGV9	Reverse	TTG ATT GTC GAC TTT ATG ATT TCT CTC C
3	TRDV1	Forward	AAG CTG GCT AGC CAC CGC CCA GAA GGT TAC
	TRGV4	Reverse	TTG ATT GTC GAC TTT ATG ATT TCT CTC C
4	TRAV19	Forward	AAG CTG GCT AGC CAC CGC TCA GAA GGT AAC
	TRBV7-2	Reverse	TTG ATT GTC GAC TTT AGA AAT CCT TTC TC
5	TRAV24	Forward	AAG CTG GCT AGC CAC CAT ACT GAA CGT G
	TRBV2	Reverse	TTG ATT GTC GAC TTT AGC CTC TGG AAT C

Table 3: PCR programme for gBlock fragment amplification with Q5 High-Fidelity DNA polymerase

Temperature (°C)	Time (hh:mm:ss)	Number of cycles
98	00:00:30	1
98	00:00:10	35
56	00:00:16	
72	00:01:00	
72	00:01:30	1
4	Hold	

Vector and gBlock DNA fragments digestion and purification

The JM22 pELNS LV vector (from the Mansour lab) and gBlock DNA fragments were digested with the restriction enzymes NheI and SalI (NEB). For the vector, the digestion was carried out in a reaction that contained 6µg of plasmid DNA, 1X NEBuffer, 60 units of each restriction enzyme, and made up to a final volume of 300µl with water. For the gBlock fragment, the digestions were carried out in separate tubes for each sample, in reactions that contained 60ng of each gBlock, 1X NEBuffer, 10 units of each restriction enzyme, and made up to a final volume of 50µl with water. The reactions were then incubated at 37°C for 15 minutes, followed by 20 minutes at 65°C. The resulting products of both reactions were purified using a NucleoSpin Gel and PCR Clean Up kit (Macherey-Nagel), as per the manufacturer's instructions. For the vector digestion, the sample was first run on a 1%

agarose gel at 90V for 30 minutes before being visualised on a GelDoc machine (BioRad). The desired bands at ~8000bp were excised from the gel and then purified. For the gBlock fragments, the samples were eluted in 20µl of elution buffer at concentrations between 12.5-18 ng/µl following purification.

Quick Ligation reaction

The digested vector and gBlock gene fragments were ligated using a Quick Ligation Kit (NEB) as per the manufacturer's instructions. Briefly, for each sample, a 20µl reaction was set up; 50ng of the vector backbone was added along with 32ng of the digested gBlock fragment, 1X Quick Ligase reaction buffer with 1µl of Quick Ligase, and remaining volume was made up with water. The reaction was mixed with a pipette and incubated for 15 minutes at room temperature before being placed on ice and used to transform bacteria.

DNA Assembly reaction

The digested vector and gBlock gene fragments were ligated using an NEBuilder HiFi DNA Assembly Master Mix (NEB) as per the manufacturer's instructions. Briefly, the vector (50ng) and gBlock fragments were added in a 1:2 ratio, along with 10µl NEBuilder HiFi DNA Assembly Master Mix, and made up to 20µl with water. The reaction was mixed with a pipette and incubated for 15 minutes at 50^{o}C before being placed on ice and used to transform bacteria.

Transformation of E. Coli bacteria and DNA analysis

Stable Competent *E. coli* (NEB) was transformed with the plasmid products from the Quick Ligation reaction (5ng), or 2µl of the DNA Assembly reaction. In both instances, the 10µl of *E. coli* was thawed on ice for each sample, and the DNA was added and mixed with a pipette. The mixtures were then placed on ice for 30 minutes before being heat shocked at 42^{o}C for 30 seconds, and returned on ice for 2 minutes. 100µl of room temperature SOC media (NEB) was added to each sample and the tubes were incubated at 37^{o}C for 30 minutes with shaking (250 rpm). LB Agar plates containing ampicillin were warmed at 37^{o}C, and the samples were added to the plates and spread and incubated at 37^{o}C overnight. Colonies that grew were picked and grown in 5ml of LB broth containing carbenicillin

(1:1000) before extracting the DNA using a QIAprep Spin Miniprep kit (Qiagen). The DNA samples were then sent to Genewiz for sequencing.

Statistical analysis

The statistical significance of the efficiency of enrichment of CD1c-reactive T cells following several rounds of expansion was tested using unpaired t-test and Wilcoxon test. Furthermore, a one-way ANOVA and Tukey's multiple comparison test was used to test the differences in CD1c expression on MoDCs at different time points. Cytotoxicity measured via the ToxiLight assay was tested using a two-way ANOVA and Tukeys multiple comparison test. This was used in the experiments where the effects of the T cell dose-dependent response, and MOI effect were investigated. This was also used in earlier optimisation experiments to test differences between both T cell lines when cultured with infected THP1-CD1c. Additionally, two-way ANOVA and Tukeys multiple comparison test was carried out for all Luminex data analysis to test the statistical significance of the cytokines released under different conditions. Moreover, a two-way ANOVA and Šídák's multiple comparisons test was carried out to test the differences between both T cell lines when cultured with infected and uninfected THP1-CD1c. Lastly, paired t-tests were used to test the statistical significance of the biotinylation of CD1c proteins, and the effectiveness of THP1-CD1c mediated T cell expansion; as well as to test the statistical significance of the cytotoxicity caused by the T cell lines when cultured with THP1-KO and THP1-CD1c (infected), when increasing the MOI of UV killed TB. Prior to carrying out statistical analyses, the normality of all data sets were tested by the Shapiro-Wilk test. GraphPad Prism 10 Software was used for all statistical analyses.

Chapter 3 Optimising the methodology for the specific expansion of CD1c-autoreactive T cells

In order to characterise CD1c immunity in TB, we first sought to expand CD1c-auotreactive T cells from human blood. Our aim was to first generate a robust and consistent method of expanding these populations so that they may be applied in TB infection models to study cellular responses. We utilised CD1c expressing cell lines, as well as artificial systems to expand CD1c-autoreactive T cells; we also generated our own CD1c tetramers in-house using a bacterial expression system, so that they could be used in tetramer guided cell sorting. Additionally, we identified several cell-mediated expansion methods that were successful to different extents, these are reviewed below.

Initially, we used MoDCs as they can be robustly differentiated from monocytes and express high levels of CD1c. Using trained and traditional MoDCs mediated expansion was successful to a certain extent. However, we found that although MoDCs resulted in slight expansions in the CD1c-reactive T cell populations, using THP1-CD1c mediated T cell expansion appears to be a more specific and efficient method of expansion. Additionally, in order to further increase the proficiency of this method, the CTV negative T cells were isolated using CD1c-SL tetramers; this is an extra measure to ensure that the T cells have specifically proliferated in response to CD1c. However, whilst CD1c-SL tetramers have been an invaluable tool in identifying and isolating CD1c-autoreactive T cells, due to issues in the production process we decided to use CD1c tetramers generated using a mammalian expression system. Mammalian CD1c tetramers can be generated robustly and are widely used in the field to identify CD1c-autoreactive T cells. Overall, the T cells expanded with MoDCs can certainly be used to derive clones. However, we utilised THP1-mediated T cell expansion due to its higher specificity and efficiency.

Generation of working CD1c-SL tetramers by oxidative refolding

Our lab has recently utilised CD1c tetramers to clone αβ [303] and γδ T cells [378]. Hence, the specific staining and isolation of CD1c-autoreactive T cells were attempted by using fluorescently labelled human CD1c tetramers.

To produce CD1c proteins for tetramer studies, fully refolded and biotinylated CD1c-lipid complexes were generated through oxidative refolding. To this end, completely denatured and reduced CD1c heavy chain and β2m inclusion bodies were expressed in *E. coli* Rosetta strains. The bacterial cultures were subsequently sonicated to release inclusion bodies that were then homogenised and washed.

The inclusion body proteins were solubilised in 6M guanidine solution; and 10ug of each protein was analysed on an SDS-PAGE gel. The results shown in Figure 5A indicate the presence of clear bands for CD1c and β2m in lanes 2 and 3, respectively. These proteins underwent oxidative refolding in the presence of detergents and lipids. The refolded proteins were then purified using SEC, and further purified using anion-exchange chromatography (data not shown) whereby proteins are eluted on a salt gradient to identify different molecular species. Column fractions were collected and subsequently analysed on an SDS-PAGE gel to ensure the purest fraction was used for tetramerisation and subsequent T cell staining.

The presence of correctly refolded proteins in several fractions are indicated in the SDS-PAGE gels (Figure 5B). However, through extensive previous optimisation in our lab, we found that only fraction 2 stains T cells effectively. The refolded proteins were biotinylated, this is essential as it allows their tetramerisation and conjugation to fluorochromes. To confirm protein biotinylation, a biotin ELISA is carried out. The results revealed that refolded CD1c was biotinylated as observed by a strong biotinylation signal when compared to the negative control (Figure 6). To produce tetramers, the biotinylated proteins were conjugated to phycoerythrin (PE)- or Brilliant Violet 421 (BV421) - streptavidin. The tetramers were subsequently investigated for their binding to Jurkat T cell lines expressing the CD1c autoreactive TCR NM4 [303]. Figure 7 demonstrates the gating strategy employed when analysing the flow cytometry data for Jurkat T cells. The results indicated that CD1c-SL tetramers stained Jurkat NM4 T cells brightly, but they did not stain parental negative control Jurkats (Figure 8A & 8B) nor Jurkats expressing a CD1d reactive TCR (Figure 8C). Furthermore, CD1d tetramers stained Jurkat 4C12 but not Jurkat NM4, therefore confirming CD1c reactivity for NM4 TCR and further validating the specificity of CD1c-SL tetramers (Figure 8D & 8E).

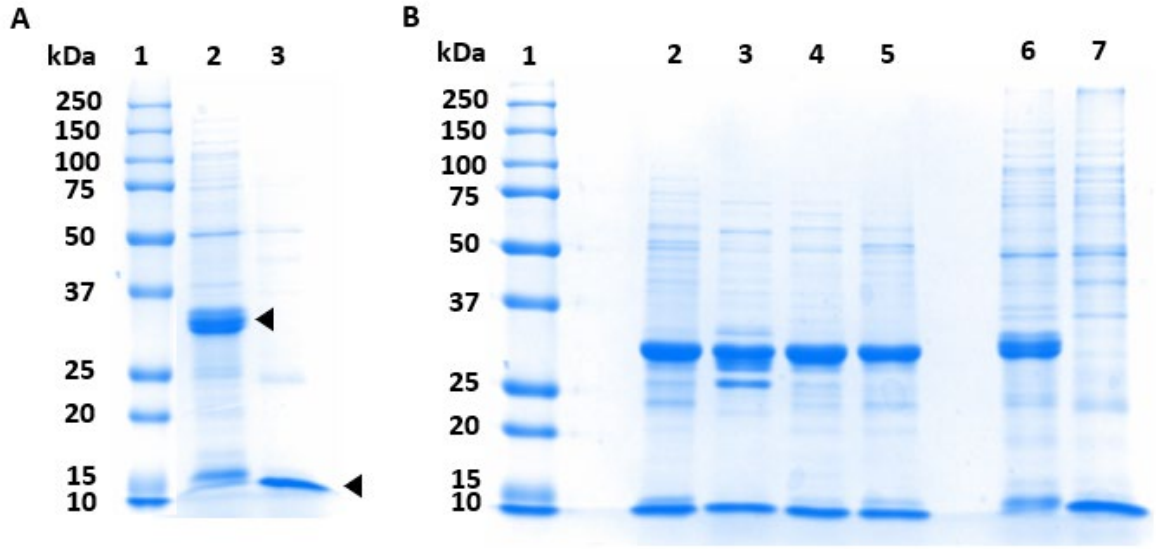

Figure 5: Separation of purified inclusion body proteins and refolded CD1c protein fractions. Representative images of SDS-PAGE gels separation confirming the formation and presence of CD1c proteins. (**A**) Lane 1: protein ladder, lane 2: CD1c heavy chain (indicated by black arrowhead), lane 3: β-2-microglobulin (indicated by black arrowhead). (**B**) Lane 1: protein ladder, lane 2: pre anion exchange (AE) refolded protein, lane 3: post AE fraction 1, lane 4: post AE fraction 2, lane 5: post AE fraction 3, lane 6: CD1c heavy chain, lane 7: β-2-microglobulin (lanes 6 and 7 were used as positive controls).

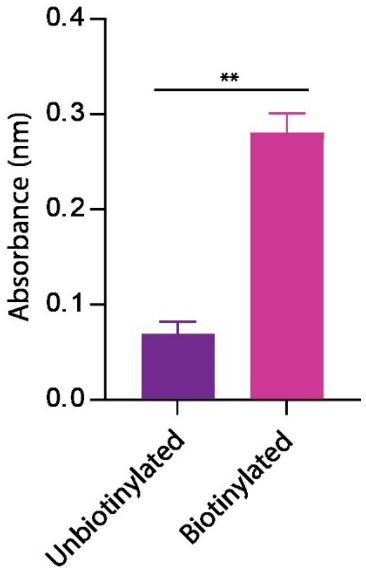

Figure 6: Confirmation of the biotinylation of CD1c proteins. Bar graph of biotinylated CD1c protein complex (grey bar) showing high levels of absorbance compared to an unbiotinylated control (purple bar) (*n*=3). Error bars represent SEM. ** $P < 0.01$ (paired t-test).

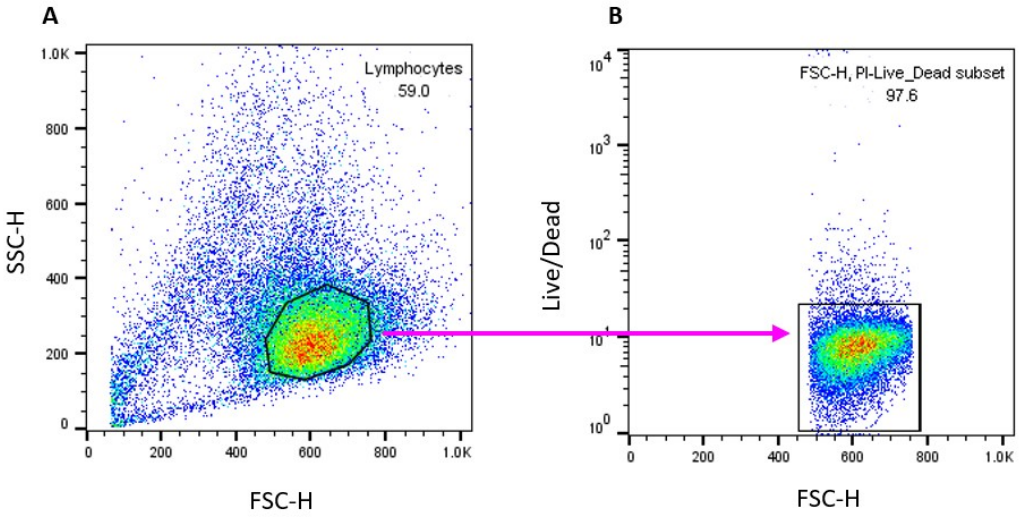

Figure 7: Flow cytometry gating strategy for Jurkat T cells. The flow cytometry dot plots indicate that cells were pre-gated on Jurkat lymphocytes (**A**), and viable cells that were PI negative were gated on for downstream analysis (**B**). Arrow indicates gating hierarchy.

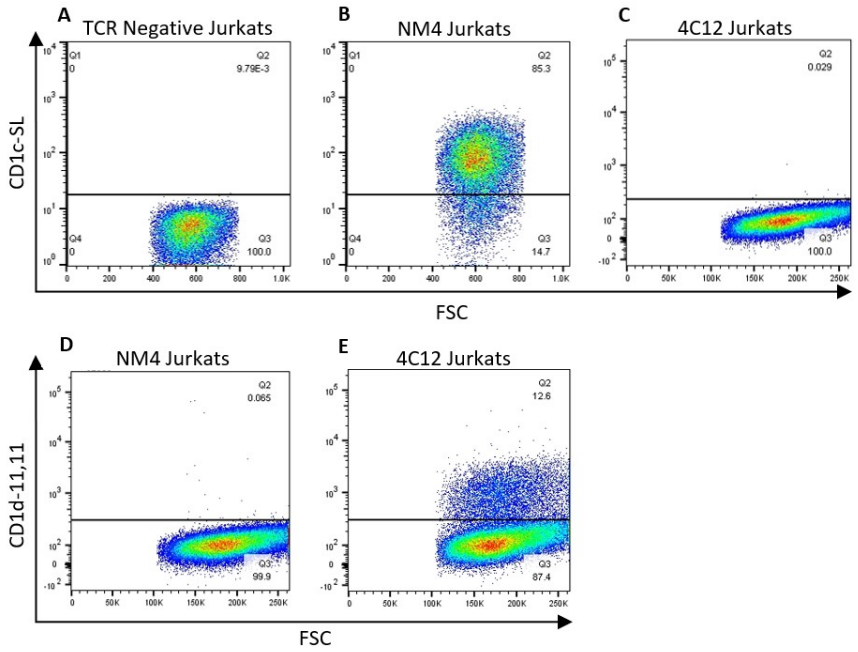

Figure 8: NM4 Jurkats express a CD1c reactive TCR that only stains with CD1c-SL tetramers. Flow cytometry dot plots showing CD1c-SL tetramer staining of NM4 Jurkats, which do not stain with a CD1d tetramer (CD1d-11,11). Parental "TCR negative" Jurkat T cells (**A**), and (**E**) CD1d restricted cells "4C12 Jurkats" served as controls when staining with CD1c-SL tetramers, highlighting the specificity of the tetramers to CD1c reactive TCR.

Various methods of T cell expansion

Having validated our CD1c tetramers as tools that stain specific T cells, we next sought to expand CD1c-autoreactive T cells using diverse *in vitro* expansion methods for subsequent tetramer guided T cell sorting and cloning.

MACSi beads

MACSi beads can be used as an artificial APC (aAPC) to activate T cells and stimulate their proliferation. To investigate whether MACSi beads can be used to specifically expand CD1c autoreactive T cells, anti-biotin MACSi beads (Miltenyi) were coated with biotinylated CD2, CD28, and CD1c. One million T cells were stimulated with one million beads before culturing for 5 days in the presence of IL-2. To investigate whether CD1c autoreactive T cells were specifically expanded, cultures were stained on day 5 with CD1c-SL tetramers. Figure 9 demonstrates the gating strategy employed when analysing the flow cytometry data for cultures expanded with MACSi beads. The results visibly showed CD1c tetramer bound cells in cultures stimulated with CD1c MACSi beads compared to control (Figure 10A & B). In parallel, cultures were re-stimulated with MACSi beads overnight before staining with the T cell activation markers CD25 and CD137. In agreement with the tetramer staining, the results confirmed a modest expansion of CD1c autoreactive T cells in cultures grown in the presence of CD1c conjugated MACSi beads (Figure 10C & D). Overall, despite the results suggesting that MACSi beads resulted in a slight increase in CD1c autoreactive T cells, they were not pursued further due to poor T cell expansions.

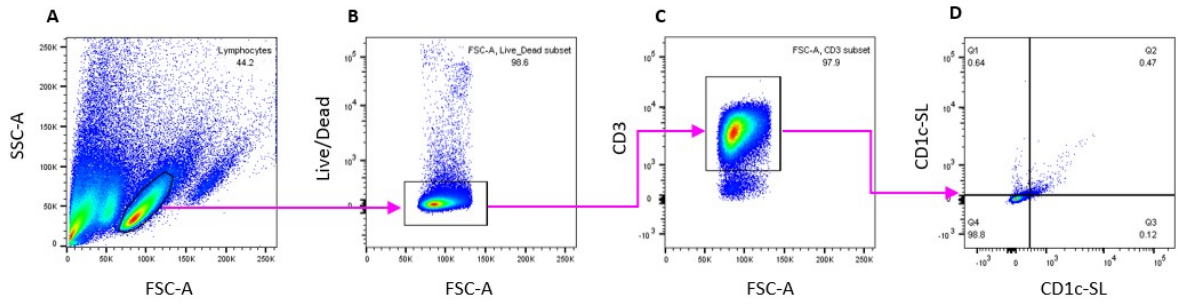

Figure 9: Gating strategy of cultured primary T cells. Representative flow cytometry dot plots showing the gating strategy employed to identify $CD3^+$ $tetramers^+$ T cells. Cells were first gated on lymphocytes (**A**), PI negative, live lymphocytes were then gated on (**B**), followed by $CD3^+$ T cells (**C**), before analysing double tetramer positive T cells (**D**). This gating strategy was used for all cultured T cells. Arrows indicate gating hierarchy.

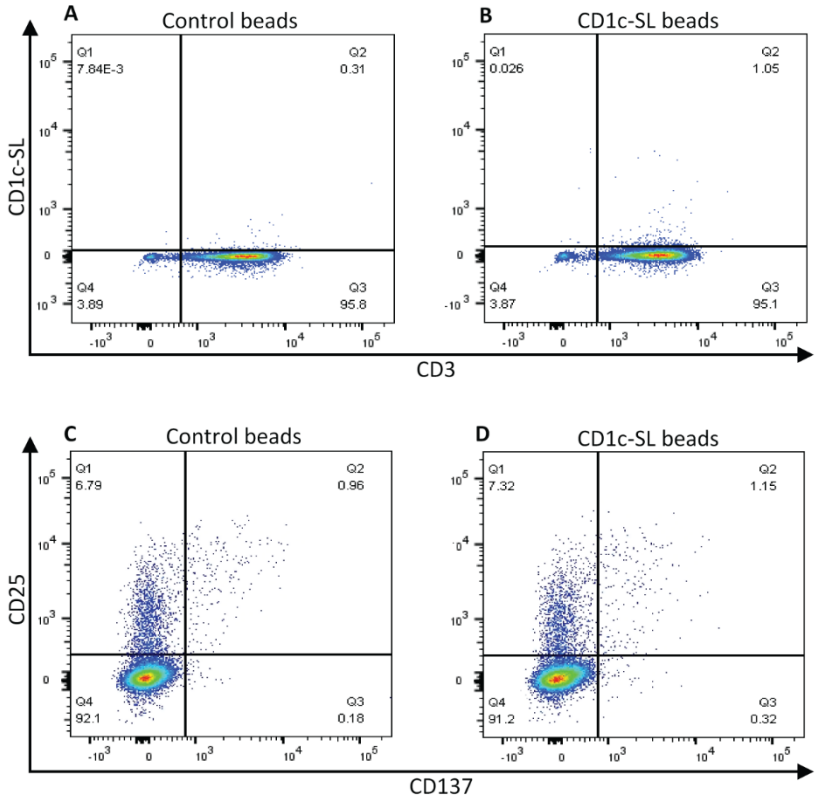

Figure 10: CD1c-SL conjugated MACSi beads resulted in weak expansion of CD1c reactive T cell populations. $CD3^+$ T cells were enriched by negative selection before culturing with MACSi beads (*n*=1 healthy blood donor). Flow cytometry dot plots show that CD1c-SL beads resulted in small populations of T cells that stained with CD1c-SL tetramers (**B**), and were $CD25^+$ $CD137^+$ (**D**). The control MACSi beads used were not coated with CD1c-SL (**A** & **C**).

Traditional and trained MoDC mediated T cell expansion

The generation of CD1c-reactive T cells using MoDCs is well established in the literature and has been applied for over 20 years [329]. MoDCs express high levels of CD1c and are able to effectively expand autologous T cells resulting in the enrichment of specific populations. Subsequently, CD1c-reactive T cells can be derived and cloned from these populations, and their phenotype and function further investigated.

Additionally, monocytes that are briefly stimulated with a bacterial antigen have been shown to generate a greater immune response upon restimulation with a secondary bacterial stimulus, this is due to epigenetic reprogramming resulting in a long-term proinflammatory phenotype in stimulated cells [464]; this is known as trained immunity. The response is reminiscent of adaptive immunity but takes place in innate cells such as monocytes. We reasoned that monocytes that have been trained

and subsequently differentiated to MoDCs may express even higher levels of CD1c and may potentially be more potent APCs, thus resulting in a better expansion of CD1c-autoreactive T cells.

Confirmation of CD14⁺ cell enrichment

Following the isolation of CD14⁺ cells from PBMCs using a MACS Miltenyi kit, flow cytometric analysis was carried out to confirm their enrichment. Post enrichment, CD14⁺ cells comprised 94.7% of the cell population (Figure 11). CD14⁺ cells were then either differentiated to MoDCs or trained as monocytes/MoDC as mentioned below.

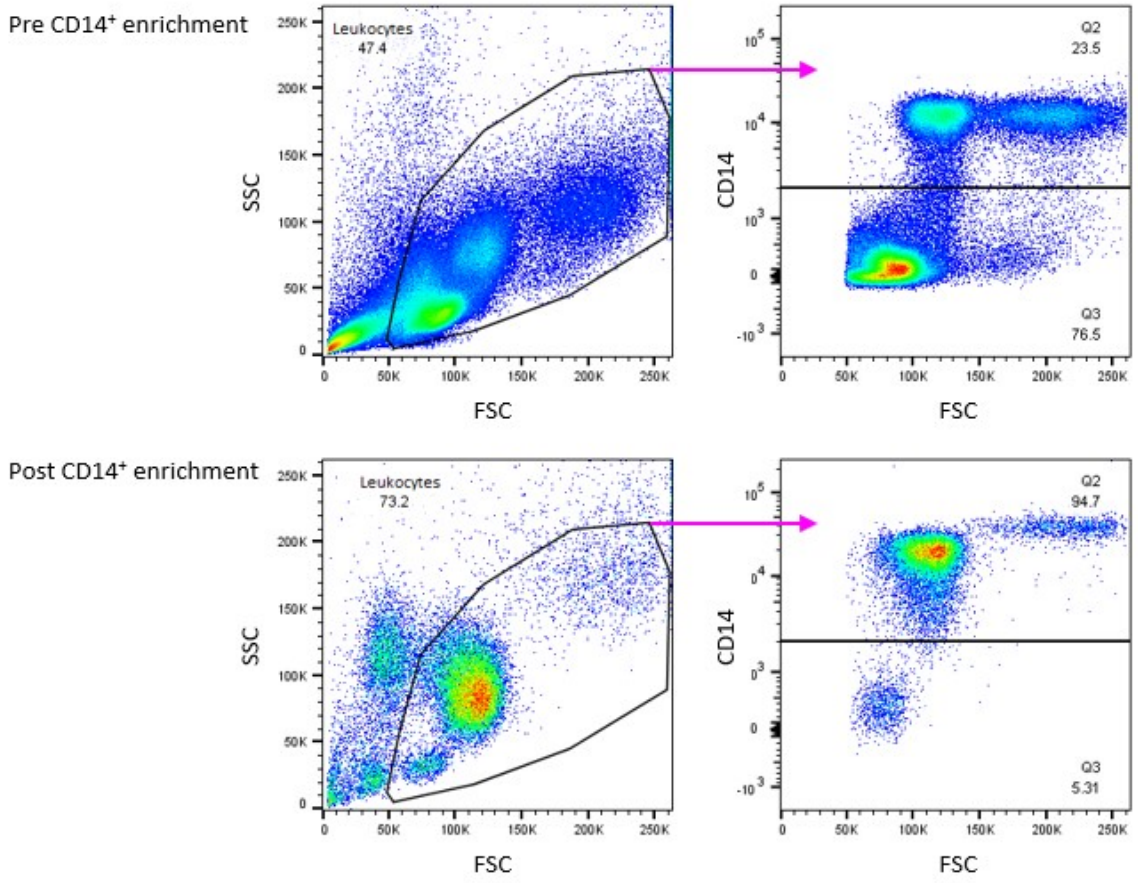

Figure 11: CD14⁺ cells are enriched post MACS isolation. Flow cytometry dot plots representative of the gating strategy used to confirm the enrichment of CD14⁺ monocytes that were isolated using magnetic sorting. Pre-enrichment, the majority of leukocytes gated were CD14⁻, whilst post CD14 MACS isolation the majority were CD14⁺. Arrows indicate gating hierarchy.

Determining peak CD1c expression in MoDCs

In order to ensure maximum efficiency of MoDC mediated expansion of CD1c-autoreactive T cells, flow cytometric analysis was carried out to determine a time point at which CD1c expression on MoDC surface was at its greatest. Cells were stained on day 0, to establish a baseline, followed by staining on days 4 and 6 post the addition of IL-4 and GM-CSF. The data suggested that between days 4 and 6, the expression of CD1c on MoDCs is at its peak (Figure 12). Consequently, day 5 was chosen as the time point at which T cells would be cultured with the MoDCs.

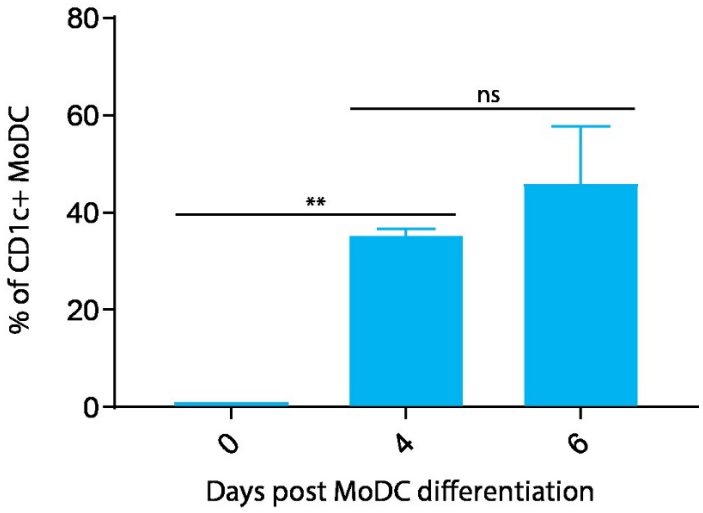

Figure 12: Peak expression of CD1c on MoDC cell surface occurs between days 4 and 6. MoDCs that were stained with anti-CD1c on days 0, 4, and 6 determined that CD1c cell surface expression plateaus by day 6 (*n* =3). Error bars represent SEM. ** $P < 0.01$ (one-way ANOVA).

Trained monocytes

Several published studies have demonstrated that monocytes exposed to various challenges develop a stronger immune response when encountering a secondary stimulus; trained innate immune cells are able to build short term immunological memory due to epigenetic reprogramming [465, 466]. We hypothesised that trained $CD1c^+$ monocytes may be efficient APCs that can expand CD1c autoreactive T cells. Firstly, we attempted to train monocytes using various stimuli, such as LPS, β-

glucan, UV-killed TB, and Mevalonate, before investigating their CD1c expression. MACS sorted $CD14^+$ monocytes were cultured with each stimulus for 24 hours, before being washed and cultured in media containing 10% human AB serum for 5 days at which point CD1c expression was analysed. On day 5, the expression of CD1c was absent on the cell surface of the trained monocytes as there was a similar lack of visible staining between anti-CD1c antibody, and its isotype control (Figure 13). It is important to note however, that by day 5, monocyte cell survival was very poor (data not shown), this could have impacted the expression of proteins. As an alternative solution, we attempted to train the monocytes before differentiating them into MoDCs.

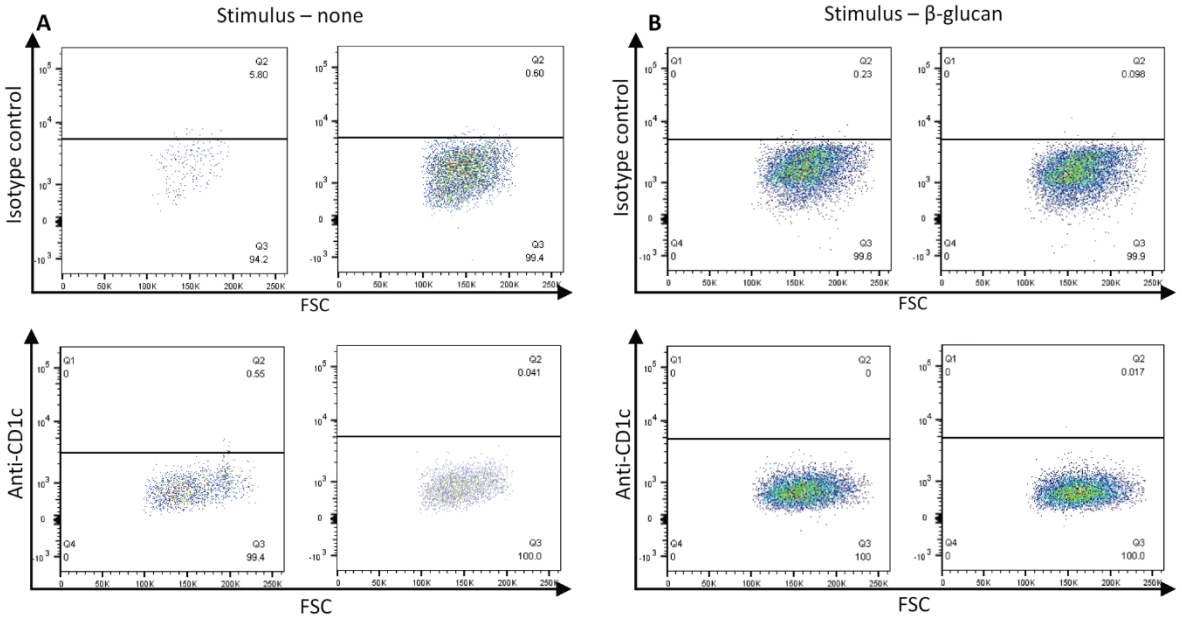

Figure 13: Trained monocytes do not express CD1c. $CD14^+$ monocytes from a subject previously exposed to TB were stimulated with various stimuli that induce trained immunity; CD1c expression was determined five days post stimulation. Flow cytometry dot plots representative of CD1c expression on monocytes that did not receive stimulus and were stained with either the isotype control (upper panel), or with an anti-CD1c antibody (lower panel) (**A**). Training with a stimulus such as β-glucan did not result in an increase in CD1c expression as shown by the flow cytometry dot plots of monocytes that were stimulated with β-glucan and stained with the isotype control (upper panel), or with an anti-CD1c antibody (lower panel) (**B**). This experiment was repeated twice, with triplicate wells in each experiment (*n*=2).

Trained MoDCs

In anticipation of better cell survival and to observe an upregulation of CD1c expression, MoDCs that were trained with various stimuli prior to differentiation were generated. MACS sorted $CD14^+$ monocytes were incubated with either LPS, β-glucan, UV-killed TB, or Mevalonate for 24 hours. Cells were then washed and cultured in MoDC media for 5 days to generate $CD1^+$ DCs [467]. Cell surface CD1c expression was determined by staining with anti-CD1c and its isotype control at day 5. We found that, of the total cells stained, untrained MoDCs had the highest frequency of $CD1c^+$ cells at 67.3%, with β-glucan, UV-killed TB, and Mevalonate having 41.6%, 37.6%, and 45.9% $CD1c^+$ cells, respectively; this suggested that training modulates expression of CD1c by MoDCs (Figure 14). Nevertheless, having found that monocytes did not express high levels of CD1c (Figure 13), whereas MoDCs did (Figure 16), we hypothesised that trained MoDCs might express even higher levels of CD1c, thus would be more potent at expanding CD1c-autoreactive T cells. We therefore utilised trained MoDCs as APCs and cultured them with autologous T cells at a 10:1 ratio (T cells:DCs). After 14 days of culture, T cells were stained with CD1c-SL tetramers. In addition, we employed double tetramer staining to further validate the binding of tetramers to bona fide CD1c-autoreactive T cells; a method previously employed in the literature [309]. Our results show that there were double tetramer bound T cells in wells cultured with β-glucan and mevalonate trained MoDCs (Figure 15B). However, due to 1) low number of cells acquired on the flow cytometer, and 2) poor viability of cultures, results from this experiment were inconclusive and this initial data set was not substantial enough to warrant proceeding with, or repeating these experiments.

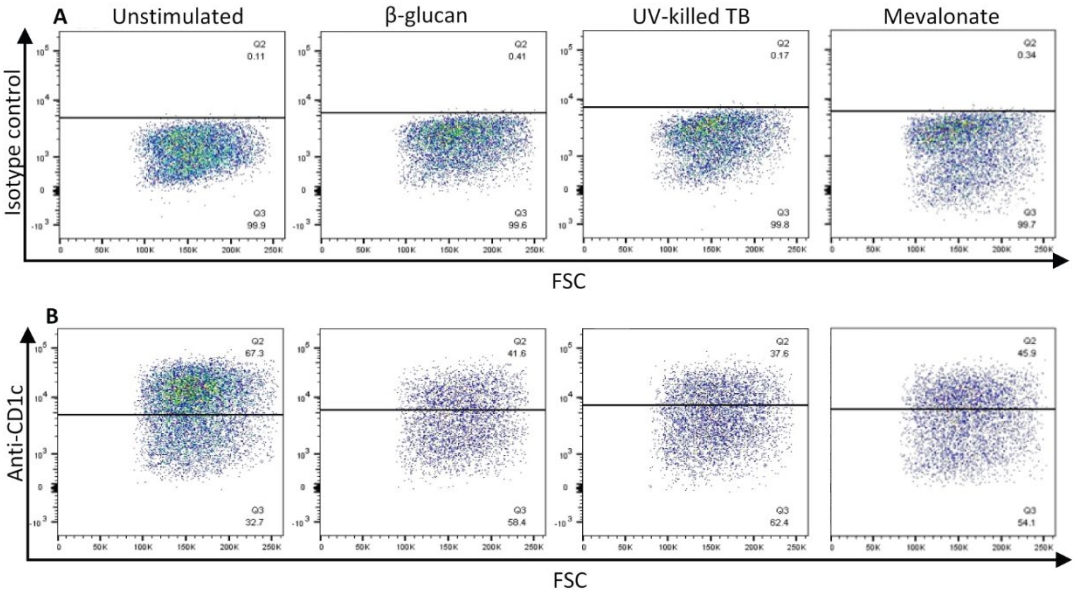

Figure 14: Training with specific stimuli seemingly modulates CD1c expression on MoDCs. $CD14^{+}$ monocytes were either unstimulated or stimulated with molecules that induce trained immunity in monocytes (*n*=1 blood donor previously exposed to TB). Flow cytometry dot plots show that training MoDCs with β-glucan, UV-killed TB, or mevalonate impacts CD1c expression, as indicated by CD1c staining (**B**). MoDCs stimulated with various stimuli were also stained with an isotype control antibody (negative control) (**A**).

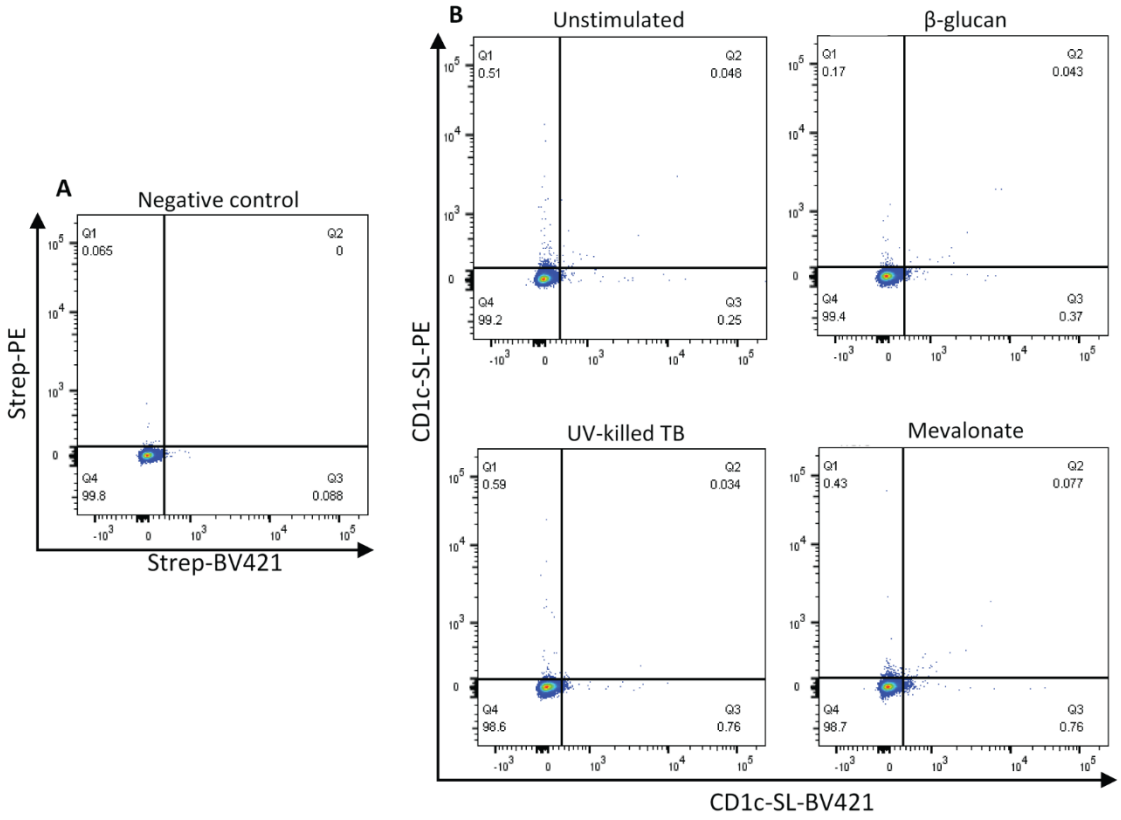

Figure 15: T cells stimulated with trained MoDCs stain with CD1c-SL tetramers. 14 days post stimulation with MoDCs trained with β-glucan, UV-killed TB, or mevalonate, live $CD3^+$ T cells were stained with CD1c-SL tetramers (*n*=1). Flow cytometry dot plots show that post stimulation with the various trained MoDCs, small populations of T cells that were double positive for CD1c-SL tetramers were present.

The use of trained MoDCs did not amplify the expansion of CD1c-restricted T cells as we had anticipated. We therefore sought an alternative MoDC mediated method, this time the cells were not trained prior to differentiation, and were generated in the traditional way.

Traditional MoDCs

In parallel to the above, CD1c-autoreactive T cells were also generated by culturing autologous T cells with MoDCs from 4 donors. MACS isolated $CD14^+$ monocytes were differentiated to MoDCs by culturing in MoDC media containing IL-4 and GM-CSF for 5 days. Cell surface CD1c expression was determined by staining with anti-CD1c at day 5 (Figure 16). The results revealed that across all

donors, 96.9-99.6% of MoDCs expressed CD1c. To expand CD1c-autoreactive T cells, autologous MoDC-T cell cultures were set up at a ratio of 10:1 (T cells:DCs) for 14 days before staining with two CD1c-SL tetramers (Figure 17). Not all donors had convincing CD1c tetramer$^+$ populations at day 14 (Figure 17B). Cultures derived from donors 1 and 3 did not have any CD1c tetramer$^+$ T cells by day 14 and were not cultured further. There were clear populations of CD1c-SL double tetramer$^+$ T cells present in cultures derived from donors 2 and 4 (Figure 17B). Furthermore, our results corroborate findings in the literature, as they indicated that traditional immature MoDCs were effective at proliferating CD1c reactive T cells. [327, 357].

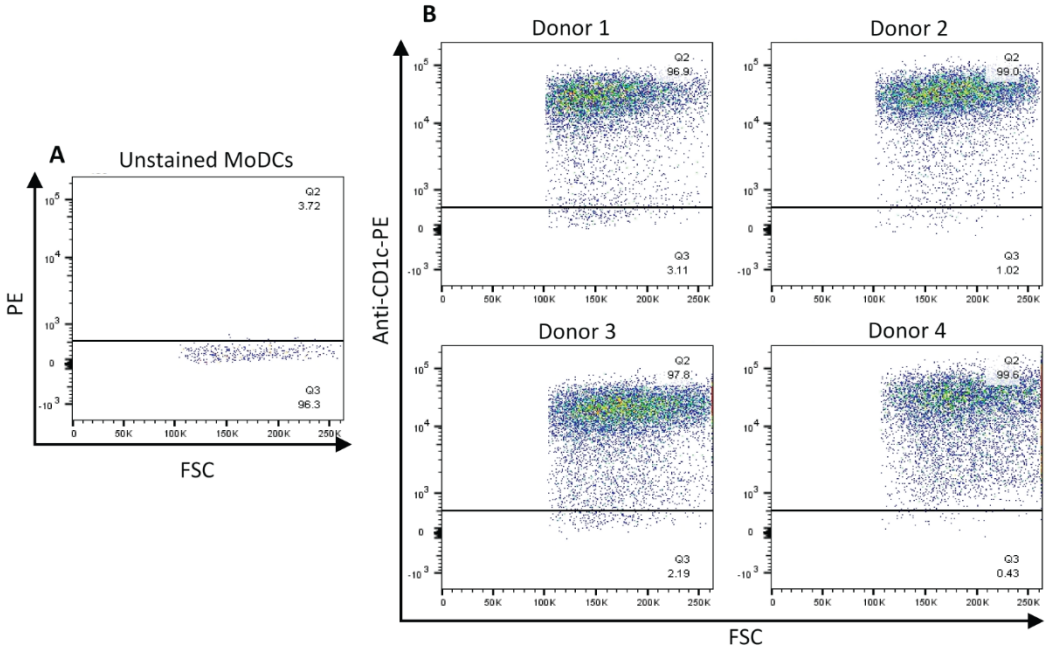

Figure 16: MoDCs express high levels of CD1c. MoDCs from several donors were stained with anti-CD1c antibody 5 days post differentiation (*n*=4; donors 1 & 2 are healthy subjects, donors 3 & 4 have previously been exposed to TB). Flow cytometry dot plots show that across all donors, MoDCs readily stained with CD1c. Unstained MoDCs were used as negative control due to unavailability of an isotype control at the time.

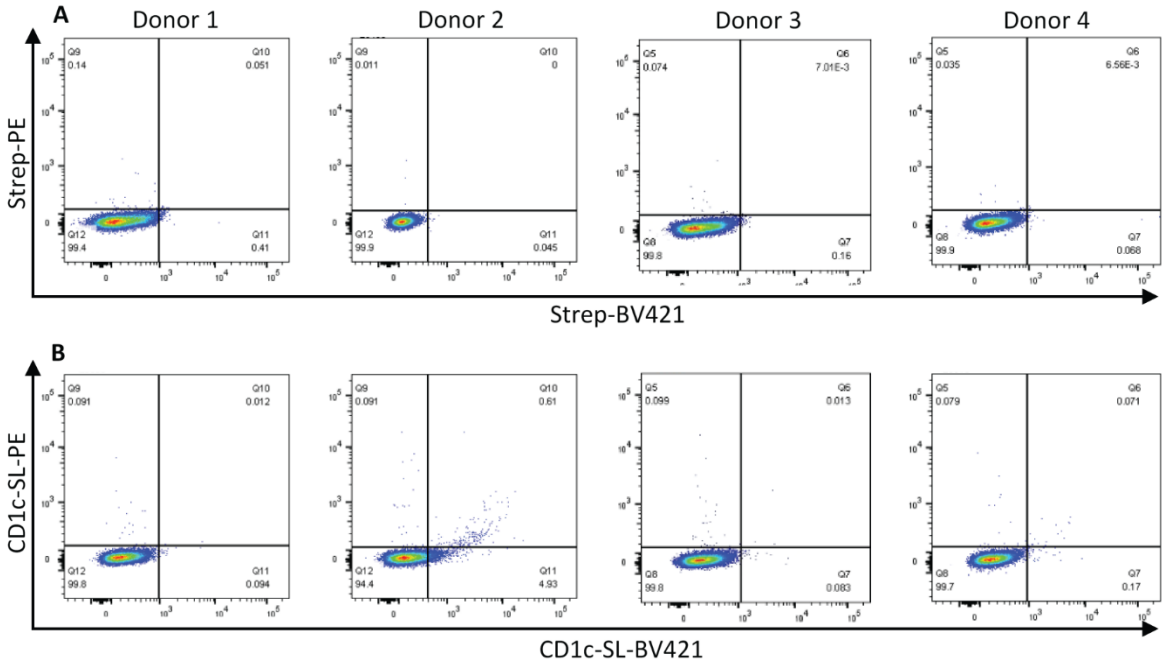

Figure 17: T cells stimulated with traditional MoDCs stain with CD1c-SL tetramers. T cells from healthy subjects (donors 1 & 2), and from subjects previously exposed to TB (donors 3 & 4), were isolated and stimulated with autologous MoDCs. This resulted in the expansion of T cell populations that were double tetramers positive (*n*=4). Flow cytometry dot plots show the negative control staining of T cells with CD1 unconjugated streptavidin-PE and streptavidin-BV421 (**A**), and the presence of single and double tetramer positive populations in T cells from all donors stained with CD1c-SL-PE and CD1c-SL-BV421 (**B**).

Tetramer guided enrichment of T cells

In order to enrich the CD1c-reactive T cell populations, T cells from donors with the greatest frequencies of CD1c-SL double tetramer$^+$ populations, namely cells from donors 2 and 4 were isolated. Sorted cells were seeded in 96-well plates at a density of 100-500 cells per well with irradiated feeder cells and stimulated with PHA. Two days post seeding, IL-2 was added to the culture media to enhance their proliferation. When large cell pellets formed, every set of 8 wells were pooled to generate T cell lines and maintained to promote culture expansion. After a sufficient number of cells proliferated, lines from both donors were screened again for CD1c-SL double tetramer$^+$ cells. A small population of T cells derived from donor 2 stained with both tetramers, but not cells from donor 4 (data not shown). Expansion and maintenance of T cell cultures continued with those derived from donor 2 only. Six T cell lines were eventually generated: P4.11, P4.12, P4.13, P9.33, P9.34, and P10. Fourteen days later, these lines were stained again, and CD1c-SL double

tetramer^{+} cells were sorted (Figure 18). This cycle was repeated 4 times in total to enrich the tetramer^{+} populations. This enrichment is evident in Figure 19. CD1c-autoreactive T cell clones can be derived from these lines for further characterisation.

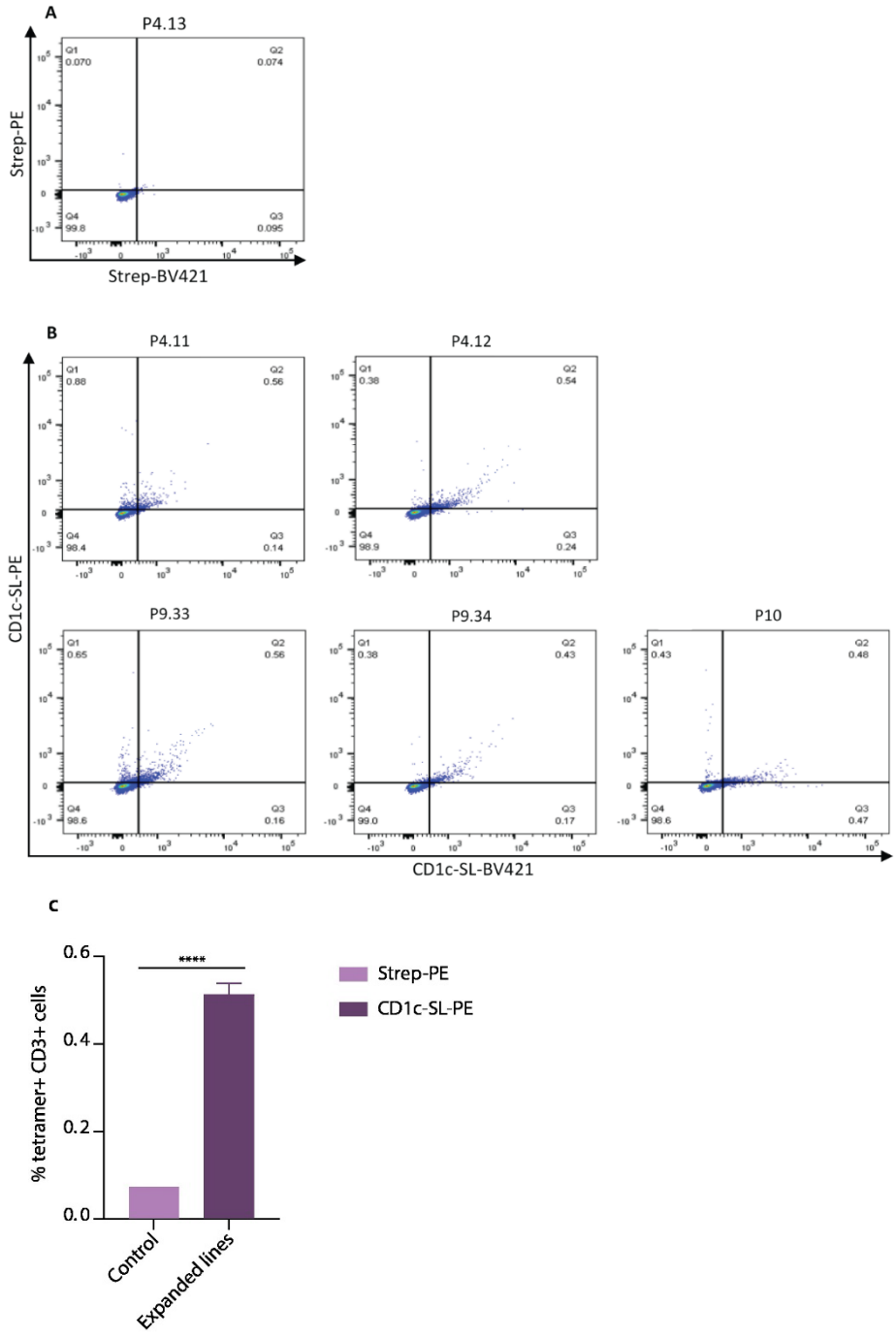

Figure 18: Sorted T cells stain with CD1c-SL tetramers. T cells that were isolated from a healthy blood donor using CD1c-SL tetramers guided sorting were expanded *in vitro* to generate several lines, and stained with CD1c-SL tetramers to confirm expansion of CD1c-reactive T cell populations (*n*=5). Flow cytometry dot plots showing negative control stain of a T cell line with CD1 unconjugated streptavidin-PE and streptavidin-BV421 (**A**), and dual staining of CD1c-SL (PE and BV421) tetramers in all T cell lines (**B**). Bar graph shows that expanded T cell lines contain a significantly greater percentage of tetramer positive T cells than control (**C**). Error bars represent SEM. **** $P < 0.0001$ (unpaired t-test).

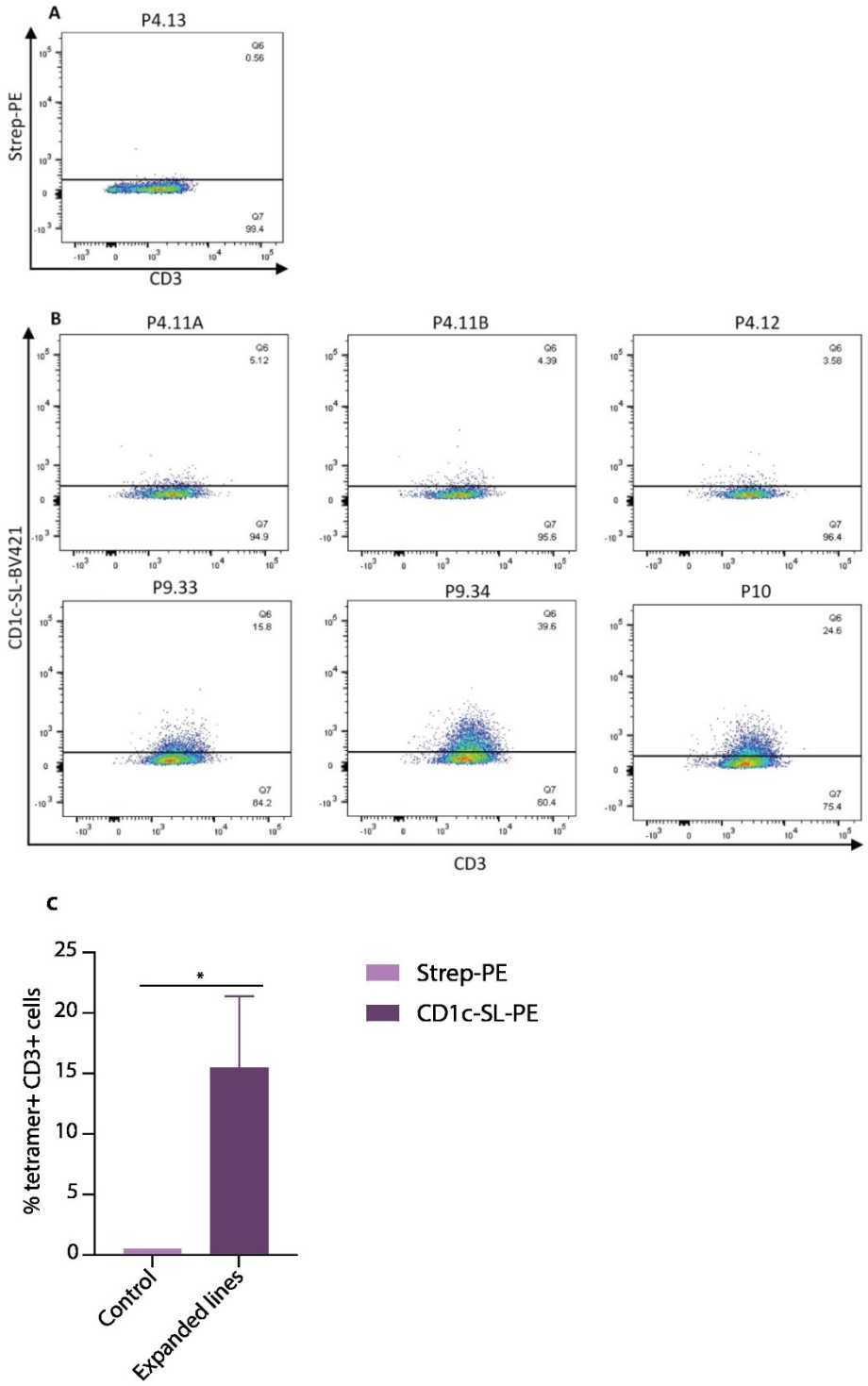

Figure 19: CD1c-reactive T cells initially expanded with MoDCs are enriched following several rounds of tetramer guided sorting. Flow cytometry dot plots show staining of an expanded T cell line with a negative tetramer (**A**), and expanded T cell lines with CD1c-SL tetramers (**B**), which determined that several lines were enriched (*n*=6). Following four cycles of sorting, T cell lines P9.33, P9.34, and P10 exhibited convincing tetramer positive populations, which can be further studied. Bar graph shows that expanded T cell lines contain a significantly greater percentage of tetramer positive T cells than control (**C**). Error bars represent SEM. * $P < 0.05$ (Wilcoxon test).

Whilst the traditional MoDC mediated T cell expansion was more effective than trained MoDCs, the APCs still express other cell surface markers that may cause the expansion of T cells in a non-specific manner. We therefore explored other methods which are more specific to CD1c, such as an engineered cell line overexpressing CD1c which does not express other antigen presenting molecules such as MHC class I and II.

THP1-CD1c mediated T cell expansion

THP1 cells are a commercially available human monocytic leukaemia cell line. They are often used in studies as APCs to validate T cell reactivity, or to expand specific T cell populations by expressing specific antigen receptors on their cell surface. For example, the role of CD1a-autoreactive T cells in the response to contact sensitisers has been validated using THP1 cell lines expressing CD1a. Skin T cells were activated by THP1-CD1a in the absence of exogenous antigens, and the stimulatory response was blocked by anti-CD1a antibodies [468]. Additionally, THP1 cells transduced with MR1 were used to expand and isolate MR1-autoreactive T cells allowing their characterisation [469].

THP1 cell lines are immortalised and easy to maintain in culture, which is particularly advantageous for long term experiments. Moreover, they are readily transduced and express consistent and stable levels of protein, whereas MoDCs can be short lived in comparison and can have donor-dependent variation in their expression of proteins [468].

Here, THP1 cells that are CIITA/β2m double knockouts and have been transduced with CD1c (THP-CD1c) are used to expand CD1c-autoreactive T cells. The aim was to establish a more robust and consistent method of deriving antigen specific T cells that can be further characterised in downstream studies.

Validation of THP1 cell lines

The THP1-CD1c and THP1-KO cell lines were generated by our collaborators at Immunocore. First, β2m and Class II transactivator (CIITA) were knocked out from the THP1-WT cell line using CRISPR-Cas9 technology. Knocking out β2m results in the lack of expression of any protein associated with β2m on the cell surface. With regards to antigen presenting molecules, this means that whilst members of the CD1 family, MR1, and MHC class I proteins are still synthesised intracellularly, they do not traverse to the cell surface as their expression requires β2m. Additionally, CIITA is a

transcriptional co-activator that regulates the transcription of MHC class II genes [470]. Consequently, knocking out CIITA results in the inability of these cells to upregulate the expression of MHC class II proteins upon activation. Following the knockout of β2m and CIITA, the cells were transduced using a lentivirus system with a plasmid containing a β2m-CD1c single chain gene construct (Figure 20) to generate the THP1-CD1c cell line. Three days post transduction, $CD1c^+$ cells were sorted and maintained in culture.

THP1-CD1c cells were subsequently used to expand T cells. This is regarded as a more stringent method of expanding CD1c-autoreactive T cells specifically due to the lack of expression of other antigen presenting molecules on the cell surface. MHC class II may be present but does not become upregulated upon activation of THP1-CD1c due to the absence of CIITA, thus does not contribute sufficiently to overcome the CD1c-mediated expansion of T cells. To validate the cell surface expression of CD1c on both these cell lines, flow cytometric analysis was carried out. The data in Figure 21 confirms the absence of CD1c on the THP1-KO cells, and its expression on THP1-CD1c cells. Additionally, to further validate these cell lines and ensure that the expression of HLA class I & II molecules were not upregulated upon activation, and thus could interfere with CD1c specific expansion, an IFN-γ assay was carried out. The cells were stimulated overnight with IFN-γ before being stained for HLA class I, class II, CD1c, and β2m, and undergoing flow cytometric analysis. IFN-γ does not result in increased staining of HLA class I & II in THP1-KO and THP1-CD1c whilst it does in THP1-WT cells (Figure 22).

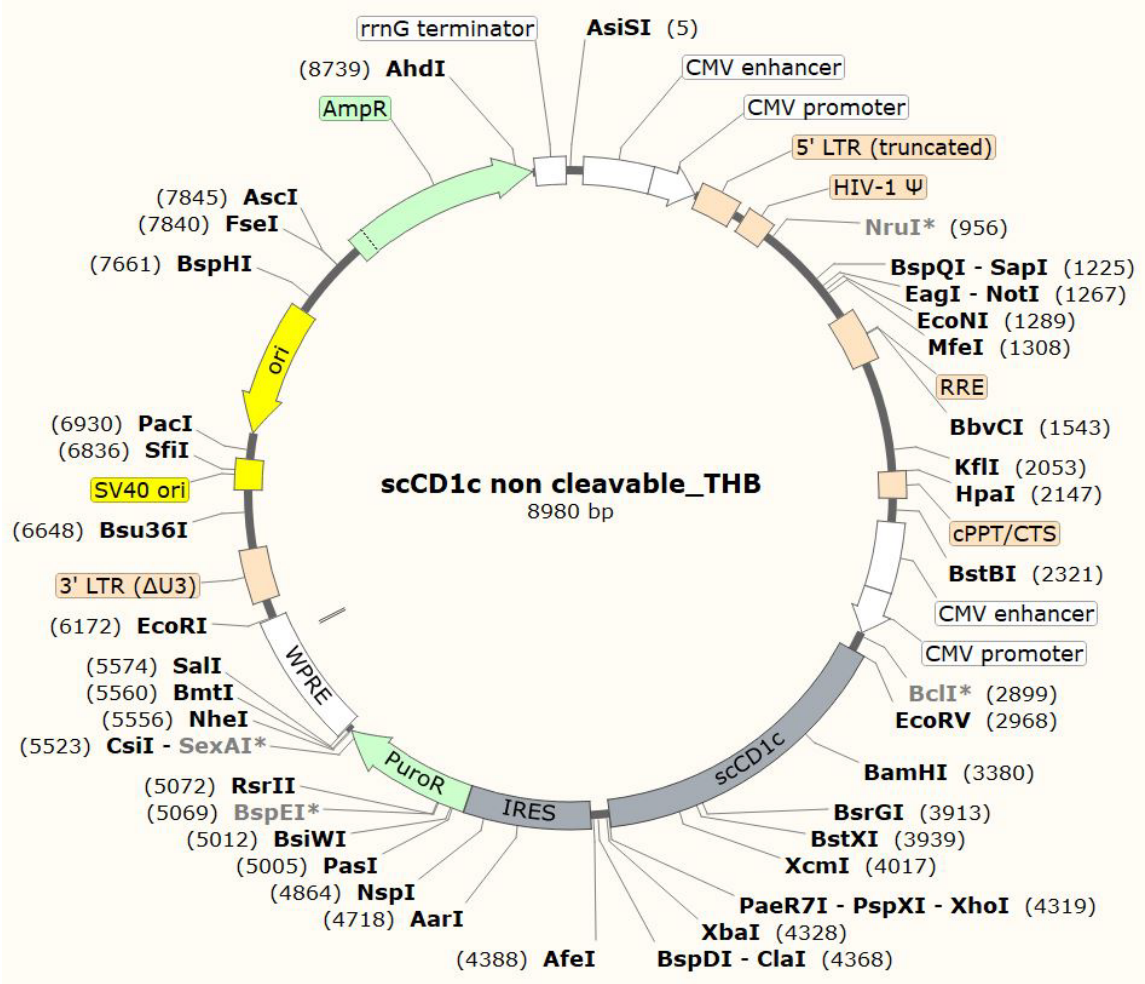

Figure 20: Schematic of lentivirus vector encoding CD1c used in the transduction of THP1 cells. CMV enhancer – human cytomegalovirus (CMV) immediate early enhancer; CMV promoter – CMV immediate early promoter; 5’ LTR (truncated) – truncated 5’ long terminal repeat (LTR) from HIV-1; HIV-1 Ψ – packaging signal of HIV – 1; RRE – the Rev response element (RRE) of HIV-1 allows for Rev dependent mRNA export; cPPT/CTS – central polypurine tract and central termination sequence of HIV-1; scCD1c – CD1c heavy chain and associated β2m; IRES – internal ribosome entry site of the encephalomyocarditis virus (EMCV); PuroR – puromycin resistance; WPRE – woodchuck hepatitis virus posttranscriptional regulatory element; 3’ LTR – self-inactivating 3’ long terminal repeat from HIV; SV40 ori – SV40 origin of replication; ori – ColE1/pMB1/pBR322/pUC origin of replication; AmpR – resistance to ampicillin, carbenicillin, and related antibiotics. Restriction enzymes sites indicated in bold.

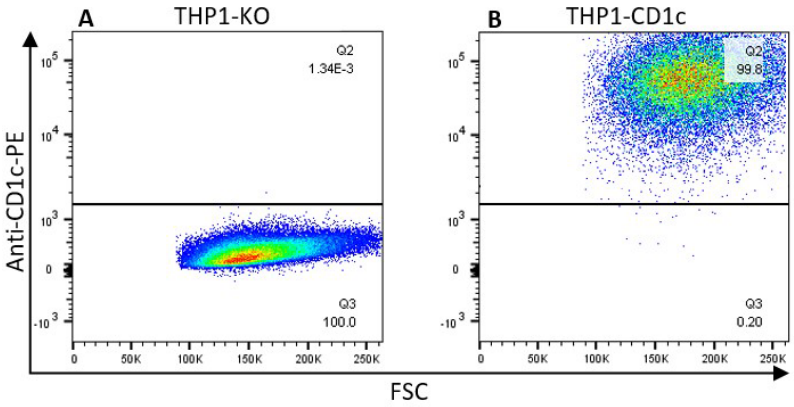

Figure 21: CD1c is expressed on THP1-CD1c and not on THP1-KO cells. Representative flow cytometry dot plots of THP1 cell lines stained with anti-CD1c show that CD1c is only expressed on THP1-CD1c cells.

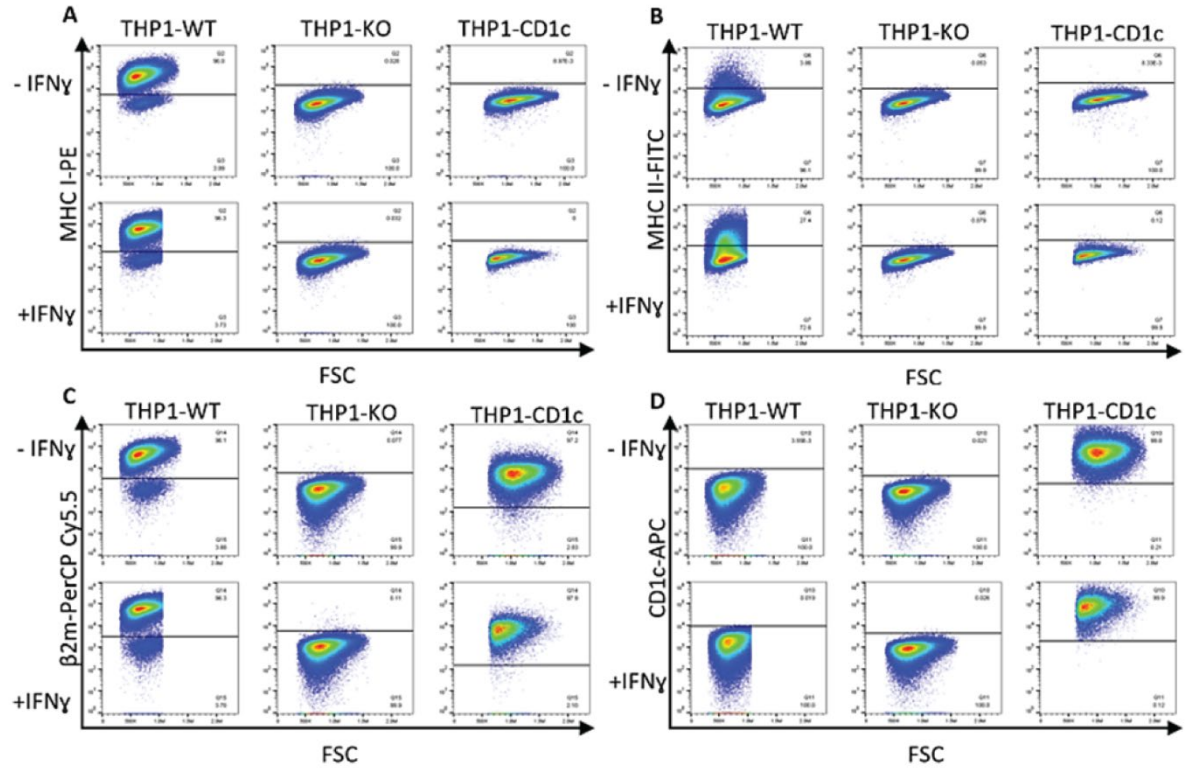

Figure 22: IFN-γ stimulation does not impact the expression of cell surface proteins on THP1 cell lines. THP1-WT, -KO, and –CD1c cells were stimulated with IFN-γ overnight and stained with (**A**) MHC I, (**B**) MHC II, (**C**) β2m, and (**D**) CD1c (*n*=1). Flow cytometry dot plots show that the expression of the cell surface proteins on the THP1-KO and THP1-CD1c were not affected by IFN-γ stimulation.

THP1-mediated expansion – day 8 CD1c tetramers staining

Using a short-term T cell expansion protocol optimised by our collaborators at Immunocore, T cells from 2 donors were cultured with irradiated THP1-CD1c cells that were used as APCs, and IL-2 was added to encourage proliferation. The THP1-KO line was used as a control. After 8 days, tetramer guided cell sorting was employed to isolate CD1c-SL tetramer^{+} T cells. To ensure that the isolated cells have proliferated in response to the APCs, the T cells were stained with Cell Trace Violet (CTV) prior to stimulation. CTV is a dye that readily crosses the plasma membrane of T cells and binds free amines in the cytoplasm and is retained intracellularly. As cells proliferate, their CTV signal diminishes as it gets diluted. This is demonstrated in Figure 23 A2 & B2, where T cells stimulated with THP1-CD1c have proliferated, exhibiting increased CTV^{lo} populations than those stimulated with THP1-KO (Figure 23 A1 & B1). Of the CTV^{lo} cell populations, those that are tetramer^{+} were sorted, and expanded as one line per donor. Subsequently, CD1c tetramer^{+} T cells (Figure 24A & B) were sorted again where they were seeded at lower densities per well to increase cloning efficiency. These sorting experiments generated 6 T cell lines per donor. The results in Figure 25 demonstrate the presence of tetramer^{+} populations in representative T cell lines from 2 donors. All T cell lines were cryopreserved for later use.

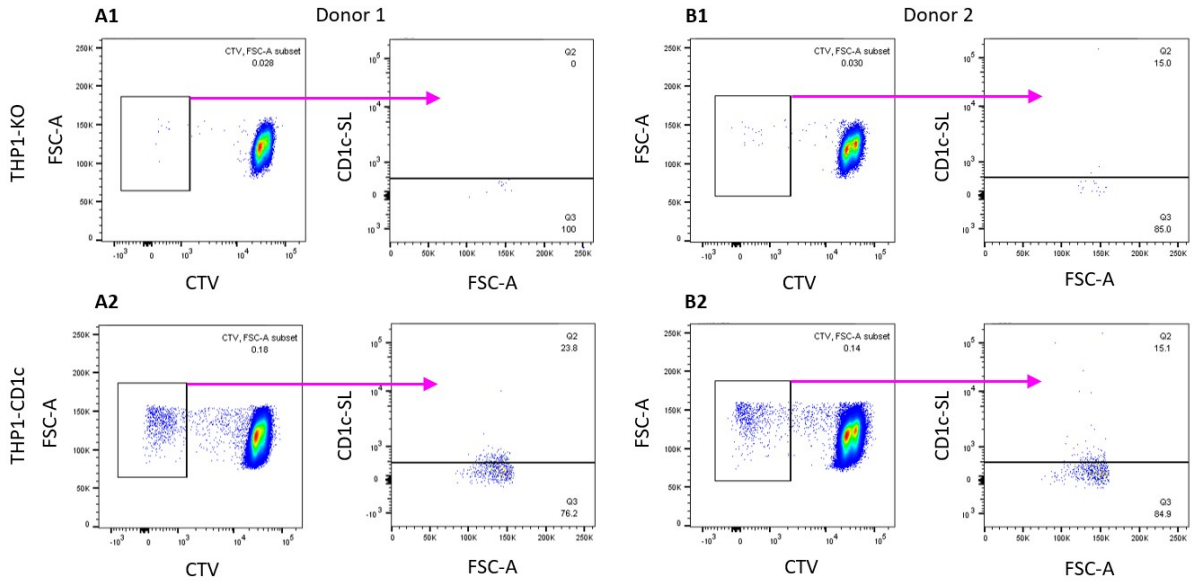

Figure 23: CTV staining further validates the expansion of CD1c-reactive T cells (first round of sorting). T cells expanded with THP1-CD1c had larger populations of CTV^{lo} newly proliferated cells that were also CD1c-SL tetramer positive (*n*=2. Donor 1 is a healthy subject, and donor 2 has previously been exposed to TB). T cells stained with CTV prior to stimulation indicate proliferation as the CTV signal diminishes, whilst CD1c-SL tetramers staining determines their specificity. Flow cytometry dot plots show live T cells that are CTV^{lo}, and were stained with CD1c-SL tetramers. T cells from both donors were stimulated with THP1-KO (**A1** & **B1**), and THP1-CD1c (**A2** & **B2**).

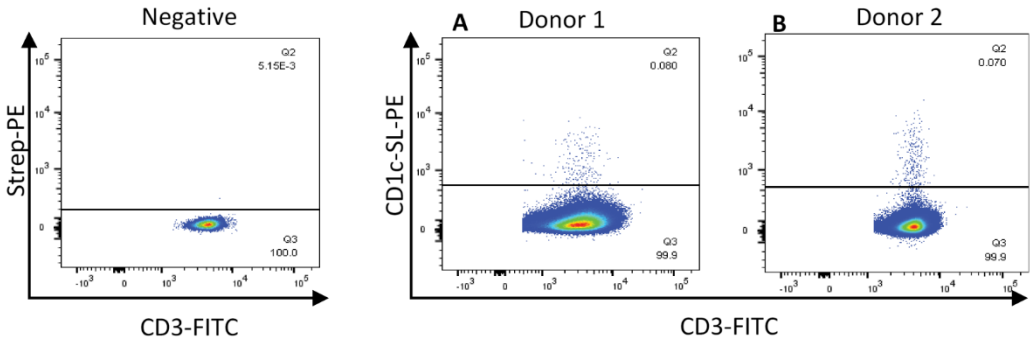

Figure 24: CD1c-reactive T cells that were initially sorted on CD1c-SL tetramer are enriched (second round of sorting). (**A** & **B**) Flow cytometry dot plots show live CD3^{+} cells with CD1c-SL tetramer^{+} populations in both donors (*n*=2).

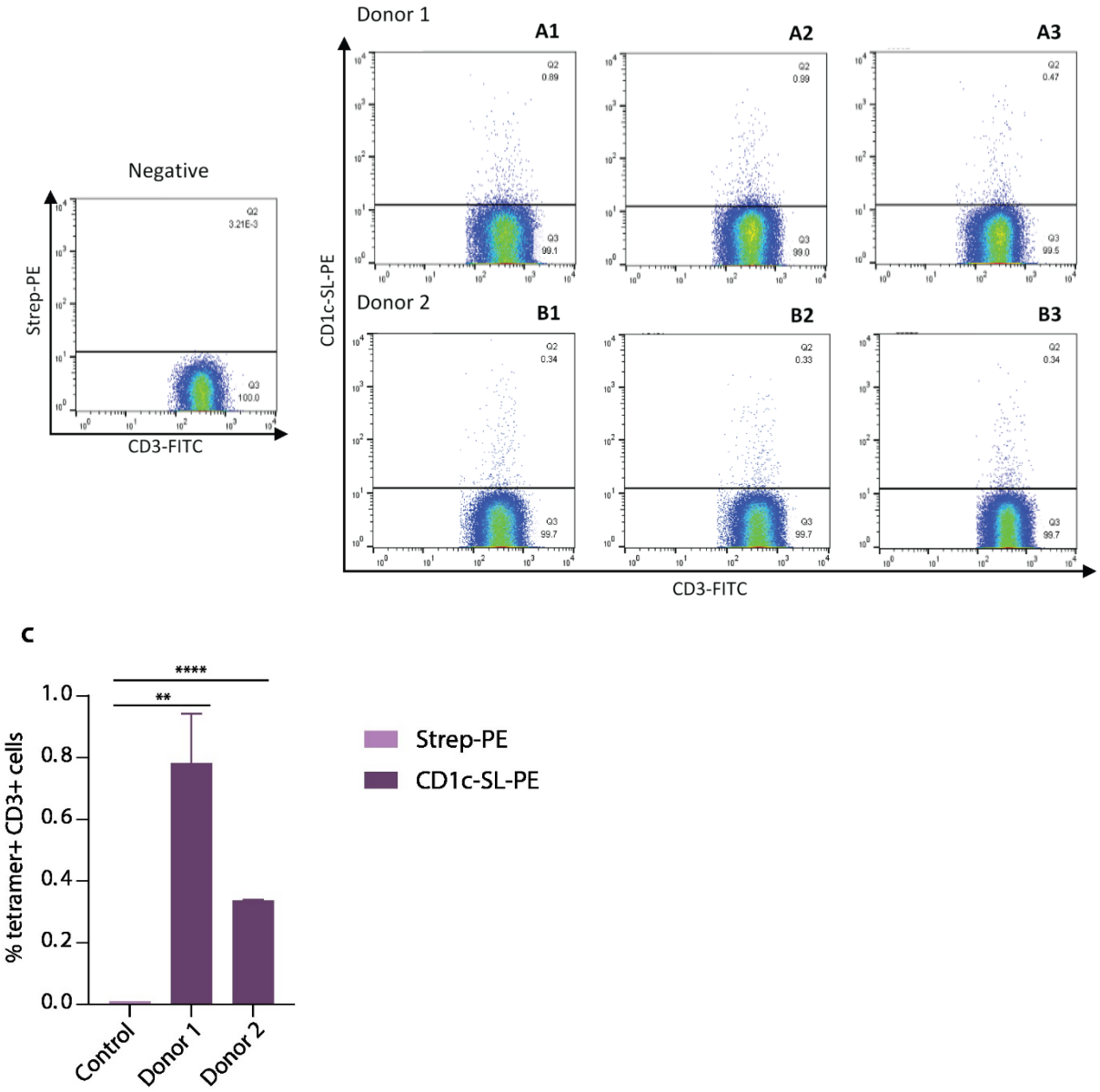

Figure 25: Cells that were initially sorted on CD1c-SL tetramers are enriched post expansion and stain with CD1c-SL tetramers. Representative flow cytometry dot plots show live $CD3^+$ CD1c-SL $tetramer^+$ populations in lines derived from both donor 1 (healthy subject) (**A1**-**A3**), and donor 2 (previously exposed to TB) (**B1**-**B3**) following several rounds of sorting and expansion (*n*=6). Bar graph shows that T cell lines from both donors contain significantly greater percentages of tetramer positive T cells than control (**C**). Error bars represent SEM. ** $P < 0.01$, **** $P < 0.0001$ (unpaired t-test).

THP1-mediated expansion – day 9 cell sort post 24h activation

To confirm reactivity of expanded T cell lines to CD1c, an Activation Induced Marker (AIM) assay was carried out. On day 8 post stimulation with THP1-KO or THP1-CD1c cells, T cells were stimulated for 24 hours with either THP1-KO or THP1-CD1c cells, before staining with the activation markers CD25 and CD137. Cells that were $CD25^{+}CD137^{+}$ were sorted and cultured further. Using activation markers in the isolation of CD1c-restricted T cells is a way of ensuring that the sorted cells are specifically reactive to CD1c. This is demonstrated in Figure 26, where we found larger populations of $CD25^{+}CD137^{+}$ T cells in cultures stimulated with THP1-CD1c compared to those cultured with THP1-KO cells. These cells underwent several rounds of sorting and subsequent expansion before staining with CD1c-SL tetramers (Figure 27). Further rounds of sorting and expansion generated 6 lines per donor. The results in Figure 28 demonstrates the presence of $tetramer^{+}$ populations in representative T cell lines.

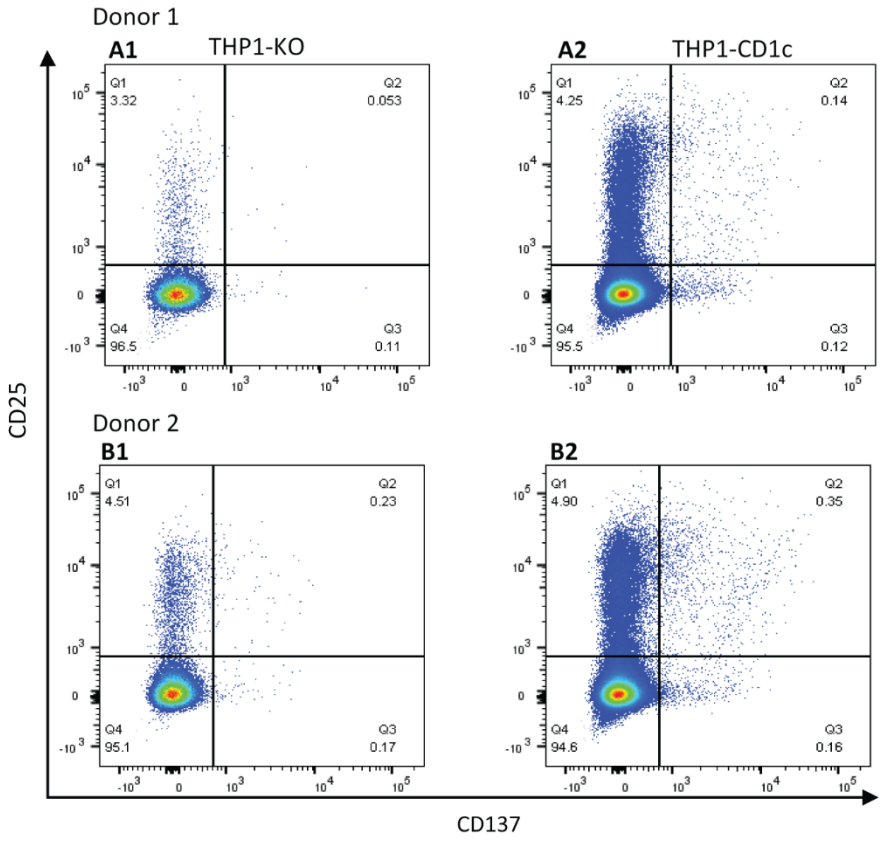

Figure 26: Stimulation of T cells with THP1 cell lines for 24 hours resulted in increased expression of activation markers. Flow cytometry dot plots of $CD3^{+}$ cells from two donors (donor 1 is a healthy subject, and donor 2 has previously been exposed to TB), stained with CD25 and CD137 show that stimulation with THP1-CD1c cells result in larger populations of $CD25^{+}$ $CD137^{+}$ T cells (**A2** &**B2**), than those stimulated with THP1-KO (**A1** & **B1**) (*n*=2).

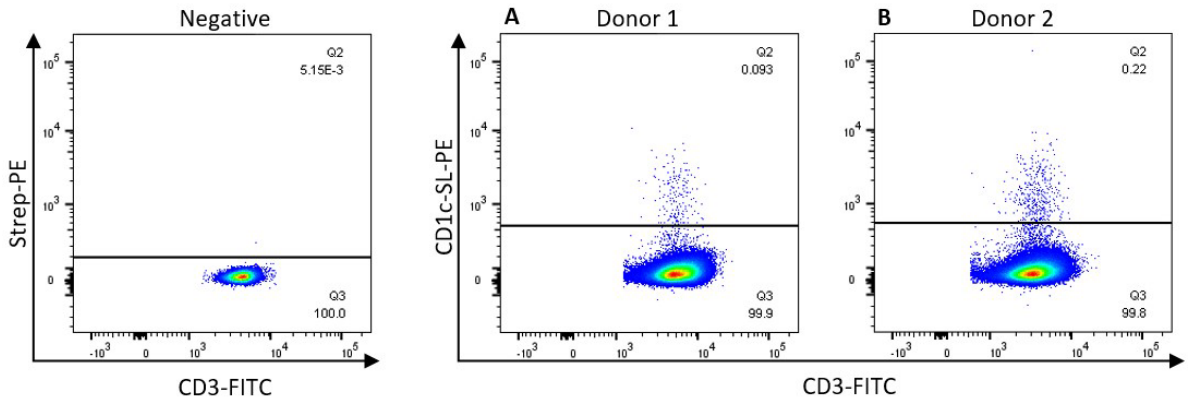

Figure 27: T cells that were CD25$^+$ CD137$^+$ were sorted post stimulation with THP1-CD1c and are CD1c-reactive (second round of sorting). (**A** & **B**) Flow cytometry dot plots show live CD3$^+$ T cells with CD1c-SL tetramer$^+$ populations in both donors (*n*=2). Donor 1 is a healthy subject, and donor 2 has previously been exposed to TB.

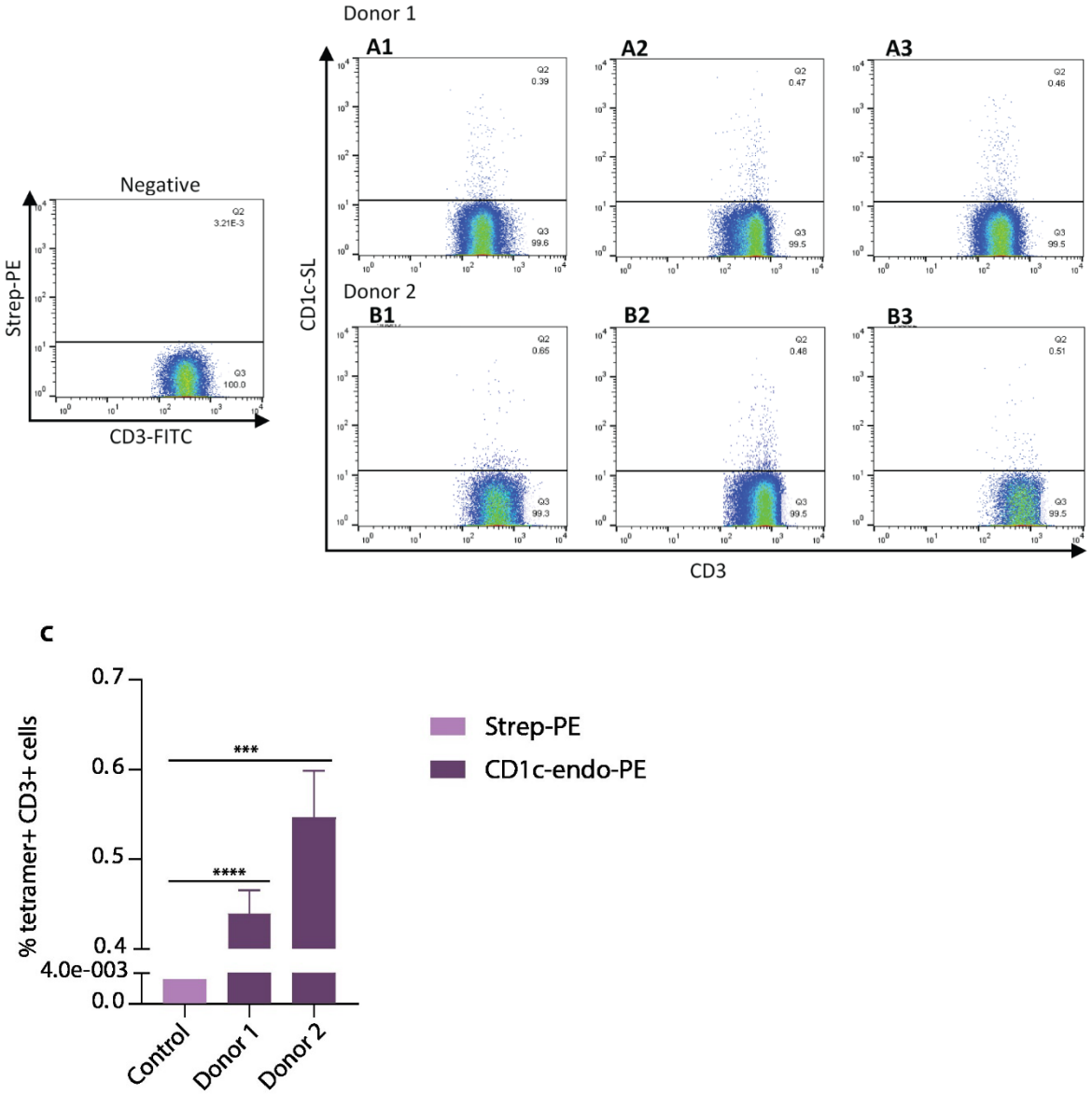

Figure 28: T cells that were initially sorted on CD25$^+$ CD137$^+$ markers were enriched in CD1c-SL tetramers$^+$ T cells post second sort. Representative flow cytometry plots showing live CD3$^+$ CD1c-SL tetramer$^+$ T cell populations in cell lines derived from both donors 1 and 2 (*n*=3 per donor). Donor 1 is a healthy subject (**A1**-**A3**), and donor 2 has previously been exposed to TB (**B1**-**B3**). Bar graph shows that T cell lines from both donors contain significantly greater percentages of tetramer positive T cells than control (**C**). Error bars represent SEM. *** $P < 0.001$, **** $P < 0.0001$ (unpaired t-test).

Summary

MoDCs and MACSi beads mediated expansion

Tetramer guided studies were carried out using CD1c proteins that were generated using both bacterial and mammalian expression systems. In the case of the trained MoDC mediated expansion, we found that irrespective of the training condition, trained MoDCs expressed lower levels of CD1c compared to the negative control. Nevertheless, we found that T cells cultured with β-glucan and mevalonate conditioned MoDC exhibited some tetramer^{+} populations when stained with CD1c-SL tetramers. However, despite the tetramer staining, the low levels of expression of CD1c on the MoDCs meant that the expansion of the desired T cells was not as efficient. Additionally, the low cell viability meant that less CD1c expressing cells were present and were likely in poor health. This experiment was only carried out once and in the interest of time it was not repeated or pursued further.

Traditional MoDCs were found to express high levels of CD1c as has previously been published [467], and resulted in the most effective expansion of CD1c-autoreactive T cells. CD1c-SL tetramer^{+} populations were repeatedly sorted to enrich T cells. The enrichment of these T cells generated parental lines from which CD1c-autoreactive T cells can be cloned. Furthermore, with regards to the MACSi beads mediated expansion, they proved to be ineffective in the expansion or the activation of CD1c-autoreactive T cells and therefore were not pursued further. However, based on our later experiments with THP1 mediated cell expansions, we found that a longer period of stimulation of at least 12 days was more effective. Therefore, future studies utilising aAPC beads should aim to extend the expansion period from 5 days to 12 days.

THP1 mediated expansion

Whilst the THP1 lines do not express β2m-associated proteins, they do express very low levels of MHC class II, however, their loss of CIITA results in the inability of these cells to upregulate the expression of MHC class II when activated. Hence, these APCs may still cause low levels of non-specific T cell activation, which was observed upon culturing T cells with THP1-KO cells (Figure 23 A1 & B1). Nevertheless, this does not contribute sufficiently to overcome the CD1c-mediated expansion of T cells. Furthermore, IFN-γ assays confirmed that the expression of MHC class I & II were not increased by IFN-γ activation in both the THP1-KO and THP1-CD1c cell lines; however, as expected,

an increase was observed in the WT THP1 cells. Additionally, following activation, CD1c expression did not decrease in the THP1-CD1c cell line. We have attempted the THP1-mediated expansion method whilst at Southampton, and again whilst on placement at Immunocore (Oxford) using the same THP1 cell lines but with slight differences in the methods which are discussed below.

THP1 mediated expansion – 8-day protocol

Initially, an 8-day expansion method was used whereby pan T cells were co-cultured with THP1-CD1c cells and THP1-KO cells as a control. Here, IL-2 was added only once, at day 4, after which the cells were left undisturbed until day 8 where they were stained with CD1c-SL tetramers. However, despite the THP1-KO line being an appropriate control, we encountered issues related to cell viability due to wells being sparsely populated due to lack of stimulation. Nonetheless, cells from both cultures were stained with CD1c-SL tetramers and $CD3^+$ CD1c-SL $tetramer^+$ cells were sorted and expanded. During the expansion, the T cells were placed in U-bottom 96-well plates along with irradiated feeders. Previously, $CD3^+$ $tetramer^+$ cells were sorted and placed in flat bottom plates where they were then stimulated, however, this method resulted in poor success rates with very few wells expanding. The use of round bottom plates led to more successful expansions, as the round well encourages close contact between the cells and thus leads to a greater chance of survival, particularly when there are very few in the culture. As the cells grow in the round bottom wells, they form a pellet which becomes larger and can be seen with the naked eye. Being able to visualise the cells quickly and without needing the microscope meant that the cultures spent less time being disturbed and out of the incubator. However, when the pellets did start to enlarge, under the microscope, activated T cells can be seen migrating away from the pellet. At this point every set of 8 wells were transferred from a 96-well plate and pooled in 1 well of a 24-well plate. As the wells became more confluent, the cells were split. The tetramer staining following this expansion revealed an enrichment in the CD1c-SL $tetramer^+$ cells which also underwent another round of sorting and expansion, the resulting 6 lines generated demonstrated further enrichment of CD1c-SL $tetramer^+$ T cells.

Activation Induced Marker (AIM) assay

In the AIM assays, T cells were stimulated for 24 hours with either THP1-CD1c or THP1-KO at the end of the 8-day expansion method, and stained with activation markers with $CD25^+$ $CD137^+$ populations being isolated. Clear differences in the levels of $CD25^+$ $CD137^+$ cells were observed in cultures stimulated with both THP1 lines. However, THP1-CD1c cells resulted in a greater number of $CD25^+$ $CD137^+$ cells which were then sorted. The first round of sorting was based on the activation markers; however, the subsequent round of sorting and expansion was conducted using CD1c-SL tetramer guided sorting in the same manner as described above. This also generated 6 T cell lines which demonstrated enrichment in CD1c-SL $tetramer^+$ T cells that can be utilised for further T cell enrichment.

Chapter 4 Generation of enriched CD1c-autoreactive T cells using THP1 cell mediated expansion and CD1c-endo tetramer guided cell sorting

Having identified a promising method of expanding CD1c-autoreactive T cells using THP1 cell lines, we optimised an effective and reliable methodology to expand and isolate CD1c-autoreactive T cell populations, using both THP1 cells and CD1c tetramers carrying self-lipids that can be robustly generated in a mammalian expression system. We employed CD1c-endo tetramer guided cell sorting to identify and isolate CD1c-autoreactive T cells. Stimulation of pan T cells with THP1-CD1c cells resulted in an expansion of CTV^{lo} cells, which were confirmed to be tetramer reactive when stained with CD1c-endo tetramers. To further confirm the efficiency of the expansion method and the specificity of the expanded population, AIM assays were carried out. The AIM assays revealed the specific activation of T cells in response to CD1c. Following expansion of pan T cells with THP1-CD1c and several rounds of tetramer guided cell sorting followed by expansion, 6 lines were generated, of which, 5 bound to CD1c-endo tetramers. The line containing the highest percentage of CD1c-endo $tetramer^{+}$ T cells was P1C5, and is autoreactive. We also found it expresses CD4, full αβ-TCRs, and hybrid δ/αβ-TCRs.

Mammalian CD1c-endo tetramers

We have previously shown that CD1c-SL tetramers bind human autoreactive T cells [303]. CD1c-SL tetramers have been used in the experiments above to isolate CD1c-autoreactive T cells previously expanded with MoDCs or THP1-CD1c cells. However, we encountered several issues with the production of CD1c-SL protein. Firstly, the yield has been low, and secondly refolded protein monomers either failed to stain T cells or stained weakly. Therefore, we sought to produce lipid loaded CD1c complexes (CD1c-endo) using the more reliable mammalian expression system. We employed CD1c-endo tetramers to isolate autoreactive T cells that recognise CD1c presenting self-lipids. CD1c-endo tetramers allow for the consistent identification of autoreactive T cells, as the CD1c proteins formed are always loaded with self-lipids derived from the mammalian cells in which they are produced [309]. Furthermore, CD1c-endo tetramers are commonly used in the field to study the autoreactivity of T cells, i.e. T cells responding to CD1c in the absence of added microbial antigens, thus confirming their autoreactivity [381, 471].

Generating CD1c-endo tetramers

In order to isolate CD1c autoreactive T cells from healthy human PBMC, CD1c-endo tetramers were generated using a mammalian expression system. HEK cells were transfected with DNA plasmid containing inserts of the CD1c heavy chain, β2m, a GS linker, a polyhistidine tag (6His), an Avi-tag, and BirA biotin ligase under a CMV promoter. The 6His tag allows the purification of the protein via immobilised metal affinity chromatography, whereby, a Nickel HisTrap column packed with Nickel ions (Ni^{2+}) traps the protein by binding its 6His tail which has high affinity to Ni^{2+} ions; the protein can then be recovered from the column by elution. The plasmid also contains an insert for BirA biotin ligase, this allows the enzymatic binding of biotin to the Avi-tag site. Collectively, with the CD1c heavy chain and β2m, the cells produce and secrete folded protein monomers into the media. Once purified, these can be labelled with streptavidin conjugated fluorochromes to produce tetramers, or to fluorescently labelled dextran backbones to produce dextramers.

Post transfection, the cultures were incubated for 5 days, during this period, the cells produce CD1c-endo monomers and secrete them into the media. The media was then collected following centrifugation to pellet the cells, and the protein was initially purified using a HisTrap column and eluted off the column in fractions. Before commencing with SEC, the fractions were analysed on an SDS-PAGE gel to ensure the presence of protein. CD1c-endo monomers were present in all the fractions as indicated by single dense bands; a single band is seen in both reduced and non-reduced fractions as the CD1c and β2m are a single polypeptide (Figure 29A). The fractions were then pooled and further purified using SEC and collected fractions were subsequently analysed on an SDS-PAGE gel to ensure the fractions were pure and can be used for tetramerisation and subsequent T cell staining (Figure 29B).

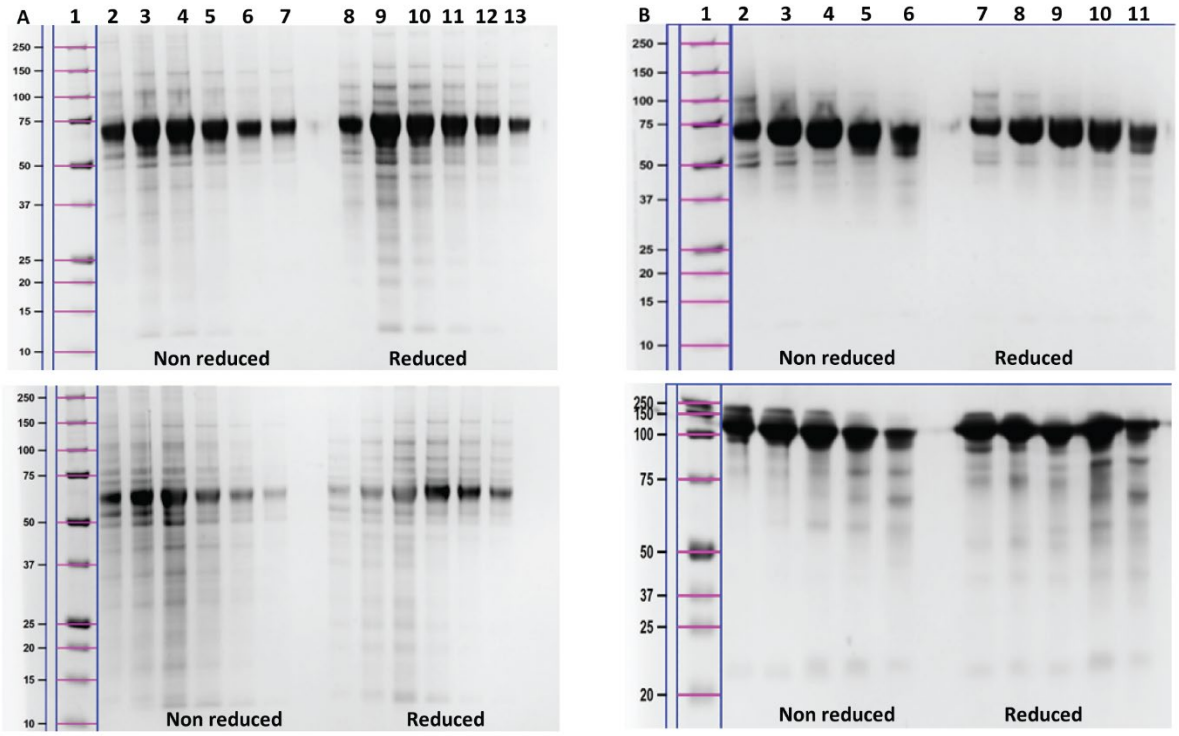

Figure 29: Separation of purified CD1c-endo protein. Representative images of SDS-PAGE gels confirming the presence and purification of CD1c-endo protein post HisTrap purification, and post SEC. (**A**) post HisTrap purification - lane 1: protein ladder, lanes 2 – 7 non reduced protein fractions, lanes 8 – 13 reduced protein fractions eluted from HisTrap column. (**B**) post SEC - lane 1: protein ladder, lanes 2 – 6: non reduced protein, lanes 7 – 11: reduced protein fractions eluted from SEC column.

Titration of tetramers and dextramers

In order to ensure maximum efficiency of staining, a direct comparison between CD1c-endo tetramers and dextramers was made. Tetramers are more frequently used, predominantly in academic settings due to the lower costs associated with generating the proteins and purchasing other components of the tetramer, particularly in long term experiments. Moreover, the use of CD1-endo tetramers has contributed significantly to our understanding of the TCRs that interact with the various CD1 proteins. Studies have used CD1b-endo tetramers to demonstrate how CD1b binds TCRs [345], whilst the use of CD1a-endo, and CD1c-endo tetramers demonstrated that CD1a- and CD1c-restricted T cells are autoreactive [309, 344]. Furthermore, Wun et al identified some of the lipids bound to CD1c when recognised by CD1c-autoreactive T cells [309]. These lipids included sphingomyelin (SM), phosphatidylcholine (PC), and monoacylglycerol (MAG). Whilst SM and PC have

previously been identified as CD1 ligands [346, 472, 473], the discovery of MAG as a CD1c ligand was a novel finding in this study [309].

A single tetramer molecule is composed of 4 CD1c-endo monomers bound to a single fluorescently labelled streptavidin molecule (Figure 30A). Whilst a single dextramer molecule is composed of a fluorescently labelled dextran backbone that has sites which allow the binding of 20 biotinylated proteins (Figure 30B). Having many binding sites for fluorescently labelled proteins gives dextramers an increased avidity and sensitivity for T cells than tetramers. However, the titration of both reagents whilst using T cells from 3 donors as well as positive and negative control cell lines, indicates that in this case, tetramers were better able to stain CD1c-autoreactive T cells (Figure 31 A2 – C2, Figure 32 & Figure 33). Moving forward, the reagent used to stain T cells were CD1c-endo tetramers at 0.33µM per $1x10^6$ T cells.

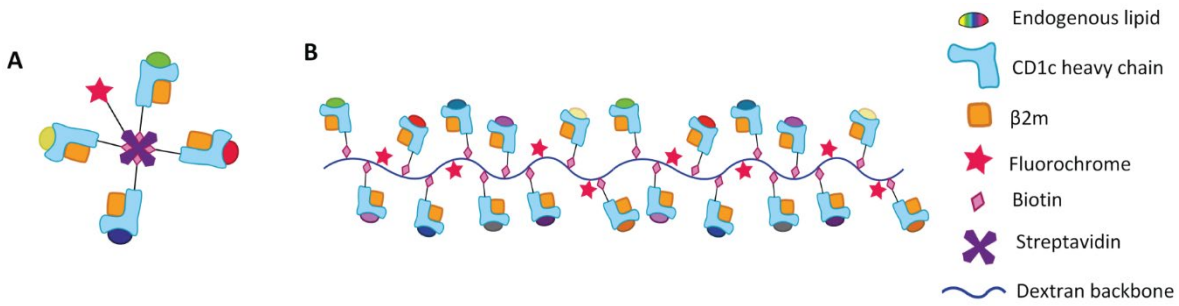

Figure 30: Illustration of CD1c-endo tetramers and dextramers. CD1c-endo tetramer is displayed with 4 monomers bound to a fluorescently labelled streptavidin (**A**), and CD1c-endo dextramer is displayed with 20 monomers bound to a fluorescently labelled dextran backbone (**B**).

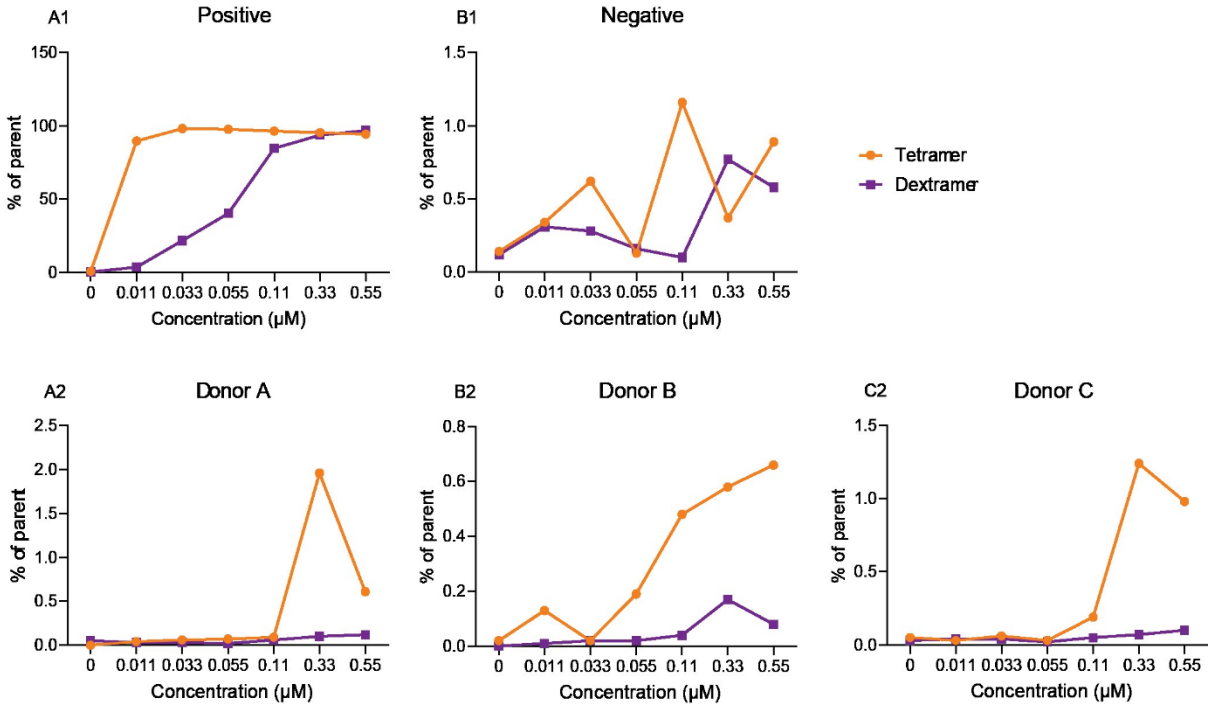

Figure 31: CD1c-endo tetramers were more effective than dextramers at staining CD1c-restricted T cells. Cumulative data of titration of CD1c-endo tetramers and dextramers show that CD1c-endo tetramers stain better than dextramers**.** (**A1**) Staining of negative control cell line has low levels of background staining with both reagents, (**B1**) positive control lines indicate that tetramers are more efficient even at lower concentrations, (**A2 – C2**) CD1c-endo tetramers are better at staining pan T cells than dextramers.

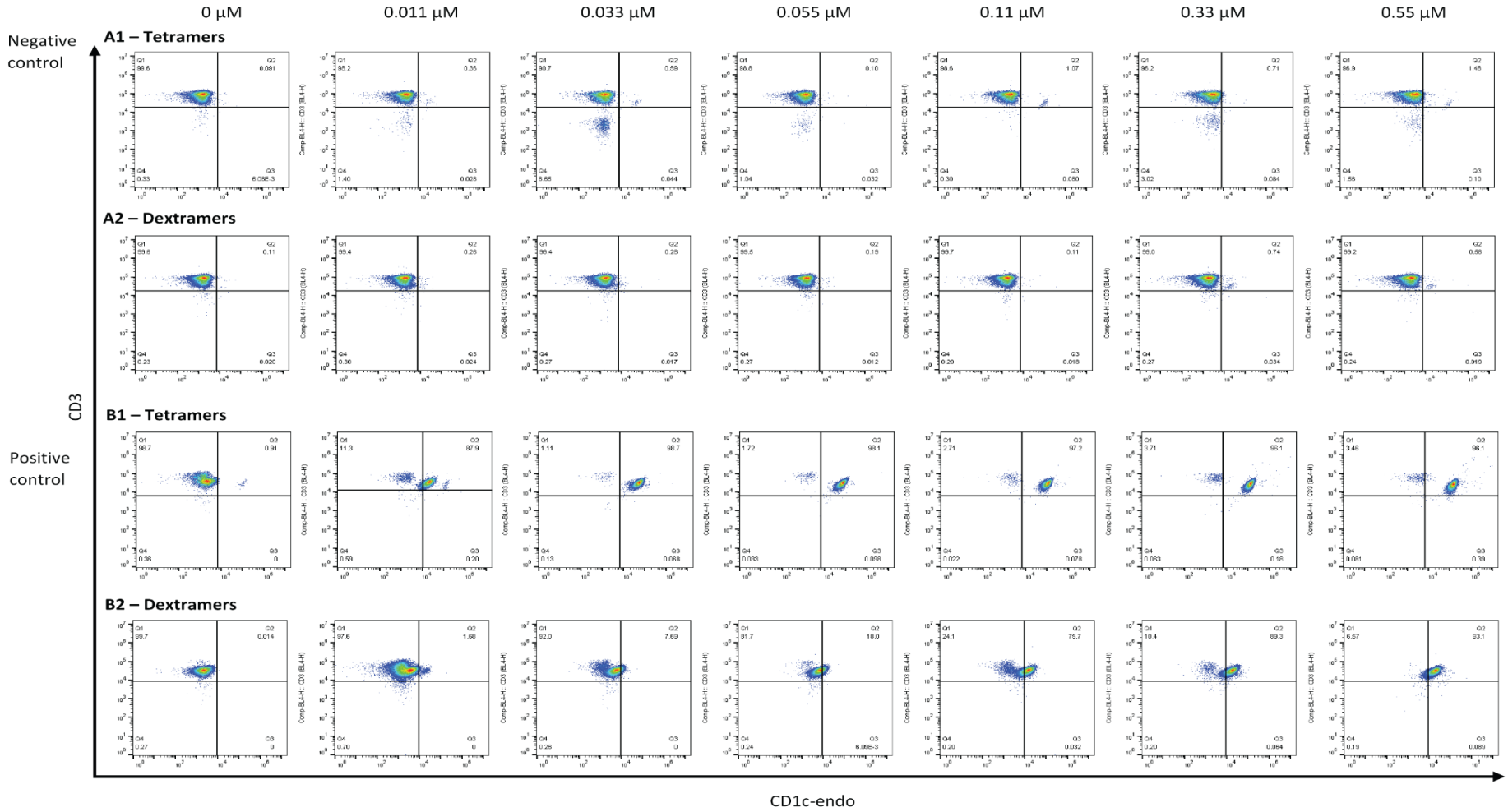

Figure 32: CD1c-endo tetramers are more effective at staining a CD1c-restricted control cell line. Titration of CD1c-endo tetramers and dextramers show that tetramers are better at identifying CD1c-restricted T cells than dextramers are. Flow cytometry dot plots show that at the lowest concentration of 0.011µM, the positive control cell line stained better with tetramers.

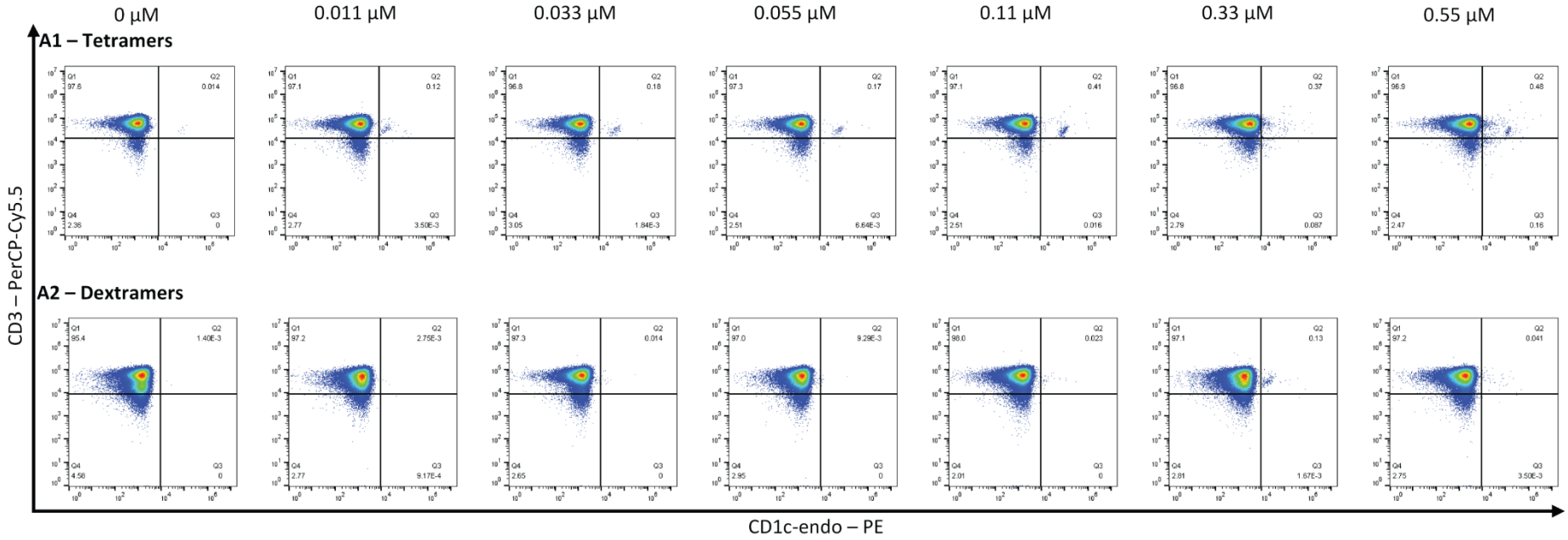

Figure 33: Titration of CD1c-endo tetramers are more effective at staining pan T cells. Flow cytometry dot plots show that pan T cells from one donor stained better with increasing concentrations of CD1c-endo tetramers than they did with dextramers.

THP1 mediated T cell expansion – 12 days method

Aside from the length of time, the main difference in this method in comparison to the 8 days expansion method (shown in Chapter 3) is that 10 IU/ml IL-2 was added every other day to the cultures stimulated with THP1-CD1c as well as the controls (T cells only) until the cells were sorted. IL-2 is a mitogenic cytokine, thus promotes the proliferation of T cells. Together with the extended period of time, this resulted in an enrichment of CD1c-endo tetramer^{+} T cells (Figure 34) upon tetramer screening of five donors. Additionally, the cultures had better overall viability, as well as an increase in CD3^{+} CTV^{lo} cells in the cultures expanded with THP1-CD1c (Figure 35 B1 – B3). However, there is also some low level of expansion in the T cell only controls as indicated by the CD3^{+} CTV^{lo} population (Figure 35 A1 – A3), this is likely due to the effect of the IL-2. Whilst this expansion method resulted in an increase in the CD1c-endo tetramer^{+} T cell population, as well as CTV^{lo} CD3^{+} T cells; in order to further validate the specificity of the expansion method, an activation assay was carried out. On day 12 of the expansion, the T cells were stimulated for 24 hours with either THP1-KO or THP1-CD1c cells, they were then stained for the activation markers CD69 and CD137. Compared to cultures stimulated with THP1-KO, cultures stimulated with THP1-CD1c exhibited increased T cell activity as demonstrated by the increase in the percentage and MFI of CD69^{+} CD137^{+} staining in all donors (Figure 36).

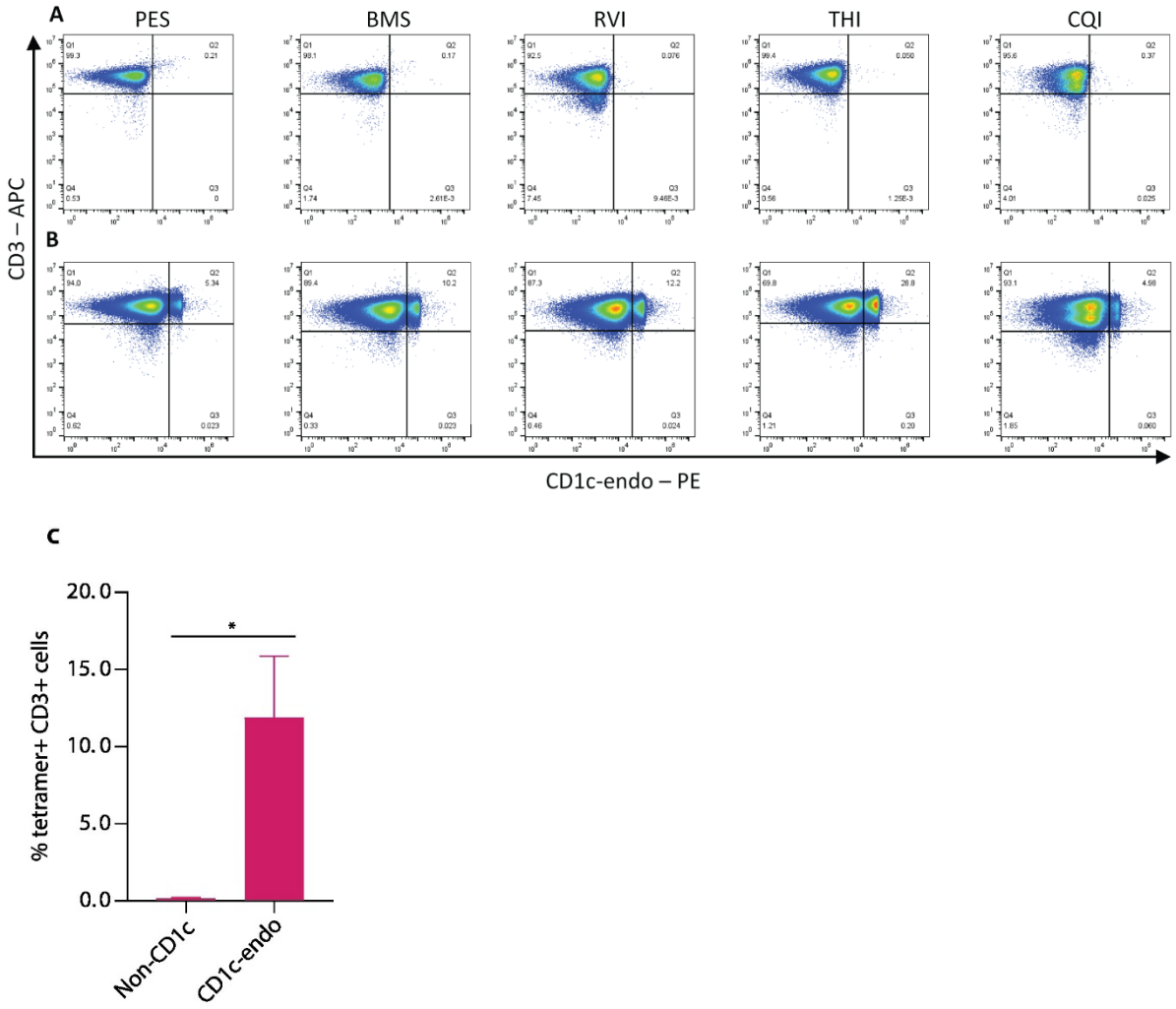

Figure 34: THP1-CD1c expands CD1c-endo tetramer$^+$ populations. Stimulation of pan T cells isolated from five blood donors with THP1-CD1c for 11 days expanded CD1c-endo tetramer$^+$ populations (*n*=5). Flow cytometry dot plots show lack of staining of pan T cells with an irrelevant control tetramer (**A**), and staining of populations of pan T cells with CD1c-endo tetramer (**B**). Bar graph shows that THP1-CD1c mediated expansion results in a significantly greater percentage of tetramer positive T cells than control (C). Error bars represent SEM. * $P < 0.05$ (paired t-test).

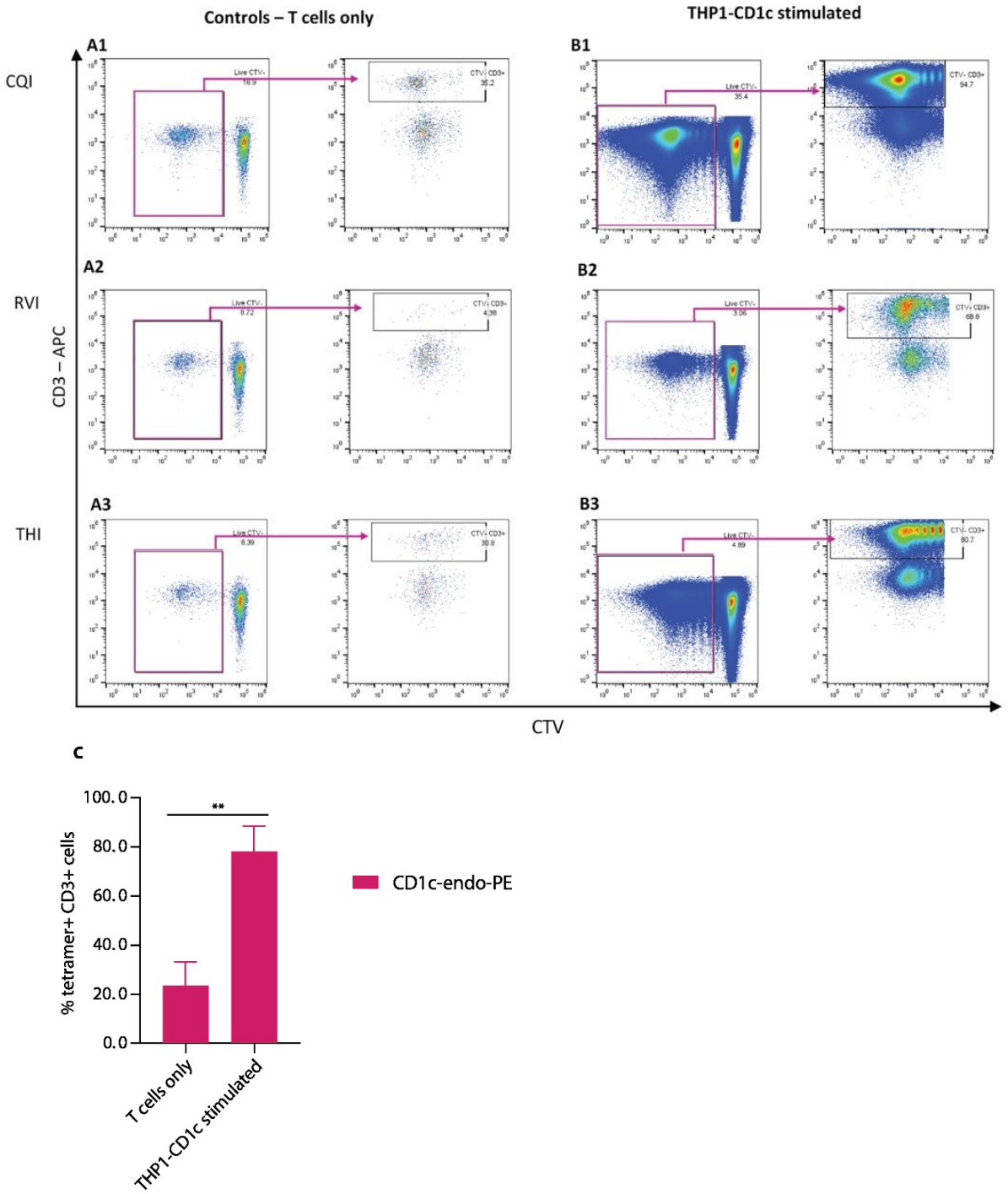

Figure 35: T cells stimulated with THP1-CD1c have a greater proliferative response (first round of sorting). Flow cytometry dot plots show live $CD3^+$ cells that have proliferated without THP1 mediated stimulation and are T cell only control cultures (**A1 – A3**), with larger populations being present in cultures where pan T cells were stimulated with THP1-CD1c in all three healthy donors (**B1 – B3**). Pink rectangular gate indicates cells that are CTV^{lo}, arrow indicates gating hierarchy, black rectangular gate indicates cells that are $CD3^+$ CTV^{lo} (*n*=3). Bar graph shows that THP1-CD1c mediated expansion results in significantly greater percentage of $CD3^+$ CTV^{lo} T cells than control (**C**). Error bars represent SEM. ** $P < 0.01$ (paired t-test).

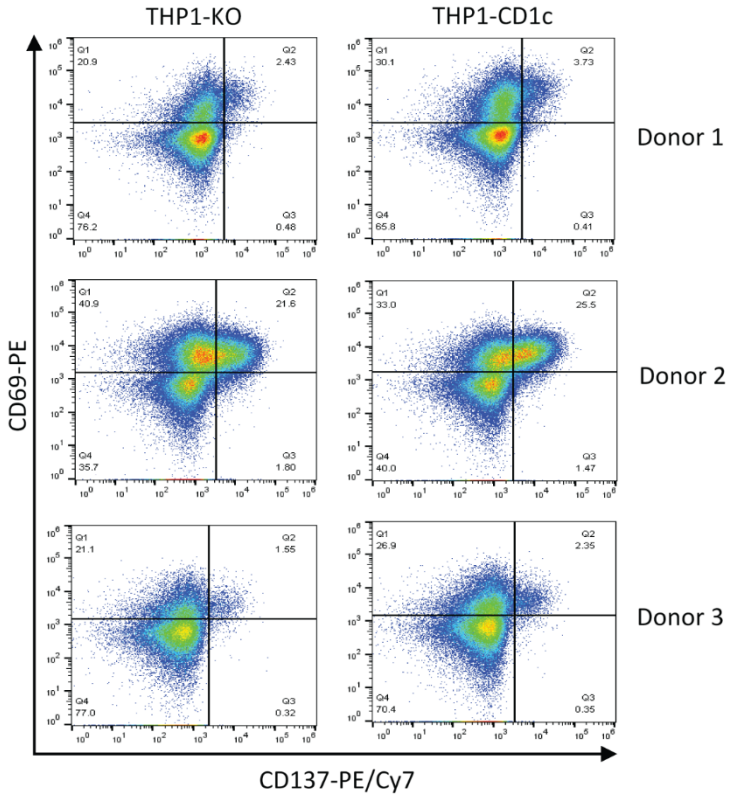

Figure 36: Expression of activation markers increased following stimulation with THP1-CD1c. More staining of activation markers was visible 24-hours post stimulation with THP1-CD1c cells and a similar pattern was observed in three donors. Flow cytometry dot plots suggested that a high level of background activation in cells stimulated with THP1-KO occurred (**A1**-**A3**), and this increased in cells stimulated with THP1-CD1c as indicated by the increase in the percentage of $CD69^+$ and $CD137^+$ stained cells (**B1**-**B3**) (*n*=3).

CD1c-endo $tetramer^+$ T cells were sorted from donors A and B and the cells were expanded with irradiated PBMCs, PHA, and IL-2. After the cultures grew, they were stained and $CD3^+$ CD1c-endo $tetramer^+$ cells were bulk sorted and expanded again (Figure 37). This process was repeated several times (*n*=7). After several rounds of sorting, six lines were generated and stained with CD1c-endo tetramers (Figure 38). Several expanded T cell lines stained with CD1c-endo tetramers as indicated by the shift in MFI compared to the negative control (Figure 38). However, one particular T cell line, P1C5 (Figure 38 B3), stained brightly with CD1c-endo tetramers.

Line P1C5 was expanded with irradiated PBMCs, PHA, and IL-2. Flow cytometric analysis was used to phenotype this polyclonal cell line; as well as being autoreactive, the line was found to be $CD4^+$, and expresses full αβ-TCRs as well as a hybrid δ/αβ-TCRs (Figure 39E). Further flow cytometric analysis

identified the lack of Vδ1 T cells among the γδ population (Figure 39H). Additional characterisation is required to identify the subtype of gamma delta TCRs present in this polyclonal T cell line.

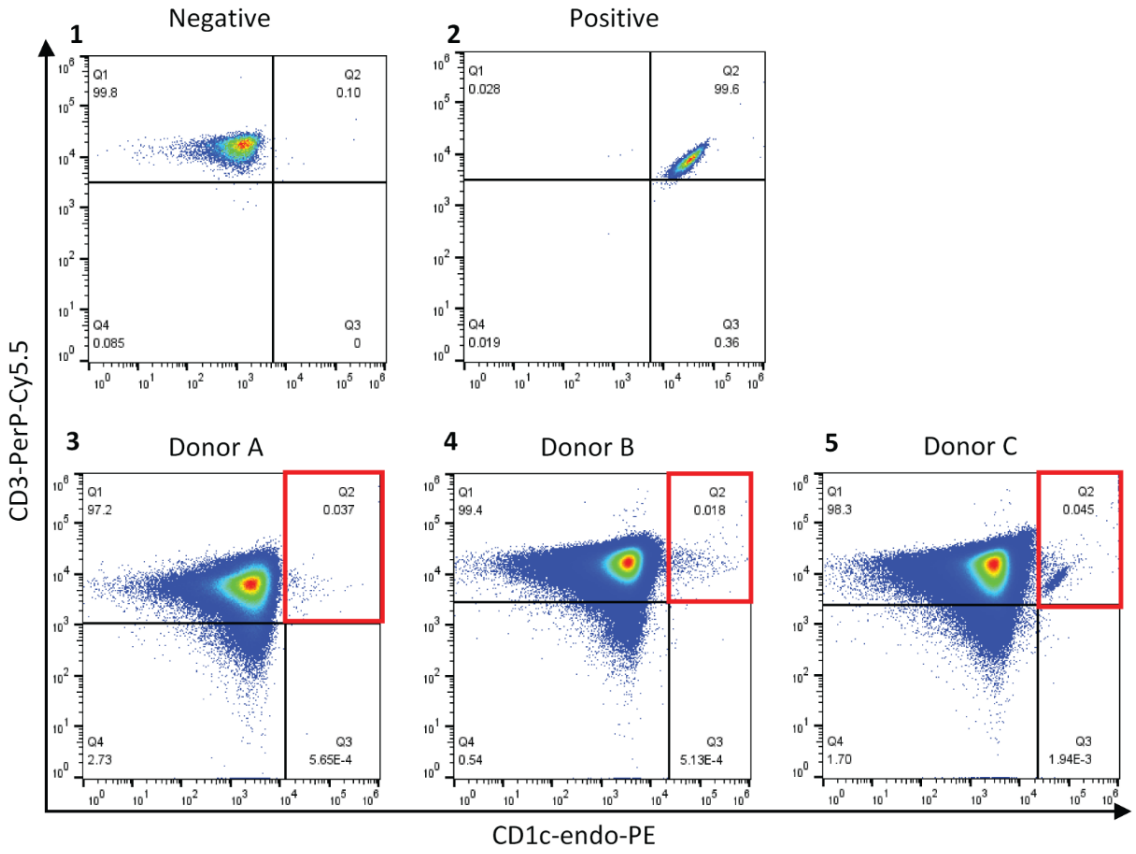

Figure 37: CD3⁺ T cells that were initially sorted on CD3⁺ CTV^{lo} stained with CD1c-endo tetramers (second round of sorting). Flow cytometry dot plots show staining of live CD3⁺ CD1c-endo tetramer⁺ populations in T cells from three donors that were previously sorted on CD3⁺ CTV^{lo} (**3 – 5**). Tetramer positive populations are indicated within the red gates, and were sorted (*n*=3).

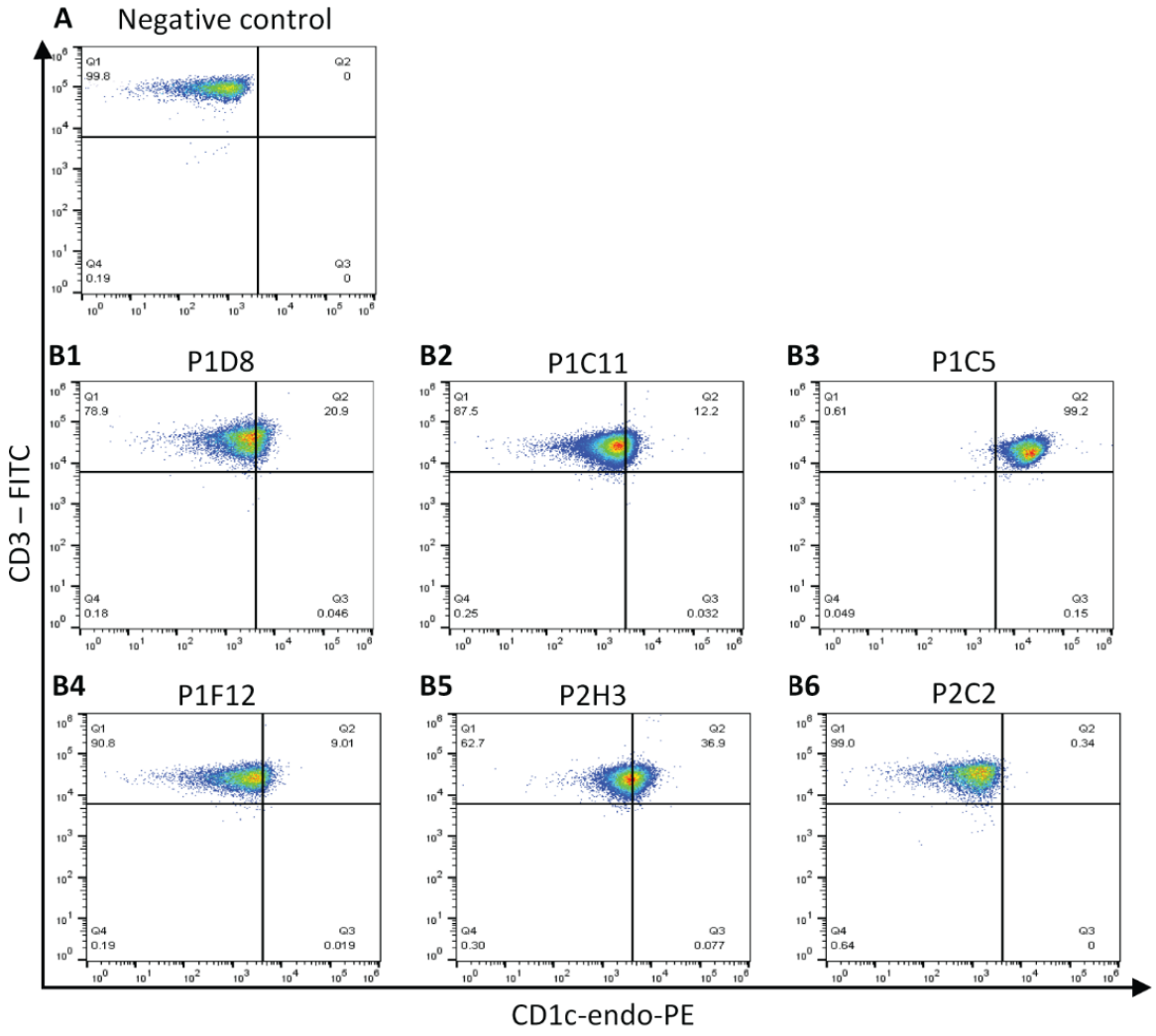

Figure 38: T cell lines that were previously sorted using CD1c-endo tetramers were enriched in CD1c-endo tetramer^{+} cells post expansion. Flow cytometry dot plots show that five out of six lines stained with CD1c-endo tetramers to different extents (**B1-B6**) (*n*=6). Data indicates that all the T cell lines bind the tetramers except line P2C2.

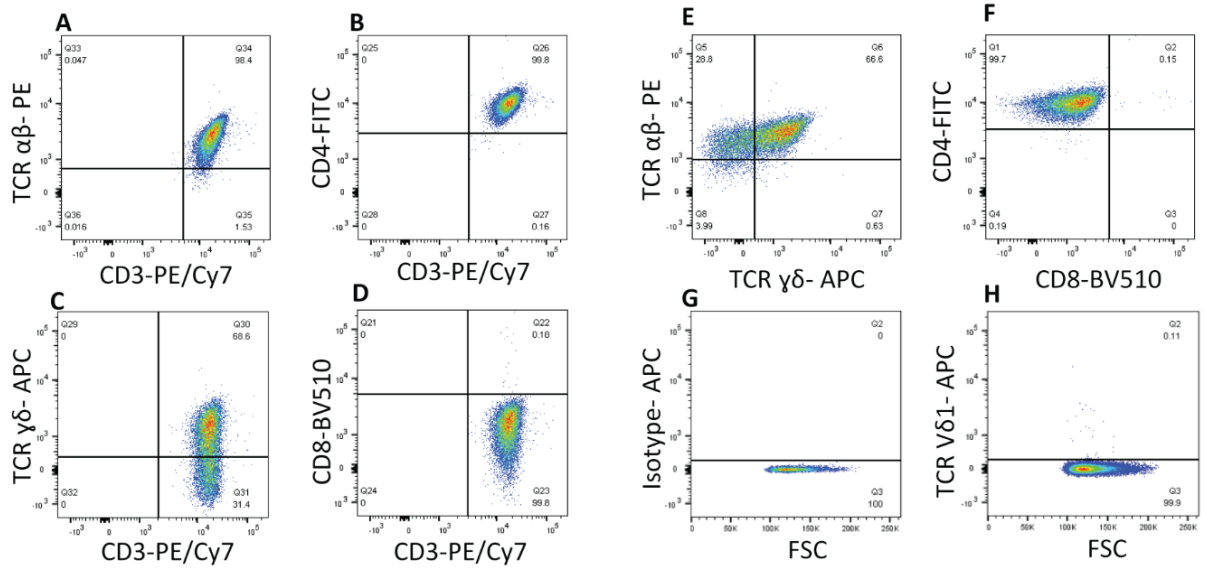

Figure 39: P1C5 T cells are polyclonal and express both αβ- and γδ-TCRs, and are CD4⁺.
Phenotypic analysis of P1C5 T cells determined their co-receptor status, and mixed TCR subset expression. Flow cytometry dot plots show single staining of pan αβ TCR (**A**), CD4 (**B**), pan γδ TCR (**C**), and dual staining of αβ and γδ TCRs (**E**). The Vδ1 TCR stain determined that P1C5 T cells did not express Vδ1 TCR (**G & H**).

Summary

Apart from the main difference in the 8-day and 12-day expansion protocols being the length of time, the tetramers used following the 12-day method were CD1c tetramers generated in a mammalian expression system and loaded with endogenous proteins. Furthermore, the 12-day method involves the addition of IL-2 to the cultures every other day from day 4 onwards. This resulted in a more effective expansion as shown by the flow cytometry plots of CTV^{lo} populations on day 12 (Figure 35) in comparison to day 8 (Figure 23). The frequent addition of IL-2 ensures that T cells initially stimulated by THP1 cells remain activated and promotes their proliferation. Whilst donor variability does play a factor in how well cells respond to stimuli, the overall health of the cultures was better and cell viability was higher in the 12-day method. Additionally, as opposed to using THP1-KO as a control, T cell that were cultured alone, without the addition of APCs, were used as controls. As mentioned above, cell viability significantly declines with the length of time due to lack of stimulation. Therefore, in this experiment, T cells that were grown on their own were stimulated with IL-2 only from day 0 for the duration of the protocol. Naturally, this resulted in the proliferation of T cells as demonstrated by the increase in CTV^{lo} populations (Figure 35 A1 – 3), however, the stimulation with THP1-CD1c resulted in a higher frequency of $CD3^{+}$ CTV^{lo} cells than the T cell only control (Figure 35 B1 – 3). These cells were subsequently sorted and expanded. During the

expansion, the T cells were placed in flat bottom 96-well plates along with irradiated feeders, PHA, and IL-2. After 4 days, the T cells formed large round clumps along the bottom of the well with activated T cells migrating out, the clumps were gently broken up by pipette mixing to encourage the T cells to spread across the surface of the well and continue proliferating. As they became more confluent, the cells were split into 2 wells of a 96-well plate followed by being pooled into 1 well of a 24-well plate, the cells were continuously split as and when the wells became confluent. When several hundred cells are sorted, they can be seeded into flat bottom plates as opposed to round bottom plates, as their chances of survival are greater due to a larger number of cells together per well, additionally, the flat bottom plates allow for better visualisation of the cells and allows proliferating T cells to migrate out easier from their clumps, and the gentle and gradual splitting of cells whilst refreshing half of the media and adding more IL-2 every 48-72 hours resulted in continued proliferation and greater cell viability. The expanded $CD3^+$ CTV^{lo} T cells underwent several rounds of sorting where $CD3^+$ CD1c-endo $tetramer^+$ cells were sorted and expanded as described above. Expansions post single cell sorting were not successful, therefore, with each round, the cells were bulk sorted to maximise the chances of survival and then split into several wells to generate mini lines. This resulted in 5 out of 6 T cell lines that were CD1c-endo $tetramer^+$, with line P1C5, being almost 100% CD1c-endo $tetramer^+$ (Figure 38). This cell line was found to express both αβ- and γδ-TCRs, was Vδ1 negative, and expressed CD4 (Figure 39).

Chapter 5 CD1c-autoreactive T cells exhibit enhanced cytotoxicity towards Mtb infected target cells

A 2D infection model of THP1 target cells infected with UV killed TB was used to study the functional effect of the CD1c-autoreactive P1C5 T cell line. Our main readout in this experiment was generated from the culture media, which was used in a ToxiLight assay to measure the cytotoxic effect of P1C5 during TB infection. Following several optimisation experiments we identified an optimal time point, and the MOI required to measure T cell cytotoxicity. Our data supports the hypothesis that CD1c-autoreactive T cells may play a protective role during TB infection through their specific and enhanced killing of *Mtb* infected $CD1c^+$ target cells. This is reflected in both types of experiments whereby the cytotoxicity of P1C5 T cells increased in a dose-dependent manner when increasing both the T cell dose, and the MOI.

Infection of THP1 lines with UV killed TB

Optimisation

To investigate the functional effects of the CD1c autoreactive T cells P1C5 in TB infection, THP1 cell lines were infected with UV killed TB for 24 hours. P1C5 T cells were subsequently cultured with infected THP1 cells and cytotoxicity was then measured using the ToxiLight assay. Several factors needed to be optimised, such as the time point at which to measure cytotoxicity, and the range of MOIs required to infect the THP1 cells.

First, a time point at which to measure the cytotoxicity was determined. To do this, the impact of the infection on the cell surface expression of CD1c was first investigated. The cells were infected with a range of MOIs (0.0001, 0.001, 0.01, 0.1, 1, and 10); they were then stained with anti-CD1c, and flow cytometric analysis was carried out 24, 48, and 72 hours post infection to determine CD1c expression. At MOI 0, the expression of CD1c was at its peak on day 1 and then decreased at day 2, and maintained at day 3; at MOIs 0.0001-0.1, a similar trend is observed whereby the expression is less than that of MOI 0 on day 1, followed by a decrease at day 2, before it starts increasing again at day 3. At MOI 1, the expression is almost maintained across all 3 days with a slight decrease over the 72-hour period. MOI 10 has the most drastic change where expression on day 1 increases and continues to increase by day 3 (Figure 40).

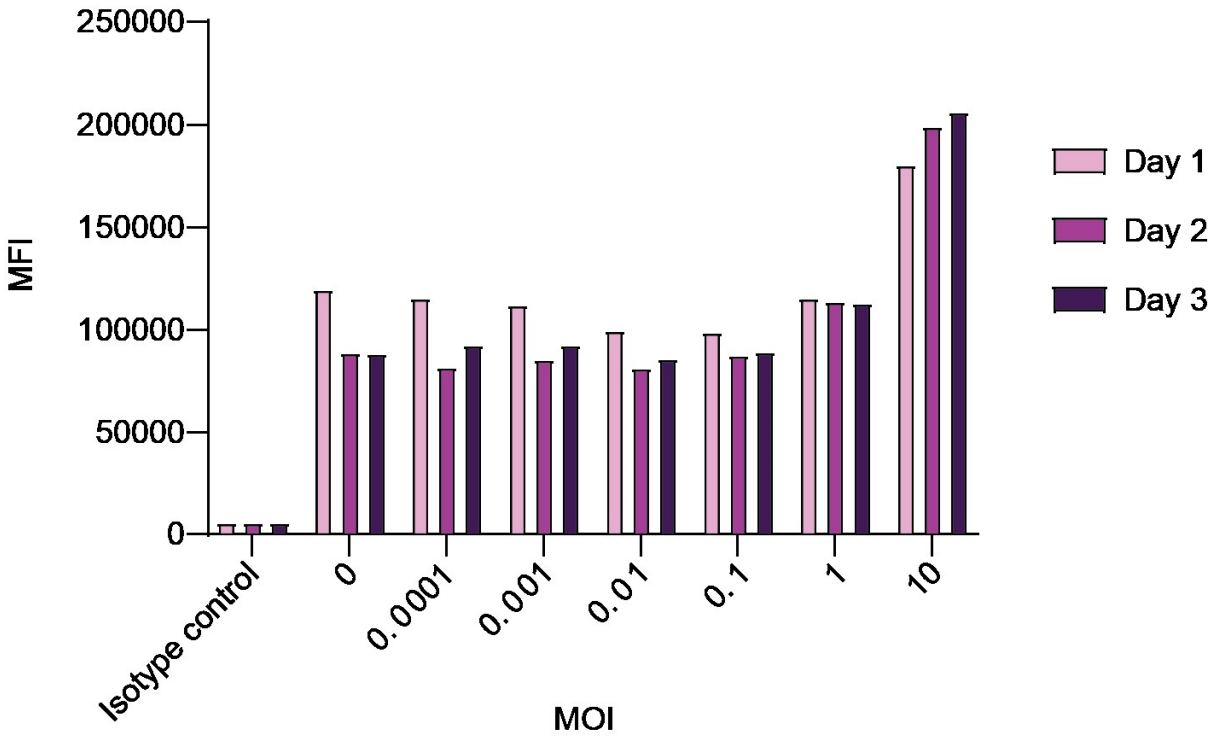

Figure 40: Mean fluorescence intensity (MFI) of CD1c expression on *Mtb* infected THP1-CD1c cells using a range of MOIs over 3 days. The changes in expression of CD1c is minimal across all MOIs, except with MOI of 10 where it increases. This experiment was carried out once.

An initial experiment to identify a time point at which to measure cytotoxicity was carried out using THP1-CD1c cells infected with UV killed TB at MOI 0.001. Following infection, CD1c-autoreactive (P1C5) and non-reactive (P3D7) T cells were added to separate wells, and a ToxiLight assay was carried out 24, and 48 hours later. The ToxiLight assay relies on the release of intracellular adenylate kinase (AK) into the media when a cell dies. AK phosphorylates ADP to ATP. The ATP was then measured by bioluminescence produced via the firefly luciferase reaction. The greater the cell death, the more AK is released into the culture media and therefore the greater the intensity of the bioluminescent signal. Compared to 24 hours, the ToxiLight assay demonstrated that 48 hours post the addition of T cells to THP1 cells exhibited a greater response (Figure 41). Based on this initial study, the ToxiLight assay was carried out at 48 hours post the addition of T cells in subsequent experiments. Furthermore, these results also revealed increased cytotoxicity of P1C5 T cells when cultured with *Mtb* infected THP1-CD1c target cells (Figure 41).

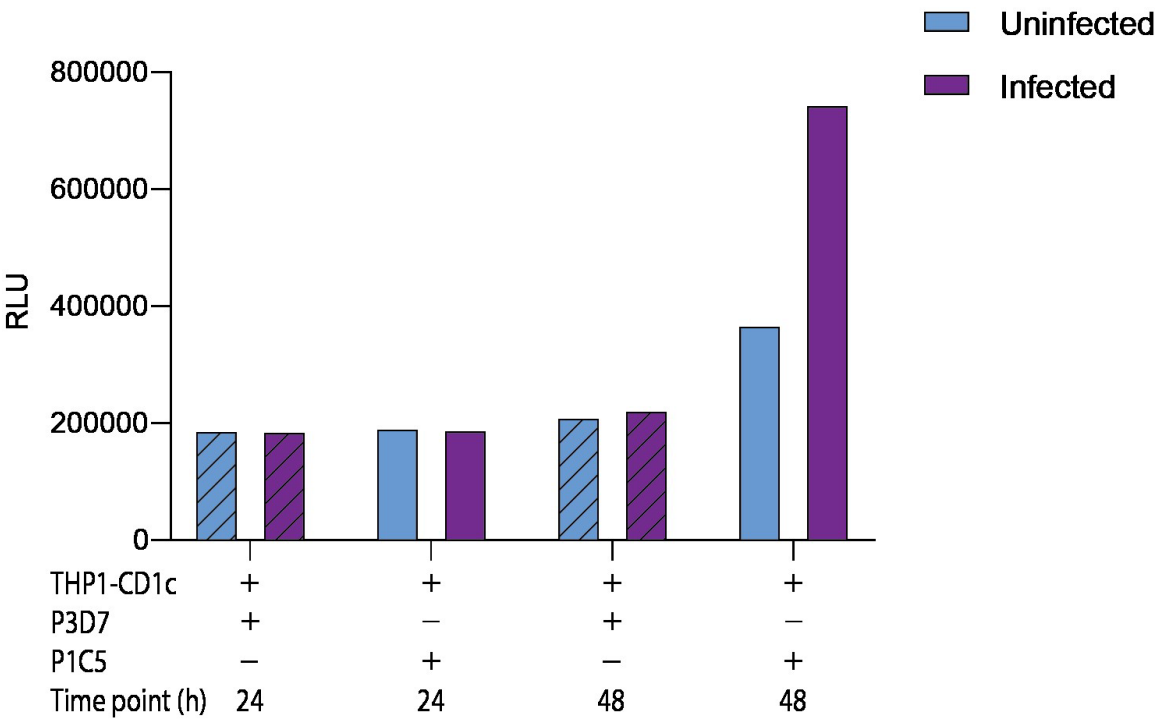

Figure 41: Cytotoxicity of P1C5 T cells is most detectable at 48h. Cytotoxicity was measured using a ToxiLight assay 24 and 48 hours post the addition of T cells to uninfected and *Mtb* infected (MOI 0.001) THP1-CD1c target cells. This experiment was carried out once in duplicate.

The experiment was subsequently repeated twice with THP1-KO target cells included as an additional control. THP1-CD1c and THP1-KO cells were infected with UV killed TB (MOI 0.001 and MOI 1) and cultured with P1C5 and P3D7 T cells.

We observed lower levels of bioluminescence when T cells were cultured with uninfected and *Mtb* infected THP1-KO cells (Figure 42A). Additionally, a greater response was observed when P1C5 T cells were cultured with uninfected THP1-CD1c cells, indicating higher levels of cytotoxicity. Importantly, we observed a significant increase in cytotoxicity when P1C5 T cells were cultured with infected THP1-CD1c target cells, with both MOIs (Figure 42A & B). Moreover, the cytotoxic role of P1C5 T cells and their specificity to CD1c was further highlighted by the significant increase in cytotoxicity when T cells were cultured with infected THP1-CD1c cells compared to infected THP1-KO cells (Figure 42C). These results indicate that P1C5 T cells respond to THP1-CD1c in an autoreactive manner, and their autoreactivity and therefore killing capacity increases during infection. An additional experiment where THP1-CD1c cells were infected with a wider range of MOI starting from 0.0001 and increasing in 10-fold increments to 10 was also carried out to determine the MOIs at

which an effect could be detected. The ToxiLight data demonstrated that between MOIs 0.0001 – 0.1 there is little difference between the uninfected and infected conditions, but a clear difference in target killing becomes detectable at an MOI of 1, and is further increased at an MOI of 10 (Figure 42D).

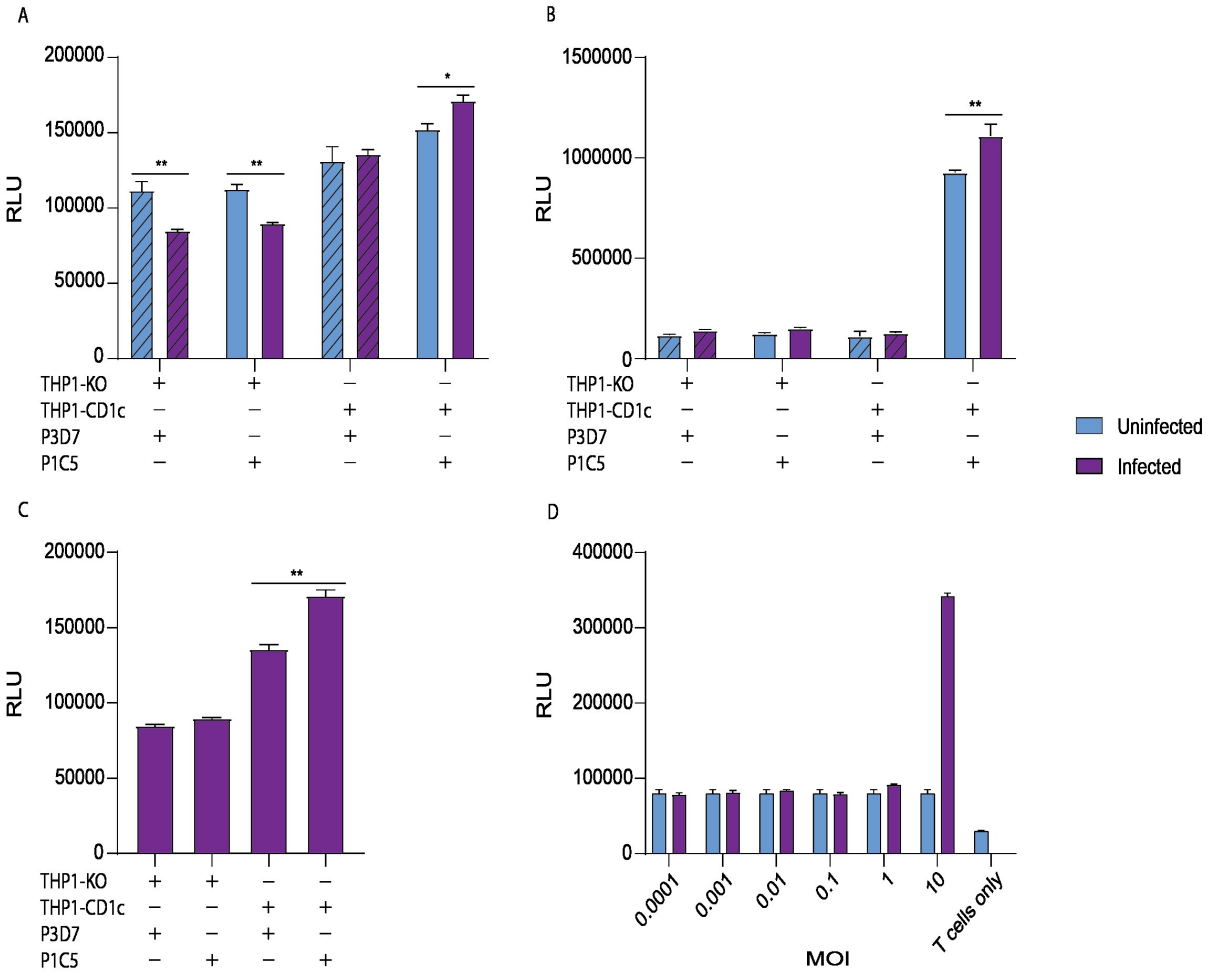

Figure 42: P1C5 T cells specifically targeted infected THP1-CD1c cells and caused greater cytotoxicity. Cytotoxicity of T cells was measured by ToxiLight assay 48 hours post addition of P1C5 and P3D7 T cells to uninfected (blue bars), and *Mtb* infected (purple bars) THP1 target cells at a 1:1 ratio. Bar graphs indicate responses at various MOIs, (**A**) *Mtb* MOI = 0.001, (**B** & **C**) *Mtb* MOI = 1, (**D**) full range of MOIs (0.0001 – 10) with *Mtb* infected or uninfected THP1-CD1c cells and P1C5 T cell line only. Data are representative of three experiments, each preformed in duplicate. Error bars represent SEM.* $P < 0.05$; ** $P < 0.01$ (two-way ANOVA).

These initial experiments demonstrated significant differences in the cytotoxic response of P1C5 T cells towards THP1 target cells in the context of TB infection. To further confirm this, dose-dependent responses were performed in 2 ways: 1) the MOI was fixed and the effect of increasing

the ratio of T cells was studied; and 2) the ratio of T cells to THP1 cells was fixed, and the MOI was increased in 10-fold increments.

The effect of increasing the T cell ratio

Infecting THP1 cells with UV killed TB at an MOI of 10 revealed the greatest difference in the initial experiments (Figure 42D), therefore, this MOI was used when investigating the effect of increasing the numbers of T cells whilst keeping the number of infected THP1 cells fixed (50,000 cells/well). Twenty-four hours post infection, T cells were added at 0.3:1, 1:1, and 3:1 ratios. A clear dose-dependent response is observed in the wells where infected THP1-CD1c cells were cultured with P1C5 T cells (Figure 43). The cytotoxicity observed in these wells is statistically significant relative to the control wells where P1C5 cells were cultured with THP1-KO, and when control P3D7 T cells were cultured with target cells (Figure 43A). Similarly, we observed a significant dose-dependent increase in cytotoxicity in wells cultured with infected THP1-CD1c and P1C5 T cells (Figure 43B). However, we did not observe a cytotoxic response in the wells where P1C5 T cells were cultured with uninfected THP1-CD1c or when control P3D7 T cells were cultured with target cells (Figure 43B).

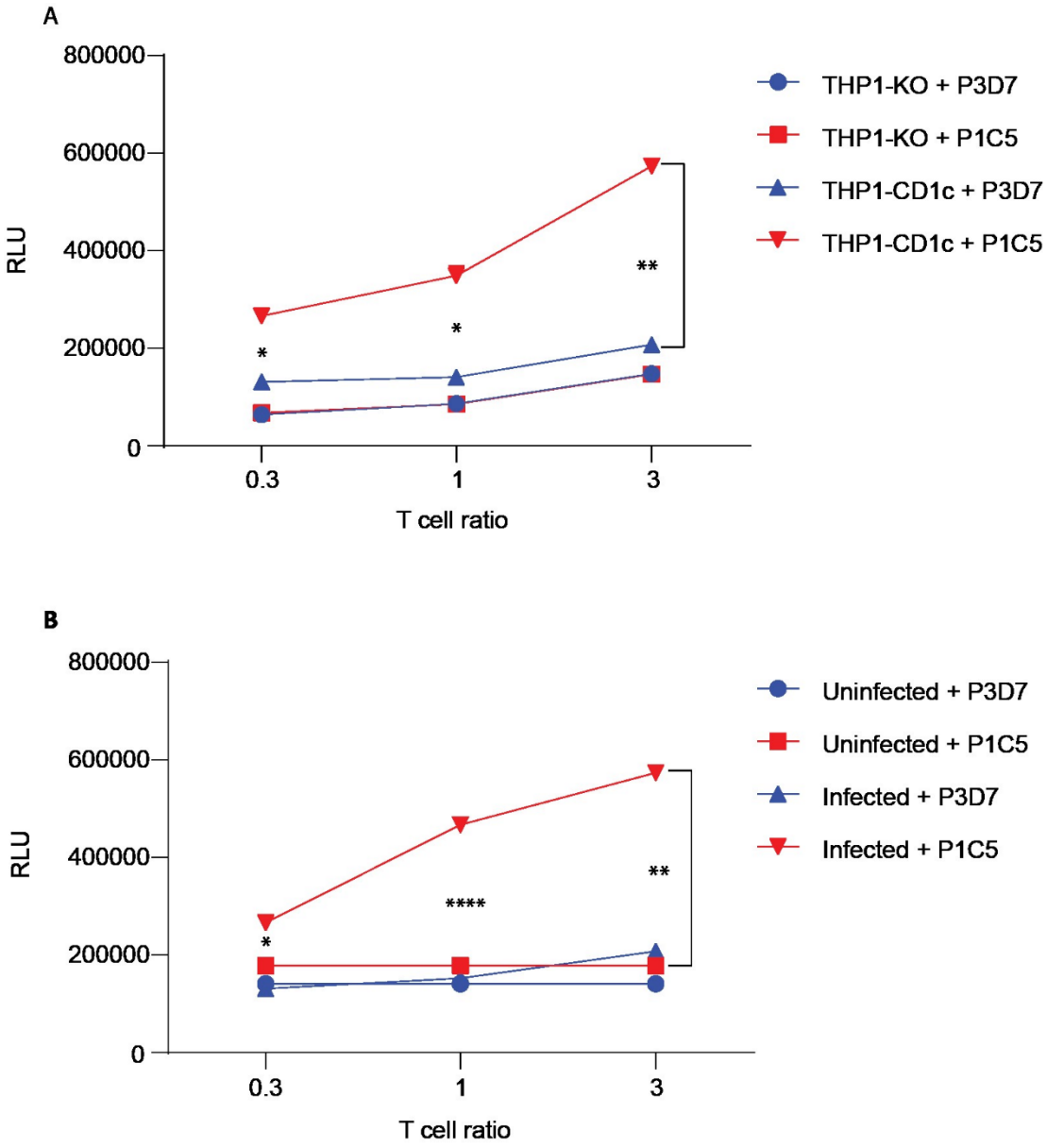

Figure 43: CD1c-reactive T cells caused an increase in cytotoxicity in a dose-dependent manner. P1C5 T cells result in greater cytotoxicity specifically when cultured with infected THP1-CD1c. Line graph shows an increase in cytotoxicity in a T cell dose-dependent manner when P1C5 T cells were cultured with infected THP1-CD1c cells compared to infected THP1-KO (**A**). This increase also occurred when P1C5 T cells were cultured with infected THP1-CD1c cells, compared to uninfected THP1-CD1c, and P3D7 T cells that were cultured with infected or uninfected THP1-CD1c cells (**B**). THP1 cells were infected with *Mtb* MOI = 10. T cells were added to THP1 cells at three different ratios 0.3:1, 1:1, and 3:1. Cytotoxicity was then measured 48 hours post the addition of T cells to THP1 cells. Data are representative of two experiments, each preformed in triplicate. * $P < 0.05$; ** $P < 0.01$; **** $P < 0.0001$ (two-way ANOVA).

The effect of increasing the MOI of UV killed TB

Our data revealed that increasing the MOI resulted in an increase in CD1c expression on THP1-CD1c cells at MOI of 10 (Figure 40). Thus, the effect of the increase in CD1c expression on cytotoxicity was investigated. THP1 cells were infected with a range of MOIs, and T cells were added 24 post infection to the THP1 cells at a fixed ratio (1:1). Forty-eight hours later, cytotoxicity was measured using the ToxiLight assay. Across all three MOIs, P1C5 T cells resulted in a significantly greater level of cytotoxicity when cultured with THP1-CD1c, compared to THP1-KO cells (Figure 44A). Furthermore, a statistically significant dose-dependent increase in cytotoxicity was observed in the wells where infected THP1-CD1c cells were cultured with P1C5 T cells, compared to the wells cultured with the control T cell line P3D7 (Figure 44B).

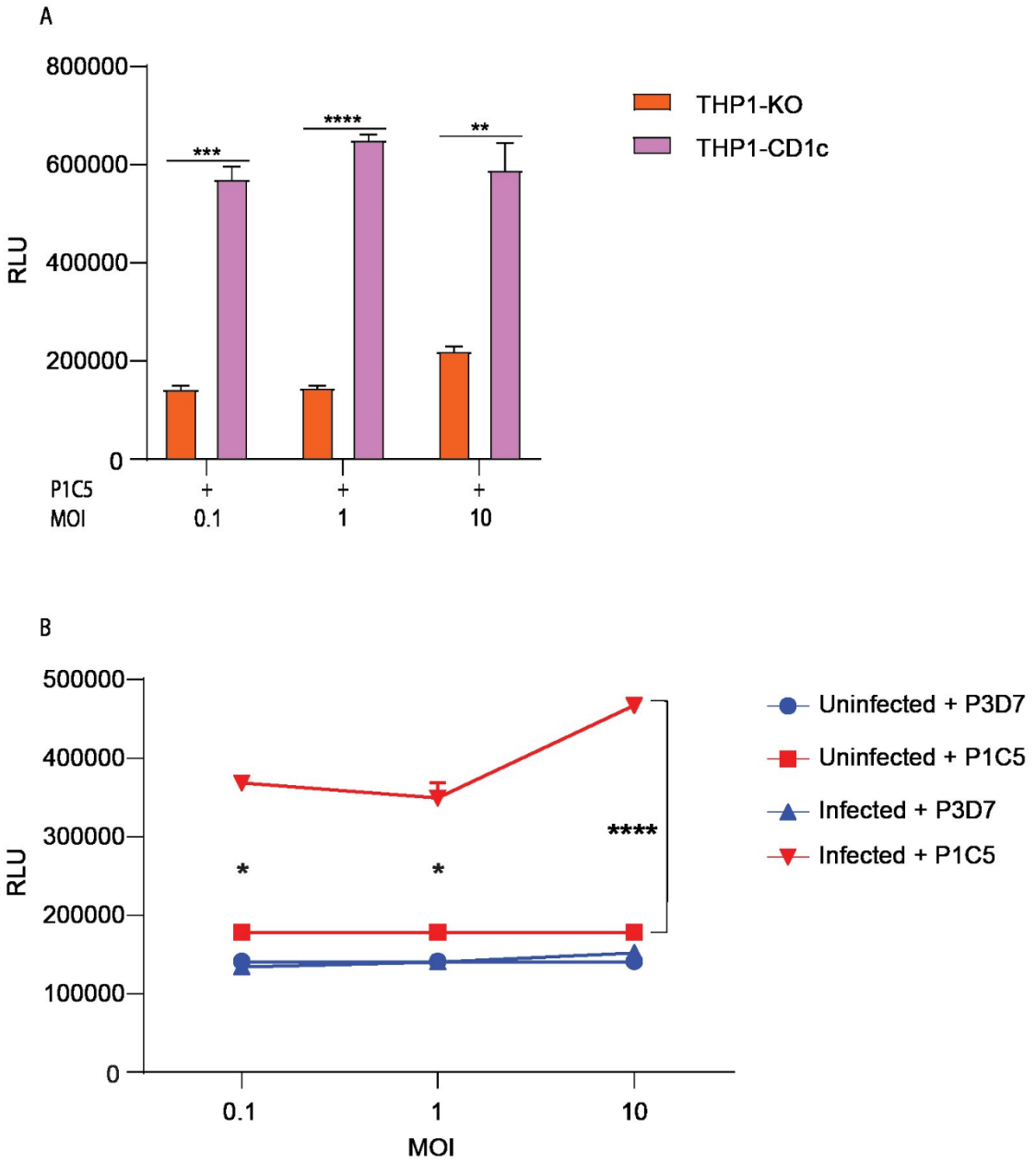

Figure 44: Increasing the MOI of UV killed TB resulted in an increase in cytotoxicity. Bar graph shows that P1C5 T cells resulted in an increase in cytotoxicity when cultured with infected THP1-CD1c cells, compared to infected THP1-KO cells (**A**). This increase in cytotoxicity also occurred when P1C5 cells were cultured with infected THP1-CD1c cells compared to uninfected THP1-CD1c, and when P3D7 cells were cultured with infected and uninfected THP1-CD1c cells (**B**). THP1 cells were infected with three different MOI of *Mtb* 0.1, 1, and 10. T cells were added to THP1 cells at a 1:1 ratio. Cytotoxicity was measured 48 hours post the addition of T cells to THP1 cells. Data are representative of two experiments, each preformed in triplicate. Error bars represent SEM. * $P < 0.05$; ** $P < 0.01$; **** $P < 0.0001$ (A, paired t-test; B, two-way ANOVA).

Summary

In order to investigate the functional effect of CD1c-autoreactive T cells during the infection of THP1 cell lines with UV killed TB, we studied the impact of two different parameters, the T cell ratio dependent-response, and the MOI dose-response of UV-killed TB. In experiments where both the THP1-KO and THP1-CD1c lines were infected with MOI = 10, and T cells were added in a ratio dependent manner, P1C5 T cells resulted in significant cell death only when cultured with infected THP1-CD1c. Meanwhile, the cytotoxicity observed in the wells with P1C5 T cells and infected THP1-KO was comparable to that of the wells that contained the infected THP1 lines with control P3D7 T cells. Furthermore, when studying the infected vs non-infected THP1-CD1c, the greatest cytotoxicity is observed only in the wells that are cultured with P1C5 T cells, and not with P3D7 T cells in both the infected vs uninfected conditions (Figure 43). Additionally, when the MOI used to infect THP1 lines was increased from 0.1 to 10 in ten-fold increments, whilst the ratio of THP1 cells:T cells remained unchanged, P1C5 T cells resulted in a significant increase in cytotoxicity in comparison to P3D7 T cells. Similarly, when studying the infected vs non-infected THP1-CD1c, the greatest cytotoxicity was observed only in the wells that are cultured with P1C5 T cells across all the MOIs, and not with P3D7 T cells in both the infected vs uninfected conditions (Figure 44). Collectively, the data demonstrates the cytotoxic effect of our CD1c-autoreactive T cell line during TB infection.

Chapter 6 CD1c-autoreactive T cells are polyfunctional and have a mixed cytokine profile

Having observed the cytotoxic effect of P1C5 T cells during *Mtb* infection, we sought to identify their cytokine profile. In order to achieve this aim, Luminex assays were carried out using supernatants from cultures of P1C5 T cells that were infected with *Mtb* at MOI = 10. We found that in response to infection, this polyclonal line released an array of cytokines such as IL-1α, IL-1RA, TNF-α, IFN-γ, IL-2, IL-12, IL-4, IL-5, IL-10, IL-13, Monokine Induced by Interferon gamma (MIG), and GM-CSF. Additionally, some cytokines were also produced in an autoreactive manner in the absence of *Mtb*. Furthermore, we identified a few cytokines released by THP1 cells in response to infection, in the absence of T cells. Altogether, the data supports the notion that P1C5 is a CD1c-autoreactive polyclonal T cell line with a mixed polyfunctional cytokine profile, and antimycobacterial properties.

THP1-CD1c cells produce cytokines in response to *Mtb* infection

We infected THP1-CD1c cells alone with UV-killed *Mtb* (MOI = 10) as controls in order to determine which cytokines they would release independent of T cells. We found that they released significant amounts of IL-8 and Regulated on Activation, Normal T cell Expressed and Secreted (RANTES) (Figure 45), both of which are chemokines involved in the recruitment of leukocytes such as neutrophils and T cells [474-476]. This supports what has previously been published, as *Mtb* infection has been shown to upregulate the expression of IL-8 in human monocytes [477]; and RANTES has been shown to become upregulated in response to *Mtb* infection in THP1 cells [474].

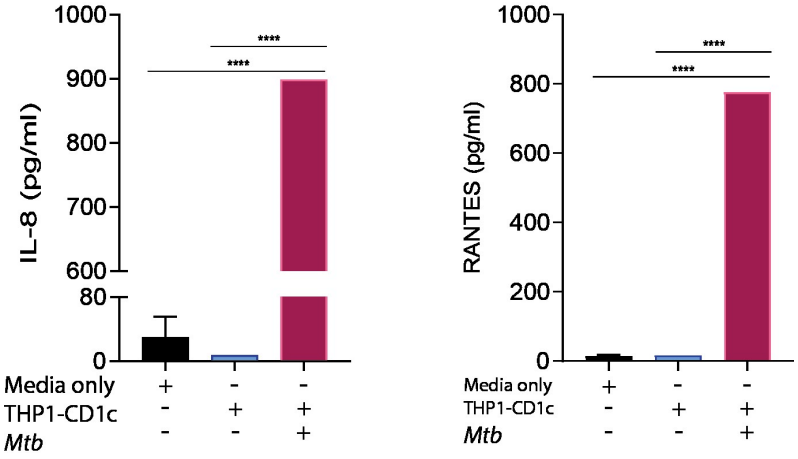

Figure 45: THP1-CD1c cells produced large amounts of chemoattractants when infected with *Mtb*. Infected THP1-CD1c cells produce significant amounts of (**A**) IL-8 and (**B**) RANTES, in comparison to media only (black bars), and uninfected THP1-CD1c cells (blue bars). THP1-CD1c cells were infected with *Mtb* MOI = 10. The data are from one experiment performed in triplicate, and results are consistent from two separate experiments performed in triplicate. Error bars represent SEM. ****$P <$ 0.0001 (two-way ANOVA).

The response of P1C5 T cells to *Mtb* infection is dependent upon TCR recognition of CD1c

Having observed the cytotoxic effect of P1C5 T cells during *Mtb* infection, we used the same supernatants to identify the cytokines released by these cells. Additionally, we observed consistent results across two experiments, with each experimental condition performed in triplicate, and determined whether this response was CD1c dependent by using P3D7 (our non-CD1c reactive T cell line) (Figure 46 & Supplementary Figure S1), as well as using THP1-KO cells that do not express CD1c (Figure 47 & Supplementary Figure S2). In all cases, THP1 cells were infected with UV-killed TB at MOI = 10, and the T cells were added at 3 different ratios relative to the THP1 cells (0.3:1, 1:1, 3:1).. Our data revealed that in response to infected THP1-CD1c cells, P1C5 T cells released significantly greater amounts of various cytokines which included IL-1α, IL-1RA, TNF-α, IL-2, IFN-γ, IL-4, IL-5, IL-10, IL-13, MIG, GM-CSF; and significantly lower amounts of RANTES, in comparison to infected THP1-KO cells (Figure 48).

Furthermore, in comparison to when P3D7 T cells were cultured with infected THP1-CD1c, we again observed that P1C5 T cells produced significantly greater amounts of various cytokines than P3D7 T

cells did (Figure 49). In both experiments, the release of some of the cytokines appear to increase in a dose dependent manner (Figure 48 & Figure 49).

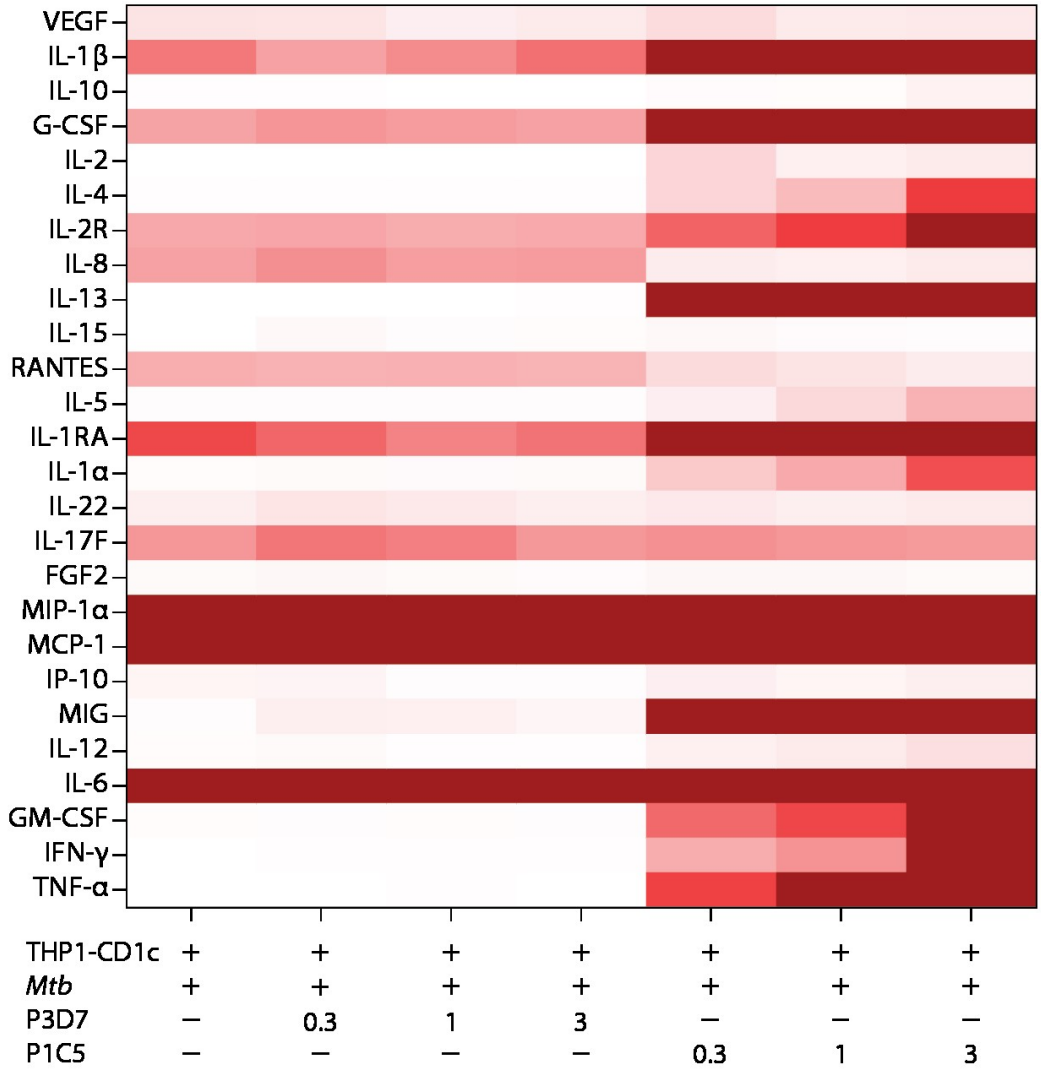

Figure 46: Heat map of cytokines secreted by P3D7 and P1C5 T cells. Heat map depicting relative levels of cytokines secreted by P3D7 and P1C5 T cells cultured with infected THP1-CD1c cells. T cells were added to infected THP1-CD1c cells (*Mtb* MOI = 10) at three different ratios 0.3:1, 1:1, and 3:1. Concentrations of cytokines released were measured 48 hours post the addition of T cells. Red and white indicate greater and lower expression, respectively.

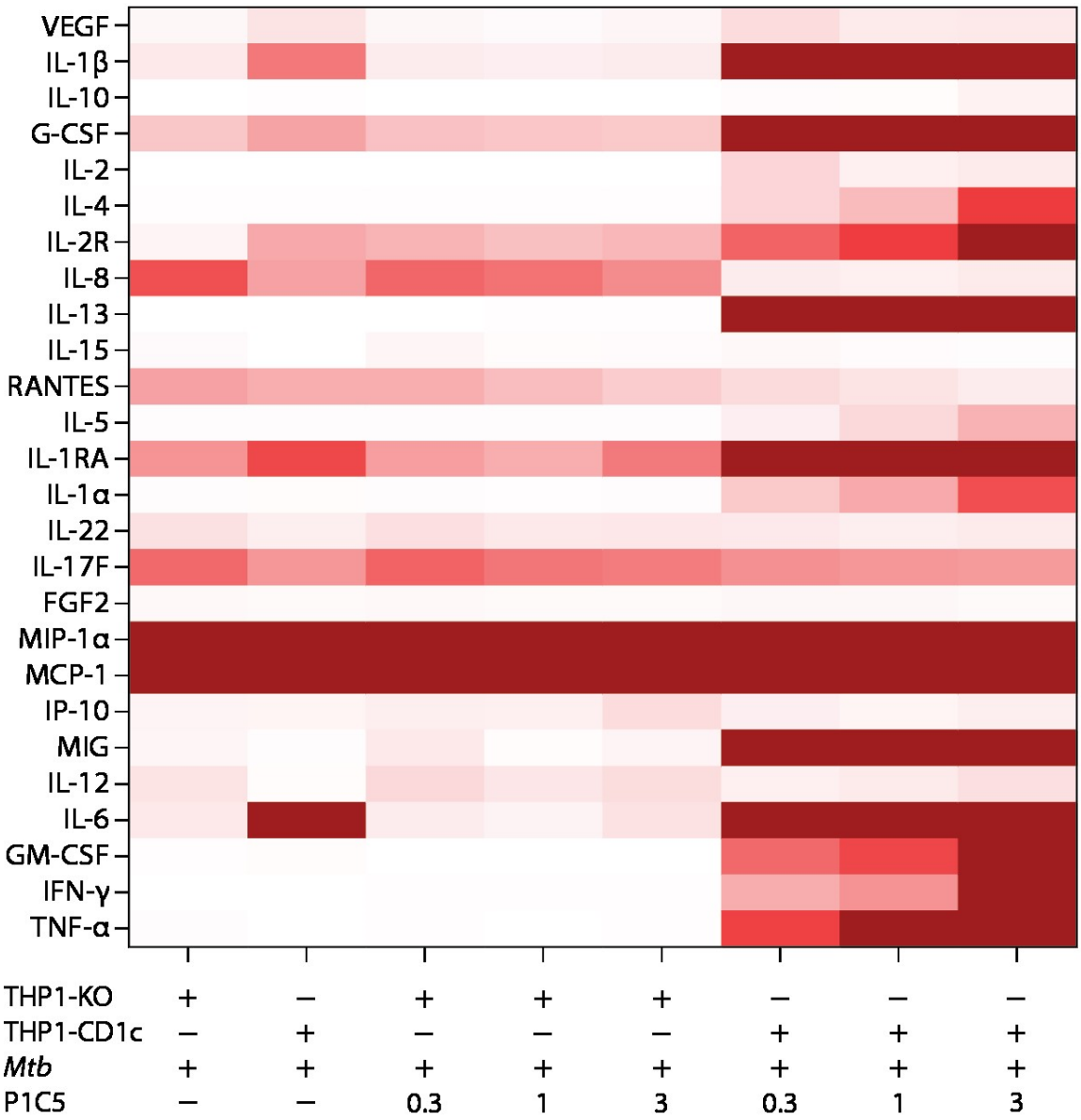

Figure 47: Heat map of cytokines secreted by P1C5 T cells in response to infected THP1 cells. Heat map depicting relative levels of cytokines secreted by P1C5 T cells cultured with infected THP1-KO and THP1-CD1c cells. T cells were added to infected THP1 cells (*Mtb* MOI = 10) at three different ratios 0.3:1, 1:1, and 3:1. Concentrations of cytokines released were measured 48 hours post the addition of T cells. Red and white indicate greater and lower expression, respectively.

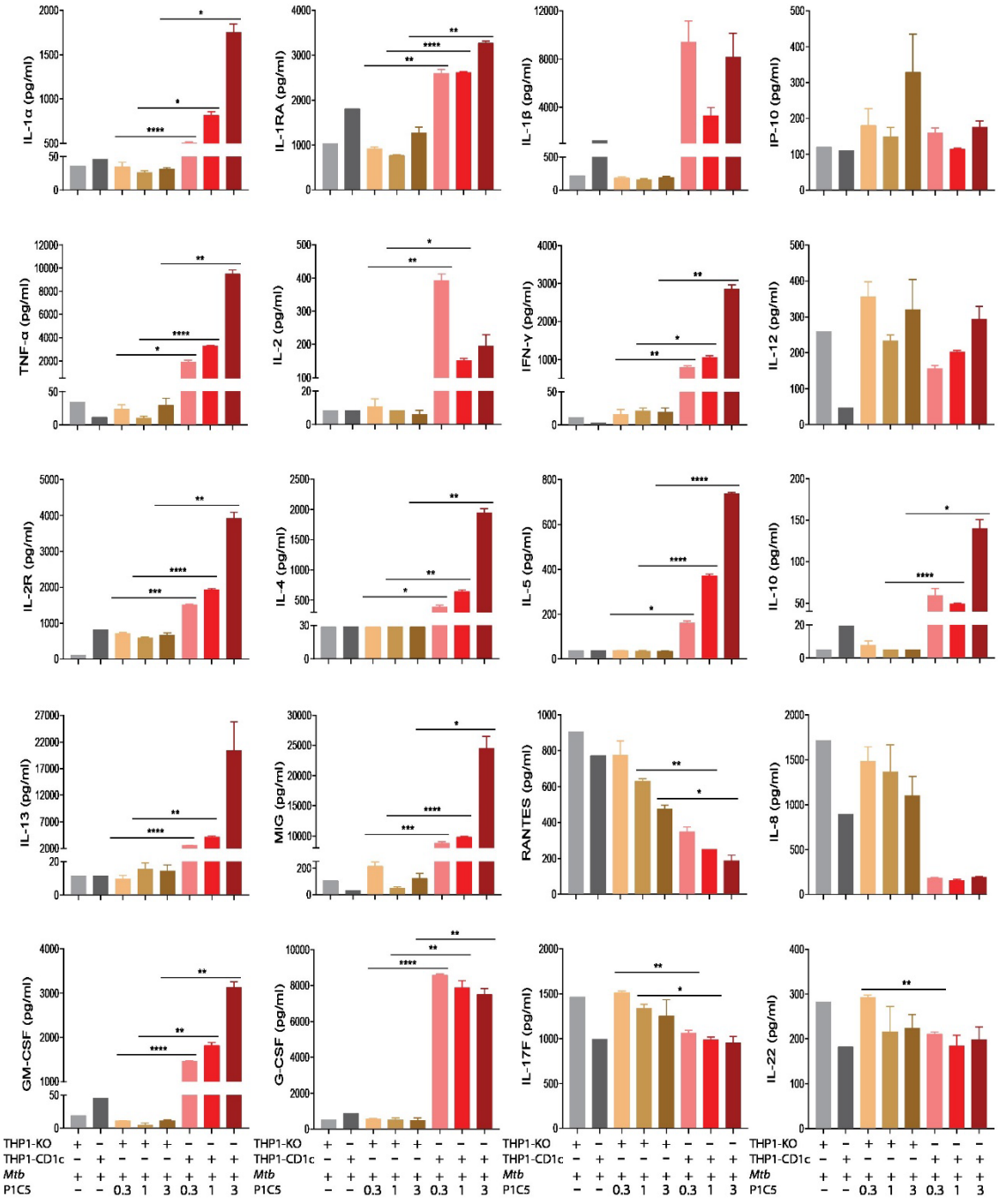

Figure 48: P1C5 T cells produced various cytokines in a CD1c dependent manner. P1C5 T cells resulted in a significant increase in cytokines associated with anti-microbial control when cultured with infected THP1-CD1c cells, this response is not observed when P1C5 T cells were cultured with infected THP1-KO cells. THP1 cells were infected with *Mtb* MOI = 10, and T cells were added at three different ratios 0.3:1, 1:1, and 3:1. Concentrations of cytokines released were measured 48 hours post the addition of T cells. The data are from one experiment performed in triplicate, and results are consistent from two separate experiments performed in triplicate. Error bars represent SEM. * $P < 0.05$; ** $P < 0.01$, *** $P < 0.0005$, **** $P < 0.0001$ (two-way ANOVA).

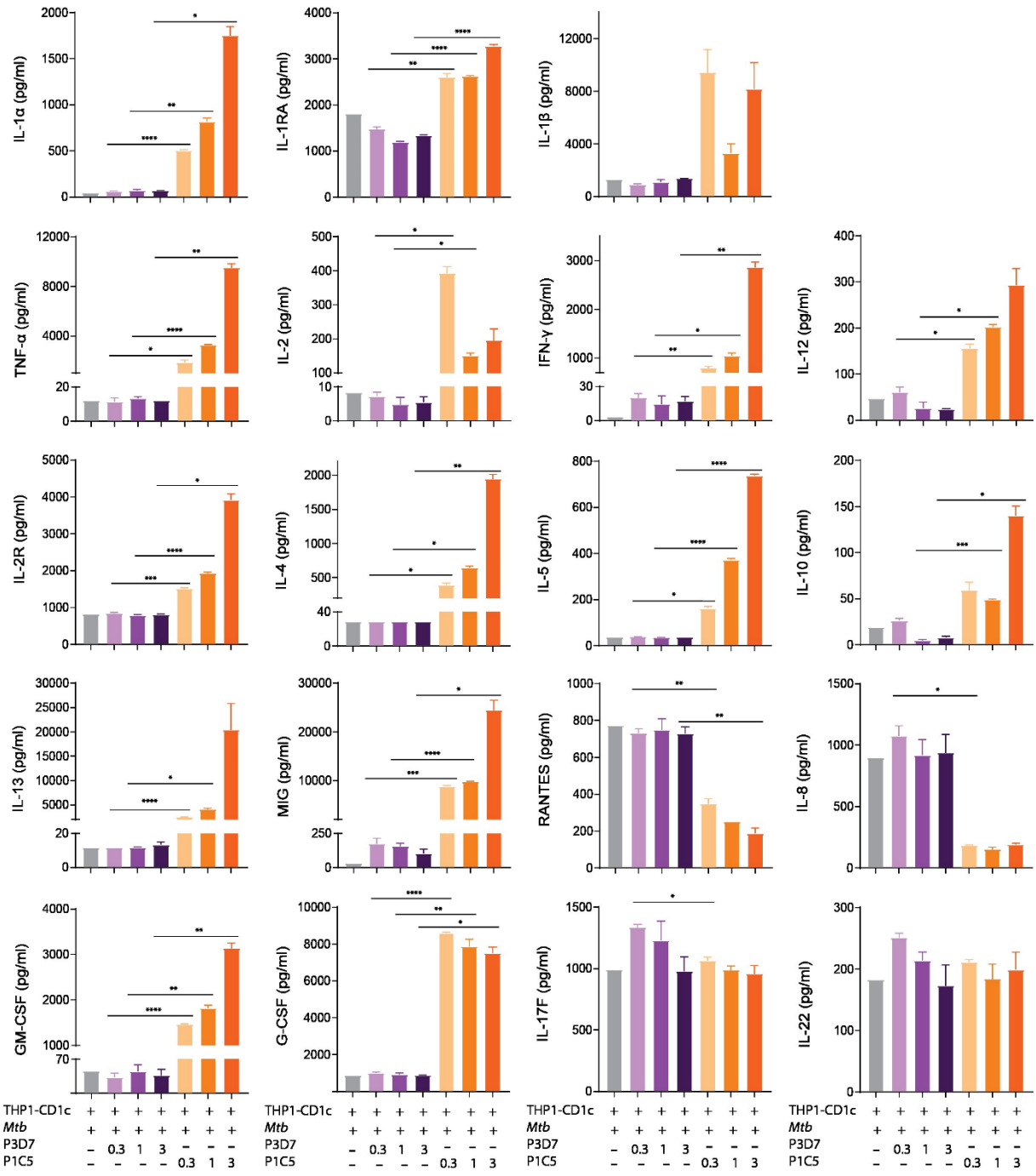

Figure 49: P1C5 T cells produced various cytokines in response to infected THP1-CD1c. P1C5 T cells result in a significant increase in cytokines associated with anti-microbial response when cultured with infected THP1-CD1c cells, this response is not observed with P3D7 T cells. THP1-CD1c cells were infected with *Mtb* MOI = 10, and T cells were added at three different ratios 0.3:1, 1:1, and 3:1. Concentrations of cytokines released were measured 48 hours post the addition of T cells. The data are from one experiment performed in triplicate, and results are consistent from two separate experiments performed in triplicate. Error bars represent SEM. * $P < 0.05$; ** $P < 0.01$, *** $P < 0.0005$, **** $P < 0.0001$ (two-way ANOVA).

P1C5 T cells display CD1c mediated autoreactive responses

In order to identify whether P1C5 T cells displayed autoreactivity towards THP1-CD1c, we measured cytokine responses from wells with uninfected THP1-CD1c cells and P1C5 T cells. We also compared these cytokine responses with those from cells cultured with infected THP1-CD1c. The THP1 cells were infected with UV-killed TB at MOI = 10, P1C5 T cells were then added at 3 different ratios relative to the THP1 cells (0.3:1, 1:1, 3:1). We found that during infection, P1C5 T cells expressed significantly greater amounts of various cytokines such as IL-1α, TNF-α, IL-2, IFN-γ, IL-12, IL-4, IL-5, IL-10, IL-13, and GM-CSF (Figure 50). Additionally, we also found that P1C5 T cells did not release as many cytokines when cultured with uninfected THP1-CD1c (Figure 51), as they did when cultured with infected THP1-CD1c (Figure 52), however, they still released several cytokines such as IL-1α, IL-1RA, IL-1β, IL-2, IFN-γ, IL-5, IL-13, IL-17F and GM-CSF (Figure 51), thus displaying autoreactivity. Importantly, they released significantly greater concentrations of cytokines when cultured with *Mtb* infected THP1-CD1c, further supporting an anti-*Mtb* role for these T cells.

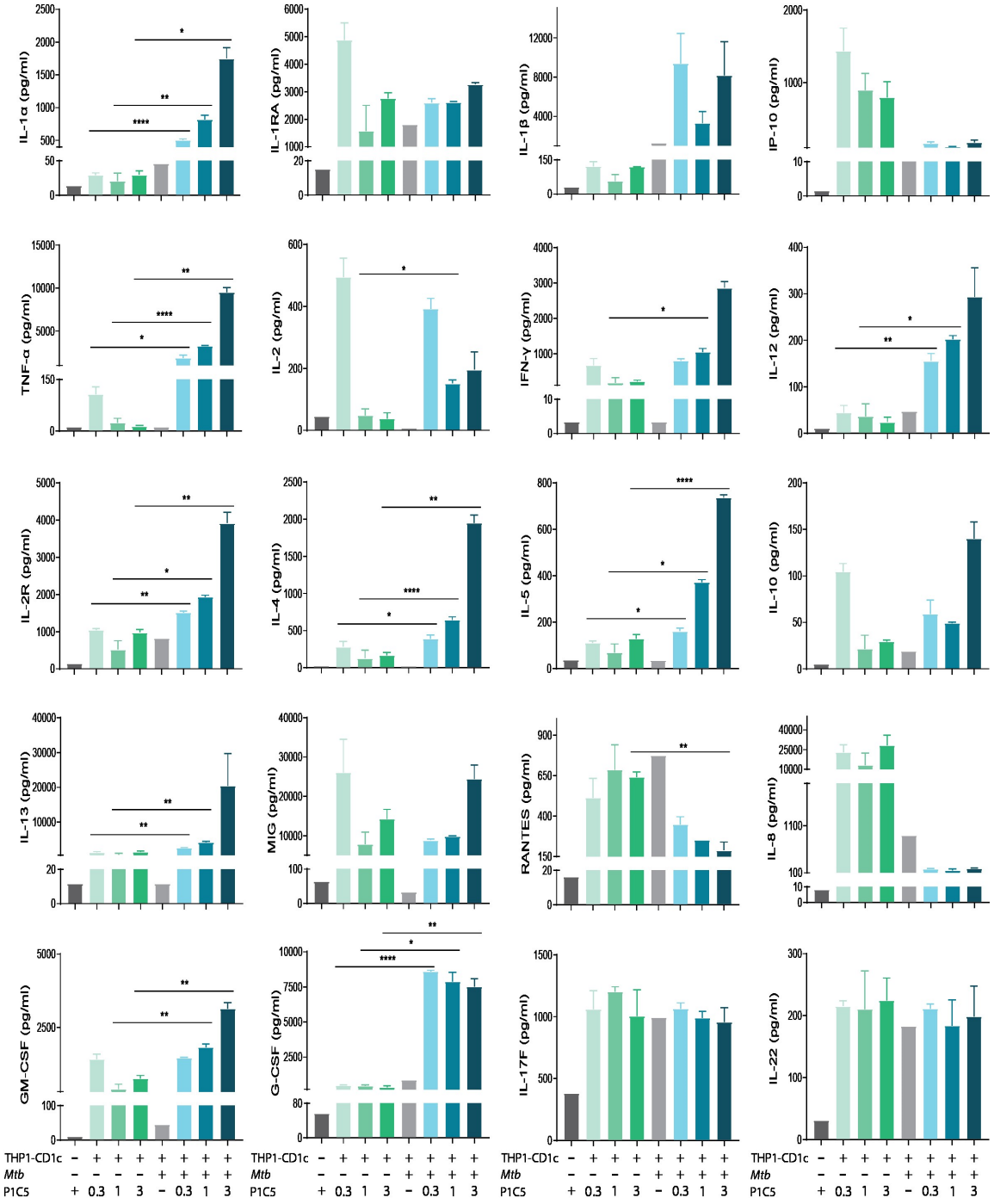

Figure 50: P1C5 T cells produce a significant amount of cytokines in response to *Mtb* infection. P1C5 T cells produce cytokines in response to uninfected THP1-CD1c, and result in a significant increase in some cytokines when cultured with infected THP1-CD1c (*Mtb* MOI = 10). T cells were added to THP1-CD1c cells at three different ratios 0.3:1, 1:1, and 3:1. Concentrations of cytokines released were measured 48 hours post the addition of T cells. The data are from one experiment performed in triplicate, and results are consistent from two separate experiments performed in triplicate. Error bars represent SEM. * $P < 0.05$; ** $P < 0.01$, *** $P < 0.0005$, **** $P < 0.0001$ (two-way ANOVA).

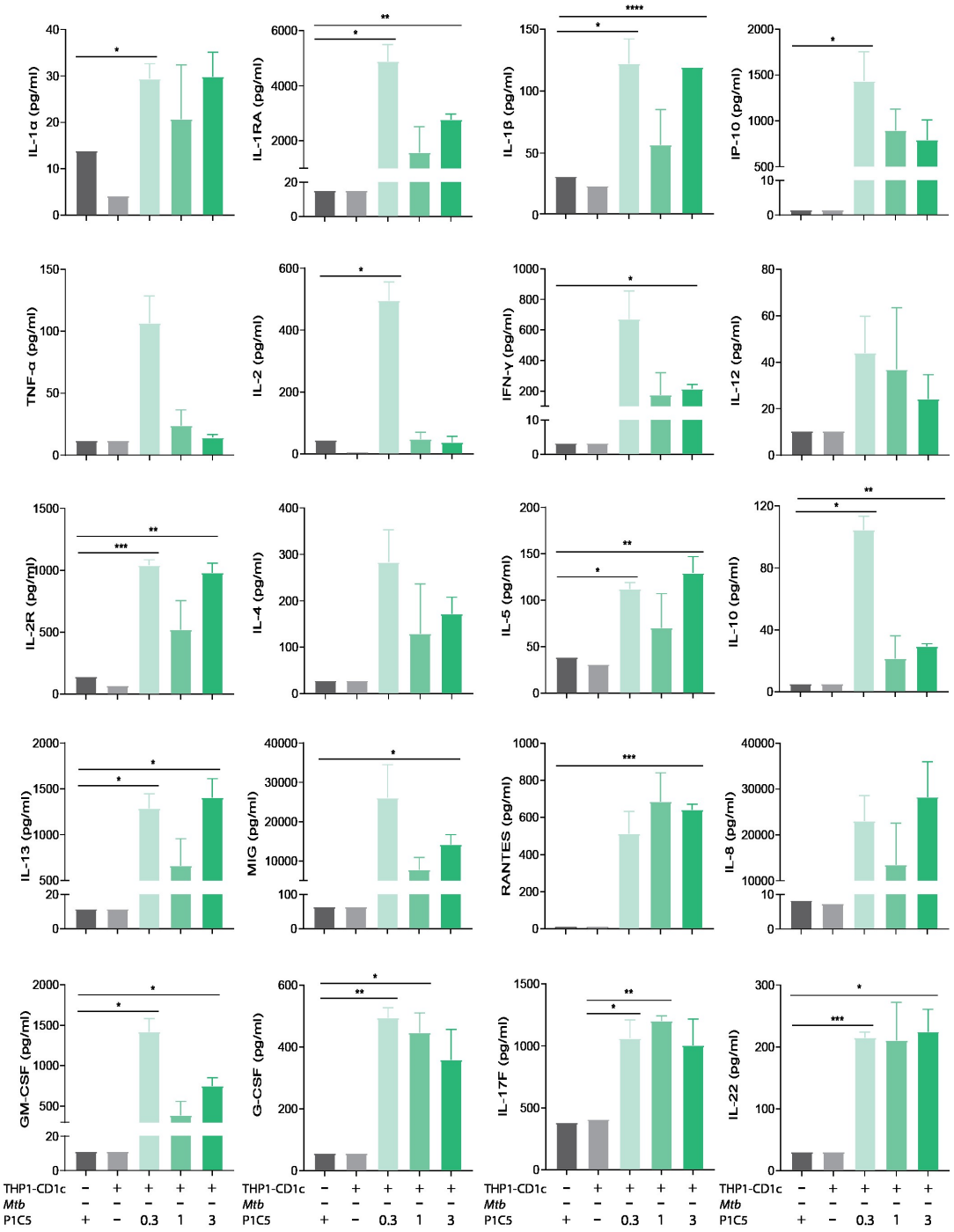

Figure 51: P1C5 T cells display autoreactive responses when cultured with uninfected THP1-CD1c. P1C5 T cells result in a significant increase in some cytokines when cultured with uninfected THP1-CD1c (green bars) compared to controls (grey bars), thus indicating their autoreactivity. T cells were added to THP1-CD1c cells at three different ratios 0.3:1, 1:1, and 3:1. Concentrations of cytokines released were measured 48 hours post the addition of T cells. The data are from one experiment performed in triplicate, and results are consistent from two separate experiments performed in triplicate. Error bars represent SEM. * $P < 0.05$; ** $P < 0.01$, *** $P < 0.0005$, **** $P < 0.0001$ (two-way ANOVA).

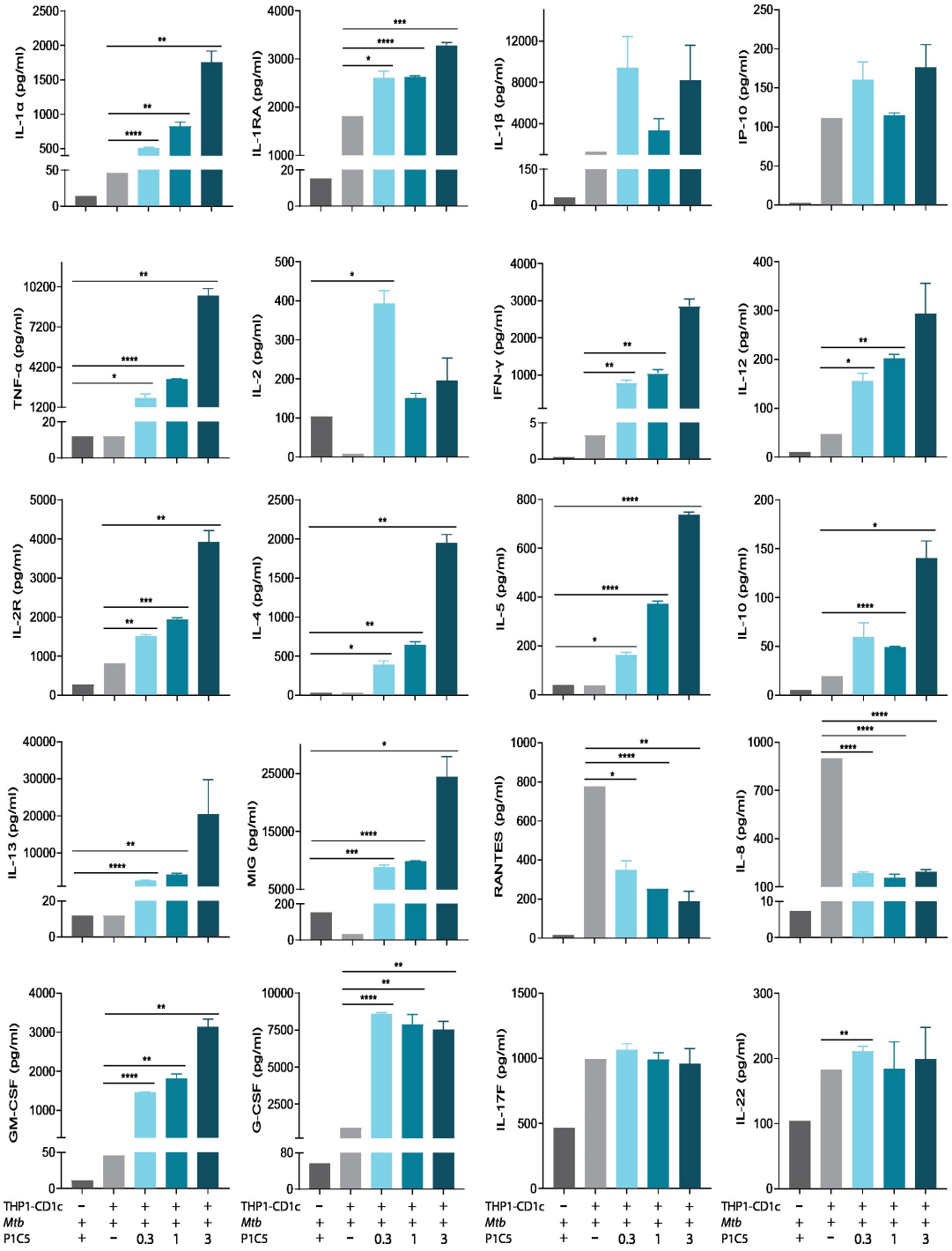

Figure 52: P1C5 T cells display dose-dependent cytokine responses when cultured with infected THP1-CD1c. P1C5 T cells result in a significant increase in some cytokines when cultured with infected THP1-CD1c (blue bars) compared to controls (grey bars). THP1-CD1c cells were infected with *Mtb* MOI = 10. T cells were added to THP1 cells at three different ratios 0.3:1, 1:1, and 3:1. Concentrations of cytokines released were measured 48 hours post the addition of T cells. The data are from one experiment performed in triplicate, and results are consistent from two separate experiments performed in triplicate. Error bars represent SEM. * $P < 0.05$; ** $P < 0.01$, *** $P < 0.0005$, **** $P < 0.0001$ (two-way ANOVA).

Summary

The use of Luminex assays determined that our P1C5 T cell line produced an array of cytokines that were not specific to one lineage. We found that when cultured in the absence of T cells, infected THP1-CD1c cells produced copious amounts of the chemokines IL-8 and RANTES; both of which have been shown to be involved during TB, and contribute to the recruitment and activation of T cells at the site of infection [477-479]. Additionally, we demonstrated that not only did P1C5 T cells respond to *Mtb* infection specifically, they also did so in a CD1c dependent manner, and displayed autoreactivity in the absence of *Mtb*. Their autoreactivity was highlighted by the release of significantly high concentrations of several cytokines when P1C5 T cells were cultured with uninfected THP1-CD1c cells. Furthermore, this response was amplified in the presence of *Mtb.* The cells exhibited an *Mtb*-specific polyfunctional response, as indicated by the significant amounts of anti-microbial cytokines released such as TNF-α, IFN-γ, IL-1, and GM-CSF, as well as Th2 cytokines such as IL-4 and IL-5. In addition, we found that in the presence of *Mtb*, P1C5 T cells produced significant amounts of IL-12. This cytokine is typically produced by APCs such as monocytes, macrophages, and DCs, and promotes the survival and expansion of activated T cells [480]. Altogether, along with the release of chemokines during infection, such as MIG, our data suggests that CD1c-reactive T cells are amongst the first line of defence and their recruitment and activation occurs readily upon infection.

Overall, this data has allowed us to further phenotype P1C5 T cells as CD1c-autoreactive T cells, and their role during TB infection. Irrespective of the controls used, we observed similar patterns across the data. The use of THP1-KO target cells, as well as using a non-CD1c reactive T cell line determined that P1C5 T cell responses were CD1c specific; and the comparison of cytokines released in the presence and absence of *Mtb* determined their autoreactive capacity. Whilst the significant increase in cytokines released during infection determined their *Mtb*-specific protective function.

Chapter 7 CD1c-autoreactive T cells express αβ and γδ T cell receptors

In order to better understand the TCR repertoire of CD1c-autoreactive T cells, sequencing of their TCRs must be carried out. This allows for further characterisation of TCRs and biochemical studies to be completed. We used tetramers to single cell sort and sequence TCRs from 3 donors. Although we identified several unique TCRs, issues in the consequent amplification and cloning steps meant that we were unfortunately unable to further characterise them during the course of this study. However, ongoing work to better understand these TCRs continues in our lab.

TCR sequencing

In order to better understand the TCR repertoire of CD1c-autoreactive T cells, sequencing of their TCRs must be carried out. This allows for further characterisation of TCRs and biochemical studies to be completed. T cells from three donors that were previously expanded with THP1-CD1c were stained with anti-CD3, and CD1c-endo tetramers. $CD3^+$ CD1c-endo $tetramer^+$ T cells were single cell sorted by flow cytometry (Figure 53) directly into PCR plates, and sequenced by the Sequencing Team at Immunocore. From the three donors, 8 unique TCR pairs were identified and sequenced (*Table 4* & *Table 5*). Half of the identified TCRs were γδ, and although they were all derived from the same donor (RVI); CD1c autoreactive TCRs derived from a different donor in an RNASeq study carried out by our lab in Southampton identified highly homologous γδ-TCRs (data not shown). Studies identifying the TCR chains of CD1c autoreactive T cells have shown that they can be either αβ- [481] or γδ-TCRs [381], however the functional implication in the context of TB infection of either TCR type remains to be investigated. Further validation and specificity studies of the TCRs derived from this experiment are yet to be carried out.

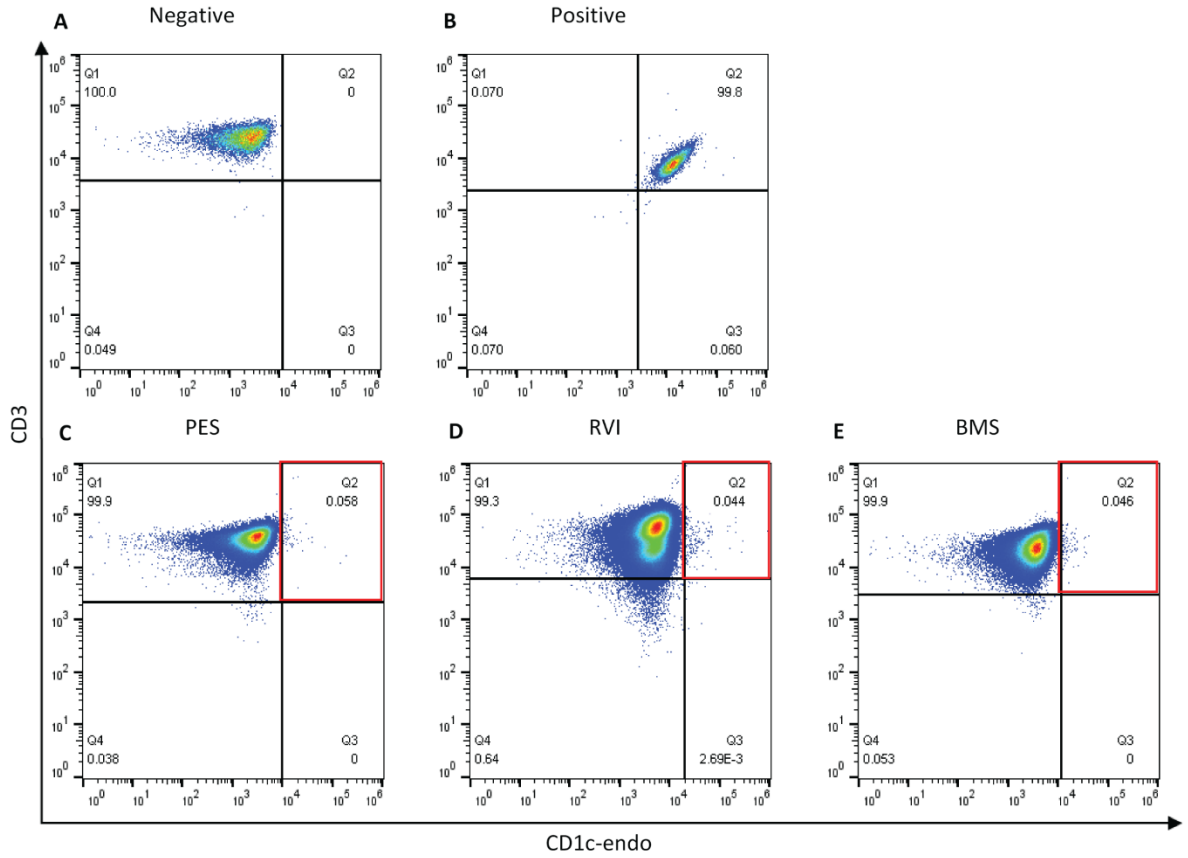

Figure 53: Single cell sorting of CD1c-endo tetramer positive T cells. Flow cytometry dot plots show CD1c-endo tetramer staining of T cells from three donors. Cells within the red gates were single cell sorted (**C-E**) (*n*=3).

Table 4: Summary of sorted cells and unique TCRs from each line

Donor	**Number of sorted single cells**	**Unique TCRs**
BMS	15	1
PES	14	2
RVI	69	5

Table 5: Sequences and frequency of unique TCRs from single cell sequencing. Some sequences redacted due to Immunocore IP.

Donor	Frequency of clonotype	Chain	V	D	J	C	CDR3
RVI	2	Delta	TRDV2	TRDD3	XXXXX	TRDC	XXXXXXXXXXXXXXXXXX
		Gamma	TRGV9	-	XXXXX	TRGC1	XXXXXXXXXXXXXXXX
RVI	1	Delta	TRDV2	TRDD3	XXXXX	TRDC	XXXXXXXXXXXXX
		Gamma	TRGV9	-	XXXXX	TRGC1	XXXXXXXXXXXXXXXX
RVI	26	Delta	TRDV1	TRDD3	XXXXX	TRDC	XXXXXXXXXXXXXXXXXX
		Gamma	TRGV4	-	XXXXXX	TRGC2	XXXXXXXXXXXXXXX
RVI	1	Alpha	TRAV5	-	XXXXXX	TRAC	XXXXXXXXXXX
		Beta	TRBV6-5	TRBD1	XXXXXX	TRBC1	XXXXXXXXXXXX
RVI	1	Delta	TRDV3	TRDD3	XXXXX	TRDC	XXXXXXXXXXXXXXXXXX
		Gamma	TRGV9	-	XXXXX	TRGC2	XXXXXXXXXXXXXXXX
BMS	6	Alpha	TRAV24	-	XXXXXX	TRAC	XXXXXXXXXXXXX
		Beta	TRBV2	TRBD2	XXXXXX	TRBC2	XXXXXXXXXXXXX
PES	5	Alpha	TRAV14DV4	-	XXXXXX	TRAC	XXXXXXXXXXXXXXXX
		Beta	TRBV2	TRBD1	XXXXXX	TRBC1	XXXXXXXXXXXXXX
PES	2	Alpha	TRAV38-2DV8	-	XXXXXX	TRAC	XXXXXXXXXXXXXX
		Beta	TRBV3-1	-	XXXXXX	TRBC1	XXXXXXXXXXXXX

Following sequencing, our aim was to clone the TCRs onto Jurkat cell lines, this would allow us to better investigate their specificity and function. We completed a set of experiments at Immunocore in an effort to achieve this aim.

Amplification of gBlocks

A robust method of cloning TCRs has been developed and is regularly used at Immunocore. This involves designing gene fragments containing the sequenced TCRs, these are then amplified via PCR to generate enough of the desired DNA segment and then cloned into a lentiviral vector. The lentiviruses are subsequently used to transduce Jurkat T cell lines resulting in cell surface expression of TCRs. The TCRs of the CD1c-endo tetramer^{+} T cells that were single cell sorted and sequenced were designed as gene fragments by our collaborators at Immunocore and synthesised externally by IDT. First, the gBlocks were attempted to be amplified using primer pairs that were specifically designed for each gBlock (primer pair gBlock table). However, the amplification was not successful. The desired fragment was amplified, but not efficiently, while other amplicons can be visualised along with the desired PCR product indicated by the blue arrows in (Figure 54). In some samples the other fragments are amplified preferentially (Figure 54). To further preferentially amplify the desired amplicon, a temperature gradient PCR was carried out. Two samples were tested, whereby the

components of the PCR reaction mixture and the conditions of the PCR programme remained the same, apart from a temperature gradient being set between 56-65°C. However, this did not result in any changes to the PCR products produced at any temperature (Figure 55). Due to the amount of starting material remaining, as well as time being limited, amplification PCRs were not explored further, and instead more direct approaches were attempted, as discussed below.

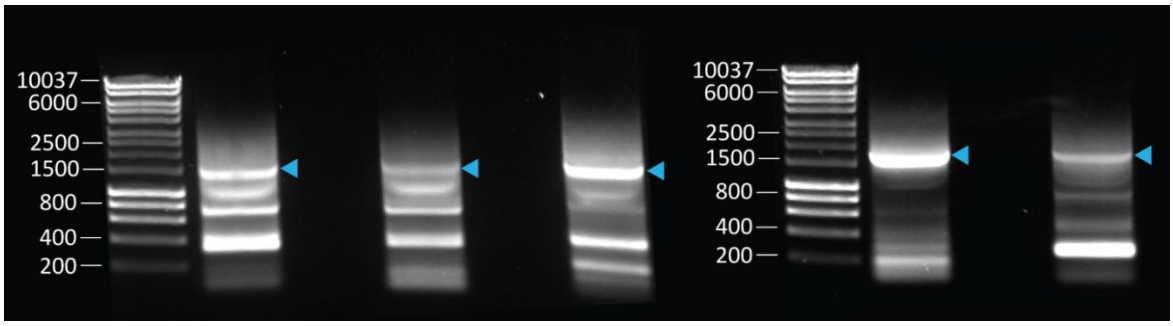

Figure 54: PCR amplification of gBlock gene fragments was not effective. Agarose gel electrophoresis separation of a PCR reaction carried out to amplify gene fragments, the desired amplicon is indicated by the blue arrowheads at ~1500kb. Amplification of the desired fragment was was ineffective despite being repeated twice. 1kb HyperLadder was used (Bioline).

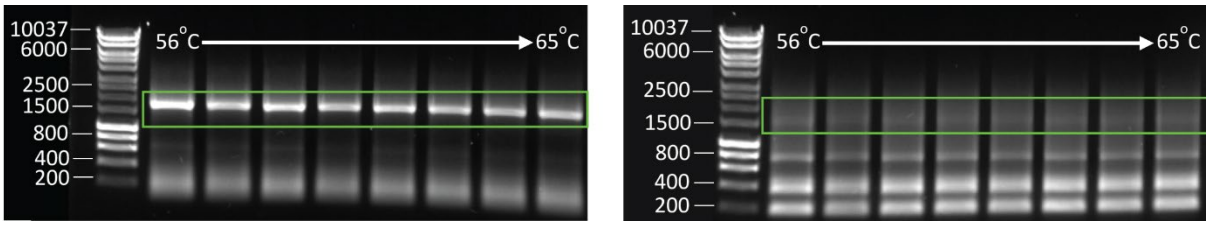

Figure 55: PCR temperature gradient of two gBlock fragments did not improve amplification of the desired fragment. Agarose gel electrophoresis separation of two different gBlock fragments with increasing annealing temperature gradients (56°C – 65°C). Temperature gradients did not improve the efficiency of the PCR reaction to amplify the desired amplicon. The desired fragments are highlighted within the green rectangle. 1kb HyperLadder was used (Bioline).

Vector and gBlock digestion and ligation

The JM22 pELNS LV vector and gBlock fragments were digested with the same restriction enzymes, NheI and SalI. Due to the size of the vector, following digestion, it was separated on an agarose gel (Figure 56) before being purified. The gBlocks were purified directly into DNA binding columns and eluted in the appropriate volume. A ligation reaction was carried out in order to ligate the vector backbone and gBlock fragment together before transforming the bacteria.

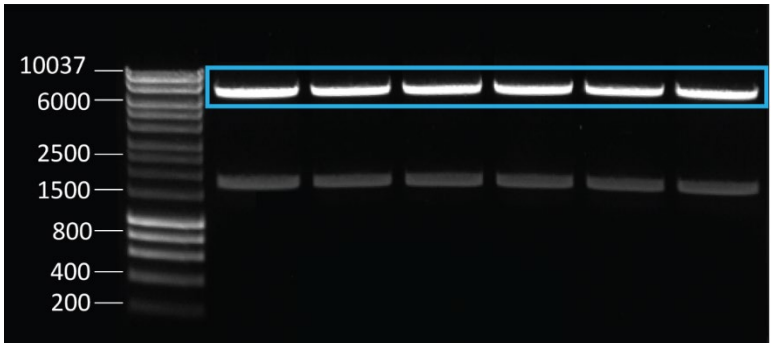

Figure 56: Effective digestion of the vector. Image of agarose gel electrophoresis separation of JM22 pELNS vector following digestion with restriction enzymes. The vector backbone fragments at ~8000kb that are highlighted within the blue rectangle were purified. 1kb HyperLadder was used (Bioline).

Transformation and DNA analysis

Following the transformation of the bacteria with plasmids consisting of the ligated gBlocks and vector backbones, colonies that grew on the agar plates were cultured in order to isolate DNA which was then purified and sent to Genewiz for sequencing. The sequences that returned determined that the insertion of the gBlock fragments into the vectors was unsuccessful, and that either the vector re-ligated to itself, or the digestions were not efficient in the first place, hence the transformed bacteria was able to propagate. Following the lack of success of these experiments, the sequences were revised at Southampton, and the absence of leader sequences in the gBlock fragments was identified. The sequences were reconstructed with the leader sequences and constant region integrated into the delta chains which were also missing in the original design (Figure 57). Finally, the complete full TCR sequences for 10 sequenced TCRs were constructed as in the example in Figure 57. These constructs were ordered for synthesis and subsequent subcloning into the Lentiviral vector by GeneScript. The vectors have since been amplified and transduction experiments are currently ongoing to express the TCRs in Jurkat T cell lines.

GCGCGCTAGCCGCCACC**atg**cagaggatctcctccctcatccatctctctcttctgggcaggagtcatgtcagccattgagttg
gtgcctgaacaccaaacagtgcctgtgtcaataggggtccctgccaccctcaggtgctccatgaaa[redacted]
[redacted]atcaactggtacagaaagacccaaggtaacacaatgactttcatataccga[redacted]atctatggccctggtttcaaagac
aatttccaaggtgacattgatattgcaaagaacctggctgtacttaagatacttgcaccatcagagagagatgaagggtcttactac
tgt[redacted]
agaagccagcctcacaccaagcctagcgtgttcgtgatgaagaacggcaccaacgtggcctgcctggtcaaagagttctaccccaag
gacatccggatcaacctggtgtccagcaagaagatcaccgagttcgaccccgccatcgtgatcagccctagcggcaagtacaacgcc
gtgaagctggggaagtacgaggacagcaatagcgtgacctgcagcgtgcagcacgacaacaagaccgtgcacagcaccgatttcgaa
gtgaaaaccgactccaccGATCACGTAAAACCTAAGGAAACTGAAAACACAAAGCAACCTTCAAAGAGCTGCCATAAACCCAAAGCC
ATAGTTCATACCGAGAAGGTGAACATGATGTCCCTCACAGTGCTTGGGCTACGAATGCTGTTTGCAAAGACTGTTGCCGTCAATTTT
CTCTTGACTGCCAAGTTATTTTTTTTGGGATCCGGCGCCACCAACTTCAGCCTGCTGAAGCAGGCCGGAGACGTGGAAGAAAACCCT
GGCCCTAGGatgctgtcactgctccacacatcaacgctggcagtccttggggctctgtgtgtatatggtgcaggtcacctagagcaa
cctcaaatttccagtactaaaacgctgtcaaaaacagcccgcctggaatgtgtggtgtct[redacted]gta
tattggtatcgagagagacctggtgaagtcatacagttcctggtgtcc[redacted]
[redacted]caggcaaatttgaggtggataggatacctgaaacgtctacatccactctcaccattcacaatgtagagaaacaggacatagct
acctactactgt[redacted]gac
aagcagctggacgccgacgtgtcccctaagcctaccatcttcctgccttctatcgccgagacaaagctgcagaaggccggcacctac
ctgtgcctgctggaaaagttcttcccagacgtgatcaagatccactgggaagagaagaagtccaataccatcctgggcagccaagag
ggcaataccatgaagaccaacgacacctacatgaagttcagctggctgacagtgcccgagaagtccctggacaaagaacacagatgc
atcgtgcgccacgagaacaacaagaacggcgtggaccaagagatcatcttcccacctatcaagacagatgtcatcacaatggacccc
aaagacaattgttcaaaagatgcaaatgatacactactgctgcagctcacaaacacctctgcatattacatgtacctcctcctgctc
ctcaagagtgtggtctattttgccatcatcacctgctgtctgcttagaagaacggctttctgctgcaatggagagaaatca**TAA**GT
CGAC

Green = Delta

Yellow = Gamma

GCTAGC NheI site

GGATCC BamHI site

CCTAGG AvrII site

GTCGAC SalI site

Full protein sequence from **ATG-TAA**

MQRISSLIHLSLFWAGVMSAIELVPEHQTVPVSIGVPATLRCSMK[redacted]INWYRKTQGNTMTFIYR
[redacted]IYGPGFKDNFQGDIDIAKNLAVLKILAPSERDEGSYYC[redacted]*R*
SQPHTKPSVFVMKNGTNVACLVKEFYPKDIRINLVSSKKITEFDPAIVISPSGKYNAVKLGKYEDSNSVT
CSVQHDNKTVHSTDFEVKTDSTDHVKPKETENTKQPSKSCHKPKAIVHTEKVNMMSLTVLGLRMLFAKTV
*AVNFLLTAKLFFL*GSGATNFSLLKQAGDVEENPGPRMLSLLHTSTLAVLGALCVYGAGHLEQPQISSTKT
LSKTARLECVVS[redacted]VYWYRERPGEVIQFLVS[redacted]RKESGIPSGKFEVDRIPETSTSTLTI
HNVEKQDIATYYC[redacted]*DKQLDADVSPKPTIFLPSIAETKLQKAGTYLCL*
LEKFFPDVIKIHWEEKKSNTILGSQEGNTMKTNDTYMKFSWLTVPEKSLDKEHRCIVRHENNKNGVDQEI
IFPPIKTDVITMDPKDNCSKDANDTLLLQLTNTSAYYMYLLLLLKSVVYFAIITCCLLRRTAFCCNGEKS
-

Leader

Delta

Gamma

CDR1 CDR2 CDR3 redacted

Italic = constant chain

2A peptide linker

Figure 57: Example of full construct of one representative TCR (a Vγ9Vδ2 TCR) within pELNS vector with multiple cloning sites. Some sequences were redacted due to Immunocore IP.

Summary

TCR sequencing studies are essential for understanding the TCR repertoire of CD1c-autoreactive T cells. Using CD1c-endo tetramers, cells from three donors that had previously been expanded with THP1-CD1c cells were isolated using tetramer guided single cell sorting. Following sequencing, eight unique TCR sequences were identified; we then attempted to amplify the sequences from gBlock gene fragments before they can be used to transduce Jurkat T cells. Amplification attempts were unsuccessful; and further revision identified issues in the gBlock sequences which have since been resolved.

Chapter 8 Discussion

Several studies have demonstrated a role for CD1c mediated responses in host immunity to TB infection [325, 329, 341, 482, 483]. In TB patients, including those with active TB, CD1c mediated immune responses have been shown to increase in the circulation [329]. Indeed, the first CD1c structures solved were bound to the *Mtb* derived cell wall lipids PMs, further supporting a role for CD1c in host immunity to infection [302, 381]. However, the functional role of CD1c mediated immune responses, including autoreactive T cell subsets, in human TB infection remains elusive. In this study, we optimised a methodology pipeline for the specific enrichment of CD1c autoreactive T cells from healthy and TB exposed individuals. Using these methods, we generated enriched CD1c-autoreactive T cells, and then explored their functional effect in TB. Studies to identify and clone CD1c-autoreactive T cells and their TCRs were carried out to investigate 1) TCR repertoire, 2) T cell phenotype, 3) T cell function in the context of TB infection, and 4) their cytokine profile.

Expansion of CD1c-restricted T cells

We explored various methods and tools in order to identify, expand, and isolate CD1c-autoreactive T cells. Several cell types were used as APCs to promote the expansion of these T cells, such as: trained and traditional (untrained) MoDCs, transduced THP1 cells that overexpress CD1c (THP1-CD1c), and CD1c coated MACSi beads. The methods varied in their success rates and limitations. Nevertheless, we ultimately developed a robust methodology for the specific isolation and expansion of CD1c-autoreactive T cells using THP1 cells, and validated the reliability and efficiency of this method using various assays.

Typically, when expanding T cells *ex vivo*, one of the most common and effective methods used are anti-CD3 and anti-CD28 coated beads [484-487], as it expands T cells without bias [488]. It is most effective when used to stimulate and expand the numbers of T cells once the desired T cell population has already been isolated. Nevertheless, we applied the concept of bead-mediated expansion by generating CD1c coated MACSi beads, however, they proved to be ineffective and were not pursued further.

When studying TB specific T cell responses, the expansion of T cells is often carried out using mycobacterial derived peptide antigens such as ESAT-6 and Ag85B [489]. However, the use of peptide mediated expansion methods give rise to conventional T cells with TCRs that recognise HLA

presenting molecules [489]. In order to expand CD1c specific T cells, we first sought to use autologous DCs. It has been well established in the literature that DCs express high levels of CD1c [490-492], and is often used as a DC marker [493]. Additionally, upon differentiation of monocytes to MoDCs, they have also been found to readily express CD1c [467, 494]. We reasoned that upon stimulation of T cells with MoDCs, their high levels of expression of CD1c would maximise the chances of CD1c-specific T cells expanding, and that trained MoDCs would do so to an even greater extent. However, using trained MoDCs did not prove to be as effective as using traditional (untrained) MoDCs. Having found that our trained MoDCs expressed lower levels than the controls, we speculated that it is possibly due to the disruption of monocyte differentiation by the various stimuli. This has previously been documented in the literature by Mariotti et al., when they investigated the impact of *Mtb* infection on CD1 expression in monocytes, they found that *Mtb* infected monocytes failed to express CD1 molecules when differentiated into MoDCs. They also found that while MoDCs infected with live *Mtb* had a greater decrease in CD1 protein expression, heat killed *Mtb* infection was also able to inhibit the expression of CD1 proteins but to a lesser extent. The study concluded that this was potentially another mechanism by which *Mtb* avoids immune recognition [495], further highlighting an important role for CD1 in *Mtb* infection.

The most effective T cell expansion method that generated robust and consistent results was mediated by THP1 cells. We also used these cell lines to validate the specificity of this expansion method by carrying out several assays such as an IFN-γ assay, AIM assay, and proliferation assay. Following expansion, we used CD1c-endo tetramers to confirm the presence and increase of CD1c-auoreactive T cells.

In order to expand CD1c restricted T cells, we used the THP1-KO and THP1-CD1c cell lines generated by our collaborators at Immunocore. They also developed a short-term T cell expansion method using these lines (personal communication, Marco Lepore). When expanding unconventional T cells, Lepore et al. had previously demonstrated the use of similar MHC KO lines expressing MR1 (A375-MR1) to isolate and further characterise the function of MR1-autoreactive T cells [496]. Generally, the use of commercially available APC cell lines that are engineered to express a specific molecule, thus resulting in the stimulation and expansion a particular population of T cells *ex vivo,* is well established [6, 496-498]. Additionally, Latouche et al. also found that the use engineered APCs generated a better and more effective T cell response than autologous DCs [498].

Similarly, we found that the use of THP1-CD1c mediated expansion was a more stringent and specific method of expanding CD1c-autoreactive T cells than the other methods we attempted. To further validate the THP1 lines, we carried out IFN-γ assays. We confirmed that the expression of MHC class I & II did not increase upon activation with IFN-γ in both the THP1-KO and THP1-CD1c cell lines.

One of the main issues we encountered when culturing T cells with THP1-KO, was poor viability. This was due to lack of stimulation, which resulted in poor proliferative responses. Consequently, by day 8, only around 8% of the cells were viable from those originally seeded. Therefore, the number of cells available for staining was very low. A potential way to rectify this was to increase the initial number of T cells seeded with THP1-KO, however, this meant that less cells would be seeded with THP1-CD1c cells. The percentage of CD1c-autoreactive cells is relatively low in human blood [341], we therefore sought to maximise the chances of expanding these T cells *in vitro*. We observed that the greater the number of T cells cultured initially with THP1-CD1c cells, the more efficient the T cell expansion was.

To further validate our expansion method, we used an AIM assay. Our lab has previously optimised an AIM assay in order to identify activated T cells. Assays studying cellular activation typically rely on the analysis of the cytokines produced by cells. However, the main drawback of these assays, such as ELISPOTs is that they are limited to mostly Th1 responses [499, 500], thus the subtypes of T cells they can detect is restricted as T cells that produce non-Th1 cytokines will not be detected. On the other hand, AIM assays circumvent this issue as they are capable of detecting a wider range of T cell subtypes; the assay relies on the expression of cell surface markers that are expressed during activation in response to an antigen [469, 471, 499, 501]. In our AIM assays, we stained for the activation markers CD25 and CD137 to detect activated T cells, which were then isolated.

Additionally, our proliferation assay demonstrated the specificity of the THP1-CD1c mediated expansion. When isolation MR1-restricted T cells, Lepore et al. previously demonstrated the use of CTV to identify cells that have newly proliferated in response to an antigen, before sorting the cells that were positive for activation markers [469]. We validated our expansion method by confirming the presence of large CTV^{lo} populations that were present 12 days after co-culturing T cells with THP1-CD1c, that were otherwise smaller in our control conditions.
Lastly, we used CD1c tetramers that were generated in a mammalian expression system, and loaded with endogenous proteins. This allowed for the identification of CD1c-autoreactive T cells since CD1c-endo is loaded with self-lipids [309]. The use of CD1 proteins loaded with endogenous lipids whether they are used as monomers, tetramers, or dextramers, to identify CD-reactive T cells is well established in the literature. CD1b-endo dextramers were used to identify CD1b-autoreactive T cells [346]; CD1c-endo monomers were used to expand CD1c-reactive T cells [471], and CD1c-endo tetramers were able to demonstrate that *Mtb* antigen specific CD1c reactive T cells also displayed autoreactivity [381]; additionally, CD1d-endo tetramers were used to identify autoreactive populations of iNKTs [502]. After the $CD3^{+}$ CTV^{lo} T cells were expanded, they underwent several

rounds of tetramer guided sorting where we used our CD1c-endo tetramers to isolate $CD3^+$ CD1c-endo $tetramer^+$ cells. Eventually, we generated 6 lines, out of which, 5 lines were CD1c-endo $tetramer^+$, with line P1C5, being almost 100% CD1c-endo $tetramer^+$ (Figure 38).

Overall, perhaps the most important and challenging factor whilst expanding T cells is the maintenance of high cell density and viability. Cultures of *ex vivo* T cell expansions have been shown to undergo apoptosis at low density but expand rapidly at high densities. The apoptosis that occurs in low density cultures was found to be due to oxidative stress [503]. Whilst T cells in high density cultures also produce ROS, they also produce higher levels of catalase, this is an enzyme that accumulates in the media and decomposes ROS, thus allowing cells to continue growing [504]. CD1c restricted T cells are notoriously tricky to culture, they require a fine balance between having enough space in the well, and not having too much space to grow in, as well as being in the right state of activation where they are actively proliferating and secreting growth factors [503]. The activation state of the T cells is very important, and adding IL-2 to the cultures is central to keeping T cells in an activated state. However, they do eventually enter a resting phase which can be visualised as their morphology changes from an elongated "boomerang"-like shape, to small round cells. The resting phase persists despite the addition of IL-2, at this point the cell viability begins to decrease, and the cells must either be cryopreserved or re-stimulated with PHA, IL-2 and feeder cells. Moreover, T cell lines also differ in the speed at which the cells proliferate, and the same line can in fact have variable proliferation efficiencies with every round of stimulation.

Published studies that have isolated and expanded unconventional T cells, including CD1-restricted T cells, have used various techniques and methods to specifically expand these populations. Our optimised method of expanding and isolating CD1c-autoreactive T cells used a combination of different elements of published studies. These include the expansion of T cells with autologous APCs (e.g. MoDC) or engineered APCs, tetramer and dextramer guided cell sorting by flow cytometry, and cell sorting based on activation marker assays or cytokine release [346, 373, 375, 496, 502, 505]. These methods were applied when sorting bacterial lipid specific T cells [375, 505] or self-lipid specific "autoreactive" T cells [373, 471, 502, 506].

Antigen specific CD1b-restricted T cells were isolated from the blood of TB patients [482]. Freshly isolated T cells were first stained with GMM loaded CD1b tetramers (CD1b-GMM) and sorted, and then stimulated and expanded in round bottom plates with allogenic irradiated feeder cells, IL-2, IL-15, and anti-CD3 [375]. DeWitt et al. also isolated CD1b-restricted T cells using CD1b-GMM tetramers with a slight variation in the expansion of the T cells post tetramer sorting. Following

staining of $CD14^+$ depleted PBMCs with CD1b-GMM tetramers and anti-CD3; $tetramer^+$ T cells were sorted and placed in round bottom plates with EBV-transformed B cells and irradiated PBMCs as feeder cells, PHA and IL-2. Half the media was replaced every other day until clusters were large and round, and then pooled in larger wells prior to being screened again by tetramer staining [505]. Moreover, CD1b dextramers loaded with *Staphylococcus aureus* derived lipids were used to isolate CD1b-antigen specific T cells from freshly harvested T cells. The sorted cells were expanded with allogenic feeder cells in the presence of IL-2, IL-15, and anti-CD3. This was followed by another round of sorting and expansion to further enrich the T cell population [346]. The cells were found to be autoreactive as they bound to "mock" loaded CD1b dextramers; these dextramers were loaded with a mixture of endogenous phospholipids [346].

Additionally, autoreactive CD1d-restricted iNKTs cells were identified and isolated using a combination of APCs and tetramer guided sorting. A K562 cell line deficient in HLA class I and II were transduced with CD1d, CD83 and CD80 (K562-CD1d), a cell line similar to our engineered THP1 cells. T cells were then stimulated with irradiated K562-CD1d cells that were pulsed with αGalCer and stimulated every 7 days, with IL-2 being added every 3 days. The cells were then sorted using CD1d-endo which was generated in a mammalian system using HEK cells, thus allowing for the staining, isolation and consequent expansion of CD1d-autoreactive iNKTs. This identified a panel of iNKT TCRs with a range of autoreactivity [502].

Furthermore, *Mtb* antigen specific and autoreactive T cells restricted by CD1c were isolated using PM loaded CD1c tetramers (CD1c-PM) using similar methodology [373]. Freshly isolated T cells were sorted after staining with CD1c-PM-tetramers and expanded by limiting dilution. This was followed by another round of screening with tetramers, sorting, and expansion to generate enriched CD1c-restricted T cells. Although initially isolated using CD1c-PM, some of the T cell lines isolated displayed some autoreactivity by binding to CD1c-endo tetramers made using an insect expression system [381].

Also, Guo et al. used CD1c-endo monomers instead of tetramers and a K562 cell line engineered to express CD1c (K562-CD1c) to identify CD1c autoreactive T cells. T cells that were negatively selected from PBMCs were stimulated with irradiated K562-CD1c cells in the absence of exogenous lipids, and IL-2 was added every 3-4 days. The cells were restimulated every 7 days to give rise to CD1c-autoreactive T cells [471]. CD1c-endo monomers were used in a plate bound assay to stimulate T cells in the presence or absence of anti-CD1c, and the T cells were then stained with CD69 as an activation marker to identify CD1c-endo "autoreactive" T cells for FACS. Additionally, K562-CD1c cells were used in an activation assay whereby the T cells were stimulated and then stained with

CD154 as a readout for activation, and cytokine production were measured to determine the cytokine profile of CD1c-autoreactive T cells [471].

Several other studies were also able to identify unconventional T cells without the use of tetramers. De Jong et al. expanded CD1a-autoreactive T cells by first differentiating MoDCs from PBMCs, and then stimulating T cell expansion by culturing with autologous MoDCs in the presence of IL-2 and IL-15 [506]. After 14 days, reactivity was tested by stimulating the T cells with K562 cells expressing CD1a, in the presence or absence of anti-CD1a blocking antibody. Cytokine release was measured during the blocking assay to determine CD1a autoreactive T cells. The authors subsequently went on to derive CD1a-autoreactive T cell clones by limiting dilution [506].

Moreover, Lepore et al. identified MR1-restricted T cells by stimulating purified T cells with an APC cell line (A375 cells) engineered to express MR1. The T cells were stimulated for 2 weeks and cultured in the presence of IL-2 [469]. The cells were then stimulated again overnight and $CD3^{+}CD69^{+}CD137^{+}$ T cells were sorted by FACS. They were then cloned by limiting dilution and T cell expansion was achieved using PHA, IL-2 and irradiated allogenic feeder cells [469].

In summary, unconventional T cells have been isolated by tetramer or dextramer guided cell sorting, followed by expansion with irradiated allogenic feeder cells, and a combination of cytokines and other reagents to encourage proliferation, usually PHA or anti-CD3, IL-2, and IL-15. Alternatively, they are first stimulated with APC lines expressing the target protein and are then sorted with tetramers or dextramers prior to expansion. In studies where tetramers were not used, engineered APCs and flow cytometric analysis based on activation assays along with cytokine profiling, such as an IFN-γ capture assay [469, 471, 506], allowed for the identification and isolation of T cell clones.

Our approach uses a combination of methodology with similarity to previously published work which allows us to cover most bases. There is no standard method by which unconventional T cells can be identified, isolated, and cloned. Using CD1-endo proteins, and tetramers thereof, generated in mammalian systems, which are loaded with self-lipids, allows for the detection and isolation of CD1c-autoreactive T cells. In our case, tetramers were used instead of dextramers as optimisation experiments demonstrated that tetramer staining was more robust (Figure 32). Additionally, the use of dextramers in an academic setting is costly and is not sustainable in long-term experiments. We also used THP1-CD1c mediated T cell expansion to grow CD1c-autoreactive T cells prior to sorting with tetramers, this expansion method yielded the best result, in comparison to autologous $CD1c^{+}$ MoDCs. Perhaps the efficiency of the MoDCs mediated expansion could be improved by increasing the length of the time the cells are co-cultured *in vitro*. Furthermore, the T cells cultured with the MoDCs were stained with our CD1c-SL tetramers that were generated using a bacterial expression

system. Whilst this showed promising enrichment of CD1c-autoreactive cells, the lesser efficiency of the expansion method and issues with the production pipeline of the bacterial CD1c-SL tetramer meant that both the expansion method, and CD1c-SL tetramers were no longer pursued. Instead, the main reagent used in our lab became CD1c-endo, which is generated using HEK cells. Additionally, in conjunction to the use of tetramers, we used activation assays to further validate the specificity of the CD1c-autoreactive T cells post tetramer guided sorting. In terms of expanding T cells post sorting, we used irradiated allogenic feeder cells, PHA, and IL-2, which is common practice in the field.

Tetramers are a powerful tool, and their use is standard practice when identifying CD1-reactive T cells. However, irrespective to whether CD1c-SL or CD1c-endo tetramer was used, the detection of CD1c autoreactive T cells is challenging. Previous studies have demonstrated that TCRs that respond to self-antigens do so with lesser affinity than those that respond to pathogen derived antigens [374, 507]. Consequently, autoreactive T cells bind CD1c-SL, and CD1c-endo tetramers with low affinity and can have high dissociation rates [374, 508]. Whilst the interaction between TCRs and their antigens occur with low avidity, the use of tetramers is supposed to circumvent this by engaging multiple TCRs on the same cell, thus increasing the half-life of the interaction as well as its avidity [374]. Nevertheless, in terms of staining, this low affinity binding can result in lower staining intensity [374], causing populations to appear negative. With regards to the 6 lines that were sorted and stained with CD1c-endo tetramers (Figure 38), some populations appear positive with the rest appearing negative, this could simply be due to low affinity binding. Thus, CD1c-autoreactive T cells can be missed during staining due to lower affinity binding to self-antigen as opposed to microbial antigen [374, 507, 508].

Additionally, the use of CD1c-SL or -endo means that due to tetramers having mixed cargo, even when CD1c-autoreactive T cells are identified and sorted, detecting them again may not prove as easy due to the batch-to-batch variation in the tetramers, and therefore the possible differences in the composition of the lipid cargo between each batch. Also, the cells being derived from different donors naturally results in variability in terms of their extent of stimulation, further adding to the challenges of isolating and culturing these populations.

Nevertheless, continuous efforts in our lab are ongoing to improve and refine the tools being used to isolate CD1c-restricted T cells. We found that using CD1c-endo Strep-tag coated beads were efficient at enriching these populations, and several rounds of enrichments can be made from *ex vivo* derived T cells. This method is also less time consuming as it circumvents the need for several rounds of tetramer guided sorting, and the expansion downtime required after each sort. Members of our lab have already generated pure T cell lines using this method after a single round of sorting following

the Strep-tag mediated enrichment. In this study, due to time constraints, we were unable to use this method to derive other CD1c restricted T cell lines from different donors, and investigate their role in TB. However, it has been optimised, and is starting to be used robustly by a current student in our lab.

P1C5 T cells

Our approach for the expansion of CD1c-autoreactive T cells generated several T cell lines that were stained with CD1c-endo tetramers. Of which, P1C5 stained brightly with CD1c-endo tetramers, and was therefore taken forward for phenotyping and for functional anti-TB studies. Phenotyping of P1C5 T cells identified that they were double positive when stained for pan αβ- as well as γδ-TCRs (Figure 39E). T cells that are hybrids and express both δ- and αβ-TCRs have previously been reported in the literature [509, 510]. Pellicci et al. first identified δ/αβ TCRs that recognised peptide antigens, as well as lipid antigens, which are presented by HLA molecules and CD1d, respectively. They also found that these cells comprised almost 50% of all $V\delta1^+$ T cells [510]. Furthermore, Edwards et al. identified hybrid αβ-γδ T cells in both murine and human samples, however, in this study they identified the δ chain as being Vδ2, with around 10% of all $V\delta2^+$ cells in human samples also expressing αβ TCRs. In a murine model, they were able to demonstrate that hybrid αβ-γδ T cells were proinflammatory based on their cytokine profile and were able to promote bacterial clearance following infection with *Staphylococcus aureus* [509]. In the case of P1C5 T cells, due to time constraints, brief flow cytometric analysis was carried out which determined that they were Vδ1 negative, and $CD4^+$. Consequently, further analyses on these T cells are required to better determine their phenotype and to further define their function. Using this cell line, we completed functional studies in the context of TB infection to investigate their cytotoxicity effect, and cytokine profile.

Cytotoxicity during TB infection

Our lab has previously observed that single cell RNA-Seq analyses of CD1c-endo tetramer positive T cells from several donors suggest that they are highly cytotoxic (personal communication, Mansour lab). We investigated the role of P1C5 T cells during the infection of THP1 cell lines with UV killed TB. Killing TB with UV allows the bacilli to remain whole with its extracellular proteins and lipids intact, this is important as the *Mtb* derived lipid antigens are mostly components of its cell wall. The use of THP1 cells as an infection model to study the function of unconventional T cells is well established in

the literature. This includes their use in proliferation, cytotoxicity, AIM, and cytokine profiling assays. Jackman et al. used THP1 cell lines infected with live virulent *Mtb* to study the impact of a tail deletion in CD1b on the antigen presentation capacity of the protein [511], they measured cytokine secretion from CD1b-restricted *Mtb* antigen specific T cell lines in response to *Mtb* infected THP1 cells with a CD1b tail mutation [511]. Other THP1 based infection models such as those infected with *E.Coli* have also been used to study the cytotoxic and proliferative responses of MAIT cells [512], as well as cytokine release [513].

In this study, we observed that P1C5 T cells resulted in significant cytotoxicity in a T cell ratio dependent manner when cultured with TB infected THP1-CD1c. Additionally, cytotoxic responses of P1C5 T cells with infected THP1-KO were comparable to those of P3D7 T cells with infected THP1 lines. We also observed the same significant increase in cytotoxicity caused by P1C5 T cells when increasing the MOI of UV killed TB in 10-fold increments, which was not observed in control conditions. This suggests that the cytotoxic responses were occurred upon recognition of CD1c by the T cells. To further validate that the cytotoxicity was CD1c-mediated, blocking assays could be carried out, where the target molecule is blocked and the effect of this on the cytotoxic function of the T cells is studied [512, 514]. Altogether, the data clearly highlights the cytotoxic function of P1C5 T cells during TB infection when cultured with *Mtb* infected APCs expressing CD1c.

Evidence of the cytotoxic function of $CD4^+$ T cells has been reported in the context of other diseases. Cytotoxic $CD4^+$ T cells have been found in patients with Epstein-Barr virus (EBV) [515], and expansion of antigen specific populations have also been detected [516], which were able to recognise and kill infected B cells [517]. Furthermore, they have also been found in the PBMCs of patients with infectious diseases such as hepatitis [518], human cytomegalovirus (CMV) [519] and HIV [520]. During influenza A virus infection, $CD4^+$ T cells with a Th1 effector phenotype have been found to express granzyme B and perforin [521] and have killing capacity [522]. Additionally, a recent study in patients infected with SARS-CoV-2 also identified cytotoxic $CD4^+$ T cells [523]. Aside from infectious diseases, expanded cytotoxic $CD4^+$ T cells have been found in tumours from patients with different cancers, such as breast cancer [524], osteosarcoma [525], lung cancer [526], and colorectal cancer [527].

With regards to TB infection, various studies have established that $CD4^+$ T cells play a key role in the immune response to TB. This is further supported by the evidence from studies with HIV patients where *Mtb* reactivation, reinfection and primary infection was linked to the depletion of $CD4^+$ T cells [528, 529]. Furthermore, despite $CD8^+$ T cells and other immune cells being present, they cannot compensate for the role that $CD4^+$ T cells play against *Mtb* [528].

Moreover, a transcriptomic study profiling $CD4^+$ T cells in subjects with LTBI identified genes that were involved in cytotoxic cell killing such as granzyme A, perforin and granzyme K; and suggested a role for these cells in the control of the disease in subjects with LTBI to prevent the reactivation of the disease from latent to the active state [530].

Furthermore, it is well established that αβ T cells differentiate into cytotoxic $CD8^+$ T cells or $CD4^+$ helper T cells. This determination in lineage is determined by key transcription factors, which includes the helper T cell master regulator ThPOK. This is a crucial gene and is highly conserved across species [531]; which has been shown to suppress the cytolytic function in $CD4^+$ T cells [531-534]. Mucida et al. found that the helper T cell fate of $CD4^+$ T cells could be reversed and that antigen stimulated mature $CD4^+$ T cells can terminate the expression of the gene encoding ThPOK and reactivate genes of the CD8 lineage, thus resulting in cytotoxic $CD4^+$ T cells [535]. Canaday et al. found that upon stimulation with *Mtb*, $CD4^+$ and $CD8^+$ subsets both upregulated mRNA expression of perforin, Fas ligand, granzyme A and B, as well as granulysin at similar levels, and lysed *Mtb* infected monocytes [536].

$CD4^+$ CD1c-restricted T cells have previously been reported in the literature, and have been found to recognise a lipid mycobacterial antigen, resulting in the lysis of *Mtb* infected target cells [537]. Additionally, they are able to inhibit the growth of intracellular bacteria [537]. Similarly, $CD8^+$ CD1c-restricted T cells have also been found to have antimicrobial functions and release granulysin [96, 355, 537].

Cytokine responses from cytotoxic CD1c-autoreactive T cells

CD1c-autoreactive T cells also demonstrated antimicrobial activity and were found to be cross reactive with several mycobacteria, whereby they recognised target cells infected with *M.leprae* or *Mtb*, and secreted TNF-α upon stimulation [356]. Moreover, CD1c-autoreactive T cells are present in healthy human blood, and have been shown to release IFN-γ and IL-2 in response to $CD1c^+$ APCs carrying self-lipids [341, 538]. Spada et al. also isolated CD1c antigen specific γδ T cells that were able to lyse $CD1c^+$ target cells, and had a Th1 cytokine profile producing IL-2 and IFN-γ. Additionally, they were shown to have cytotoxic effects via a perforin dependent pathway [355]. This pathway plays a role in bacterial resistance and antiviral immunity as it is a primary cytotoxic effector mechanism in host defence [539]. Furthermore, the T cells identified were shown to express granulysin, and respond to APCs in the absence of exogenous lipids, thus indicating autoreactivity [355]. Moreover, CD1c-autoreactive T cells have been found to mediate the maturation of DCs [540].

In the absence of exogenous lipids, CD1c-autoreactive T cells were able to trigger DC maturation via cell-to-cell contact and TNF-α secretion. This was found to be particularly beneficial as it rapidly generates a pool of mature DCs early on in microbial infections. This maturation effect was inhibited by blocking CD1c [540].

In an *in vivo* mouse study, several CD1-restricted T cell lines that recognise *Mtb* antigens were identified in a humanised CD1 Tg mouse model, the majority of these lines were found to be autoreactive [416]. The T cells were able to lyse mouse as well as human cell lines, suggesting the recognition of conserved self-antigens across species. Furthermore, Felio et al. found that the autoreactive T cells resulted in an enhanced response to microbial antigens as has previously been published [508]. They speculated that the autoreactive responses are enhanced through the activation of DCs which increase the expression of endogenous glycolipids that are then presented by CD1 proteins [416].

In the context of non-microbial diseases such as cancer, the cytotoxic capacity of CD1c-autoreactive T cells was also highlighted due to their ability to recognise and kill $CD1c^+$ acute leukaemia cells by identifying mLPAs that build up in leukaemia cells [352].

Whilst CD1c-autoreactive T cells have been identified in healthy subjects, TB patients, and a humanised mouse model, and their antimicrobial and cytotoxic capacity has been well documented in the literature [341, 352, 355, 471, 508, 537]. The role they play in the immune response to TB is not very well defined. We hypothesised that CD1c-autoreactive T cells play a role in human TB infection and identified their cytotoxic capacity when cultured with TB infected $CD1c^+$ APCs.

Overall, the phenotypical and functional characteristics of P1C5 T cells require further investigation. Particularly in terms of identifying other cell surface markers, as well as studying the role of these cells during live TB infection, and their cytokine profile. Nevertheless, our results show for the first time, that CD1c-autoreactive T cells exhibit direct cytotoxicity towards *Mtb* infected target cells which warrants further study.

Luminex assay

Recent studies have demonstrated that activated CD1c-restricted T cells release TNF-α or IFN-γ and can develop a Th0 or Th1 phenotype, and result in the lysis of target cells infected with *Mtb* due to the release of granulysin and perforins [275, 316, 483]. In addition, Wun et al. found that following

stimulation of autoreactive T cells with APCs expressing CD1c, IFN-γ was released [309]. Also, De Lalla et al. demonstrated that the release of IFN-γ was significantly decreased from CD1c-autoreactive T cells that were screened against THP1-CD1c cells after blocking with anti-CD1c mAb [341].

The mixed cytokine profile, and polyfunctional effects we have observed in our CD1c-autoreactive T cell line (P1C5) corroborates what has been previously published in the literature. Although a comprehensive study of the cytokine profile of CD1c-autoreactive T cells was not carried out in the context of TB infection, CD1c-autoreactive T cells derived from patients with systemic lupus erythematosus were shown to be polyfunctional and produced IFN-γ and IL-4 [541]. Additionally, a protective role for polyfunctional CD1-restricted T cells was also identified a few years ago during *Staphylococcus aureus* (SA) infection. Using an adoptive transfer approach, Visvabharathy et al. were able to demonstrate that CD1c-restricted SA-lipid specific T cells were able to reduce the bacterial load in the kidneys; and had better overall pathology overall in comparison to control mice, and produced cytokines such as IFN-γ and IL-17A [542].

Although CD1c remains the most understudied member of the group 1 CD1 family of proteins, the cytokine profiles of other CD1-autoreactive T cells such as CD1a and CD1b-autoreactive T cells have been identified. Autoreactive CD1a clones isolated from PBMCs were mostly found to produce IL-22, and did not produce IL-17 nor IFN-γ [506]; this phenotype was also true to CD1a-restricted T cells isolated from human skin[506]. Additionally, polyclonal CD1a-restricted T cell lines that were isolated from skin were found to express CD4 and produced IL-22 upon stimulation [344]; and in response to antigens derived from house dust mites during atopic dermatitis, CD1a-restricted T cells were found to release IL-13, GM-CSF, and IFN-γ [543, 544]. Likewise, we found that our polyclonal CD1c-autoreactive T cell line (P1C5) also produced IL-13, GM-CSF, and IFN-γ, as well as other cytokines such as IL-1A, TNF-α, IL-2, IL-2R, IL-5, and IL-4 upon recognition of *Mtb*-infected THP1-CD1c cells (Figure 52).

Isolated CD1b-autoreactive T cell lines that recognise PG were also found to be polyfunctional, and in response to APCs expressing CD1b (C1R cell line), were found to express a range of cytokines that include both Th1 and Th2 cytokines such as IFN-γ, TNF, IL-2, IL-4, IL-8, IL-13, and GM-CSF [346]. Similarly, P1C5 also produced IFN-γ, IL-2, IL-13, and GM-CSF in response to CD1c expressed on THP1 cells in the absence UV-killed *Mtb* (Figure 51).

The first *in vivo* study to demonstrate the functional effect of a mycolic acid specific CD1b-restricted T cell clone (DN1), and its protective anti-mycobacterial effect during *Mtb* infection was carried out by Zhao et al. [462]. These findings were made using a transgenic mouse model where the group generated mice which expressed human DN1, as well as human group 1 CD1 proteins (hCD1Tg)

[462]. Following the adoptive transfer of DN1 T cells to hCD1Tg mice infected with TB, they identified that DN1 T cells played an anti-mycobacterial role and resulted in a reduction of the bacterial load in various organs such as in the spleen, lungs and liver. Zhao et al. demonstrated that DN1 T cells are polyfunctional and secrete TNF-α, IFN-γ and IL-2, and were cytotoxic, thus resulting in their protective effects [462].

Additionally, DN1 T cells became activated and proliferated faster than Ag85B specific T cells [462]. Zhao et al. suggested that the difference in the kinetics between both cell types might be a mechanism by which the infection is controlled, whereby both cell types contribute at different stages of infection. The faster proliferative and activation response of DN1 T cells relative to Ag85B specific T cells is thought to be due to the ability of CD1b molecules to present their antigens faster than MHC class II molecules [462]. A study has previously demonstrated that following *Mtb* infection, the rapid maturation of DCs results in the inefficient loading of antigens, whereas CD1b proteins are regularly patrolling phagosomes and therefore can load and present lipid antigens earlier more effectively [545]. Although this has only been demonstrated using CD1b, this could ring true for other members of the group 1 CD1 family such as CD1a and CD1c, as they are readily available and patrol cellular compartments. Additionally, although not a group 1 CD1 protein, CD1d-restricted T cells were also shown to secrete GM-CSF which was protective against mycobacteria [334]. Altogether, although we have not studied our line P1C5 in an *in vivo* model, our data aligns with previously published studies of other CD1-restricted T cells, whereby P1C5 is polyfunctional and has a mixed cytokine profile, as well as cytotoxic effects in response to *Mtb* infection.

The protective capacity of polyfunctional peptide specific conventional $CD4^+$ T cells has also been demonstrated in several studies, where cells produced TNF-α, IFN-γ and IL-2, and displayed protective effects against mycobacterial infections [264, 270]. Furthermore, a study carried out in TB patients by Amelio et al. also identified T cells with a mixed Th1/Th2 cytokine profile where the cells had an increased GATA-3 expression, and reduced T-bet expression [546].

The occurrence of co-infection with TB and helminths is common in certain parts of the world [546]. However, both microorganisms are known to elicit different T cell responses. T cell mediated responses to TB have typically been found to be Th1 responses that lead to the production of TNF-α or IFN-γ, which stimulates macrophages and recruits other immune cells such as monocytes [8, 547]. On the other hand, helminths promote a Th2 response and result in the production of IL-4, IL-5, and IL-13 [548-551]. Taking this into consideration, Amelio et al. investigated whether the different responses elicited by both pathogens would have an impact on the functional profile of *Mtb* specific T cells [546]. In *Mtb* specific T cell cultures stimulated with *Mtb* peptides such as ESAT-6 and CFP-10,

they identified Th1 and Th2 responses using a Luminex assay [546]. The cells were found to produce high levels of IL-2, TNF-α, IFN-γ, IL-4, IL-5, IL-10, IL-13, IL-17A, and IL-17F [546].

Although these mixed Th1/Th2 responses were stimulated by peptide antigens, they are reminiscent of what we have observed with only *Mtb* infection where lipid antigens were presented by CD1c to CD1c-reactive T cells (Figure 49). During *Mtb* infection, we also detected a significant increase in other cytokines such as MIG, IL-1α, IL-1β, and IL-1RA; and a significant decrease in IL-8 and RANTES (Figure 49). MIG is a member of the CXC subfamily of chemokines [552] and acts as a chemotactic molecule for T cells and is involved in their activation; its expression is inducible by IFN-γ [553]. MIG is highly expressed in the serum of TB patients [554], and is lowered with TB treatment as the bacterial burden lessens [555], and has been suggested as a promising diagnostic marker for pulmonary TB [556]. Moreover, IL-1α, IL-1β, and IL-1RA are the most studied cytokines from the IL-1 family in TB [557, 558]. Although they are different isoforms, IL-1α and IL-1β are sometimes collectively referred to as IL-1, and both cytokines bind to the IL-1 receptor 1 (IL-1R1) [559]. IL-1RA which is an antagonist cytokine, also binds to IL-1R1, thus inhibiting the binding of both IL-1 isoforms and preventing their effects [559]. Several mouse models of TB infection have clearly highlighted an important role for IL-1 in the protection against *Mtb* infection. Murine models with impaired synthesis of IL-1R1, IL-1α and IL-1β tend to have severe lung pathology, high bacterial loads, and an increase in mortality rates [560-564].

Lastly, IL-8 and RANTES have both been found to be equally potent at inducing chemotaxis of T cells, neutrophils, and monocytes and have an established role as key mediators of leukocyte recruitment during TB infection [475, 476, 565]**.** Increased concentrations of IL-8 have been identified in the plasma [566], bronchoalveolar lavage fluid [567, 568] of TB patients, as well as in human tissue infected with *Mtb* [569, 570]**.** Additionally, various studies demonstrated that the phagocytosis of *Mtb* by monocytic cells stimulates IL-8 production [571-574], and during the course of TB infection, infected phagocytes such as monocytes and macrophages have been shown to be the main source of IL-8 [81, 477, 571]**.** Similarly, we observed a significant increase in IL-8 secretion from *Mtb* infected THP1-CD1c cells in the absence of T cells (Figure 45). We then observed a significant decrease in IL-8 when our CD1c-reactive T cell line P1C5 was added to infected THP1-CD1c cells, in comparison to a non-CD1c reactive cell line (Figure 49). Whilst we have not directly investigated the reason behind this decrease, studies have suggested that other cytokines may negatively regulate the expression of IL-8 [574], or that phagocytes may physically consume IL-8 molecules [575]**,** hence decreasing their overall concentration. When studying the effects of Th2 cytokines on the capacity of *Mtb* infected monocytes to secrete IL-8, Ameixa et al. demonstrated that certain Th2 cytokines such as IL-4, and -10 were able to inhibit the secretion of IL-8 by *Mtb* infected monocytes [574]**.** The reduction of IL-8 mediated by IL-10, in particular, was likely due to decreased binding of the transcription factor NF-κB,

which regulates IL-8 expression [574]. Meanwhile, IL-4 has been shown to downregulate IL-8 post transcription by enhancing degradation of its mRNA [576, 577]**.** This corroborates our findings whereby IL-8 levels decreased as IL-4 and IL-10 increased, and was specific to co-cultures where infected THP1-CD1c cells were cultured with P1C5 T cells (Figure 49 & Figure 50). Furthermore, Krupa et al. demonstrated that IL-8 is able to physically bind to *Mtb* bacilli. Consequently, this binding enhances the ability of phagocytes to ingest and destroy the bacteria, thus enhancing their antimicrobial function [575]. Using THP1 cells that were differentiated into macrophages, Krupa et al. demonstrated that *Mtb* bacilli coated with IL-8 were more readily phagocytosed by macrophages than IL-8-free bacilli. Consequently resulting in a decrease in the levels of "free" IL-8 in the culture media [575].

The expression of RANTES and its receptor (CCR5) are upregulated during TB infection [578], and specific *Mtb* derived antigens such as *Mtb* Heat Shock Protein 70 (HSP70) can result in this increase [579]. RANTES has been shown to induce Th1 responses [580], and contributes to the protective effects of the BCG vaccine, which enhanced its expression and Th1 response in an *in vivo* guinea pig model of TB [581]**.** Furthermore, to address the functional impact of RANTES on mycobacterial infection, Salam et al. differentiated DCs using CFP10, an *Mtb* antigen, to generate CFP10-DCs; the cells were then conditioned with RANTES prior to infection [582]. The group found that conditioning CFP10-DCs resulted in the recruitment of T cells with enhanced cytotoxicity, that were more effective at eliminating BCG infected macrophages than unconditioned CFP10-DCs [582]. When tested *in vivo*, the study demonstrated that the adoptive transfer of RANTES conditioned CFP10-DCs successfully cleared *Mtb* infection in a mouse model. Their data collectively suggested that RANTES, particularly when secreted by DCs that are differentiated by *Mtb* antigens, play an important role not only in the recruitment of T cells, but also in priming their effector response [582]. Moreover, transcriptomic analysis of *Mtb* infected THP1 cells demonstrated that RANTES is upregulated during infection [474]. Similarly, we found that infection of THP1-CD1c cells with *Mtb* resulted in a significant increase in RANTES (Figure 45), however, the addition of P1C5 T cells resulted in a decrease in RANTES (Figure 48 & Figure 49). Whilst RANTES is a key chemokine in the immune response to TB, there is little evidence regarding potential mechanisms by which RANTES is downregulated during TB infection. One explanation for the reduction we observed is that activated T cells sequester the cytokine, resulting in less RANTES being available for detection in the media. Additionally, RANTES sequestration by CD1c-autoreactive T cells might enhance their activity and subsequent cytotoxicity which is a hypothesis that warrants further investigation.

BCG vaccination has been shown to induce polyfunctional mycobacteria specific T cells in a mouse TB model which resulted in protection from *Mtb* infection [264, 583]. Evidence for the role of $CD4^+$ polyfunctional T cells that co-express IFN-γ, TNF-α and IL-2, in the immune response to TB have previously been documented in the literature. The production of IL-2 by Th1 $CD4^+$ T cells that also produce TNF-α and/or IFN-γ has been linked to *Mtb* containment as individuals develop LTBI, whilst absence of IL-2 results in active TB, despite the presence of TNF-α and IFN-γ [584-587]. IL-2 is essential for the proliferation and survival of activated T cells [588]. Subsequently, its main role during TB infection is to support the maintenance and proliferation of T cell responses. It also plays a role in T cell tolerance, and mice deficient in IL-2 and IL-2R have greater susceptibility to autoimmune disease [588]. In the context of TB infection, the proliferation of IL-2 producing $CD4^+$ T cells correlates with protection, and their loss is associated with detrimental outcomes [262].

Additionally, humans deficient in IFN-γ signalling or receptor expression [589], or IL-12 receptor expression [590] have increased susceptibility to mycobacterial infection. Whilst IFN-γ derived specifically from $CD4^+$ T cells has been shown to mediate protection during TB infection, and promotes $CD8^+$ T cell responses [184]. Mouse TB models have demonstrated that a way by which IFN-γ exerts its protective effects during infection is via the activation of macrophages which result in the inhibition of mycobacterial growth [591]. The protective effect of TNF-α has also been highlighted during TB infection, and was shown to mediate protection prior to the activity of the adaptive immune response by activating macrophages [592]. Moreover, deficiencies in TNF-α or its receptor result in an increased susceptibility to TB in mice [10, 398], and TNF-α blockade as a treatment for rheumatologic conditions results in increased susceptibility to TB in humans [11, 593].

Polyfunctional T cell responses have also been associated with successful TB treatment and results in a decrease in bacterial burden [594]. Although not yet defined, the mechanisms by which polyfunctional T cells are able to elicit protective responses are likely due to the synergistic effects of the cytokines they produce. This was demonstrated in a study using a *Leishmania major* infection model where the effects of TNF-α and IFN-γ enhanced the capacity of macrophages to contain the infection [595, 596]. Similar results were also demonstrated using a murine macrophage cell line which was able to inhibit *Mtb* replication due to the synergistic effects of IFN-γ and TNF- α [597].

Additionally, blood from infants that were vaccinated with BCG or controls that were unvaccinated was stimulated overnight with *Mtb* purified protein derivative (PPD) and their $CD4^+$ T cell responses were measured [598]. The most abundant response identified were by polyfunctional PPD specific $IL\text{-}2^+$/ $TNF\text{-}\alpha^+$/$IFN\text{-}\gamma^+$ $CD4^+$ T cells, which also resulted in significant inhibition of mycobacterial growth. The study also identified a transient Th17 response. They concluded that BCG vaccination in UK

infants results in a polyfunctional Th1 response, as well as a short lived Th17 response, both of which have anti-mycobacterial effects [598]. Another study carried out in 149 children with active TB or potential LTBI, identified that stimulation with different TB derived antigens as opposed to whole heat-killed *Mtb* resulted in slightly different functional profiles. CFP-10 and ESAT-6 stimulation gave rise to IL-2$^+$/TNF-α$^+$, IL-2$^+$/ TNF-α$^+$/IFN-γ$^+$, TNF-α$^+$ only, IFN-γ$^+$ only, or TNF-α$^+$/IFN-γ$^+$; whilst whole heat-killed *Mtb* stimulation resulted in T cells that were TNF-α$^+$ only, IFN-γ$^+$ only, IL-17$^+$ only, TNF-α$^+$/IFN-γ$^+$, IL-2$^+$/TNF-α$^+$/IL-17$^+$, or IL-2$^+$/IL-17$^+$ [599]. The IL-17 response has been captured in mouse studies whereby after being vaccinated and subsequently infected with *Mtb*, an IL-17 response occurs just before the rapid expansion of Th1 cells [600]. Additionally, following BCG vaccination of mice, an IL-17/IL-23 response was essential in generating an effective Th1 response that may have otherwise been inhibited by IL-10 [601].

TCR sequencing and cloning

Sequencing of single T cells that were single cell sorted using CD1c-endo tetramers, and sequenced, identified 4 TCRs that were αβ-TCRs, and 4 that were γδ-TCRs. These findings were in line with what is present in the current literature [341, 355, 381, 481]. However, further characterisation of the TCRs was due to be carried out to better understand their specificity and function. The first step was to clone the TCRs onto pLNES vectors. However, this presented some challenges. Firstly, the gBlock gene fragments that were designed at Immunocore and synthesised externally were supposed to be robustly amplified by PCR, and then digested by restriction enzymes whose sites were integrated in the gBlock fragment. Several PCRs were attempted with troubleshooting and optimisation, to no avail. This included changing the composition of the PCR master mix, as well as testing temperature gradient PCRs. Following the unsuccessful amplification attempts, and in the interest of time, the gBlock fragments were directly digested and purified. After they were digested with the same restriction enzymes as the vector backbone and re-ligated to form DNA plasmids to transfect bacteria, the DNA was purified and sequenced to confirm that the insertion of the gBlock gene fragment into the vector backbone was successful. The sequencing data returned determined that the insertion was not successful, and that the backbone had most likely re-ligated. Whilst these experiments were carried out at Immunocore to make the most of their expertise and facilities, following the lack of success, the sequences of the gBlock gene fragments were revised at Southampton in the Mansour lab. The revision identified that the gBlock fragments were missing the leader sequence, this sequence is important for expression of genes products in mammalian cells;

and the constant region was also missing. With this finding, the sequences were redesigned at Southampton and sent to GeneScript to be synthesised.

Chapter 9 Future work and concluding remarks

Future work

CD1c-autoreactive T cells during TB infection

It is well established in the literature that CD1c-restricted and *Mtb* lipid specific T cells are present in TB patients and appear to play a role in the immune response to TB, however, the role of CD1c-autoreactive T cells in TB is unknown; whether they are beneficial or detrimental to the host, is yet to be elucidated. This set of data demonstrates that CD1c-autoreactive T cells are able to selectively kill TB infected target cells. However, to more deeply delve into the role these cells play, and whether they are a true "friend or foe", additional studies must be carried out.

This study identifies the functional effect of P1C5 T cells during TB infection, where their cytotoxic capacity and cytokine profile have been determined, using ToxiLight, and Luminex assays, respectively. However, the mechanisms by which these cells achieve cytotoxicity, are yet to be determined. Additionally, while the co-receptor status in this line has been identified, studies such as blocking assays can help us better understand whether the co-receptor status modulates T cell function. Moreover, other cell surface markers remain to be identified, as well as studying the role of these cells during live TB infection. The functional role of our T cells can be studied using the 3D granuloma infection model at Southampton. Here, the interaction between bona fide CD1c-autoreactive T cells and a more accurate model of live *Mtb* infection can be investigated. In this model, various parameters can be measured including *Mtb* growth, flow cytometric analyses of immune cell parameters, host cell survival, and cytokine release by Luminex assays.

TCR cloning

Tetramers have been an invaluable tool in the field of unconventional T cell research. Tetramer guided studies have allowed for the identification of various subtypes of T cells. In this study, 8 unique TCR sequences (x4 αβ-TCR and x4 γδ-TCR) were generated from tetramer guided single cell sorting, and are yet to be cloned into Jurkat cell lines for further analysis. Plasmids containing the sequences have been synthesised externally and will be used to transform bacteria to produce DNA vectors containing the paired TCRs. The vectors will be used to virally transduce Jurkat T cells in order

to express the TCRs extracellularly. At which point, the Jurkats can be used to confirm the reactivity of TCRs with CD1c-endo, and further T cell activity experiments can be performed with the Jurkats. Additionally, due to the nature of the lipid cargo that CD1c-endo can be loaded with, an array of TCRs with different affinities to the lipid antigen can be detected. Therefore, the generation of other T cell lines or clones that are identified and isolated using the CD1c tetramers would be interesting. It is possible that other lines isolated using CD1c tetramers can exhibit differences to P1C5, in terms of their specificity, and possibly their function. Indeed, another CD1c-autoreactive T cell line was generated from another healthy donor in our laboratory recently. These T cells express αβ TCRs, are $CD4^+$ and they exhibit significantly enhanced activity towards $CD1c^+$ targets infected with live TB. These unpublished data are in further support of our findings with P1C5 T cells, and they suggest that CD1c-autoreactive T cells may have a central role in the host immune response to TB infection.

Conclusion

The latest WHO Global TB report highlighted that in 2022, approximately 10.6 million people contracted TB and 1.3 million died from the disease, an estimated 167,000 of whom were also HIV positive [426]. As with almost everything in the world, the COVID-19 global pandemic had an impact on TB. The diagnosis and treatment of the disease, as well as funding towards TB studies were detrimentally affected. The need for effective therapeutics and vaccines against TB remain as imperative as ever. Despite strides being made over the past few decades in understanding the immune response to TB, and identifying key immune responses, a gap in our understanding of the full breadth of the host pathogen interaction during TB infection remains. Unconventional responses such as CD1-restricted T cells have been steadily gaining recognition for their involvement in TB infection for more than 20 years. Whilst their increased numbers in the circulation of TB patients have been established in the literature, most studies have focused on the ligands they interact with, the specificity and affinity of their TCRs to various lipid antigens, and the molecular mechanisms by which the TCR-ligand interaction occurs [308, 602-604]. The functional role of these T cells, particularly CD1-autoreactive T cells, has not been defined in the context of TB infection. Here, we identified and isolated CD1c-autoreactive T cells and demonstrated a functional role for these cells in the immune response to TB. We identified polyclonal $CD4^+$ T cells expressing αβ or hybrid δ/αβ TCRs that bind to CD1c-endo tetramers, respond in an autoreactive manner to CD1c in the absence of added foreign lipids, and functionally result in the death of *Mtb* infected target cells.

Currently, the most heavily studied CD1-reactive T cell subset are iNKTs due to their tumour killing capacity [605, 606]. Evidence from clinical trials carried out using adoptive transfer of iNKTs in various cancer types demonstrated that iNKTs expanded *in vivo* and produced IFN-γ [607-609]. However, although this was well tolerated, they have not yet resulted in any clinically significant outcomes [610]. Alternatively, instead of adoptive transfer of T cells, DCs pulsed with αGalCer were trialled in patients with different cancers in order to expand iNKT cells *in vivo* [611-613], however, this was also well tolerated yet not clinically significant [611-613]. This method remains promising particularly due to it being tolerated well, however requires refinement, it has been suggested that selecting specific iNKTs subpopulations may improve outcomes [614].

Despite CD1c-autoreactive T cells recognising self-lipids, they may be suitable candidates for adoptive T cell therapy. In diseases such as leukaemia, Lepore et al. demonstrated a protective role for CD1c-autoreactive T cells as they recognised a host derived lipid, mLPA, which accumulates in leukaemic cells. The T cells selectively lysed leukaemic cells, and poorly recognised non-tumour cells that expressed CD1c [352]. *Mtb* has previously been shown to dysregulate host lipid metabolism [350, 615, 616], therefore could elicit responses specific to infected cells similar to those observed in leukaemia. Additionally, CD1-autoreactive T cells with dual recognition of both bacterial and self-antigens such as CD1b-autoreactive T cells, whilst unable to differentiate between human and bacterial PG, they can become activated more avidly by bacterial PG [346]. This is suggested to occur in a concentration dependent manner as PG is much more abundant in bacterial than in human cells, so the levels of PG in human cells is considered below the threshold of detection, and they become activated by the bacterial PG instead due to its abundance [347].

Several studies have demonstrated the impact of *Mtb* on CD1c expression on infected APCs [416, 495]. In human monocytes, *Mtb* infection resulted in lack of expression of CD1 proteins when differentiated into MoDCs [495], whilst DCs from CD1 Tg mice exhibited delayed kinetics in CD1 protein expression after *Mtb* infection [416]. Whilst it is yet to be established, despite delayed kinetics in CD1 expression, the resultant stress that the cell undergoes during infection may result in a change in the lipidome. These stress lipids may not be TB derived, but are host derived and indicate an infection state for direct sensing by autoreactive T cells. Such mechanisms have been described for CD1d-restricted iNKT cells, an inherently autoreactive T cell subset, which are activated by stimulatory self-lipids synthesised by APCs during infection [617]. The accumulation of self-antigens may result in the activation of autoreactive T cells similarly to how host PG may activate CD1b-autoreactive T cells in times of mitochondrial stress [346].

Despite studies highlighting several functions for CD1c-autoreactive T cells such as their direct cytotoxicity in disease states [352, 355, 537], impacting maturation of DCs [540], and having

enhanced responses during infection [508]; due to their autoreactive nature, a clear understanding of the mechanism by which these cells are regulated in healthy humans is important, yet remain to be fully elucidated.

It has been established that autoreactive TCRs interact with self-antigens with low avidity [618]. Although CD1c-autoreactive T cells are detectable in human blood [309, 538], their chances of "bumping into" enough CD1c proteins loaded with self-antigen to trigger an autoimmune response are not very high. CD1c is expressed on APCs such as DCs, macrophages and B cells, and an upregulation in its expression typically occurs during inflammatory conditions [619]. However, under normal conditions, components of human serum have been shown to inhibit the expression of CD1c on monocytes [620], and once CD1c is expressed, decoy receptors such as Ig-like transcript 4 (ILT4), which is an inhibitory receptor expressed by APCs may bind to CD1c to block CD1c-TCR interaction, thus dampening T cell activation [39]. This suggests that the inducible expression of CD1c by cytokines or TLR activation during infection is a way by which autoreactivity is controlled [308].

Another mechanism by which autoreactivity of CD1 restricted T cells is thought to be regulated is by the conformational changes that occur in the CD1c protein when a lipid is loaded onto it, thus altering the TCR binding surface. The lipid antigens that bind CD1c can be small and fully seated within the protein thus facilitating TCR interaction with the CD1c protein itself [309], or they can be larger lipids that cause conformational changes in the protein whereby the TCR interacts with the lipid as well as the CD1c protein [303]. Therefore, differences in the mechanisms that determine TCR recognition, as well as the nature of the lipid cargo, are key factors in determining autoreactive responses [303, 309].

Altogether, our studies demonstrate a potential protective role for CD1c-autoreactive T cells in TB. The non-polymorphic nature of CD1c-mediated responses lends itself to potentially being a powerful immunotherapeutic tool as it can be applied globally [457]. CD1c-autoreactive T cells have demonstrated cytotoxic and antimicrobial functions in various studies, including those using cells from healthy subjects, TB patients, or humanised mice [341, 352, 355, 471, 508, 537]. However, due to autoreactive responses, the development of effective therapies requires a thorough understanding of the host-pathogen interaction during TB infection, and techniques such as adoptive transfer of T cells in TB mouse models can be exploited to further shed light on this *in vivo*.

References

1. Kaczmarek, R., et al., *CD1: A Singed Cat of the Three Antigen Presentation Systems.* Arch Immunol Ther Exp (Warsz), 2017. **65**(3): p. 201-214.
2. Hershberg, R., et al., *High functional diversity in Mycobacterium tuberculosis driven by genetic drift and human demography.* PLoS Biol, 2008. **6**(12): p. e311.
3. Gutierrez, M.C., et al., *Ancient origin and gene mosaicism of the progenitor of Mycobacterium tuberculosis.* PLoS Pathog, 2005. **1**(1): p. e5.
4. Ryndak, M.B. and S. Laal, *Mycobacterium tuberculosis Primary Infection and Dissemination: A Critical Role for Alveolar Epithelial Cells.* Front Cell Infect Microbiol, 2019. **9**: p. 299.
5. Hoffmann, C., et al., *Disclosure of the mycobacterial outer membrane: cryo-electron tomography and vitreous sections reveal the lipid bilayer structure.* Proc Natl Acad Sci U S A, 2008. **105**(10): p. 3963-7.
6. Zuber, B., et al., *Direct visualization of the outer membrane of mycobacteria and corynebacteria in their native state.* J Bacteriol, 2008. **190**(16): p. 5672-80.
7. Alcais, A., et al., *Tuberculosis in children and adults: two distinct genetic diseases.* J Exp Med, 2005. **202**(12): p. 1617-21.
8. Flynn, J.L. and J. Chan, *Immunology of tuberculosis.* Annu Rev Immunol, 2001. **19**: p. 93-129.
9. Cooper, A.M., *Cell-mediated immune responses in tuberculosis.* Annu Rev Immunol, 2009. **27**: p. 393-422.
10. Flynn, J.L., et al., *Tumor necrosis factor-alpha is required in the protective immune response against Mycobacterium tuberculosis in mice.* Immunity, 1995. **2**(6): p. 561-72.
11. Keane, J., et al., *Tuberculosis associated with infliximab, a tumor necrosis factor alpha-neutralizing agent.* N Engl J Med, 2001. **345**(15): p. 1098-104.
12. Barry, C.E., 3rd, et al., *The spectrum of latent tuberculosis: rethinking the biology and intervention strategies.* Nat Rev Microbiol, 2009. **7**(12): p. 845-55.
13. Young, D., J. Stark, and D. Kirschner, *Systems biology of persistent infection: tuberculosis as a case study.* Nature Reviews Microbiology, 2008. **6**(7): p. 520-528.
14. Karakousis, P.C., W.R. Bishai, and S.E. Dorman, *Mycobacterium tuberculosis cell envelope lipids and the host immune response.* Cell Microbiol, 2004. **6**(2): p. 105-16.
15. Neyrolles, O. and C. Guilhot, *Recent advances in deciphering the contribution of Mycobacterium tuberculosis lipids to pathogenesis.* Tuberculosis (Edinb), 2011. **91**(3): p. 187-95.
16. De Libero, G. and L. Mori, *The T-cell response to lipid antigens of Mycobacterium tuberculosis.* Frontiers in Immunology, 2014. **5**.
17. Trauner, A., et al., *The dormancy regulator DosR controls ribosome stability in hypoxic mycobacteria.* J Biol Chem, 2012. **287**(28): p. 24053-63.
18. O'Garra, A., et al., *The immune response in tuberculosis.* Annu Rev Immunol, 2013. **31**: p. 475-527.
19. Ryndak, M.B., et al., *Transcriptional profile of Mycobacterium tuberculosis replicating in type II alveolar epithelial cells.* PLoS One, 2015. **10**(4): p. e0123745.
20. Teitelbaum, R., et al., *The M cell as a portal of entry to the lung for the bacterial pathogen Mycobacterium tuberculosis.* Immunity, 1999. **10**(6): p. 641-650.
21. Roy, M.G., et al., *Muc5b is required for airway defence.* Nature, 2014. **505**(7483): p. 412-6.
22. Nicholas, B., et al., *Shotgun proteomic analysis of human-induced sputum.* Proteomics, 2006. **6**(15): p. 4390-401.
23. Brandtzaeg, P., *Secretory IgA: Designed for Anti-Microbial Defense.* Front Immunol, 2013. **4**: p. 222.
24. Whitsett, J.A. and T. Alenghat, *Respiratory epithelial cells orchestrate pulmonary innate immunity.* Nat Immunol, 2015. **16**(1): p. 27-35.
25. AlMatar, M., et al., *Antimicrobial peptides as an alternative to anti-tuberculosis drugs.* Pharmacol Res, 2018. **128**: p. 288-305.

26. Peters, W. and J.D. Ernst, *Mechanisms of cell recruitment in the immune response to Mycobacterium tuberculosis.* Microbes Infect, 2003. **5**(2): p. 151-8.
27. Chai, Q., Z. Lu, and C.H. Liu, *Host defense mechanisms against Mycobacterium tuberculosis.* Cell Mol Life Sci, 2020. **77**(10): p. 1859-1878.
28. Strunk, R.C., D.M. Eidlen, and R.J. Mason, *Pulmonary alveolar type II epithelial cells synthesize and secrete proteins of the classical and alternative complement pathways.* J Clin Invest, 1988. **81**(5): p. 1419-26.
29. Arcos, J., et al., *Human lung hydrolases delineate Mycobacterium tuberculosis-macrophage interactions and the capacity to control infection.* J Immunol, 2011. **187**(1): p. 372-81.
30. Arcos, J., et al., *Lung Mucosa Lining Fluid Modification of Mycobacterium tuberculosis to Reprogram Human Neutrophil Killing Mechanisms.* J Infect Dis, 2015. **212**(6): p. 948-58.
31. Elkington, P.T., et al., *Mycobacterium tuberculosis up-regulates matrix metalloproteinase-1 secretion from human airway epithelial cells via a p38 MAPK switch.* J Immunol, 2005. **175**(8): p. 5333-40.
32. Lee, H.M., et al., *Dectin-1 is inducible and plays an essential role for mycobacteria-induced innate immune responses in airway epithelial cells.* J Clin Immunol, 2009. **29**(6): p. 795-805.
33. Rothfuchs, A.G., et al., *Dectin-1 interaction with Mycobacterium tuberculosis leads to enhanced IL-12p40 production by splenic dendritic cells.* J Immunol, 2007. **179**(6): p. 3463-71.
34. Hertz, C.J., et al., *Activation of Toll-like receptor 2 on human tracheobronchial epithelial cells induces the antimicrobial peptide human beta defensin-2.* J Immunol, 2003. **171**(12): p. 6820-6.
35. Ferguson, J.S. and L.S. Schlesinger, *Pulmonary surfactant in innate immunity and the pathogenesis of tuberculosis.* Tuber Lung Dis, 2000. **80**(4-5): p. 173-84.
36. Sidobre, S., et al., *Lipoglycans are putative ligands for the human pulmonary surfactant protein A attachment to mycobacteria. Critical role of the lipids for lectin-carbohydrate recognition.* J Biol Chem, 2000. **275**(4): p. 2415-22.
37. Hall-Stoodley, L., et al., *Mycobacterium tuberculosis binding to human surfactant proteins A and D, fibronectin, and small airway epithelial cells under shear conditions.* Infect Immun, 2006. **74**(6): p. 3587-96.
38. Chroneos, Z.C., et al., *Pulmonary surfactant and tuberculosis.* Tuberculosis (Edinb), 2009. **89 Suppl 1**: p. S10-4.
39. Li, Y., Y. Wang, and X. Liu, *The role of airway epithelial cells in response to mycobacteria infection.* Clin Dev Immunol, 2012. **2012**: p. 791392.
40. Bowie, A.G., *Translational mini-review series on Toll-like receptors: recent advances in understanding the role of Toll-like receptors in anti-viral immunity.* Clin Exp Immunol, 2007. **147**(2): p. 217-26.
41. Heeg, K., et al., *Structural requirements for uptake and recognition of CpG oligonucleotides.* Int J Med Microbiol, 2008. **298**(1-2): p. 33-8.
42. Aliprantis, A.O., et al., *Cell activation and apoptosis by bacterial lipoproteins through toll-like receptor-2.* Science, 1999. **285**(5428): p. 736-9.
43. Farhat, K., et al., *Heterodimerization of TLR2 with TLR1 or TLR6 expands the ligand spectrum but does not lead to differential signaling.* J Leukoc Biol, 2008. **83**(3): p. 692-701.
44. Uciechowski, P., et al., *Susceptibility to tuberculosis is associated with TLR1 polymorphisms resulting in a lack of TLR1 cell surface expression.* J Leukoc Biol, 2011. **90**(2): p. 377-88.
45. Takeuchi, O., et al., *Cutting edge: role of Toll-like receptor 1 in mediating immune response to microbial lipoproteins.* J Immunol, 2002. **169**(1): p. 10-4.
46. Biragyn, A., et al., *Toll-like receptor 4-dependent activation of dendritic cells by beta-defensin 2.* Science, 2002. **298**(5595): p. 1025-9.
47. Mayer, A.K., et al., *Differential recognition of TLR-dependent microbial ligands in human bronchial epithelial cells.* J Immunol, 2007. **178**(5): p. 3134-42.
48. Harriff, M.J., G.E. Purdy, and D.M. Lewinsohn, *Escape from the Phagosome: The Explanation for MHC-I Processing of Mycobacterial Antigens?* Front Immunol, 2012. **3**: p. 40.

49. Gold, M.C., et al., *Human mucosal associated invariant T cells detect bacterially infected cells.* PLoS Biol, 2010. **8**(6): p. e1000407.
50. Awuh, J.A. and T.H. Flo, *Molecular basis of mycobacterial survival in macrophages.* Cell Mol Life Sci, 2017. **74**(9): p. 1625-1648.
51. Ehrt, S. and D. Schnappinger, *Mycobacterial survival strategies in the phagosome: defence against host stresses.* Cell Microbiol, 2009. **11**(8): p. 1170-8.
52. Silver, R.F., et al., *Human alveolar macrophage gene responses to Mycobacterium tuberculosis strains H37Ra and H37Rv.* Am J Respir Cell Mol Biol, 2009. **40**(4): p. 491-504.
53. Gleeson, L.E., et al., *Cutting Edge: Mycobacterium tuberculosis Induces Aerobic Glycolysis in Human Alveolar Macrophages That Is Required for Control of Intracellular Bacillary Replication.* J Immunol, 2016. **196**(6): p. 2444-9.
54. Gou, X., et al., *The association between vitamin D status and tuberculosis in children: A meta-analysis.* Medicine (Baltimore), 2018. **97**(35): p. e12179.
55. Yuk, J.M., et al., *Vitamin D3 induces autophagy in human monocytes/macrophages via cathelicidin.* Cell Host Microbe, 2009. **6**(3): p. 231-43.
56. Sturgill-Koszycki, S., et al., *Lack of acidification in Mycobacterium phagosomes produced by exclusion of the vesicular proton-ATPase.* Science, 1994. **263**(5147): p. 678-81.
57. Ramachandra, L., et al., *Phagosomal processing of Mycobacterium tuberculosis antigen 85B is modulated independently of mycobacterial viability and phagosome maturation.* Infect Immun, 2005. **73**(2): p. 1097-105.
58. Zhai, W., et al., *The Immune Escape Mechanisms of Mycobacterium Tuberculosis.* Int J Mol Sci, 2019. **20**(2).
59. Houben, D., et al., *ESX-1-mediated translocation to the cytosol controls virulence of mycobacteria.* Cell Microbiol, 2012. **14**(8): p. 1287-98.
60. Watson, R.O., P.S. Manzanillo, and J.S. Cox, *Extracellular M. tuberculosis DNA targets bacteria for autophagy by activating the host DNA-sensing pathway.* Cell, 2012. **150**(4): p. 803-15.
61. Sreejit, G., et al., *The ESAT-6 protein of Mycobacterium tuberculosis interacts with beta-2-microglobulin (beta2M) affecting antigen presentation function of macrophage.* PLoS Pathog, 2014. **10**(10): p. e1004446.
62. van der Wel, N., et al., *M. tuberculosis and M. leprae translocate from the phagolysosome to the cytosol in myeloid cells.* Cell, 2007. **129**(7): p. 1287-98.
63. Lewis, K.N., et al., *Deletion of RD1 from Mycobacterium tuberculosis mimics bacille Calmette-Guerin attenuation.* J Infect Dis, 2003. **187**(1): p. 117-23.
64. Gatfield, J. and J. Pieters, *Essential role for cholesterol in entry of mycobacteria into macrophages.* Science, 2000. **288**(5471): p. 1647-50.
65. Ferrari, G., et al., *A coat protein on phagosomes involved in the intracellular survival of mycobacteria.* Cell, 1999. **97**(4): p. 435-47.
66. Flynn, J.L. and J. Chan, *Immune evasion by Mycobacterium tuberculosis: living with the enemy.* Curr Opin Immunol, 2003. **15**(4): p. 450-5.
67. Hussell, T. and T.J. Bell, *Alveolar macrophages: plasticity in a tissue-specific context.* Nat Rev Immunol, 2014. **14**(2): p. 81-93.
68. Shapouri-Moghaddam, A., et al., *Macrophage plasticity, polarization, and function in health and disease.* J Cell Physiol, 2018. **233**(9): p. 6425-6440.
69. Day, J., A. Friedman, and L.S. Schlesinger, *Modeling the immune rheostat of macrophages in the lung in response to infection.* Proc Natl Acad Sci U S A, 2009. **106**(27): p. 11246-51.
70. Lavalett, L., et al., *Alveolar macrophages from tuberculosis patients display an altered inflammatory gene expression profile.* Tuberculosis (Edinb), 2017. **107**: p. 156-167.
71. Bonecini-Almeida, M.G., et al., *Down-modulation of lung immune responses by interleukin-10 and transforming growth factor beta (TGF-beta) and analysis of TGF-beta receptors I and II in active tuberculosis.* Infect Immun, 2004. **72**(5): p. 2628-34.
72. O'Leary, S., M.P. O'Sullivan, and J. Keane, *IL-10 blocks phagosome maturation in mycobacterium tuberculosis-infected human macrophages.* Am J Respir Cell Mol Biol, 2011. **45**(1): p. 172-80.

73. Chang, S.T., J.J. Linderman, and D.E. Kirschner, *Multiple mechanisms allow Mycobacterium tuberculosis to continuously inhibit MHC class II-mediated antigen presentation by macrophages.* Proc Natl Acad Sci U S A, 2005. **102**(12): p. 4530-5.
74. Guenin-Mace, L., R. Simeone, and C. Demangel, *Lipids of pathogenic Mycobacteria: contributions to virulence and host immune suppression.* Transbound Emerg Dis, 2009. **56**(6-7): p. 255-68.
75. Shukla, S., et al., *Mycobacterium tuberculosis lipoprotein LprG binds lipoarabinomannan and determines its cell envelope localization to control phagolysosomal fusion.* PLoS Pathog, 2014. **10**(10): p. e1004471.
76. Welin, A., et al., *Incorporation of Mycobacterium tuberculosis lipoarabinomannan into macrophage membrane rafts is a prerequisite for the phagosomal maturation block.* Infect Immun, 2008. **76**(7): p. 2882-7.
77. Vergne, I., J. Chua, and V. Deretic, *Tuberculosis toxin blocking phagosome maturation inhibits a novel Ca2+/calmodulin-PI3K hVPS34 cascade.* J Exp Med, 2003. **198**(4): p. 653-9.
78. Eum, S.Y., et al., *Neutrophils are the predominant infected phagocytic cells in the airways of patients with active pulmonary TB.* Chest, 2010. **137**(1): p. 122-8.
79. Lerner, T.R., S. Borel, and M.G. Gutierrez, *The innate immune response in human tuberculosis.* Cell Microbiol, 2015. **17**(9): p. 1277-85.
80. Tan, B.H., et al., *Macrophages acquire neutrophil granules for antimicrobial activity against intracellular pathogens.* J Immunol, 2006. **177**(3): p. 1864-71.
81. Riedel, D.D. and S.H. Kaufmann, *Chemokine secretion by human polymorphonuclear granulocytes after stimulation with Mycobacterium tuberculosis and lipoarabinomannan.* Infect Immun, 1997. **65**(11): p. 4620-3.
82. Kroon, E.E., et al., *Neutrophils: Innate Effectors of TB Resistance?* Front Immunol, 2018. **9**: p. 2637.
83. Zhang, Y., et al., *PD-L1 blockade improves survival in experimental sepsis by inhibiting lymphocyte apoptosis and reversing monocyte dysfunction.* Crit Care, 2010. **14**(6): p. R220.
84. Martineau, A.R., et al., *Neutrophil-mediated innate immune resistance to mycobacteria.* J Clin Invest, 2007. **117**(7): p. 1988-94.
85. Yang, C.T., et al., *Neutrophils exert protection in the early tuberculous granuloma by oxidative killing of mycobacteria phagocytosed from infected macrophages.* Cell Host Microbe, 2012. **12**(3): p. 301-12.
86. Alvarez-Jimenez, V.D., et al., *Extracellular Vesicles Released from Mycobacterium tuberculosis-Infected Neutrophils Promote Macrophage Autophagy and Decrease Intracellular Mycobacterial Survival.* Front Immunol, 2018. **9**: p. 272.
87. Khan, N., et al., *Distinct Strategies Employed by Dendritic Cells and Macrophages in Restricting Mycobacterium tuberculosis Infection: Different Philosophies but Same Desire.* Int Rev Immunol, 2016. **35**(5): p. 386-398.
88. Mihret, A., *The role of dendritic cells in Mycobacterium tuberculosis infection.* Virulence, 2012. **3**(7): p. 654-9.
89. Marino, S., et al., *Dendritic cell trafficking and antigen presentation in the human immune response to Mycobacterium tuberculosis.* J Immunol, 2004. **173**(1): p. 494-506.
90. Hanekom, W.A., et al., *Mycobacterium tuberculosis inhibits maturation of human monocyte-derived dendritic cells in vitro.* J Infect Dis, 2003. **188**(2): p. 257-66.
91. Wu, T., et al., *Interaction between mannosylated lipoarabinomannan and dendritic cell-specific intercellular adhesion molecule-3 grabbing nonintegrin influences dendritic cells maturation and T cell immunity.* Cell Immunol, 2011. **272**(1): p. 94-101.
92. Balboa, L., et al., *Mycobacterium tuberculosis impairs dendritic cell response by altering CD1b, DC-SIGN and MR profile.* Immunol Cell Biol, 2010. **88**(7): p. 716-26.
93. Georgieva, M., et al., *Mycobacterium tuberculosis GroEL2 Modulates Dendritic Cell Responses.* Infect Immun, 2018. **86**(2).

94. Gagliardi, M.C., et al., *Cell wall-associated alpha-glucan is instrumental for Mycobacterium tuberculosis to block CD1 molecule expression and disable the function of dendritic cell derived from infected monocyte.* Cell Microbiol, 2007. **9**(8): p. 2081-92.
95. Wen, Q., et al., *MiR-381-3p Regulates the Antigen-Presenting Capability of Dendritic Cells and Represses Antituberculosis Cellular Immune Responses by Targeting CD1c.* J Immunol, 2016. **197**(2): p. 580-9.
96. Stenger, S., K.R. Niazi, and R.L. Modlin, *Down-regulation of CD1 on antigen-presenting cells by infection with Mycobacterium tuberculosis.* J Immunol, 1998. **161**(7): p. 3582-8.
97. Lozza, L., et al., *Communication between Human Dendritic Cell Subsets in Tuberculosis: Requirements for Naive CD4(+) T Cell Stimulation.* Front Immunol, 2014. **5**: p. 324.
98. Venturini, E., et al., *CD3, CD4, CD8, CD19 and CD16/CD56 positive cells in tuberculosis infection and disease: Peculiar features in children.* Int J Immunopathol Pharmacol, 2019. **33**: p. 2058738419840241.
99. Schierloh, P., et al., *Increased susceptibility to apoptosis of CD56dimCD16+ NK cells induces the enrichment of IFN-gamma-producing CD56bright cells in tuberculous pleurisy.* J Immunol, 2005. **175**(10): p. 6852-60.
100. Garand, M., et al., *Functional and Phenotypic Changes of Natural Killer Cells in Whole Blood during Mycobacterium tuberculosis Infection and Disease.* Front Immunol, 2018. **9**: p. 257.
101. Esin, S. and G. Batoni, *Natural killer cells: a coherent model for their functional role in Mycobacterium tuberculosis infection.* J Innate Immun, 2015. **7**(1): p. 11-24.
102. Arora, P., E.L. Foster, and S.A. Porcelli, *CD1d and natural killer T cells in immunity to Mycobacterium tuberculosis.* Adv Exp Med Biol, 2013. **783**: p. 199-223.
103. Esin, S., et al., *Interaction of Mycobacterium tuberculosis cell wall components with the human natural killer cell receptors NKp44 and Toll-like receptor 2.* Scand J Immunol, 2013. **77**(6): p. 460-9.
104. Esin, S., et al., *Direct binding of human NK cell natural cytotoxicity receptor NKp44 to the surfaces of mycobacteria and other bacteria.* Infect Immun, 2008. **76**(4): p. 1719-27.
105. Gabrilovich, D.I. and S. Nagaraj, *Myeloid-derived suppressor cells as regulators of the immune system.* Nat Rev Immunol, 2009. **9**(3): p. 162-74.
106. du Plessis, N., et al., *Increased frequency of myeloid-derived suppressor cells during active tuberculosis and after recent mycobacterium tuberculosis infection suppresses T-cell function.* Am J Respir Crit Care Med, 2013. **188**(6): p. 724-32.
107. Bronte, V., et al., *Recommendations for myeloid-derived suppressor cell nomenclature and characterization standards.* Nat Commun, 2016. **7**: p. 12150.
108. Kotze, L.A., et al., *Mycobacterium tuberculosis and myeloid-derived suppressor cells: Insights into caveolin rich lipid rafts.* EBioMedicine, 2020. **53**: p. 102670.
109. Cassetta, L., et al., *Deciphering myeloid-derived suppressor cells: isolation and markers in humans, mice and non-human primates.* Cancer Immunol Immunother, 2019. **68**(4): p. 687-697.
110. Bennett, J.A. and J.C. Marsh, *Relationship of Bacillus Calmette-Guerin-induced suppressor cells to hematopoietic precursor cells.* Cancer Res, 1980. **40**(1): p. 80-5.
111. Kendall, L. and E. Sabbadini, *Effect of Bacillus Calmette-Guerin on the in vitro generation of cytotoxic T lymphocytes. I. Effect of BCG on the frequency of cytotoxic T lymphocyte precursors and on the production of helper factors.* J Immunol, 1981. **127**(1): p. 234-8.
112. Srivastava, S., J.D. Ernst, and L. Desvignes, *Beyond macrophages: the diversity of mononuclear cells in tuberculosis.* Immunol Rev, 2014. **262**(1): p. 179-92.
113. El Daker, S., et al., *Granulocytic myeloid derived suppressor cells expansion during active pulmonary tuberculosis is associated with high nitric oxide plasma level.* PLoS One, 2015. **10**(4): p. e0123772.
114. Klimpel, G.R., M. Okada, and C.S. Henney, *Inhibition of in vitro cytotoxic responses by BCG-induced macrophage-like suppressor cells. II. Suppression occurs at the level of a "helper" T cell.* J Immunol, 1979. **123**(1): p. 350-7.

115. Kato, K. and K. Yamamoto, *Suppression of BCG cell wall-induced delayed-type hypersensitivity by BCG pre-treatment. II. Induction of suppressor T cells by heat-killed BCG injection.* Immunology, 1982. **45**(4): p. 655-61.
116. Yang, B., et al., *Identification of CD244-expressing myeloid-derived suppressor cells in patients with active tuberculosis.* Immunol Lett, 2014. **158**(1-2): p. 66-72.
117. Wang, Z., et al., *A myeloid cell population induced by Freund adjuvant suppresses T-cell-mediated antitumor immunity.* J Immunother, 2010. **33**(2): p. 167-77.
118. Goldmann, O., A. Beineke, and E. Medina, *Identification of a Novel Subset of Myeloid-Derived Suppressor Cells During Chronic Staphylococcal Infection That Resembles Immature Eosinophils.* J Infect Dis, 2017. **216**(11): p. 1444-1451.
119. Nisini, R., et al., *beta-Glucan of Candida albicans cell wall causes the subversion of human monocyte differentiation into dendritic cells.* J Leukoc Biol, 2007. **82**(5): p. 1136-42.
120. Condamine, T., et al., *Lectin-type oxidized LDL receptor-1 distinguishes population of human polymorphonuclear myeloid-derived suppressor cells in cancer patients.* Sci Immunol, 2016. **1**(2).
121. Agrawal, N., et al., *Human Monocytic Suppressive Cells Promote Replication of Mycobacterium tuberculosis and Alter Stability of in vitro Generated Granulomas.* Front Immunol, 2018. **9**: p. 2417.
122. Ribechini, E., et al., *Novel GM-CSF signals via IFN-gammaR/IRF-1 and AKT/mTOR license monocytes for suppressor function.* Blood Adv, 2017. **1**(14): p. 947-960.
123. Guirado, E., et al., *Characterization of host and microbial determinants in individuals with latent tuberculosis infection using a human granuloma model.* mBio, 2015. **6**(1): p. e02537-14.
124. Huang, L., et al., *Growth of Mycobacterium tuberculosis in vivo segregates with host macrophage metabolism and ontogeny.* J Exp Med, 2018. **215**(4): p. 1135-1152.
125. Du Plessis, N., et al., *Phenotypically resembling myeloid derived suppressor cells are increased in children with HIV and exposed/infected with Mycobacterium tuberculosis.* Eur J Immunol, 2017. **47**(1): p. 107-118.
126. Cadena, A.M., S.M. Fortune, and J.L. Flynn, *Heterogeneity in tuberculosis.* Nat Rev Immunol, 2017. **17**(11): p. 691-702.
127. Magcwebeba, T., A. Dorhoi, and N. du Plessis, *Corrigendum: The Emerging Role of Myeloid-Derived Suppressor Cells in Tuberculosis.* Front Immunol, 2019. **10**: p. 1528.
128. Dorhoi, A. and N. Du Plessis, *Monocytic Myeloid-Derived Suppressor Cells in Chronic Infections.* Front Immunol, 2017. **8**: p. 1895.
129. Gil-Santana, L., et al., *Diabetes Is Associated with Worse Clinical Presentation in Tuberculosis Patients from Brazil: A Retrospective Cohort Study.* PLoS One, 2016. **11**(1): p. e0146876.
130. Tumino, N., et al., *In HIV-positive patients, myeloid-derived suppressor cells induce T-cell anergy by suppressing CD3zeta expression through ELF-1 inhibition.* AIDS, 2015. **29**(18): p. 2397-407.
131. Vollbrecht, T., et al., *Chronic progressive HIV-1 infection is associated with elevated levels of myeloid-derived suppressor cells.* AIDS, 2012. **26**(12): p. F31-7.
132. Faurholt-Jepsen, D., et al., *Diabetes is a strong predictor of mortality during tuberculosis treatment: a prospective cohort study among tuberculosis patients from Mwanza, Tanzania.* Trop Med Int Health, 2013. **18**(7): p. 822-9.
133. Tumino, N., et al., *Granulocytic Myeloid-Derived Suppressor Cells Increased in Early Phases of Primary HIV Infection Depending on TRAIL Plasma Level.* J Acquir Immune Defic Syndr, 2017. **74**(5): p. 575-582.
134. Gama, L., et al., *Expansion of a subset of CD14highCD16negCCR2low/neg monocytes functionally similar to myeloid-derived suppressor cells during SIV and HIV infection.* J Leukoc Biol, 2012. **91**(5): p. 803-16.
135. Bowers, N.L., et al., *Immune suppression by neutrophils in HIV-1 infection: role of PD-L1/PD-1 pathway.* PLoS Pathog, 2014. **10**(3): p. e1003993.
136. Wang, L., et al., *Expansion of myeloid-derived suppressor cells promotes differentiation of regulatory T cells in HIV-1+ individuals.* AIDS, 2016. **30**(10): p. 1521-1531.

137. Qin, A., et al., *Expansion of monocytic myeloid-derived suppressor cells dampens T cell function in HIV-1-seropositive individuals.* J Virol, 2013. **87**(3): p. 1477-90.
138. Garg, A. and S.A. Spector, *HIV type 1 gp120-induced expansion of myeloid derived suppressor cells is dependent on interleukin 6 and suppresses immunity.* J Infect Dis, 2014. **209**(3): p. 441-51.
139. Meng, Z., et al., *Antiretroviral Therapy Normalizes Autoantibody Profile of HIV Patients by Decreasing CD33(+)CD11b(+)HLA-DR(+) Cells: A Cross-Sectional Study.* Medicine (Baltimore), 2016. **95**(15): p. e3285.
140. Gupta, S., et al., *Suppressor Cell-Depleting Immunotherapy With Denileukin Diftitox is an Effective Host-Directed Therapy for Tuberculosis.* J Infect Dis, 2017. **215**(12): p. 1883-1887.
141. Daniel, J., et al., *Mycobacterium tuberculosis uses host triacylglycerol to accumulate lipid droplets and acquires a dormancy-like phenotype in lipid-loaded macrophages.* PLoS Pathog, 2011. **7**(6): p. e1002093.
142. Silva Miranda, M., et al., *The tuberculous granuloma: an unsuccessful host defence mechanism providing a safety shelter for the bacteria?* Clin Dev Immunol, 2012. **2012**: p. 139127.
143. Bishai, W.R., *Rekindling old controversy on elusive lair of latent tuberculosis.* Lancet, 2000. **356**(9248): p. 2113-4.
144. Adams, D.O., *The granulomatous inflammatory response. A review.* Am J Pathol, 1976. **84**(1): p. 164-92.
145. Sandor, M., J.V. Weinstock, and T.A. Wynn, *Granulomas in schistosome and mycobacterial infections: a model of local immune responses.* Trends Immunol, 2003. **24**(1): p. 44-52.
146. de Martino, M., et al., *Immune Response to Mycobacterium tuberculosis: A Narrative Review.* Front Pediatr, 2019. **7**: p. 350.
147. Belton, M., et al., *Hypoxia and tissue destruction in pulmonary TB.* Thorax, 2016. **71**(12): p. 1145-1153.
148. Volkman, H.E., et al., *Tuberculous granuloma induction via interaction of a bacterial secreted protein with host epithelium.* Science, 2010. **327**(5964): p. 466-9.
149. Walker, N.F., et al., *Doxycycline and HIV infection suppress tuberculosis-induced matrix metalloproteinases.* Am J Respir Crit Care Med, 2012. **185**(9): p. 989-97.
150. Kalsdorf, B., et al., *HIV-1 infection impairs the bronchoalveolar T-cell response to mycobacteria.* Am J Respir Crit Care Med, 2009. **180**(12): p. 1262-70.
151. Cho, S., et al., *Antimicrobial activity of MHC class I-restricted CD8+ T cells in human tuberculosis.* Proc Natl Acad Sci U S A, 2000. **97**(22): p. 12210-5.
152. Chan, E.D., J. Chan, and N.W. Schluger, *What is the role of nitric oxide in murine and human host defense against tuberculosis?Current knowledge.* Am J Respir Cell Mol Biol, 2001. **25**(5): p. 606-12.
153. Medzhitov, R., *Recognition of microorganisms and activation of the immune response.* Nature, 2007. **449**(7164): p. 819-26.
154. Pellicci, D.G., H.F. Koay, and S.P. Berzins, *Thymic development of unconventional T cells: how NKT cells, MAIT cells and gammadelta T cells emerge.* Nat Rev Immunol, 2020. **20**(12): p. 756-770.
155. Zhu, X. and J. Zhu, *CD4 T Helper Cell Subsets and Related Human Immunological Disorders.* Int J Mol Sci, 2020. **21**(21).
156. Ruterbusch, M., et al., *In Vivo CD4(+) T Cell Differentiation and Function: Revisiting the Th1/Th2 Paradigm.* Annu Rev Immunol, 2020. **38**: p. 705-725.
157. Zhu, J., H. Yamane, and W.E. Paul, *Differentiation of effector CD4 T cell populations (*).* Annu Rev Immunol, 2010. **28**: p. 445-89.
158. Annunziato, F., C. Romagnani, and S. Romagnani, *The 3 major types of innate and adaptive cell-mediated effector immunity.* J Allergy Clin Immunol, 2015. **135**(3): p. 626-35.
159. Fang, D. and J. Zhu, *Dynamic balance between master transcription factors determines the fates and functions of CD4 T cell and innate lymphoid cell subsets.* J Exp Med, 2017. **214**(7): p. 1861-1876.

160. Gurram, R.K. and J. Zhu, *Orchestration between ILC2s and Th2 cells in shaping type 2 immune responses.* Cell Mol Immunol, 2019. **16**(3): p. 225-235.
161. Stockinger, B. and S. Omenetti, *The dichotomous nature of T helper 17 cells.* Nat Rev Immunol, 2017. **17**(9): p. 535-544.
162. Dominguez-Villar, M. and D.A. Hafler, *Regulatory T cells in autoimmune disease.* Nat Immunol, 2018. **19**(7): p. 665-673.
163. Shevach, E.M., *CD4+ CD25+ suppressor T cells: more questions than answers.* Nat Rev Immunol, 2002. **2**(6): p. 389-400.
164. Crotty, S., *T Follicular Helper Cell Biology: A Decade of Discovery and Diseases.* Immunity, 2019. **50**(5): p. 1132-1148.
165. Evans, C.M. and R.G. Jenner, *Transcription factor interplay in T helper cell differentiation.* Brief Funct Genomics, 2013. **12**(6): p. 499-511.
166. Lighvani, A.A., et al., *T-bet is rapidly induced by interferon-gamma in lymphoid and myeloid cells.* Proc Natl Acad Sci U S A, 2001. **98**(26): p. 15137-42.
167. Mikhak, Z., et al., *STAT1 in peripheral tissue differentially regulates homing of antigen-specific Th1 and Th2 cells.* J Immunol, 2006. **176**(8): p. 4959-67.
168. Zhu, J., et al., *The transcription factor T-bet is induced by multiple pathways and prevents an endogenous Th2 cell program during Th1 cell responses.* Immunity, 2012. **37**(4): p. 660-73.
169. Wei, L., et al., *Discrete roles of STAT4 and STAT6 transcription factors in tuning epigenetic modifications and transcription during T helper cell differentiation.* Immunity, 2010. **32**(6): p. 840-51.
170. Lyadova, I.V. and A.V. Panteleev, *Th1 and Th17 Cells in Tuberculosis: Protection, Pathology, and Biomarkers.* Mediators Inflamm, 2015. **2015**: p. 854507.
171. Wei, G., et al., *Global mapping of H3K4me3 and H3K27me3 reveals specificity and plasticity in lineage fate determination of differentiating CD4+ T cells.* Immunity, 2009. **30**(1): p. 155-67.
172. Lee, Y.K., et al., *Late developmental plasticity in the T helper 17 lineage.* Immunity, 2009. **30**(1): p. 92-107.
173. Leveton, C., et al., *T-cell-mediated protection of mice against virulent Mycobacterium tuberculosis.* Infect Immun, 1989. **57**(2): p. 390-5.
174. Mogues, T., et al., *The relative importance of T cell subsets in immunity and immunopathology of airborne Mycobacterium tuberculosis infection in mice.* J Exp Med, 2001. **193**(3): p. 271-80.
175. Caruso, A.M., et al., *Mice deficient in CD4 T cells have only transiently diminished levels of IFN-gamma, yet succumb to tuberculosis.* J Immunol, 1999. **162**(9): p. 5407-16.
176. Flory, C.M., R.D. Hubbard, and F.M. Collins, *Effects of in vivo T lymphocyte subset depletion on mycobacterial infections in mice.* J Leukoc Biol, 1992. **51**(3): p. 225-9.
177. Muller, I., et al., *Impaired resistance to Mycobacterium tuberculosis infection after selective in vivo depletion of L3T4+ and Lyt-2+ T cells.* Infect Immun, 1987. **55**(9): p. 2037-41.
178. Orme, I.M., *Characteristics and specificity of acquired immunologic memory to Mycobacterium tuberculosis infection.* J Immunol, 1988. **140**(10): p. 3589-93.
179. Sullivan, B.M., et al., *Increased susceptibility of mice lacking T-bet to infection with Mycobacterium tuberculosis correlates with increased IL-10 and decreased IFN-gamma production.* J Immunol, 2005. **175**(7): p. 4593-602.
180. Flynn, J.L., et al., *An essential role for interferon gamma in resistance to Mycobacterium tuberculosis infection.* J Exp Med, 1993. **178**(6): p. 2249-54.
181. Cooper, A.M., et al., *Disseminated tuberculosis in interferon gamma gene-disrupted mice.* J Exp Med, 1993. **178**(6): p. 2243-7.
182. Lin, P.L., et al., *CD4 T cell depletion exacerbates acute Mycobacterium tuberculosis while reactivation of latent infection is dependent on severity of tissue depletion in cynomolgus macaques.* AIDS Res Hum Retroviruses, 2012. **28**(12): p. 1693-702.
183. Sia, J.K. and J. Rengarajan, *Immunology of Mycobacterium tuberculosis Infections.* Microbiol Spectr, 2019. **7**(4).

184. Green, A.M., R. Difazio, and J.L. Flynn, *IFN-gamma from CD4 T cells is essential for host survival and enhances CD8 T cell function during Mycobacterium tuberculosis infection.* J Immunol, 2013. **190**(1): p. 270-7.
185. Browne, S.K., *Anticytokine autoantibody-associated immunodeficiency.* Annu Rev Immunol, 2014. **32**: p. 635-57.
186. Filipe-Santos, O., et al., *Inborn errors of IL-12/23- and IFN-gamma-mediated immunity: molecular, cellular, and clinical features.* Semin Immunol, 2006. **18**(6): p. 347-61.
187. Zhu, J., et al., *Conditional deletion of Gata3 shows its essential function in T(H)1-T(H)2 responses.* Nat Immunol, 2004. **5**(11): p. 1157-65.
188. Wei, G., et al., *Genome-wide analyses of transcription factor GATA3-mediated gene regulation in distinct T cell types.* Immunity, 2011. **35**(2): p. 299-311.
189. Wohlfert, E.A., et al., *GATA3 controls Foxp3(+) regulatory T cell fate during inflammation in mice.* J Clin Invest, 2011. **121**(11): p. 4503-15.
190. Fang, D., et al., *Bcl11b, a novel GATA3-interacting protein, suppresses Th1 while limiting Th2 cell differentiation.* J Exp Med, 2018. **215**(5): p. 1449-1462.
191. Chung, Y., et al., *Critical regulation of early Th17 cell differentiation by interleukin-1 signaling.* Immunity, 2009. **30**(4): p. 576-87.
192. Guo, L., et al., *IL-1 family members and STAT activators induce cytokine production by Th2, Th17, and Th1 cells.* Proc Natl Acad Sci U S A, 2009. **106**(32): p. 13463-8.
193. Dolff, S., O. Witzke, and B. Wilde, *Th17 cells in renal inflammation and autoimmunity.* Autoimmun Rev, 2019. **18**(2): p. 129-136.
194. Park, H., et al., *A distinct lineage of CD4 T cells regulates tissue inflammation by producing interleukin 17.* Nat Immunol, 2005. **6**(11): p. 1133-41.
195. Veldhoen, M., et al., *TGFbeta in the context of an inflammatory cytokine milieu supports de novo differentiation of IL-17-producing T cells.* Immunity, 2006. **24**(2): p. 179-89.
196. Pawlak, M., A.W. Ho, and V.K. Kuchroo, *Cytokines and transcription factors in the differentiation of CD4(+) T helper cell subsets and induction of tissue inflammation and autoimmunity.* Curr Opin Immunol, 2020. **67**: p. 57-67.
197. Sakaguchi, S., et al., *Immunologic self-tolerance maintained by activated T cells expressing IL-2 receptor alpha-chains (CD25). Breakdown of a single mechanism of self-tolerance causes various autoimmune diseases.* J Immunol, 1995. **155**(3): p. 1151-64.
198. Khattri, R., et al., *An essential role for Scurfin in CD4+CD25+ T regulatory cells.* Nat Immunol, 2003. **4**(4): p. 337-42.
199. Hori, S., T. Nomura, and S. Sakaguchi, *Control of regulatory T cell development by the transcription factor Foxp3.* Science, 2003. **299**(5609): p. 1057-61.
200. Fontenot, J.D., M.A. Gavin, and A.Y. Rudensky, *Foxp3 programs the development and function of CD4+CD25+ regulatory T cells.* Nat Immunol, 2003. **4**(4): p. 330-6.
201. Kang, S.M., Q. Tang, and J.A. Bluestone, *CD4+CD25+ regulatory T cells in transplantation: progress, challenges and prospects.* Am J Transplant, 2007. **7**(6): p. 1457-63.
202. Curotto de Lafaille, M.A. and J.J. Lafaille, *Natural and adaptive foxp3+ regulatory T cells: more of the same or a division of labor?* Immunity, 2009. **30**(5): p. 626-35.
203. Groux, H., et al., *A CD4+ T-cell subset inhibits antigen-specific T-cell responses and prevents colitis.* Nature, 1997. **389**(6652): p. 737-42.
204. Zorn, E., et al., *IL-2 regulates FOXP3 expression in human CD4+CD25+ regulatory T cells through a STAT-dependent mechanism and induces the expansion of these cells in vivo.* Blood, 2006. **108**(5): p. 1571-9.
205. Takimoto, T., et al., *Smad2 and Smad3 are redundantly essential for the TGF-beta-mediated regulation of regulatory T plasticity and Th1 development.* J Immunol, 2010. **185**(2): p. 842-55.
206. Burchill, M.A., et al., *IL-2 receptor beta-dependent STAT5 activation is required for the development of Foxp3+ regulatory T cells.* J Immunol, 2007. **178**(1): p. 280-90.
207. Shevach, E.M., *Mechanisms of foxp3+ T regulatory cell-mediated suppression.* Immunity, 2009. **30**(5): p. 636-45.

208. Spolski, R., P. Li, and W.J. Leonard, *Biology and regulation of IL-2: from molecular mechanisms to human therapy.* Nat Rev Immunol, 2018. **18**(10): p. 648-659.
209. Liu, Z., et al., *Immune homeostasis enforced by co-localized effector and regulatory T cells.* Nature, 2015. **528**(7581): p. 225-30.
210. Grossman, W.J., et al., *Human T regulatory cells can use the perforin pathway to cause autologous target cell death.* Immunity, 2004. **21**(4): p. 589-601.
211. Akkaya, B., et al., *Regulatory T cells mediate specific suppression by depleting peptide-MHC class II from dendritic cells.* Nat Immunol, 2019. **20**(2): p. 218-231.
212. Onishi, Y., et al., *Foxp3+ natural regulatory T cells preferentially form aggregates on dendritic cells in vitro and actively inhibit their maturation.* Proc Natl Acad Sci U S A, 2008. **105**(29): p. 10113-8.
213. Quinn, K.M., et al., *Inactivation of CD4+ CD25+ regulatory T cells during early mycobacterial infection increases cytokine production but does not affect pathogen load.* Immunol Cell Biol, 2006. **84**(5): p. 467-74.
214. Brighenti, S. and D.J. Ordway, *Regulation of Immunity to Tuberculosis.* Microbiol Spectr, 2016. **4**(6).
215. Sharma, S.K., et al., *Cytokine polarization in miliary and pleural tuberculosis.* J Clin Immunol, 2002. **22**(6): p. 345-52.
216. Lienhardt, C., et al., *Active tuberculosis in Africa is associated with reduced Th1 and increased Th2 activity in vivo.* Eur J Immunol, 2002. **32**(6): p. 1605-13.
217. Herrera, M.T., et al., *Compartmentalized bronchoalveolar IFN-gamma and IL-12 response in human pulmonary tuberculosis.* Tuberculosis (Edinb), 2009. **89**(1): p. 38-47.
218. Spolski, R. and W.J. Leonard, *Interleukin-21: a double-edged sword with therapeutic potential.* Nat Rev Drug Discov, 2014. **13**(5): p. 379-95.
219. Nurieva, R.I., et al., *Bcl6 mediates the development of T follicular helper cells.* Science, 2009. **325**(5943): p. 1001-5.
220. Fazilleau, N., et al., *The function of follicular helper T cells is regulated by the strength of T cell antigen receptor binding.* Nat Immunol, 2009. **10**(4): p. 375-84.
221. Vinuesa, C.G., et al., *Follicular Helper T Cells.* Annu Rev Immunol, 2016. **34**: p. 335-68.
222. Han, S., et al., *Cellular interaction in germinal centers. Roles of CD40 ligand and B7-2 in established germinal centers.* J Immunol, 1995. **155**(2): p. 556-67.
223. Zotos, D., et al., *IL-21 regulates germinal center B cell differentiation and proliferation through a B cell-intrinsic mechanism.* J Exp Med, 2010. **207**(2): p. 365-78.
224. Linterman, M.A., et al., *IL-21 acts directly on B cells to regulate Bcl-6 expression and germinal center responses.* J Exp Med, 2010. **207**(2): p. 353-63.
225. da Silva, M.V., et al., *Complexity and Controversies over the Cytokine Profiles of T Helper Cell Subpopulations in Tuberculosis.* J Immunol Res, 2015. **2015**: p. 639107.
226. Rahman, S., et al., *Compartmentalization of immune responses in human tuberculosis: few CD8+ effector T cells but elevated levels of FoxP3+ regulatory t cells in the granulomatous lesions.* Am J Pathol, 2009. **174**(6): p. 2211-24.
227. Munk, M.E. and M. Emoto, *Functions of T-cell subsets and cytokines in mycobacterial infections.* Eur Respir J Suppl, 1995. **20**: p. 668s-675s.
228. Kaufmann, S.H., *Protection against tuberculosis: cytokines, T cells, and macrophages.* Ann Rheum Dis, 2002. **61 Suppl 2**(Suppl 2): p. ii54-8.
229. Rook, G.A., *Th2 cytokines in susceptibility to tuberculosis.* Curr Mol Med, 2007. **7**(3): p. 327-37.
230. Newcomb, D.C., et al., *A functional IL-13 receptor is expressed on polarized murine CD4+ Th17 cells and IL-13 signaling attenuates Th17 cytokine production.* J Immunol, 2009. **182**(9): p. 5317-21.
231. Ribeiro-Rodrigues, R., et al., *A role for CD4+CD25+ T cells in regulation of the immune response during human tuberculosis.* Clin Exp Immunol, 2006. **144**(1): p. 25-34.
232. Guyot-Revol, V., et al., *Regulatory T cells are expanded in blood and disease sites in patients with tuberculosis.* Am J Respir Crit Care Med, 2006. **173**(7): p. 803-10.

233. Chen, X., et al., *CD4(+)CD25(+)FoxP3(+) regulatory T cells suppress Mycobacterium tuberculosis immunity in patients with active disease.* Clin Immunol, 2007. **123**(1): p. 50-9.
234. Semple, P.L., et al., *Regulatory T cells attenuate mycobacterial stasis in alveolar and blood-derived macrophages from patients with tuberculosis.* Am J Respir Crit Care Med, 2013. **187**(11): p. 1249-58.
235. Hougardy, J.M., et al., *Regulatory T cells depress immune responses to protective antigens in active tuberculosis.* Am J Respir Crit Care Med, 2007. **176**(4): p. 409-16.
236. Mahan, C.S., et al., *CD4+ CD25(high) Foxp3+ regulatory T cells downregulate human Vdelta2+ T-lymphocyte function triggered by anti-CD3 or phosphoantigen.* Immunology, 2009. **127**(3): p. 398-407.
237. Dieli, F., et al., *Granulysin-dependent killing of intracellular and extracellular Mycobacterium tuberculosis by Vgamma9/Vdelta2 T lymphocytes.* J Infect Dis, 2001. **184**(8): p. 1082-5.
238. Harris, J., et al., *T helper 2 cytokines inhibit autophagic control of intracellular Mycobacterium tuberculosis.* Immunity, 2007. **27**(3): p. 505-17.
239. Gordon, S., *Alternative activation of macrophages.* Nat Rev Immunol, 2003. **3**(1): p. 23-35.
240. Skapenko, A., et al., *The IL-4 receptor alpha-chain-binding cytokines, IL-4 and IL-13, induce forkhead box P3-expressing CD25+CD4+ regulatory T cells from CD25-CD4+ precursors.* J Immunol, 2005. **175**(9): p. 6107-16.
241. Geginat, J., et al., *Plasticity of human CD4 T cell subsets.* Front Immunol, 2014. **5**: p. 630.
242. Dorman, S.E. and S.M. Holland, *Interferon-gamma and interleukin-12 pathway defects and human disease.* Cytokine Growth Factor Rev, 2000. **11**(4): p. 321-33.
243. Casanova, J.L. and L. Abel, *Genetic dissection of immunity to mycobacteria: the human model.* Annu Rev Immunol, 2002. **20**: p. 581-620.
244. Altare, F., et al., *Impairment of mycobacterial immunity in human interleukin-12 receptor deficiency.* Science, 1998. **280**(5368): p. 1432-5.
245. Cooper, A.M., et al., *Interleukin 12 (IL-12) is crucial to the development of protective immunity in mice intravenously infected with mycobacterium tuberculosis.* J Exp Med, 1997. **186**(1): p. 39-45.
246. Scanga, C.A., et al., *Depletion of CD4(+) T cells causes reactivation of murine persistent tuberculosis despite continued expression of interferon gamma and nitric oxide synthase 2.* J Exp Med, 2000. **192**(3): p. 347-58.
247. Mittrucker, H.W., et al., *Poor correlation between BCG vaccination-induced T cell responses and protection against tuberculosis.* Proc Natl Acad Sci U S A, 2007. **104**(30): p. 12434-9.
248. Nandi, B. and S.M. Behar, *Regulation of neutrophils by interferon-gamma limits lung inflammation during tuberculosis infection.* J Exp Med, 2011. **208**(11): p. 2251-62.
249. Gallegos, A.M., et al., *A gamma interferon independent mechanism of CD4 T cell mediated control of M. tuberculosis infection in vivo.* PLoS Pathog, 2011. **7**(5): p. e1002052.
250. Lazar-Molnar, E., et al., *Programmed death-1 (PD-1)-deficient mice are extraordinarily sensitive to tuberculosis.* Proc Natl Acad Sci U S A, 2010. **107**(30): p. 13402-7.
251. Barber, D.L., et al., *CD4 T cells promote rather than control tuberculosis in the absence of PD-1-mediated inhibition.* J Immunol, 2011. **186**(3): p. 1598-607.
252. Zeng, G., G. Zhang, and X. Chen, *Th1 cytokines, true functional signatures for protective immunity against TB?* Cell Mol Immunol, 2018. **15**(3): p. 206-215.
253. Sahiratmadja, E., et al., *Plasma granulysin levels and cellular interferon-gamma production correlate with curative host responses in tuberculosis, while plasma interferon-gamma levels correlate with tuberculosis disease activity in adults.* Tuberculosis (Edinb), 2007. **87**(4): p. 312-21.
254. Gerosa, F., et al., *CD4(+) T cell clones producing both interferon-gamma and interleukin-10 predominate in bronchoalveolar lavages of active pulmonary tuberculosis patients.* Clin Immunol, 1999. **92**(3): p. 224-34.
255. Verbon, A., et al., *Serum concentrations of cytokines in patients with active tuberculosis (TB) and after treatment.* Clin Exp Immunol, 1999. **115**(1): p. 110-3.

256. Sutherland, J.S., et al., *Pattern and diversity of cytokine production differentiates between Mycobacterium tuberculosis infection and disease.* Eur J Immunol, 2009. **39**(3): p. 723-9.
257. Redford, P.S., P.J. Murray, and A. O'Garra, *The role of IL-10 in immune regulation during M. tuberculosis infection.* Mucosal Immunol, 2011. **4**(3): p. 261-70.
258. Saraiva, M., et al., *Interleukin-10 production by Th1 cells requires interleukin-12-induced STAT4 transcription factor and ERK MAP kinase activation by high antigen dose.* Immunity, 2009. **31**(2): p. 209-19.
259. Moreira-Teixeira, L., et al., *T Cell-Derived IL-10 Impairs Host Resistance to Mycobacterium tuberculosis Infection.* J Immunol, 2017. **199**(2): p. 613-623.
260. Redford, P.S., et al., *Enhanced protection to Mycobacterium tuberculosis infection in IL-10-deficient mice is accompanied by early and enhanced Th1 responses in the lung.* Eur J Immunol, 2010. **40**(8): p. 2200-10.
261. Jasenosky, L.D., et al., *T cells and adaptive immunity to Mycobacterium tuberculosis in humans.* Immunol Rev, 2015. **264**(1): p. 74-87.
262. Sakai, S., K.D. Mayer-Barber, and D.L. Barber, *Defining features of protective CD4 T cell responses to Mycobacterium tuberculosis.* Curr Opin Immunol, 2014. **29**: p. 137-42.
263. McMurtrey, C., et al., *T cell recognition of Mycobacterium tuberculosis peptides presented by HLA-E derived from infected human cells.* PLoS One, 2017. **12**(11): p. e0188288.
264. Darrah, P.A., et al., *Multifunctional TH1 cells define a correlate of vaccine-mediated protection against Leishmania major.* Nat Med, 2007. **13**(7): p. 843-50.
265. Flynn, J.L. and J. Chan, *Tuberculosis: latency and reactivation.* Infect Immun, 2001. **69**(7): p. 4195-201.
266. Almeida, J.R., et al., *Superior control of HIV-1 replication by CD8+ T cells is reflected by their avidity, polyfunctionality, and clonal turnover.* J Exp Med, 2007. **204**(10): p. 2473-85.
267. Lindenstrom, T., et al., *Tuberculosis subunit vaccination provides long-term protective immunity characterized by multifunctional CD4 memory T cells.* J Immunol, 2009. **182**(12): p. 8047-55.
268. Forbes, E.K., et al., *Multifunctional, high-level cytokine-producing Th1 cells in the lung, but not spleen, correlate with protection against Mycobacterium tuberculosis aerosol challenge in mice.* J Immunol, 2008. **181**(7): p. 4955-64.
269. Derrick, S.C., et al., *Vaccine-induced anti-tuberculosis protective immunity in mice correlates with the magnitude and quality of multifunctional CD4 T cells.* Vaccine, 2011. **29**(16): p. 2902-9.
270. Aagaard, C., et al., *Protection and polyfunctional T cells induced by Ag85B-TB10.4/IC31 against Mycobacterium tuberculosis is highly dependent on the antigen dose.* PLoS One, 2009. **4**(6): p. e5930.
271. Sharpe, S., et al., *Alternative BCG delivery strategies improve protection against Mycobacterium tuberculosis in non-human primates: Protection associated with mycobacterial antigen-specific CD4 effector memory T-cell populations.* Tuberculosis (Edinb), 2016. **101**: p. 174-190.
272. Mohagheghpour, N., et al., *CTL response to Mycobacterium tuberculosis: identification of an immunogenic epitope in the 19-kDa lipoprotein.* J Immunol, 1998. **161**(5): p. 2400-6.
273. Lalvani, A., et al., *Human cytolytic and interferon gamma-secreting CD8+ T lymphocytes specific for Mycobacterium tuberculosis.* Proc Natl Acad Sci U S A, 1998. **95**(1): p. 270-5.
274. Stenger, S., et al., *An antimicrobial activity of cytolytic T cells mediated by granulysin.* Science, 1998. **282**(5386): p. 121-5.
275. Stenger, S., et al., *Differential effects of cytolytic T cell subsets on intracellular infection.* Science, 1997. **276**(5319): p. 1684-7.
276. Behar, S.M., et al., *Susceptibility of mice deficient in CD1D or TAP1 to infection with Mycobacterium tuberculosis.* J Exp Med, 1999. **189**(12): p. 1973-80.
277. Sousa, A.O., et al., *Relative contributions of distinct MHC class I-dependent cell populations in protection to tuberculosis infection in mice.* Proc Natl Acad Sci U S A, 2000. **97**(8): p. 4204-8.

278. Heinzel, A.S., et al., *HLA-E-dependent presentation of Mtb-derived antigen to human CD8+ T cells.* J Exp Med, 2002. **196**(11): p. 1473-81.
279. Sieling, P.A., et al., *CD1-restricted T cell recognition of microbial lipoglycan antigens.* Science, 1995. **269**(5221): p. 227-30.
280. Kinjo, Y., et al., *Recognition of bacterial glycosphingolipids by natural killer T cells.* Nature, 2005. **434**(7032): p. 520-5.
281. Godfrey, D.I., et al., *The burgeoning family of unconventional T cells.* Nat Immunol, 2015. **16**(11): p. 1114-23.
282. Treiner, E., et al., *Selection of evolutionarily conserved mucosal-associated invariant T cells by MR1.* Nature, 2003. **422**(6928): p. 164-9.
283. Kjer-Nielsen, L., et al., *MR1 presents microbial vitamin B metabolites to MAIT cells.* Nature, 2012. **491**(7426): p. 717-23.
284. Dias, J., et al., *The CD4(-)CD8(-) MAIT cell subpopulation is a functionally distinct subset developmentally related to the main CD8(+) MAIT cell pool.* Proc Natl Acad Sci U S A, 2018. **115**(49): p. E11513-E11522.
285. Downey, A.M., P. Kaplonek, and P.H. Seeberger, *MAIT cells as attractive vaccine targets.* FEBS Lett, 2019. **593**(13): p. 1627-1640.
286. Le Bourhis, L., et al., *Antimicrobial activity of mucosal-associated invariant T cells.* Nat Immunol, 2010. **11**(8): p. 701-8.
287. Kwon, Y.S., et al., *Mucosal-associated invariant T cells are numerically and functionally deficient in patients with mycobacterial infection and reflect disease activity.* Tuberculosis (Edinb), 2015. **95**(3): p. 267-74.
288. Kauffman, K.D., et al., *Limited Pulmonary Mucosal-Associated Invariant T Cell Accumulation and Activation during Mycobacterium tuberculosis Infection in Rhesus Macaques.* Infect Immun, 2018. **86**(12).
289. Sada-Ovalle, I., et al., *Innate invariant NKT cells recognize Mycobacterium tuberculosis-infected macrophages, produce interferon-gamma, and kill intracellular bacteria.* PLoS Pathog, 2008. **4**(12): p. e1000239.
290. Kee, S.J., et al., *Dysfunction of natural killer T cells in patients with active Mycobacterium tuberculosis infection.* Infect Immun, 2012. **80**(6): p. 2100-8.
291. Snyder-Cappione JE, N.D., Loo CP, Chapman JM, Meiklejohn DA, and e.a. Melo FF, *Individuals with Pulmonary Tuberculosis Have Lower Levels of Circulating CD1d-Restricted NKT Cells.* J Infect Dis, 2007. **195**(9): p. 1361–4.
292. Montoya CJ, C.J., Ramirez Z, Rugeles MT, Wilson SB, Landay AL., *Invariant NKT cells from HIV-1 or Mycobacterium tuberculosis-infected patients express an activated phenotype.* Clin Immunol, 2008. **1**(127): p. 6.
293. Okamoto Yoshida, Y., et al., *Essential role of IL-17A in the formation of a mycobacterial infection-induced granuloma in the lung.* J Immunol, 2010. **184**(8): p. 4414-22.
294. Vorkas, C.K., et al., *Mucosal-associated invariant and gammadelta T cell subsets respond to initial Mycobacterium tuberculosis infection.* JCI Insight, 2018. **3**(19).
295. De Libero, G. and L. Mori, *The T-Cell Response to Lipid Antigens of Mycobacterium tuberculosis.* Front Immunol, 2014. **5**: p. 219.
296. Brigl, M. and M.B. Brenner, *CD1: antigen presentation and T cell function.* Annu Rev Immunol, 2004. **22**: p. 817-90.
297. Zajonc, D.M., et al., *Crystal structure of CD1a in complex with a sulfatide self antigen at a resolution of 2.15 A.* Nat Immunol, 2003. **4**(8): p. 808-15.
298. Zajonc, D.M., et al., *Molecular mechanism of lipopeptide presentation by CD1a.* Immunity, 2005. **22**(2): p. 209-19.
299. Cheng, J.M., et al., *Total Synthesis of Mycobacterium tuberculosis Dideoxymycobactin-838 and Stereoisomers: Diverse CD1a-Restricted T Cells Display a Common Hierarchy of Lipopeptide Recognition.* Chemistry, 2017. **23**(7): p. 1694-1701.
300. Batuwangala, T., et al., *The crystal structure of human CD1b with a bound bacterial glycolipid.* J Immunol, 2004. **172**(4): p. 2382-8.

301. Gadola, S.D., et al., *Structure of human CD1b with bound ligands at 2.3 A, a maze for alkyl chains.* Nat Immunol, 2002. **3**(8): p. 721-6.
302. Scharf, L., et al., *The 2.5 A structure of CD1c in complex with a mycobacterial lipid reveals an open groove ideally suited for diverse antigen presentation.* Immunity, 2010. **33**(6): p. 853-62.
303. Mansour, S., et al., *Cholesteryl esters stabilize human CD1c conformations for recognition by self-reactive T cells.* Proc Natl Acad Sci U S A, 2016. **113**(9): p. E1266-75.
304. Koch, M., et al., *The crystal structure of human CD1d with and without alpha-galactosylceramide.* Nat Immunol, 2005. **6**(8): p. 819-26.
305. Van Kaer, L., L. Wu, and S. Joyce, *Mechanisms and Consequences of Antigen Presentation by CD1.* Trends in Immunology, 2016. **37**(11): p. 738-754.
306. Ly, D. and D.B. Moody, *The CD1 size problem: lipid antigens, ligands, and scaffolds.* Cell Mol Life Sci, 2014. **71**(16): p. 3069-79.
307. Porcelli, S., et al., *Recognition of cluster of differentiation 1 antigens by human CD4-CD8- cytolytic T lymphocytes.* Nature, 1989. **341**(6241): p. 447-50.
308. Cotton, R.N., et al., *Lipids hide or step aside for CD1-autoreactive T cell receptors.* Curr Opin Immunol, 2018. **52**: p. 93-99.
309. Wun, K.S., et al., *T cell autoreactivity directed toward CD1c itself rather than toward carried self lipids.* Nat Immunol, 2018. **19**(4): p. 397-406.
310. Borg, N.A., et al., *CD1d-lipid-antigen recognition by the semi-invariant NKT T-cell receptor.* Nature, 2007. **448**(7149): p. 44-9.
311. Wegrecki, M., et al., *Atypical sideways recognition of CD1a by autoreactive γδ T cell receptors.* Nat Commun, 2022. **13**(1): p. 3872.
312. Mori, L., M. Lepore, and G. De Libero, *The Immunology of CD1- and MR1-Restricted T Cells.* Annu Rev Immunol, 2016. **34**: p. 479-510.
313. Rossjohn, J., et al., *Recognition of CD1d-restricted antigens by natural killer T cells.* Nat Rev Immunol, 2012. **12**(12): p. 845-57.
314. Van Rhijn, I., D. Ly, and D.B. Moody, *CD1a, CD1b, and CD1c in immunity against mycobacteria.* Adv Exp Med Biol, 2013. **783**: p. 181-97.
315. Krutzik, S.R., et al., *TLR activation triggers the rapid differentiation of monocytes into macrophages and dendritic cells.* Nat Med, 2005. **11**(6): p. 653-60.
316. Sieling, P.A., et al., *CD1 expression by dendritic cells in human leprosy lesions: correlation with effective host immunity.* J Immunol, 1999. **162**(3): p. 1851-8.
317. Buettner, M., et al., *Inverse correlation of maturity and antibacterial activity in human dendritic cells.* J Immunol, 2005. **174**(7): p. 4203-9.
318. Moody, D.B., et al., *T cell activation by lipopeptide antigens.* Science, 2004. **303**(5657): p. 527-31.
319. Van Rhijn, I. and D.B. Moody, *CD1 and mycobacterial lipids activate human T cells.* Immunol Rev, 2015. **264**(1): p. 138-53.
320. Van Rhijn, I., et al., *CD1b-mycolic acid tetramers demonstrate T-cell fine specificity for mycobacterial lipid tails.* European Journal of Immunology, 2017. **47**(9): p. 1525-1534.
321. Moody, D.B., et al., *Structural requirements for glycolipid antigen recognition by CD1b-restricted T cells.* Science, 1997. **278**(5336): p. 283-6.
322. Garcia-Alles, L.F., et al., *Structural reorganization of the antigen-binding groove of human CD1b for presentation of mycobacterial sulfoglycolipids.* Proceedings of the National Academy of Sciences of the United States of America, 2011. **108**(43): p. 17755-17760.
323. Lopez, K., et al., *CD1b Tetramers Broadly Detect T Cells That Correlate With Mycobacterial Exposure but Not Tuberculosis Disease State.* Front Immunol, 2020. **11**: p. 199.
324. Busch, M., et al., *Lipoarabinomannan-Responsive Polycytotoxic T Cells Are Associated with Protection in Human Tuberculosis.* Am J Respir Crit Care Med, 2016. **194**(3): p. 345-55.
325. Gilleron, M., et al., *Diacylated sulfoglycolipids are novel mycobacterial antigens stimulating CD1-restricted T cells during infection with Mycobacterium tuberculosis.* Journal of Experimental Medicine, 2004. **199**(5): p. 649-659.

326. Moody, D.B., et al., *Lipid length controls antigen entry into endosomal and nonendosomal pathways for CDIb presentation.* Nature Immunology, 2002. **3**(5): p. 435-442.
327. Beckman, E.M., et al., *CD1c restricts responses of mycobacteria-specific T cells. Evidence for antigen presentation by a second member of the human CD1 family.* J Immunol, 1996. **157**(7): p. 2795-803.
328. Rosat, J.P., et al., *CD1-restricted microbial lipid antigen-specific recognition found in the CD8(+) alpha beta T cell pool.* Journal of Immunology, 1999. **162**(1): p. 366-371.
329. Moody, D.B., et al., *CD1c-mediated T-cell recognition of isoprenoid glycolipids in Mycobacterium tuberculosis infection.* Nature, 2000. **404**(6780): p. 884-888.
330. Kawano, T., et al., *CD1d-restricted and TCR-mediated activation of valpha14 NKT cells by glycosylceramides.* Science, 1997. **278**(5343): p. 1626-9.
331. Fischer, K., et al., *Mycobacterial phosphatidylinositol mannoside is a natural antigen for CD1d-restricted T cells.* Proc Natl Acad Sci U S A, 2004. **101**(29): p. 10685-90.
332. Sutherland, J.S., et al., *High granulocyte/lymphocyte ratio and paucity of NKT cells defines TB disease in a TB-endemic setting.* Tuberculosis (Edinb), 2009. **89**(6): p. 398-404.
333. Montoya, C.J., et al., *Characterization of human invariant natural killer T subsets in health and disease using a novel invariant natural killer T cell-clonotypic monoclonal antibody, 6B11.* Immunology, 2007. **122**(1): p. 1-14.
334. Rothchild, A.C., et al., *iNKT cell production of GM-CSF controls Mycobacterium tuberculosis.* PLoS Pathog, 2014. **10**(1): p. e1003805.
335. Chancellor, A., et al., *Quantitative and qualitative iNKT repertoire associations with disease susceptibility and outcome in macaque tuberculosis infection.* Tuberculosis (Edinb), 2017. **105**: p. 86-95.
336. Hermans, I.F., et al., *NKT cells enhance CD4+ and CD8+ T cell responses to soluble antigen in vivo through direct interaction with dendritic cells.* J Immunol, 2003. **171**(10): p. 5140-7.
337. Gansert, J.L., et al., *Human NKT cells express granulysin and exhibit antimycobacterial activity.* J Immunol, 2003. **170**(6): p. 3154-61.
338. Carreno, L.J., N.A. Saavedra-Avila, and S.A. Porcelli, *Synthetic glycolipid activators of natural killer T cells as immunotherapeutic agents.* Clin Transl Immunology, 2016. **5**(4): p. e69.
339. Siddiqui, S., L. Visvabharathy, and C.R. Wang, *Role of group 1 CD1-restricted T cells in infectious disease.* Frontiers in Immunology, 2015. **6**.
340. Li, S., et al., *Autoreactive CD1b-restricted T cells: a new innate-like T-cell population that contributes to immunity against infection.* Blood, 2011. **118**(14): p. 3870-8.
341. de Lalla, C., et al., *High-frequency and adaptive-like dynamics of human CD1 self-reactive T cells.* European Journal of Immunology, 2011. **41**(3): p. 602-610.
342. Roura-Mir, C., et al., *CD1a and CD1c activate intrathyroidal T cells during graves' disease and Hashimoto's thyroiditis.* Journal of Immunology, 2005. **174**(6): p. 3773-3780.
343. Alshenawy, H.A. and E.A. Hasby, *Immunophenotyping of dendritic cells in lesional, perilesional and distant skin of chronic plaque psoriasis.* Cell Immunol, 2011. **269**(2): p. 115-9.
344. Cotton, R.N., et al., *Human skin is colonized by T cells that recognize CD1a independently of lipid.* J Clin Invest, 2021. **131**(1).
345. Shahine, A., et al., *A T-cell receptor escape channel allows broad T-cell response to CD1b and membrane phospholipids.* Nat Commun, 2019. **10**(1): p. 56.
346. Van Rhijn, I., et al., *Human autoreactive T cells recognize CD1b and phospholipids.* Proc Natl Acad Sci U S A, 2016. **113**(2): p. 380-5.
347. Shahine, A., et al., *A molecular basis of human T cell receptor autoreactivity toward self-phospholipids.* Sci Immunol, 2017. **2**(16).
348. Shamshiev, A., et al., *The alpha beta T cell response to self-glycolipids shows a novel mechanism of CD1b loading and a requirement for complex oligosaccharides.* Immunity, 2000. **13**(2): p. 255-264.
349. Sekiya, M., et al., *The role of neutral cholesterol ester hydrolysis in macrophage foam cells.* J Atheroscler Thromb, 2011. **18**(5): p. 359-64.

350. Russell, D.G., et al., *Foamy macrophages and the progression of the human tuberculosis granuloma.* Nat Immunol, 2009. **10**(9): p. 943-8.
351. Melian, A., et al., *CD1 expression in human atherosclerosis. A potential mechanism for T cell activation by foam cells.* Am J Pathol, 1999. **155**(3): p. 775-86.
352. Lepore, M., et al., *A novel self-lipid antigen targets human T cells against CD1c(+) leukemias.* J Exp Med, 2014. **211**(7): p. 1363-77.
353. Adams, E.J., *Diverse antigen presentation by the Group 1 CD1 molecule, CD1c.* Mol Immunol, 2013. **55**(2): p. 182-5.
354. Faure, F., et al., *CD1c as a target recognition structure for human T lymphocytes: analysis with peripheral blood gamma/delta cells.* Eur J Immunol, 1990. **20**(3): p. 703-6.
355. Spada, F.M., et al., *Self-recognition of CD1 by gamma/delta T cells: implications for innate immunity.* J Exp Med, 2000. **191**(6): p. 937-48.
356. Sieling, P.A., et al., *Evidence for human CD4+ T cells in the CD1-restricted repertoire: derivation of mycobacteria-reactive T cells from leprosy lesions.* J Immunol, 2000. **164**(9): p. 4790-6.
357. Porcelli, S., C.T. Morita, and M.B. Brenner, *CD1b restricts the response of human CD4-8- T lymphocytes to a microbial antigen.* Nature, 1992. **360**(6404): p. 593-7.
358. Vincent, M.S., et al., *CD1-dependent dendritic cell instruction.* Nat Immunol, 2002. **3**(12): p. 1163-8.
359. Siddiqui, S., L. Visvabharathy, and C.R. Wang, *Role of Group 1 CD1-Restricted T Cells in Infectious Disease.* Front Immunol, 2015. **6**: p. 337.
360. Kasmar, A.G., et al., *CD1b tetramers bind alphabeta T cell receptors to identify a mycobacterial glycolipid-reactive T cell repertoire in humans.* J Exp Med, 2011. **208**(9): p. 1741-7.
361. Takahashi, T., et al., *Cutting edge: analysis of human V alpha 24+CD8+ NK T cells activated by alpha-galactosylceramide-pulsed monocyte-derived dendritic cells.* J Immunol, 2002. **168**(7): p. 3140-4.
362. Brennan, P.J., M. Brigl, and M.B. Brenner, *Invariant natural killer T cells: an innate activation scheme linked to diverse effector functions.* Nat Rev Immunol, 2013. **13**(2): p. 101-17.
363. Chen, C.Y., et al., *A critical role for CD8 T cells in a nonhuman primate model of tuberculosis.* PLoS Pathog, 2009. **5**(4): p. e1000392.
364. O'Reilly, V., et al., *Distinct and overlapping effector functions of expanded human CD4+, CD8alpha+ and CD4-CD8alpha- invariant natural killer T cells.* PLoS One, 2011. **6**(12): p. e28648.
365. Thedrez, A., et al., *CD4 engagement by CD1d potentiates activation of CD4+ invariant NKT cells.* Blood, 2007. **110**(1): p. 251-8.
366. Altman, J.D., et al., *Phenotypic analysis of antigen-specific T lymphocytes.* Science, 1996. **274**(5284): p. 94-6.
367. Layton, E.D., et al., *Validation of a CD1b tetramer assay for studies of human mycobacterial infection or vaccination.* J Immunol Methods, 2018. **458**: p. 44-52.
368. Benlagha, K., et al., *In vivo identification of glycolipid antigen-specific T cells using fluorescent CD1d tetramers.* J Exp Med, 2000. **191**(11): p. 1895-903.
369. Karadimitris, A., et al., *Human CD1d-glycolipid tetramers generated by in vitro oxidative refolding chromatography.* Proc Natl Acad Sci U S A, 2001. **98**(6): p. 3294-8.
370. Matsuda, J.L., et al., *Tracking the response of natural killer T cells to a glycolipid antigen using CD1d tetramers.* Journal of Experimental Medicine, 2000. **192**(5): p. 741-753.
371. James, C.A., et al., *CD1b Tetramers Identify T Cells that Recognize Natural and Synthetic Diacylated Sulfoglycolipids from Mycobacterium tuberculosis.* Cell Chemical Biology, 2018. **25**(4): p. 392-+.
372. Kasmar, A.G., et al., *Cutting Edge: CD1a Tetramers and Dextramers Identify Human Lipopeptide-Specific T Cells Ex Vivo.* Journal of Immunology, 2013. **191**(9): p. 4499-4503.
373. Ly, D., et al., *CD1c tetramers detect ex vivo T cell responses to processed phosphomycoketide antigens.* J Exp Med, 2013. **210**(4): p. 729-41.
374. Wooldridge, L., et al., *Tricks with tetramers: how to get the most from multimeric peptide-MHC.* Immunology, 2009. **126**(2): p. 147-164.

375. Van Rhijn, I., et al., *A conserved human T cell population targets mycobacterial antigens presented by CD1b.* Nat Immunol, 2013. **14**(7): p. 706-13.
376. Van Rhijn, I., et al., *TCR bias and affinity define two compartments of the CD1b-glycolipid-specific T Cell repertoire.* J Immunol, 2014. **192**(9): p. 4054-60.
377. Fowlkes, B.J., et al., *A novel population of T-cell receptor alpha beta-bearing thymocytes which predominantly expresses a single V beta gene family.* Nature, 1987. **329**(6136): p. 251-4.
378. Melandri, D., et al., *The gammadeltaTCR combines innate immunity with adaptive immunity by utilizing spatially distinct regions for agonist selection and antigen responsiveness.* Nat Immunol, 2018. **19**(12): p. 1352-1365.
379. Luoma, A.M., et al., *Crystal structure of Vdelta1 T cell receptor in complex with CD1d-sulfatide shows MHC-like recognition of a self-lipid by human gammadelta T cells.* Immunity, 2013. **39**(6): p. 1032-42.
380. Uldrich, A.P., et al., *CD1d-lipid antigen recognition by the gammadelta TCR.* Nat Immunol, 2013. **14**(11): p. 1137-45.
381. Roy, S., et al., *Molecular Analysis of Lipid-Reactive Vdelta1 gammadelta T Cells Identified by CD1c Tetramers.* J Immunol, 2016. **196**(4): p. 1933-42.
382. Williams, A. and I.M. Orme, *Animal Models of Tuberculosis: An Overview.* Microbiol Spectr, 2016. **4**(4).
383. Davis, J.M., et al., *Real-time visualization of mycobacterium-macrophage interactions leading to initiation of granuloma formation in zebrafish embryos.* Immunity, 2002. **17**(6): p. 693-702.
384. Swaim, L.E., et al., *Mycobacterium marinum infection of adult zebrafish causes caseating granulomatous tuberculosis and is moderated by adaptive immunity.* Infect Immun, 2006. **74**(11): p. 6108-17.
385. Cosma, C.L., et al., *Zebrafish and frog models of Mycobacterium marinum infection.* Curr Protoc Microbiol, 2006. **Chapter 10**: p. Unit 10B 2.
386. Ramakrishnan, L., *The zebrafish guide to tuberculosis immunity and treatment.* Cold Spring Harb Symp Quant Biol, 2013. **78**: p. 179-92.
387. Cronan, M.R. and D.M. Tobin, *Fit for consumption: zebrafish as a model for tuberculosis.* Dis Model Mech, 2014. **7**(7): p. 777-84.
388. Flynn, J.L., *Lessons from experimental Mycobacterium tuberculosis infections.* Microbes Infect, 2006. **8**(4): p. 1179-88.
389. Nusbaum, R.J., et al., *Pulmonary Tuberculosis in Humanized Mice Infected with HIV-1.* Sci Rep, 2016. **6**: p. 21522.
390. Heuts, F., et al., *CD4+ cell-dependent granuloma formation in humanized mice infected with mycobacteria.* Proc Natl Acad Sci U S A, 2013. **110**(16): p. 6482-7.
391. Grover, A., et al., *Humanized NOG mice as a model for tuberculosis vaccine-induced immunity: a comparative analysis with the mouse and guinea pig models of tuberculosis.* Immunology, 2017. **152**(1): p. 150-162.
392. Calderon, V.E., et al., *A humanized mouse model of tuberculosis.* PLoS One, 2013. **8**(5): p. e63331.
393. Arrey, F., et al., *Humanized Mouse Model Mimicking Pathology of Human Tuberculosis for in vivo Evaluation of Drug Regimens.* Front Immunol, 2019. **10**: p. 89.
394. Traggiai, E., et al., *Development of a human adaptive immune system in cord blood cell-transplanted mice.* Science, 2004. **304**(5667): p. 104-7.
395. Ishikawa, F., et al., *Development of functional human blood and immune systems in NOD/SCID/IL2 receptor gamma chain(null) mice.* Blood, 2005. **106**(5): p. 1565-73.
396. Hiramatsu, H., et al., *Complete reconstitution of human lymphocytes from cord blood CD34+ cells using the NOD/SCID/gammacnull mice model.* Blood, 2003. **102**(3): p. 873-80.
397. Saunders, B.M., et al., *CD4 is required for the development of a protective granulomatous response to pulmonary tuberculosis.* Cell Immunol, 2002. **216**(1-2): p. 65-72.
398. Bean, A.G., et al., *Structural deficiencies in granuloma formation in TNF gene-targeted mice underlie the heightened susceptibility to aerosol Mycobacterium tuberculosis infection, which is not compensated for by lymphotoxin.* J Immunol, 1999. **162**(6): p. 3504-11.

399. Bente, D.A., et al., *Dengue fever in humanized NOD/SCID mice.* J Virol, 2005. **79**(21): p. 13797-9.
400. Libby, S.J., et al., *Humanized nonobese diabetic-scid IL2rgammanull mice are susceptible to lethal Salmonella Typhi infection.* Proc Natl Acad Sci U S A, 2010. **107**(35): p. 15589-94.
401. Arnold, L., et al., *Further improvements of the P. falciparum humanized mouse model.* PLoS One, 2011. **6**(3): p. e18045.
402. Sun, Z., et al., *Intrarectal transmission, systemic infection, and CD4+ T cell depletion in humanized mice infected with HIV-1.* J Exp Med, 2007. **204**(4): p. 705-14.
403. Marsden, M.D., et al., *HIV latency in the humanized BLT mouse.* J Virol, 2012. **86**(1): p. 339-47.
404. Sonnenberg, P., et al., *HIV-1 and recurrence, relapse, and reinfection of tuberculosis after cure: a cohort study in South African mineworkers.* Lancet, 2001. **358**(9294): p. 1687-93.
405. Ongaya, A., et al., *Mycobacterium tuberculosis-specific CD8+ T cell recall in convalescing TB subjects with HIV co-infection.* Tuberculosis (Edinb), 2013. **93 Suppl**: p. S60-5.
406. Law, K.F., et al., *Tuberculosis in HIV-positive patients: cellular response and immune activation in the lung.* Am J Respir Crit Care Med, 1996. **153**(4 Pt 1): p. 1377-84.
407. Fahey, J.L., et al., *Prognostic significance of plasma markers of immune activation, HIV viral load and CD4 T-cell measurements.* AIDS, 1998. **12**(13): p. 1581-90.
408. Polyak, S., et al., *Impaired class II expression and antigen uptake in monocytic cells after HIV-1 infection.* J Immunol, 1997. **159**(5): p. 2177-88.
409. Jambo, K.C., et al., *Small alveolar macrophages are infected preferentially by HIV and exhibit impaired phagocytic function.* Mucosal Immunol, 2014. **7**(5): p. 1116-26.
410. Imperiali, F.G., et al., *Increased Mycobacterium tuberculosis growth in HIV-1-infected human macrophages: role of tumour necrosis factor-alpha.* Clin Exp Immunol, 2001. **123**(3): p. 435-42.
411. Mellors, J.W., et al., *Plasma viral load and CD4+ lymphocytes as prognostic markers of HIV-1 infection.* Ann Intern Med, 1997. **126**(12): p. 946-54.
412. Lee, J., et al., *Engrafted human cells generate adaptive immune responses to Mycobacterium bovis BCG infection in humanized mice.* BMC Immunol, 2013. **14**: p. 53.
413. Hunter, R.L., et al., *Pathogenesis of post primary tuberculosis: immunity and hypersensitivity in the development of cavities.* Ann Clin Lab Sci, 2014. **44**(4): p. 365-87.
414. Pinho, S.T., et al., *Impact of tuberculosis treatment length and adherence under different transmission intensities.* Theor Popul Biol, 2015. **104**: p. 68-77.
415. Gillespie, S.H., et al., *Four-month moxifloxacin-based regimens for drug-sensitive tuberculosis.* N Engl J Med, 2014. **371**(17): p. 1577-87.
416. Felio, K., et al., *CD1-restricted adaptive immune responses to Mycobacteria in human group 1 CD1 transgenic mice.* J Exp Med, 2009. **206**(11): p. 2497-509.
417. Capuano, S.V., 3rd, et al., *Experimental Mycobacterium tuberculosis infection of cynomolgus macaques closely resembles the various manifestations of human M. tuberculosis infection.* Infect Immun, 2003. **71**(10): p. 5831-44.
418. Pena, J.C. and W.Z. Ho, *Monkey models of tuberculosis: lessons learned.* Infect Immun, 2015. **83**(3): p. 852-62.
419. Flynn, J.L., et al., *Immunology studies in non-human primate models of tuberculosis.* Immunol Rev, 2015. **264**(1): p. 60-73.
420. Mehra, S., et al., *Reactivation of latent tuberculosis in rhesus macaques by coinfection with simian immunodeficiency virus.* J Med Primatol, 2011. **40**(4): p. 233-43.
421. Lin, P.L., et al., *Tumor necrosis factor neutralization results in disseminated disease in acute and latent Mycobacterium tuberculosis infection with normal granuloma structure in a cynomolgus macaque model.* Arthritis Rheum, 2010. **62**(2): p. 340-50.
422. Elkington, P., et al., *In Vitro Granuloma Models of Tuberculosis: Potential and Challenges.* J Infect Dis, 2019. **219**(12): p. 1858-1866.
423. Tezera, L.B., M.K. Bielecka, and P.T. Elkington, *Bioelectrospray Methodology for Dissection of the Host-pathogen Interaction in Human Tuberculosis.* Bio Protoc, 2017. **7**(14).
424. Tezera, L.B., et al., *Dissection of the host-pathogen interaction in human tuberculosis using a bioengineered 3-dimensional model.* Elife, 2017. **6**.

425. Torres, M., et al., *Role of phagosomes and major histocompatibility complex class II (MHC-II) compartment in MHC-II antigen processing of Mycobacterium tuberculosis in human macrophages.* Infect Immun, 2006. **74**(3): p. 1621-30.
426. *Global tuberculosis report 2023. Geneva: World Health Organization; 2023*. Available from: https://www.who.int/teams/global-tuberculosis-programme/tb-reports/global-tuberculosis-report-2023.
427. Andersen, P. and K.B. Urdahl, *TB vaccines; promoting rapid and durable protection in the lung.* Curr Opin Immunol, 2015. **35**: p. 55-62.
428. Urdahl, K.B., S. Shafiani, and J.D. Ernst, *Initiation and regulation of T-cell responses in tuberculosis.* Mucosal Immunol, 2011. **4**(3): p. 288-93.
429. Irvine, E.B., et al., *Robust IgM responses following intravenous vaccination with Bacille Calmette-Guerin associate with prevention of Mycobacterium tuberculosis infection in macaques.* Nat Immunol, 2021. **22**(12): p. 1515-1523.
430. Dijkman, K., et al., *Prevention of tuberculosis infection and disease by local BCG in repeatedly exposed rhesus macaques.* Nat Med, 2019. **25**(2): p. 255-262.
431. Dijkman, K., et al., *Pulmonary MTBVAC vaccination induces immune signatures previously correlated with prevention of tuberculosis infection.* Cell Rep Med, 2021. **2**(1): p. 100187.
432. Darrah, P.A., et al., *Prevention of tuberculosis in macaques after intravenous BCG immunization.* Nature, 2020. **577**(7788): p. 95-102.
433. Perley, C.C., et al., *The human antibody response to the surface of Mycobacterium tuberculosis.* PLoS One, 2014. **9**(2): p. e98938.
434. Nabeshima, S., et al., *Serum antibody response to tuberculosis-associated glycolipid antigen after BCG vaccination in adults.* J Infect Chemother, 2005. **11**(5): p. 256-8.
435. de Valliere, S., et al., *Enhancement of innate and cell-mediated immunity by antimycobacterial antibodies.* Infect Immun, 2005. **73**(10): p. 6711-20.
436. Brown, R.M., et al., *Lipoarabinomannan-reactive human secretory immunoglobulin A responses induced by mucosal bacille Calmette-Guerin vaccination.* J Infect Dis, 2003. **187**(3): p. 513-7.
437. Chen, T., et al., *Association of Human Antibodies to Arabinomannan With Enhanced Mycobacterial Opsonophagocytosis and Intracellular Growth Reduction.* J Infect Dis, 2016. **214**(2): p. 300-10.
438. Hamasur, B., et al., *A mycobacterial lipoarabinomannan specific monoclonal antibody and its F(ab') fragment prolong survival of mice infected with Mycobacterium tuberculosis.* Clin Exp Immunol, 2004. **138**(1): p. 30-8.
439. Costello, A.M., et al., *Does antibody to mycobacterial antigens, including lipoarabinomannan, limit dissemination in childhood tuberculosis?* Trans R Soc Trop Med Hyg, 1992. **86**(6): p. 686-92.
440. Zimmermann, N., et al., *Human isotype-dependent inhibitory antibody responses against Mycobacterium tuberculosis.* EMBO Mol Med, 2016. **8**(11): p. 1325-1339.
441. Kaufmann, S.H., *Future vaccination strategies against tuberculosis: thinking outside the box.* Immunity, 2010. **33**(4): p. 567-77.
442. Cooper, A.M. and J.L. Flynn, *The protective immune response to Mycobacterium tuberculosis.* Curr Opin Immunol, 1995. **7**(4): p. 512-6.
443. Fletcher, H.A., et al., *Corrigendum: T-cell activation is an immune correlate of risk in BCG vaccinated infants.* Nat Commun, 2016. **7**: p. 11633.
444. Tameris, M.D., et al., *Safety and efficacy of MVA85A, a new tuberculosis vaccine, in infants previously vaccinated with BCG: a randomised, placebo-controlled phase 2b trial.* Lancet, 2013. **381**(9871): p. 1021-8.
445. Goonetilleke, N.P., et al., *Enhanced immunogenicity and protective efficacy against Mycobacterium tuberculosis of bacille Calmette-Guerin vaccine using mucosal administration and boosting with a recombinant modified vaccinia virus Ankara.* J Immunol, 2003. **171**(3): p. 1602-9.

446. Sharpe, S.A., et al., *Establishment of an aerosol challenge model of tuberculosis in rhesus macaques and an evaluation of endpoints for vaccine testing.* Clin Vaccine Immunol, 2010. **17**(8): p. 1170-82.
447. Ndiaye, B.P., et al., *Safety, immunogenicity, and efficacy of the candidate tuberculosis vaccine MVA85A in healthy adults infected with HIV-1: a randomised, placebo-controlled, phase 2 trial.* Lancet Respir Med, 2015. **3**(3): p. 190-200.
448. Ernst, J.D., *Mechanisms of M. tuberculosis Immune Evasion as Challenges to TB Vaccine Design.* Cell Host Microbe, 2018. **24**(1): p. 34-42.
449. Kagina, B.M., et al., *Specific T cell frequency and cytokine expression profile do not correlate with protection against tuberculosis after bacillus Calmette-Guerin vaccination of newborns.* Am J Respir Crit Care Med, 2010. **182**(8): p. 1073-9.
450. Hansen, S.G., et al., *Prevention of tuberculosis in rhesus macaques by a cytomegalovirus-based vaccine.* Nat Med, 2018. **24**(2): p. 130-143.
451. Darrah, P.A., et al., *Boosting BCG with proteins or rAd5 does not enhance protection against tuberculosis in rhesus macaques.* NPJ Vaccines, 2019. **4**: p. 21.
452. Cooper, A.M., *Mouse model of tuberculosis.* Cold Spring Harb Perspect Med, 2014. **5**(2): p. a018556.
453. Havlir, D.V. and P.F. Barnes, *Tuberculosis in patients with human immunodeficiency virus infection.* N Engl J Med, 1999. **340**(5): p. 367-73.
454. Phuah, J.Y., et al., *Activated B cells in the granulomas of nonhuman primates infected with Mycobacterium tuberculosis.* Am J Pathol, 2012. **181**(2): p. 508-14.
455. Phuah, J., et al., *Effects of B Cell Depletion on Early Mycobacterium tuberculosis Infection in Cynomolgus Macaques.* Infect Immun, 2016. **84**(5): p. 1301-1311.
456. Nunes-Alves, C., et al., *In search of a new paradigm for protective immunity to TB.* Nat Rev Microbiol, 2014. **12**(4): p. 289-99.
457. Joosten, S.A., et al., *Harnessing donor unrestricted T-cells for new vaccines against tuberculosis.* Vaccine, 2019. **37**(23): p. 3022-3030.
458. Hiromatsu, K., et al., *Induction of CD1-restricted immune responses in guinea pigs by immunization with mycobacterial lipid antigens.* J Immunol, 2002. **169**(1): p. 330-9.
459. Dascher, C.C., et al., *Immunization with a mycobacterial lipid vaccine improves pulmonary pathology in the guinea pig model of tuberculosis.* Int Immunol, 2003. **15**(8): p. 915-25.
460. Williams, A., Y. Hall, and I.M. Orme, *Evaluation of new vaccines for tuberculosis in the guinea pig model.* Tuberculosis (Edinb), 2009. **89**(6): p. 389-97.
461. Larrouy-Maumus, G., et al., *Protective efficacy of a lipid antigen vaccine in a guinea pig model of tuberculosis.* Vaccine, 2017. **35**(10): p. 1395-1402.
462. Zhao, J., et al., *Mycolic acid-specific T cells protect against Mycobacterium tuberculosis infection in a humanized transgenic mouse model.* Elife, 2015. **4**.
463. Gadola, S.D., et al., *Generation of CD1 tetramers as a tool to monitor glycolipid-specific T cells.* Philos Trans R Soc Lond B Biol Sci, 2003. **358**(1433): p. 875-7.
464. Bekkering, S., et al., *In Vitro Experimental Model of Trained Innate Immunity in Human Primary Monocytes.* Clin Vaccine Immunol, 2016. **23**(12): p. 926-933.
465. Saeed, S., et al., *Epigenetic programming of monocyte-to-macrophage differentiation and trained innate immunity.* Science, 2014. **345**(6204): p. 1251086.
466. Bekkering, S., et al., *Metabolic Induction of Trained Immunity through the Mevalonate Pathway.* Cell, 2018. **172**(1-2): p. 135-+.
467. Aquino, A., et al., *Exogenous control of the expression of Group I CD1 molecules competent for presentation of microbial nonpeptide antigens to human T lymphocytes.* Clin Dev Immunol, 2011. **2011**: p. 790460.
468. Betts, R.J., et al., *Contact sensitizers trigger human CD1-autoreactive T-cell responses.* Eur J Immunol, 2017. **47**(7): p. 1171-1180.
469. Lepore, M., et al., *Correction: Functionally diverse human T cells recognize non-microbial antigens presented by MR1.* Elife, 2017. **6**.

470. Devaiah, B.N. and D.S. Singer, *CIITA and Its Dual Roles in MHC Gene Transcription.* Front Immunol, 2013. **4**: p. 476.
471. Guo, T., et al., *A Subset of Human Autoreactive CD1c-Restricted T Cells Preferentially Expresses TRBV4-1(+) TCRs.* J Immunol, 2018. **200**(2): p. 500-511.
472. Birkinshaw, R.W., et al., *alphabeta T cell antigen receptor recognition of CD1a presenting self lipid ligands.* Nat Immunol, 2015. **16**(3): p. 258-66.
473. de Jong, A., et al., *CD1a-autoreactive T cells recognize natural skin oils that function as headless antigens.* Nat Immunol, 2014. **15**(2): p. 177-85.
474. Ragno, S., et al., *Changes in gene expression in macrophages infected with Mycobacterium tuberculosis: a combined transcriptomic and proteomic approach.* Immunology, 2001. **104**(1): p. 99-108.
475. Mukaida, N., A. Harada, and K. Matsushima, *Interleukin-8 (IL-8) and monocyte chemotactic and activating factor (MCAF/MCP-1), chemokines essentially involved in inflammatory and immune reactions.* Cytokine Growth Factor Rev, 1998. **9**(1): p. 9-23.
476. Gerszten, R.E., et al., *MCP-1 and IL-8 trigger firm adhesion of monocytes to vascular endothelium under flow conditions.* Nature, 1999. **398**(6729): p. 718-23.
477. Ameixa, C. and J.S. Friedland, *Interleukin-8 secretion from Mycobacterium tuberculosis-infected monocytes is regulated by protein tyrosine kinases but not by ERK1/2 or p38 mitogen-activated protein kinases.* Infect Immun, 2002. **70**(8): p. 4743-6.
478. Pydi, S.S., et al., *Down regulation of RANTES in pleural site is associated with inhibition of antigen specific response in tuberculosis.* Tuberculosis (Edinb), 2019. **116S**: p. S123-S130.
479. Zhao, Y., et al., *IP-10 and RANTES as biomarkers for pulmonary tuberculosis diagnosis and monitoring.* Tuberculosis (Edinb), 2018. **111**: p. 45-53.
480. Trinchieri, G., *Interleukin-12: a cytokine at the interface of inflammation and immunity.* Adv Immunol, 1998. **70**: p. 83-243.
481. Roy, S., et al., *Molecular basis of mycobacterial lipid antigen presentation by CD1c and its recognition by alphabeta T cells.* Proc Natl Acad Sci U S A, 2014. **111**(43): p. E4648-57.
482. Montamat-Sicotte, D.J., et al., *A mycolic acid-specific CD1-restricted T cell population contributes to acute and memory immune responses in human tuberculosis infection.* J Clin Invest, 2011. **121**(6): p. 2493-503.
483. Ulrichs, T., et al., *T-cell responses to CD1-presented lipid antigens in humans with Mycobacterium tuberculosis infection.* Infect Immun, 2003. **71**(6): p. 3076-87.
484. Rosenberg, S.A. and M.E. Dudley, *Cancer regression in patients with metastatic melanoma after the transfer of autologous antitumor lymphocytes.* Proc Natl Acad Sci U S A, 2004. **101 Suppl 2**(Suppl 2): p. 14639-45.
485. Riddell, S.R. and P.D. Greenberg, *The use of anti-CD3 and anti-CD28 monoclonal antibodies to clone and expand human antigen-specific T cells.* J Immunol Methods, 1990. **128**(2): p. 189-201.
486. Klapper, J.A., et al., *Single-pass, closed-system rapid expansion of lymphocyte cultures for adoptive cell therapy.* J Immunol Methods, 2009. **345**(1-2): p. 90-9.
487. Dudley, M.E., et al., *Generation of tumor-infiltrating lymphocyte cultures for use in adoptive transfer therapy for melanoma patients.* J Immunother, 2003. **26**(4): p. 332-42.
488. Garlie, N.K., et al., *T cells coactivated with immobilized anti-CD3 and anti-CD28 as potential immunotherapy for cancer.* J Immunother, 1999. **22**(4): p. 336-45.
489. Patel, S., et al., *Mycobacteria-Specific T Cells May Be Expanded From Healthy Donors and Are Near Absent in Primary Immunodeficiency Disorders.* Front Immunol, 2019. **10**: p. 621.
490. Nizzoli, G., et al., *Human CD1c+ dendritic cells secrete high levels of IL-12 and potently prime cytotoxic T-cell responses.* Blood, 2013. **122**(6): p. 932-42.
491. Jongbloed, S.L., et al., *Human CD141+ (BDCA-3)+ dendritic cells (DCs) represent a unique myeloid DC subset that cross-presents necrotic cell antigens.* J Exp Med, 2010. **207**(6): p. 1247-60.

492. Bakdash, G., et al., *Expansion of a BDCA1+CD14+ Myeloid Cell Population in Melanoma Patients May Attenuate the Efficacy of Dendritic Cell Vaccines.* Cancer Res, 2016. **76**(15): p. 4332-46.
493. Ziegler-Heitbrock, L., et al., *Nomenclature of monocytes and dendritic cells in blood.* Blood, 2010. **116**(16): p. e74-80.
494. Chen, P., et al., *Increased CD1c+ mDC1 with mature phenotype regulated by TNFalpha-p38 MAPK in autoimmune ocular inflammatory disease.* Clin Immunol, 2015. **158**(1): p. 35-46.
495. Mariotti, S., et al., *Mycobacterium tuberculosis subverts the differentiation of human monocytes into dendritic cells.* Eur J Immunol, 2002. **32**(11): p. 3050-8.
496. Lepore, M., et al., *Functionally diverse human T cells recognize non-microbial antigens presented by MR1.* Elife, 2017. **6**.
497. Maus, M.V., et al., *Ex vivo expansion of polyclonal and antigen-specific cytotoxic T lymphocytes by artificial APCs expressing ligands for the T-cell receptor, CD28 and 4-1BB.* Nat Biotechnol, 2002. **20**(2): p. 143-8.
498. Latouche, J.B. and M. Sadelain, *Induction of human cytotoxic T lymphocytes by artificial antigen-presenting cells.* Nat Biotechnol, 2000. **18**(4): p. 405-9.
499. Bowyer, G., et al., *Activation-induced Markers Detect Vaccine-Specific CD4(+) T Cell Responses Not Measured by Assays Conventionally Used in Clinical Trials.* Vaccines (Basel), 2018. **6**(3).
500. Reiss, S., et al., *Comparative analysis of activation induced marker (AIM) assays for sensitive identification of antigen-specific CD4 T cells.* PLoS One, 2017. **12**(10): p. e0186998.
501. Barham, M.S., et al., *Activation-Induced Marker Expression Identifies Mycobacterium tuberculosis-Specific CD4 T Cells in a Cytokine-Independent Manner in HIV-Infected Individuals with Latent Tuberculosis.* Immunohorizons, 2020. **4**(10): p. 573-584.
502. Chamoto, K., et al., *CDR3beta sequence motifs regulate autoreactivity of human invariant NKT cell receptors.* J Autoimmun, 2016. **68**: p. 39-51.
503. Pilling, D., et al., *High cell density provides potent survival signals for resting T-cells.* Cell Mol Biol (Noisy-le-grand), 2000. **46**(1): p. 163-74.
504. Ma, Q., et al., *Cell density plays a critical role in ex vivo expansion of T cells for adoptive immunotherapy.* J Biomed Biotechnol, 2010. **2010**: p. 386545.
505. DeWitt, W.S., et al., *A Diverse Lipid Antigen-Specific TCR Repertoire Is Clonally Expanded during Active Tuberculosis.* J Immunol, 2018. **201**(3): p. 888-896.
506. de Jong, A., et al., *CD1a-autoreactive T cells are a normal component of the human alphabeta T cell repertoire.* Nat Immunol, 2010. **11**(12): p. 1102-9.
507. Rius, C., et al., *Peptide-MHC Class I Tetramers Can Fail To Detect Relevant Functional T Cell Clonotypes and Underestimate Antigen-Reactive T Cell Populations.* J Immunol, 2018. **200**(7): p. 2263-2279.
508. Vincent, M.S., et al., *CD1a-, b-, and c-restricted TCRs recognize both self and foreign antigens.* J Immunol, 2005. **175**(10): p. 6344-51.
509. Edwards, S.C., et al., *A population of proinflammatory T cells coexpresses alphabeta and gammadelta T cell receptors in mice and humans.* J Exp Med, 2020. **217**(5).
510. Pellicci, D.G., et al., *The molecular bases of delta/alphabeta T cell-mediated antigen recognition.* J Exp Med, 2014. **211**(13): p. 2599-615.
511. Jackman, R.M., et al., *The tyrosine-containing cytoplasmic tail of CD1b is essential for its efficient presentation of bacterial lipid antigens.* Immunity, 1998. **8**(3): p. 341-51.
512. Kurioka, A., et al., *MAIT cells are licensed through granzyme exchange to kill bacterially sensitized targets.* Mucosal Immunol, 2015. **8**(2): p. 429-40.
513. Lepore, M., et al., *Parallel T-cell cloning and deep sequencing of human MAIT cells reveal stable oligoclonal TCRbeta repertoire.* Nat Commun, 2014. **5**: p. 3866.
514. Booth, J.S., et al., *Mucosal-Associated Invariant T Cells in the Human Gastric Mucosa and Blood: Role in Helicobacter pylori Infection.* Front Immunol, 2015. **6**: p. 466.
515. Choi, I.K., et al., *Signaling by the Epstein-Barr virus LMP1 protein induces potent cytotoxic CD4(+) and CD8(+) T cell responses.* Proc Natl Acad Sci U S A, 2018. **115**(4): p. E686-E695.

516. Meckiff, B.J., et al., *Primary EBV Infection Induces an Acute Wave of Activated Antigen-Specific Cytotoxic CD4(+) T Cells.* J Immunol, 2019. **203**(5): p. 1276-1287.
517. Adhikary, D., et al., *The Epstein-Barr Virus Major Tegument Protein BNRF1 Is a Common Target of Cytotoxic CD4(+) T Cells.* J Virol, 2020. **94**(15).
518. Aslan, N., et al., *Cytotoxic CD4 T cells in viral hepatitis.* J Viral Hepat, 2006. **13**(8): p. 505-14.
519. Zaunders, J.J., et al., *Identification of circulating antigen-specific CD4+ T lymphocytes with a CCR5+, cytotoxic phenotype in an HIV-1 long-term nonprogressor and in CMV infection.* Blood, 2004. **103**(6): p. 2238-47.
520. Soghoian, D.Z., et al., *HIV-specific cytolytic CD4 T cell responses during acute HIV infection predict disease outcome.* Sci Transl Med, 2012. **4**(123): p. 123ra25.
521. Brown, D.M., A.T. Lampe, and A.M. Workman, *The Differentiation and Protective Function of Cytolytic CD4 T Cells in Influenza Infection.* Front Immunol, 2016. **7**: p. 93.
522. Hua, L., et al., *Cytokine-dependent induction of CD4+ T cells with cytotoxic potential during influenza virus infection.* J Virol, 2013. **87**(21): p. 11884-93.
523. Meckiff, B.J., et al., *Imbalance of Regulatory and Cytotoxic SARS-CoV-2-Reactive CD4(+) T Cells in COVID-19.* Cell, 2020. **183**(5): p. 1340-1353 e16.
524. Zhang, Y., et al., *Single-cell analyses reveal key immune cell subsets associated with response to PD-L1 blockade in triple-negative breast cancer.* Cancer Cell, 2021. **39**(12): p. 1578-1593 e8.
525. Zhou, Y., et al., *Single-cell RNA landscape of intratumoral heterogeneity and immunosuppressive microenvironment in advanced osteosarcoma.* Nat Commun, 2020. **11**(1): p. 6322.
526. Guo, X., et al., *Global characterization of T cells in non-small-cell lung cancer by single-cell sequencing.* Nat Med, 2018. **24**(7): p. 978-985.
527. Zhang, L., et al., *Lineage tracking reveals dynamic relationships of T cells in colorectal cancer.* Nature, 2018. **564**(7735): p. 268-272.
528. Prezzemolo, T., et al., *Functional Signatures of Human CD4 and CD8 T Cell Responses to Mycobacterium tuberculosis.* Front Immunol, 2014. **5**: p. 180.
529. Barnes, P.F., et al., *Tuberculosis in patients with human immunodeficiency virus infection.* N Engl J Med, 1991. **324**(23): p. 1644-50.
530. Arlehamn, C.L., et al., *Transcriptional profile of tuberculosis antigen-specific T cells reveals novel multifunctional features.* J Immunol, 2014. **193**(6): p. 2931-40.
531. He, X., et al., *The zinc finger transcription factor Th-POK regulates CD4 versus CD8 T-cell lineage commitment.* Nature, 2005. **433**(7028): p. 826-33.
532. Aliahmad, P., et al., *TOX is required for development of the CD4 T cell lineage gene program.* J Immunol, 2011. **187**(11): p. 5931-40.
533. Pai, S.Y., et al., *Critical roles for transcription factor GATA-3 in thymocyte development.* Immunity, 2003. **19**(6): p. 863-75.
534. Wang, L., et al., *The zinc finger transcription factor Zbtb7b represses CD8-lineage gene expression in peripheral CD4+ T cells.* Immunity, 2008. **29**(6): p. 876-87.
535. Mucida, D., et al., *Transcriptional reprogramming of mature CD4(+) helper T cells generates distinct MHC class II-restricted cytotoxic T lymphocytes.* Nat Immunol, 2013. **14**(3): p. 281-9.
536. Canaday, D.H., et al., *CD4(+) and CD8(+) T cells kill intracellular Mycobacterium tuberculosis by a perforin and Fas/Fas ligand-independent mechanism.* J Immunol, 2001. **167**(5): p. 2734-42.
537. Ochoa, M.T., et al., *T-cell release of granulysin contributes to host defense in leprosy.* Nat Med, 2001. **7**(2): p. 174-9.
538. Guo, X., et al., *Publisher Correction: Global characterization of T cells in non-small-cell lung cancer by single-cell sequencing.* Nat Med, 2018. **24**(10): p. 1628.
539. van den Broek, M.F. and H. Hengartner, *The role of perforin in infections and tumour surveillance.* Exp Physiol, 2000. **85**(6): p. 681-5.
540. Leslie, D.S., et al., *CD1-mediated gamma/delta T cell maturation of dendritic cells.* J Exp Med, 2002. **196**(12): p. 1575-84.
541. Sieling, P.A., et al., *Human double-negative T cells in systemic lupus erythematosus provide help for IgG and are restricted by CD1c.* J Immunol, 2000. **165**(9): p. 5338-44.

542. Visvabharathy, L., et al., *Group 1 CD1-restricted T cells contribute to control of systemic Staphylococcus aureus infection.* PLoS Pathog, 2020. **16**(4): p. e1008443.
543. Jarrett, R., et al., *Filaggrin inhibits generation of CD1a neolipid antigens by house dust mite-derived phospholipase.* Sci Transl Med, 2016. **8**(325): p. 325ra18.
544. Hardman, C.S., et al., *CD1a presentation of endogenous antigens by group 2 innate lymphoid cells.* Sci Immunol, 2017. **2**(18).
545. Hava, D.L., et al., *Evasion of peptide, but not lipid antigen presentation, through pathogen-induced dendritic cell maturation.* Proc Natl Acad Sci U S A, 2008. **105**(32): p. 11281-6.
546. Amelio, P., et al., *Mixed Th1 and Th2 Mycobacterium tuberculosis-specific CD4 T cell responses in patients with active pulmonary tuberculosis from Tanzania.* PLoS Negl Trop Dis, 2017. **11**(7): p. e0005817.
547. Walzl, G., et al., *Immunological biomarkers of tuberculosis.* Nat Rev Immunol, 2011. **11**(5): p. 343-54.
548. Sher, A., et al., *Production of IL-10 by CD4+ T lymphocytes correlates with down-regulation of Th1 cytokine synthesis in helminth infection.* J Immunol, 1991. **147**(8): p. 2713-6.
549. Pearce, E.J., et al., *Th2 response polarization during infection with the helminth parasite Schistosoma mansoni.* Immunol Rev, 2004. **201**: p. 117-26.
550. McKee, A.S. and E.J. Pearce, *CD25+CD4+ cells contribute to Th2 polarization during helminth infection by suppressing Th1 response development.* J Immunol, 2004. **173**(2): p. 1224-31.
551. Anthony, R.M., et al., *Protective immune mechanisms in helminth infection.* Nat Rev Immunol, 2007. **7**(12): p. 975-87.
552. Farber, J.M., *Mig and IP-10: CXC chemokines that target lymphocytes.* J Leukoc Biol, 1997. **61**(3): p. 246-57.
553. Park, M.K., et al., *The CXC chemokine murine monokine induced by IFN-gamma (CXC chemokine ligand 9) is made by APCs, targets lymphocytes including activated B cells, and supports antibody responses to a bacterial pathogen in vivo.* J Immunol, 2002. **169**(3): p. 1433-43.
554. Araujo, Z., et al., *Diagnostic accuracy of combinations of serological biomarkers for identifying clinical tuberculosis.* J Infect Dev Ctries, 2018. **12**(6): p. 429-441.
555. Almeida Cde, S., et al., *Anti-mycobacterial treatment reduces high plasma levels of CXC-chemokines detected in active tuberculosis by cytometric bead array.* Mem Inst Oswaldo Cruz, 2009. **104**(7): p. 1039-41.
556. Li, Y., et al., *Monokine induced by gamma interferon for detecting pulmonary tuberculosis: A diagnostic meta-analysis.* Medicine (Baltimore), 2020. **99**(47): p. e23302.
557. Domingo-Gonzalez, R., et al., *Cytokines and Chemokines in Mycobacterium tuberculosis Infection.* Microbiol Spectr, 2016. **4**(5).
558. Cooper, A.M., K.D. Mayer-Barber, and A. Sher, *Role of innate cytokines in mycobacterial infection.* Mucosal Immunol, 2011. **4**(3): p. 252-60.
559. Boraschi, D., et al., *The family of the interleukin-1 receptors.* Immunol Rev, 2018. **281**(1): p. 197-232.
560. Mayer-Barber, K.D., et al., *Caspase-1 independent IL-1beta production is critical for host resistance to mycobacterium tuberculosis and does not require TLR signaling in vivo.* J Immunol, 2010. **184**(7): p. 3326-30.
561. Mayer-Barber, K.D., et al., *Host-directed therapy of tuberculosis based on interleukin-1 and type I interferon crosstalk.* Nature, 2014. **511**(7507): p. 99-103.
562. Juffermans, N.P., et al., *Interleukin-1 signaling is essential for host defense during murine pulmonary tuberculosis.* J Infect Dis, 2000. **182**(3): p. 902-8.
563. Bohrer, A.C., et al., *Cutting Edge: IL-1R1 Mediates Host Resistance to Mycobacterium tuberculosis by Trans-Protection of Infected Cells.* J Immunol, 2018. **201**(6): p. 1645-1650.
564. Sugawara, I., et al., *Role of interleukin (IL)-1 type 1 receptor in mycobacterial infection.* Microbiol Immunol, 2001. **45**(11): p. 743-50.
565. Lee, J.S., et al., *Expression and regulation of the CC-chemokine ligand 20 during human tuberculosis.* Scand J Immunol, 2008. **67**(1): p. 77-85.

566. Friedland, J.S., et al., *Inhibition of ex vivo proinflammatory cytokine secretion in fatal Mycobacterium tuberculosis infection.* Clin Exp Immunol, 1995. **100**(2): p. 233-8.
567. Kurashima, K., et al., *Elevated chemokine levels in bronchoalveolar lavage fluid of tuberculosis patients.* Am J Respir Crit Care Med, 1997. **155**(4): p. 1474-7.
568. Sadek, M.I., et al., *Chemokines induced by infection of mononuclear phagocytes with mycobacteria and present in lung alveoli during active pulmonary tuberculosis.* Am J Respir Cell Mol Biol, 1998. **19**(3): p. 513-21.
569. Yang, X.D., et al., *Fully human anti-interleukin-8 monoclonal antibodies: potential therapeutics for the treatment of inflammatory disease states.* J Leukoc Biol, 1999. **66**(3): p. 401-10.
570. Bergeron, A., et al., *Cytokine patterns in tuberculous and sarcoid granulomas: correlations with histopathologic features of the granulomatous response.* J Immunol, 1997. **159**(6): p. 3034-43.
571. Zhang, Y., et al., *Enhanced interleukin-8 release and gene expression in macrophages after exposure to Mycobacterium tuberculosis and its components.* J Clin Invest, 1995. **95**(2): p. 586-92.
572. Wickremasinghe, M.I., L.H. Thomas, and J.S. Friedland, *Pulmonary epithelial cells are a source of IL-8 in the response to Mycobacterium tuberculosis: essential role of IL-1 from infected monocytes in a NF-kappa B-dependent network.* J Immunol, 1999. **163**(7): p. 3936-47.
573. Friedland, J.S., et al., *Secretion of interleukin-8 following phagocytosis of Mycobacterium tuberculosis by human monocyte cell lines.* Eur J Immunol, 1992. **22**(6): p. 1373-8.
574. Ameixa, C. and J.S. Friedland, *Down-regulation of interleukin-8 secretion from Mycobacterium tuberculosis-infected monocytes by interleukin-4 and -10 but not by interleukin-13.* Infect Immun, 2001. **69**(4): p. 2470-6.
575. Krupa, A., et al., *Binding of CXCL8/IL-8 to Mycobacterium tuberculosis Modulates the Innate Immune Response.* Mediators Inflamm, 2015. **2015**: p. 124762.
576. Wang, P., et al., *Interleukin (IL)-10 inhibits nuclear factor kappa B (NF kappa B) activation in human monocytes. IL-10 and IL-4 suppress cytokine synthesis by different mechanisms.* J Biol Chem, 1995. **270**(16): p. 9558-63.
577. Standiford, T.J., et al., *Gene expression of macrophage inflammatory protein-1 alpha from human blood monocytes and alveolar macrophages is inhibited by interleukin-4.* Am J Respir Cell Mol Biol, 1993. **9**(2): p. 192-8.
578. Algood, H.M. and J.L. Flynn, *CCR5-deficient mice control Mycobacterium tuberculosis infection despite increased pulmonary lymphocytic infiltration.* J Immunol, 2004. **173**(5): p. 3287-96.
579. Wang, Y., et al., *CD40 is a cellular receptor mediating mycobacterial heat shock protein 70 stimulation of CC-chemokines.* Immunity, 2001. **15**(6): p. 971-83.
580. Dorner, B.G., et al., *MIP-1alpha, MIP-1beta, RANTES, and ATAC/lymphotactin function together with IFN-gamma as type 1 cytokines.* Proc Natl Acad Sci U S A, 2002. **99**(9): p. 6181-6.
581. Skwor, T.A., et al., *Recombinant guinea pig CCL5 (RANTES) differentially modulates cytokine production in alveolar and peritoneal macrophages.* J Leukoc Biol, 2004. **76**(6): p. 1229-39.
582. Salam, N., et al., *Protective immunity to Mycobacterium tuberculosis infection by chemokine and cytokine conditioned CFP-10 differentiated dendritic cells.* PLoS One, 2008. **3**(8): p. e2869.
583. Lindenstrom, T., et al., *Control of chronic mycobacterium tuberculosis infection by CD4 KLRG1- IL-2-secreting central memory cells.* J Immunol, 2013. **190**(12): p. 6311-9.
584. Sester, U., et al., *Whole-blood flow-cytometric analysis of antigen-specific CD4 T-cell cytokine profiles distinguishes active tuberculosis from non-active states.* PLoS One, 2011. **6**(3): p. e17813.
585. Portevin, D., et al., *Assessment of the novel T-cell activation marker-tuberculosis assay for diagnosis of active tuberculosis in children: a prospective proof-of-concept study.* Lancet Infect Dis, 2014. **14**(10): p. 931-8.
586. Harari, A., et al., *Dominant TNF-alpha+ Mycobacterium tuberculosis-specific CD4+ T cell responses discriminate between latent infection and active disease.* Nat Med, 2011. **17**(3): p. 372-6.

587. Caccamo, N., et al., *Multifunctional CD4(+) T cells correlate with active Mycobacterium tuberculosis infection.* Eur J Immunol, 2010. **40**(8): p. 2211-20.
588. Waldmann, T.A., S. Dubois, and Y. Tagaya, *Contrasting roles of IL-2 and IL-15 in the life and death of lymphocytes: implications for immunotherapy.* Immunity, 2001. **14**(2): p. 105-10.
589. Haverkamp, M.H., J.T. van Dissel, and S.M. Holland, *Human host genetic factors in nontuberculous mycobacterial infection: lessons from single gene disorders affecting innate and adaptive immunity and lessons from molecular defects in interferon-gamma-dependent signaling.* Microbes Infect, 2006. **8**(4): p. 1157-66.
590. de Jong, R., et al., *Severe mycobacterial and Salmonella infections in interleukin-12 receptor-deficient patients.* Science, 1998. **280**(5368): p. 1435-8.
591. Lewinsohn, D.A., M.C. Gold, and D.M. Lewinsohn, *Views of immunology: effector T cells.* Immunol Rev, 2011. **240**(1): p. 25-39.
592. Allie, N., et al., *Prominent role for T cell-derived tumour necrosis factor for sustained control of Mycobacterium tuberculosis infection.* Sci Rep, 2013. **3**: p. 1809.
593. Harris, J. and J. Keane, *How tumour necrosis factor blockers interfere with tuberculosis immunity.* Clin Exp Immunol, 2010. **161**(1): p. 1-9.
594. Day, C.L., et al., *Functional capacity of Mycobacterium tuberculosis-specific T cell responses in humans is associated with mycobacterial load.* J Immunol, 2011. **187**(5): p. 2222-32.
595. Liew, F.Y., Y. Li, and S. Millott, *Tumor necrosis factor-alpha synergizes with IFN-gamma in mediating killing of Leishmania major through the induction of nitric oxide.* J Immunol, 1990. **145**(12): p. 4306-10.
596. Bogdan, C., et al., *Tumor necrosis factor-alpha in combination with interferon-gamma, but not with interleukin 4 activates murine macrophages for elimination of Leishmania major amastigotes.* Eur J Immunol, 1990. **20**(5): p. 1131-5.
597. Chan, J., et al., *Killing of virulent Mycobacterium tuberculosis by reactive nitrogen intermediates produced by activated murine macrophages.* J Exp Med, 1992. **175**(4): p. 1111-22.
598. Smith, S.G., et al., *Polyfunctional CD4 T-cells correlate with in vitro mycobacterial growth inhibition following Mycobacterium bovis BCG-vaccination of infants.* Vaccine, 2016. **34**(44): p. 5298-5305.
599. Tebruegge, M., et al., *Mycobacteria-Specific Mono- and Polyfunctional CD4+ T Cell Profiles in Children With Latent and Active Tuberculosis: A Prospective Proof-of-Concept Study.* Front Immunol, 2019. **10**: p. 431.
600. Khader, S.A., et al., *IL-23 and IL-17 in the establishment of protective pulmonary CD4+ T cell responses after vaccination and during Mycobacterium tuberculosis challenge.* Nat Immunol, 2007. **8**(4): p. 369-77.
601. Gopal, R., et al., *IL-23-dependent IL-17 drives Th1-cell responses following Mycobacterium bovis BCG vaccination.* Eur J Immunol, 2012. **42**(2): p. 364-73.
602. Moody, D.B. and R.N. Cotton, *Four pathways of CD1 antigen presentation to T cells.* Curr Opin Immunol, 2017. **46**: p. 127-133.
603. Genardi, S., E. Morgun, and C.R. Wang, *CD1-Restricted T Cells in Inflammatory Skin Diseases.* J Invest Dermatol, 2022. **142**(3 Pt B): p. 768-773.
604. Chancellor, A., S.D. Gadola, and S. Mansour, *The versatility of the CD1 lipid antigen presentation pathway.* Immunology, 2018. **154**(2): p. 196-203.
605. Cui, J., et al., *Requirement for Valpha14 NKT cells in IL-12-mediated rejection of tumors.* Science, 1997. **278**(5343): p. 1623-6.
606. Crowe, N.Y., M.J. Smyth, and D.I. Godfrey, *A critical role for natural killer T cells in immunosurveillance of methylcholanthrene-induced sarcomas.* J Exp Med, 2002. **196**(1): p. 119-27.
607. Motohashi, S., et al., *Anti-tumor immune responses induced by iNKT cell-based immunotherapy for lung cancer and head and neck cancer.* Clin Immunol, 2011. **140**(2): p. 167-76.
608. Exley, M.A., et al., *Adoptive Transfer of Invariant NKT Cells as Immunotherapy for Advanced Melanoma: A Phase I Clinical Trial.* Clin Cancer Res, 2017. **23**(14): p. 3510-3519.

609. Cheng, X., et al., *Feasibility of iNKT cell and PD-1+CD8+ T cell-based immunotherapy in patients with lung adenocarcinoma: Preliminary results of a phase I/II clinical trial.* Clin Immunol, 2022. **238**: p. 108992.
610. Nair, S. and M.V. Dhodapkar, *Natural Killer T Cells in Cancer Immunotherapy.* Front Immunol, 2017. **8**: p. 1178.
611. Richter, J., et al., *Clinical regressions and broad immune activation following combination therapy targeting human NKT cells in myeloma.* Blood, 2013. **121**(3): p. 423-30.
612. Ishikawa, A., et al., *A phase I study of alpha-galactosylceramide (KRN7000)-pulsed dendritic cells in patients with advanced and recurrent non-small cell lung cancer.* Clin Cancer Res, 2005. **11**(5): p. 1910-7.
613. Chang, D.H., et al., *Sustained expansion of NKT cells and antigen-specific T cells after injection of alpha-galactosyl-ceramide loaded mature dendritic cells in cancer patients.* J Exp Med, 2005. **201**(9): p. 1503-17.
614. Look, A., et al., *Towards a better understanding of human iNKT cell subpopulations for improved clinical outcomes.* Front Immunol, 2023. **14**: p. 1176724.
615. Korb, V.C., A.A. Chuturgoon, and D. Moodley, *Mycobacterium tuberculosis: Manipulator of Protective Immunity.* Int J Mol Sci, 2016. **17**(3): p. 131.
616. Caceres, N., et al., *Evolution of foamy macrophages in the pulmonary granulomas of experimental tuberculosis models.* Tuberculosis (Edinb), 2009. **89**(2): p. 175-82.
617. Brennan, P.J., et al., *Invariant natural killer T cells recognize lipid self antigen induced by microbial danger signals.* Nat Immunol, 2011. **12**(12): p. 1202-11.
618. Wooldridge, L., et al., *Tricks with tetramers: how to get the most from multimeric peptide-MHC (vol 126, pg 147, 2009).* Immunology, 2009. **126**(3): p. 447-447.
619. Dougan, S.K., A. Kaser, and R.S. Blumberg, *CD1 expression on antigen-presenting cells.* Curr Top Microbiol Immunol, 2007. **314**: p. 113-41.
620. Leslie, D.S., et al., *Serum lipids regulate dendritic cell CD1 expression and function.* Immunology, 2008. **125**(3): p. 289-301.

Appendix

Supplementary figures

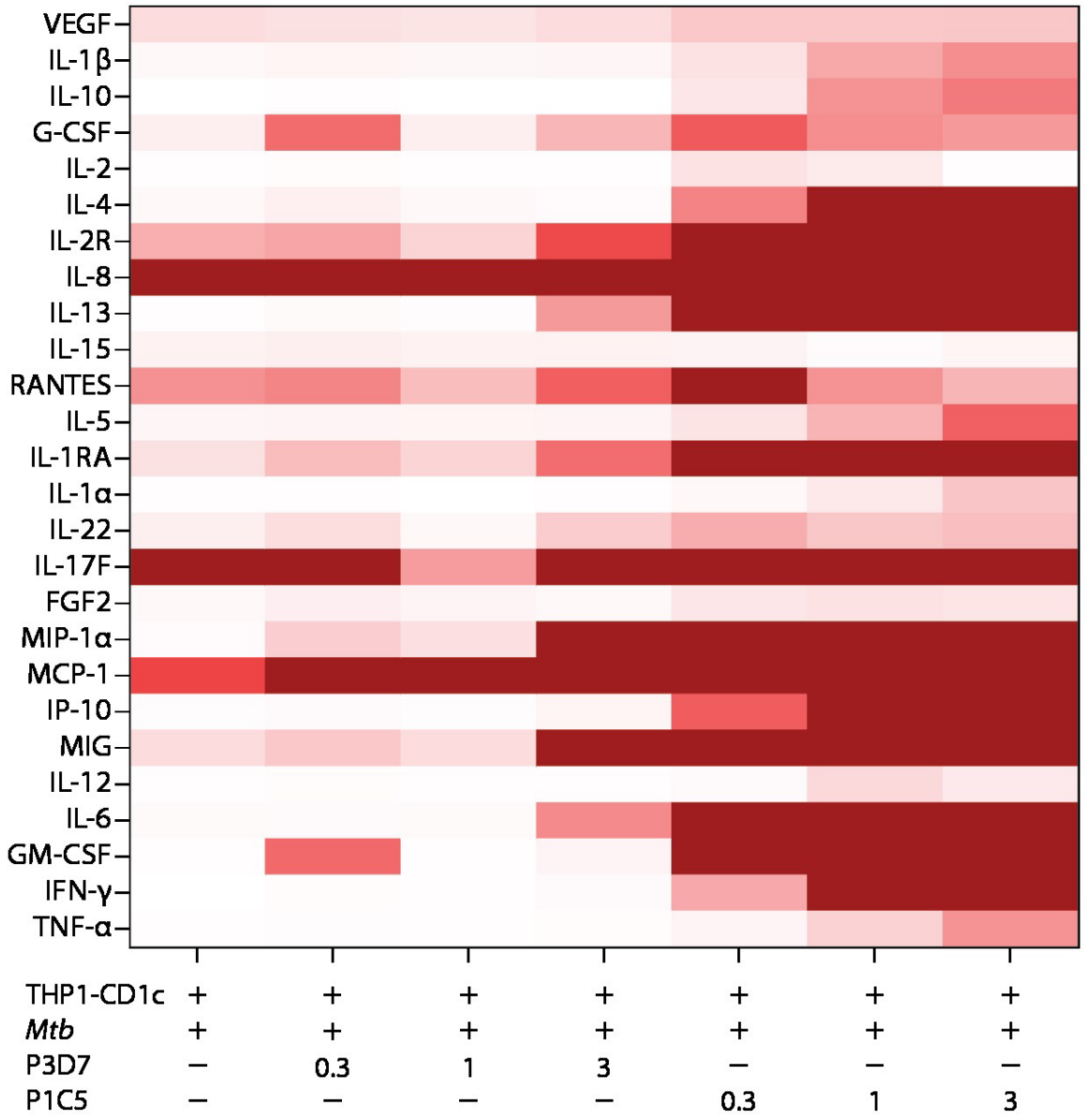

Figure S1: Heat map of cytokines secreted by P3D7 and P1C5 T cells. Heat map depicting relative levels of cytokines secreted by P3D7 and P1C5 T cells cultured with infected THP1-CD1c cells. T cells were added to infected THP1-CD1c cells (*Mtb* MOI = 10) at three different ratios 0.3:1, 1:1, and 3:1. Concentrations of cytokines released were measured 48 hours post the addition of T cells. Red and white indicate greater and lower expression, respectively.

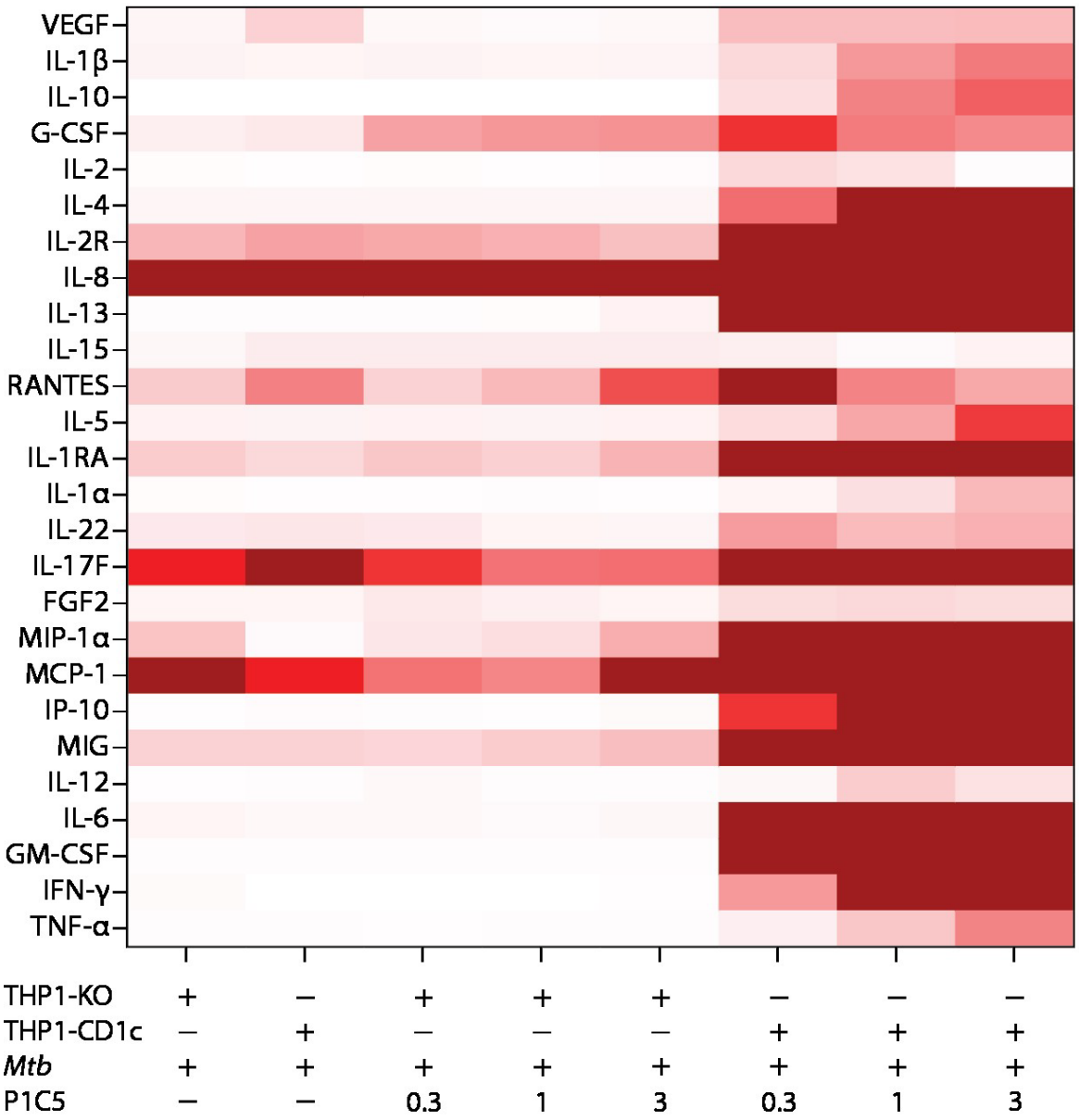

Figure S2: Heat map of cytokines secreted by P1C5 T cells in response to infected THP1 cells. Heat map depicting relative levels of cytokines secreted by P1C5 T cells cultured with infected THP1-KO and THP1-CD1c cells. T cells were added to infected THP1 cells (*Mtb* MOI = 10) at three different ratios 0.3:1, 1:1, and 3:1. Concentrations of cytokines released were measured 48 hours post the addition of T cells. Red and white indicate greater and lower expression, respectively.